Water Business Jet

Design Synthesis Exercise

Delft University of Technology

TU Delft

Jaeger

Design Synthesis Exercise

Water Business Jet

Final Report

Bachelor of Science
Aerospace Engineering
Delft University of Technology

Team 07

Member	Student Number
W.A.J. Duchateau	4369351
R.G.J. Fennema	4210476
F.H. Hartog	4359461
M. Hofwegen	4349660
J.M.W. van Kollenburg	4362594
J.A.H. Kuijpers	4353501
Y.C. Mekking	4300718
R.A. Weerheim	4358295
S.P. de Wringer	4351568
B.J.V. Zwanenburg	4393678

Tutor	Organisation
Dr. C.D. Rans	SI&C

Coach	
Ir. O. Stroosma	C&S
Dr. S. Bouarfa	ATO

Preface

This report is the fourth and final report concluding the spring Design Synthesis Exercise for group 07. Ten bachelor students from the faculty of Aerospace Engineering at Delft University of Technology have worked eleven weeks on a given assignment: the design of an executive jet with amphibious capabilities. This report is aimed at peers, meaning basic engineering knowledge at the level of a third year bachelor student is assumed of the reader throughout the report.

A report of this size does not easily come about and without the valuable advice of many people the report would not have reached its current quality. We would therefore like to express our gratitude to several people who were of invaluable help.

First of all we would like to express our deepest gratitude to our tutor Calvin Rans and two coaches Olaf Stroosma and Soufiane Bouarfa for their guidance and constructive feedback throughout the project. The time and effort they put into consulting us is much valued.

Secondly, we would like to thank Dr. ir. Keuning from the faculty of Maritime Engineering for his advice and expertise on the hydrodynamic aspects of the design. As aerospace students, this external expertise from a different field of study was of extra value.

We also would like to express our gratitude to both Dr. ir. Abhishek K. Sahai and ir. P. C. Roling from the faculty of Aerospace Engineering for the practical insight they provided regarding noise emission.

Furthermore, we would like to show our appreciation to Dr. ir. Vos, also from the faculty of Aerospace Engineering, for his expertise on high speed aerodynamics, which aided in the analysis of the hull shaped fuselage at high Mach numbers.

Lastly, the hard work of the OSCC and OSSAs in arranging all practicalities, whenever we needed them, deserves praise.

Group 07, Water Business Jet
Delft, June 2017

Executive summary

Introduction

Currently almost half of the world population lives within 100 km from a coastline. Especially major business-centric cities such as Singapore, New York City, Hong Kong and Vancouver are located directly next to oceans, seas or lakes. This provides the opportunity of utilising these large bodies of water as infrastructure for landing and takeoff. A reduction in transportation times is realisable since aircraft could taxi to the location of interest directly instead of operating out of less centrally located airports. In addition it would provide the possibility of landing at the desired location even if no landing slots are available at the local airport. Present amphibious aircraft, however, are typically aimed at remote operations. As a consequence, essentially no amphibious passenger jet aircraft currently exist. Therefore a huge potential lies in the market for executive aircraft as no business jet currently offers such a level of flexibility so often desired by typical customers. Furthermore the development of an amphibious executive aircraft can be the basis for potential spinoffs and serve as the next step in realising a more flexible approach to transport. The objective of the design project was to develop a preliminary design of a high speed executive amphibious aircraft and research its technical, operational and economic feasibility. This exercise resulted in the preliminary design of the Jaeger, a two-engine, T-tail aircraft capable of ultra-long-range missions at high speeds.

The market

The unique selling point of the Jaeger is the flexibility it provides with its amphibious capabilities. It becomes possible to directly travel to locations with no adequate airport or when there are no available landing slots. Another benefit is the potential decrease in travel time. Operating out of water can save 15 to 30 minutes compared to general airports in Vancouver for example. On a trip of 1100 nautical miles (NM), the average operating distance of the Dassault Falcon 7X, this is a relatively large gain. Further market analysis gives an optimal maximum range of 4500 NM: it is sufficient for both the current top 10 and emerging top 10 business routes; covers all possible routes within Asia which is characterised by a rapidly expanding market for executive aircraft; and provides the possibility of travelling the entire world with one stop only. With a selling price of 60 million USD and similar performance for characteristics such as cruise speed and passenger capacity, the concept is expected to be highly competitive compared to business jets with similar missions such as the 7X, Global 6000 and Gulfstream G550. Being the first to bring a business water jet to the market imposes a large first mover advantage, based both on reputation and knowledge. It would allow Jaeger to instantly gain a large share in the water aircraft market, strengthening its position for the years to come.

Design case

In addition to the market requirements, functional and requirement analyses were performed to get a full picture of the design space. Especially functions due to Jaeger's amphibious nature proved critical, because this is the point where the design obviously differs most from conventional jets. Several requirements relating to damage from the aquatic environment were therefore set up. The aircraft requirement for spray clearance is a prime example hereof. Relating to aircraft operations on water, it was found that the aircraft requires a maximum landing weight equal to its maximum takeoff weight. Additionally, a preliminary sensitivity analysis was performed to get a sense of the importance of different design parameters for the requirements set. It showed that the lift-to-drag ratio and engine specific fuel consumption are critical for meeting these requirements. Therefore, it is logical that these parameters bear relatively heavy weights in the performed tradeoffs.

Concept selection process

The concept was selected from a number of concepts using a tradeoff table. The concepts were generated from design options found from design options trees. An extensive tradeoff between the concepts was performed based on the following criteria: hydrodynamic performance, aerodynamic performance, structural performance, development risk, passenger comfort, spinoff possibilities, cost and sustainability. The concept of a canard configuration with retractable side floats was selected and formed the basis of the conceptual design phase. A risk assessment based on the conceptual design pointed out that the centre of gravity range required for in flight stability and the centre of gravity range required for acceptable trim angles at rest could possibly not be matched. Therefore the design was changed to a high wing, two-engine T-tail configuration with retractable side floats.

Concept characteristics

At the current state, the concept consists of a two-engine jet aircraft with a high wing, T-tail configuration. It has a hull shaped bottom of the fuselage, a waterjet propulsion system and retractable side floats for stability on water. An overview of this design is given in Figure 1. The most important parameters are given in Table 1 and Table 2. It is worth noting that the range requirement of 4500 NM, which followed from the market analysis, is met, even when flying at full passenger capacity including carry-on luggage.

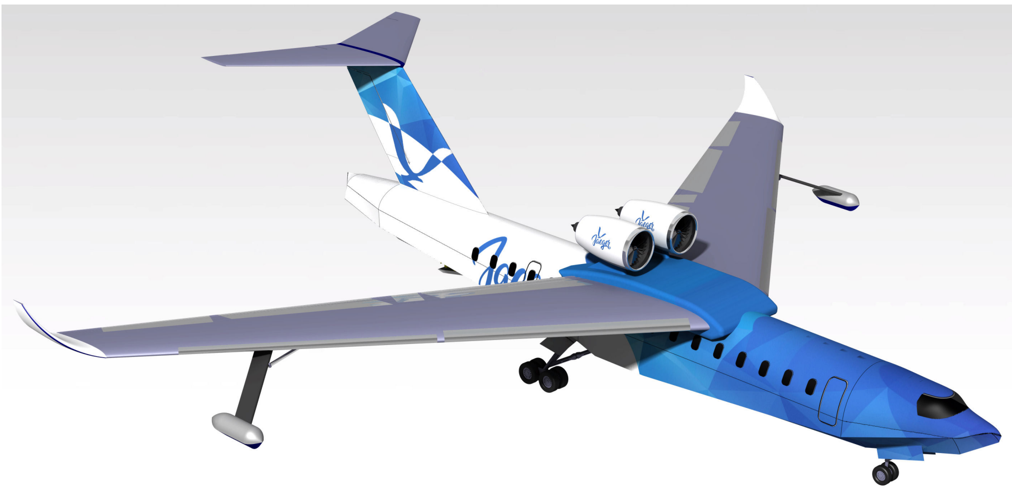

Figure 1: Isometric view of the aircraft.

Table 1: Jaeger fact and performance sheet (1)

Dimensions		
Length	27.3	m
Height	7.10	m
Diameter	2.70	m
Span	30.0	m
Cabin length	12.84	m

Weights		
Maximum takeoff weight	31,750	kg
Operational empty weight	16,941	kg
Max fuel weight	12,913	kg
Maximum landing weight	31,750	kg
Max payload weight	10,000	kg

Propulsion		
		Engines
Manufacturer	Safran	
Type	Silvercrest 2C	
Takeoff thrust	12,000	lbf
		Water jet
Power	37.0	kW
Taxi speed	6	$m\,s^{-1}$

Table 2: Jaeger fact and performance sheet (2)

Performance						
Takeoff & Landing			**Cruise**		
		Water	Approach speed	45	$m\,s^{-1}$
BFL @ MTOW	2,610	m	Maximum operating altitude	12,497	m
TOFL	1,980	m	Cruise speed	0.85	M
		Land	Maximum operating speed	0.9	M
BFL @ MTOW	1,932	m	Maximum range - no payload	6,700	NM
TOFL (sea-level)	1,618	m	Range - 0.85M, 16 VIP + carry-on luggage (2,000 kg)	6,000	NM
			Range - 0.85M, 4,000 kg PL	4,500	NM

Subsystem design and feasibility assessment

As this main objective of this report is to analyse the feasibility of a Water Business Jet, the design process focused on the items and subsystems which posed the largest risk on the feasibility. By means of a risk analysis it was found that operations on water, hydrodynamic drag, taxiing on water, hydrostatic stability and aerodynamic drag were of the most important items to allocate resources to. The most noteworthy results obtained by analysing these subsystems are presented in the remainder of this section.

Operations

The most critical aspects of the aircraft operations were landing and takeoff on water as well as (un)loading on water. An operational plan for landing near major business-centric cities and at remote locations is created. The major benefit of the plan is that essentially no new large infrastructure has to be developed. Community noise, maritime traffic and current regulations at desired landing sites form no substantial limitations on operations. For (un)loading on water four concepts were established: via a horseshoe dock, via a pier with extendable platforms, by towing the aircraft onto land via a ramp and with a small boat.

Hydrodynamic drag

For the engine sizing, landing and takeoff distance calculation and waterjet sizing it is required to determine the total drag as a function of speed for water operations. A model was created to determine this drag, based on several papers on hydrodynamic drag combined with knowledge on aerodynamic drag and lift. The model was verified, and a towing tank test was proposed to validate the results since the calculations are extrapolated from test data. Figure 3 shows the computed drag as function of speed.

Preliminary calculations on spray and hydrodynamic stability were performed. The computations predict acceptable spray. Combined with the high engine placement that uses the wings for shielding against spray this provides enough confidence, for this design phase, that spray will not pose large problems. Regarding dynamic stability, porpoising should not be a problem since the calculations based on the basic planing coefficients predict stable planing.

Water Jet Propulsion

The waterjet, which is necessary to meet the noise requirement, was sized to ensure proper aircraft manoeuvring on water. In order to make optimal use of the APU, a taxi speed of $6\,m\,s^{-1}$ was chosen. As a result, a jet output and input power of 37 and 62 kW are required, respectively. Assuming a 60 % jet efficiency, the power can therefore be delivered by the 90 kW APU, consequently eliminating the need of an extra subsystem. The waterjet is positioned into the aft of the fuselage and is deployed as shown in Figure 3.

Side floats for hydrostatic stability

One side float under each wing was selected to maintain hydrostatic stability, even with waves of 1.5 m and corresponding wind speeds creating a moment around the longitudinal axes. Furthermore, a mechanism was selected that retracts the sidefloat into the wing, thus reducing drag during cruise. This mechanism is displayed in Figure 4. However, in order to accommodate for enough space in the wing for the storage of the side float, a part of the wing box needs to be removed. This poses the need for an alternative wing box structure. Whether or not it will be able to efficiently design such an alternative structure, is considered a risk on the technical feasibility of the Jaeger.

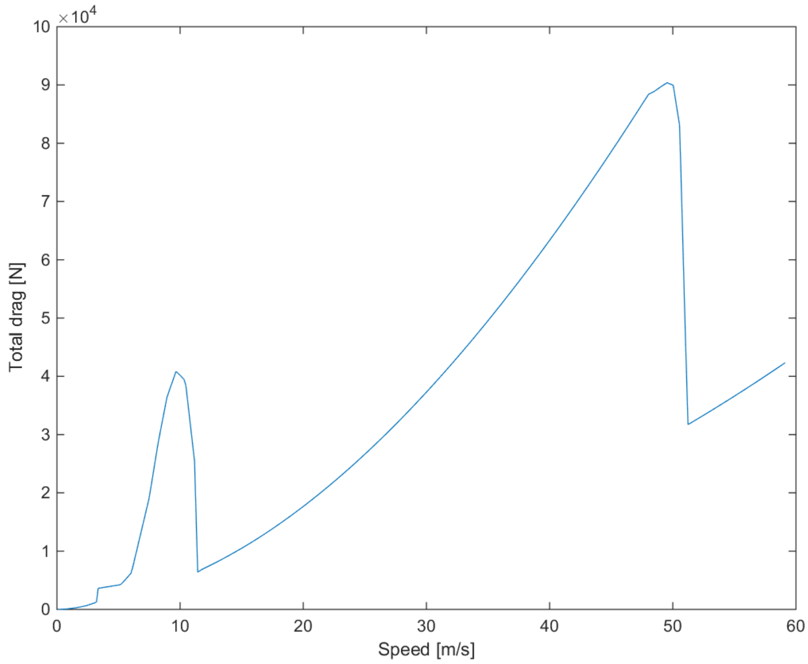

Figure 2: Total (aerodynamic and hydrodynamic) drag versus speed.

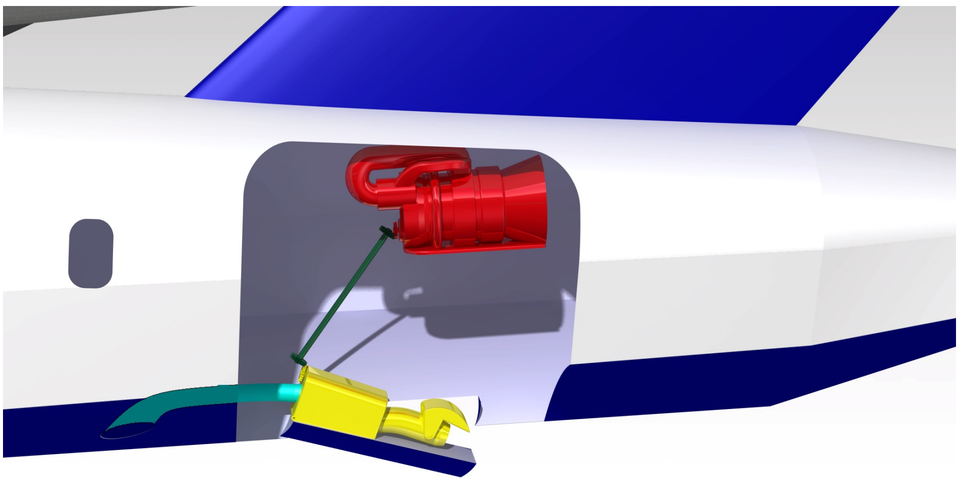

Figure 3: Deployment of the waterjet and its integration into the fuselage.

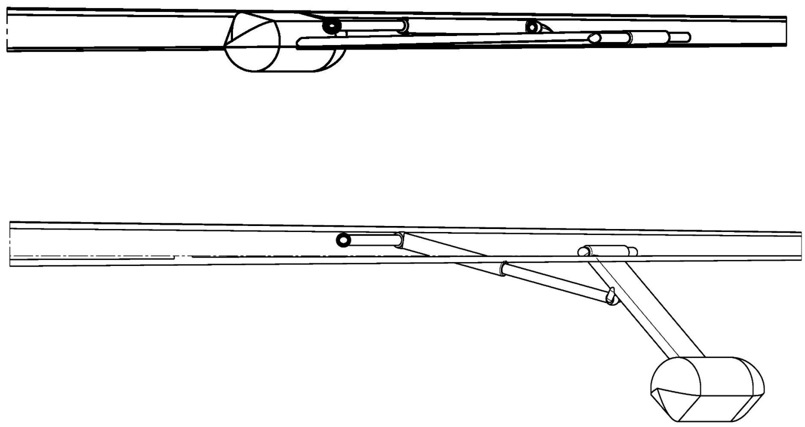

Figure 4: Side floats retracted in wing and extended.

Aerodynamics

Research into the aerodynamic performance of the Jaeger focused on drag and the effect of the hull on the flow at high speeds. This research resulted in a first indication that the drag is within the limits to meet the range requirements. However, it was found that proper validation of the model was not possible within the available resources. In addition, the model showed a high sensitivity to the hull contribution, which in turn was merely based on statistical data. Furthermore, a preliminary CFD analysis showed the occurrence of shock waves at the step in the hull in the cruise speed range.

Conclusion and recommendations

At the current state, the concept indicates technical, operational and economic feasibility. At a sales price of 60 million USD and 100 units sold, a profit of approximately 2.4 million USD is expected to be made per aircraft. Furthermore the majority of initially set requirements and identified risks have been met and mitigated respectively. Through a final risk assessment however it was identified that still a couple of noticeable risks exist which could impact the feasibility of the concept.

At the current state aerodynamic, performance is the most critical risk on the feasibility of the concept, in particular the shock waves and zero-lift drag aspects. For hydrodynamic performance the drag model has not been validated yet and little is known on the stability and impact loads during landing in rough water conditions. Consequently there still exists some uncertainty on the integration of the side floats and wing. Lastly a change in regulations could endanger the operational aspects which make the concept unique.

Due to the promising results so far it is recommended to proceed with further efforts in studying the feasibility of and developing the water business jet concept. Firstly, more research into the occurrence and effects of the shock waves and the drag in general should be performed. Furthermore the hydrodynamic drag model has to be validated by means of a towing tank test, and the effects of rough water conditions on water operations should be investigated in detail. Specifically the resulting impact loads have to be considered, also through the establishment of an extensive structural model. This also aids in further research on the integration of side floats and wing and establishment of a detailed mass estimation. Lastly it is advised to proactively work together with authorities and secure desired operational plans, and use more sophisticated cost models as the design progresses.

Contents

Nomenclature

List of symbols

Typical units are given in square brackets. If no unit is given, then the variable is dimensionless.

α	angle of attack [rad],
	angular acceleration [rad/s^2]
β	angle of deadrise [rad]
γ	flight path angle [rad]
Δ	displacement [kg],
	deflection
δ	deflection [rad]
ε	induced downwash angle [rad]
Λ	sweep angle [rad]
λ	wave length [m]
ν	kinematic viscosity [m^2/s]
ρ	density [kg/m^3]
τ	trim angle [rad]
A	aspect ratio,
	amplitude [m],
	area [m^2]
B	beamwidth [m]
a, b	engine coefficients
C_D	drag coefficient
C_F	friction drag coefficient
C_L	lift coefficient
C_R	residual drag coefficient
C_T	total drag coefficient
C_V	velocity coefficient
c	chord [m]
c_l	section lift coefficient
D	Drag [N]
E	Young's modulus [Pa]
e	Oswald efficiency factor
F	force [N]
Fr	Froude number
g	gravitational acceleration [m/s^2]
h	height [m]
I	mass moment of inertia [kg m^2],
	area moment of inertia [m^4]
K	spray coefficient
L	length [m],
	arm [m]
M	Mach number,
	moment [N m]
m	density exponent
$\dot{m}$	mass flow
N	thrust setting
n	load factor
P	sales price [million USD]
p	pressure [Pa]
R	range [NM]
Re	Reynolds number
S	surface area [m^2]
s	distance [m]
T	thrust [N],
	torque [N m]
t	time [s]
u	wave deflection [m]
V	velocity [m/s],
	shear force [N],
	volume [m^3]
$\mathbb{V}$	tail volume coefficient
v	wave speed [m/s]
W	weight [N]

Subscripts

$_0$	zero-lift
$_{ac}$	aerodynamic centre
$_{cg}$	centre of gravity
$_{cr}$	cruise
$_{eng}$	engine
$_f$	fuel
$_{fus}$	fuselage
$_h$	horizontal stabiliser
$_{LE}$	leading edge
$_{max}$	maximum
$_r$	rotating
$_s$	stall
$_{scr}$	screen
$_{sl}$	sea level
$_{sf}$	side float
$_{TO}$	takeoff
$_{ult}$	ultimate
$_v$	vertical stabiliser
$_{wl}$	waterline
$_w$	wing

List of abbreviations

ACC	Area Control Center
ADS-B	Automatic Dependent Survaillance-Broadcast
ADSEE	Aerospace Design & Systems Engineering Elements
APU	Auxiliary Power Unit
ARTCC	Air Route Traffic Control Centre
ATC	Air Traffic Control
ATCT	Air Traffic Control Tower
BFL	Balanced Field Length
BWL	Beam of Waterline
CAEP	Committee on Aviation Environmental Protection
CER	Cost Estimation Relationship
CFD	Computational Fluid Dynamics
DAPCA	Development And Procurement Cost of Aircraft
DSE	Design Synthesis Exercise
EASA	European Aviation Safety Agency
EBHA	Electric Backup Hydraulic Actuation
FAA	Federal Aviation Administration
FEM	Finite Element Method
FMECA	Failure Modes, Effects and Criticality Analysis
FTA	Fault Tree Analysis
GA	General Aviation
GPS	Global Positioning System
HLD	High-Lift Device
ICAO	International Civil Aviation Organization
INM	Integrated Noise Model
ISA	International Standard Atmosphere
ITTC	International Towing Tank Conference
LTO	Landing Takeoff
LWL	Length of Waterline
MLW	Maximum Landing Weight
MTOW	Maximum Takeoff Weight
OEW	Operational Empty Weight
RAMS	Reliability, Availability, Maintainability, and Safety
RC	Rate of Climb
SBSS	Surveillance & Broadcast Services System
SEAD	Systems Engineering & Aerospace Design
SEL	Sound Exposure Level
SFC	Specific Fuel Consumption
TBO	Time Between Overhaul
TCC	Terminal Control Centre
TOFL	Takeoff Field Length
TOP	Takeoff Parameter
TRACON	Terminal Radar Approach Control
VHF	Very High Frequency
VTS	Vessel Tracking Service
VTSCC	Vessel Tracking Service Control Centre

Introduction

Currently almost half of the world population lives within 100 km from a coastline.[1] Especially major business-centric cities such as Singapore, New York City, Hong Kong and Vancouver are located directly next to oceans or lakes. This provides the opportunity of utilising these large bodies of water as infrastructure for landing and takeoff. A reduction in transportation times is realisable since aircraft could taxi to the location of interest directly instead of operating out of less centrally located airports. In addition it would provide the possibility of landing at the desired location even if no landing slots are available at the local airport.

Present amphibious aircraft, however, are typically aimed at remote operations. As a consequence, essentially no amphibious passenger jet aircraft currently exist. Therefore a huge potential lies in the market for executive aircraft as no business jet currently offers such a level of flexibility so often desired by typical customers. Furthermore the development of an amphibious executive aircraft can be the basis for potential spinoffs and serve as the next step in realising a more flexible approach to transport.

Jaeger, named after the smaller species in the Skua family of seabirds, addresses this market potential. It is a high speed executive jet with amphibious capabilities. Figure 5 shows the conceptual design of Jaeger.

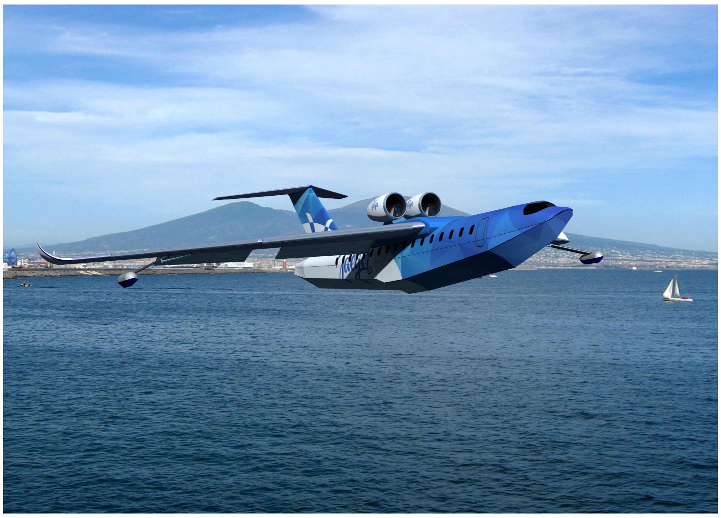

Figure 5: Impression of the Jaeger water business jet

The objective of the design project was to develop a preliminary design of a high speed executive amphibious aircraft and research its technical, operational and economic feasibility. This report concludes the Design Synthesis Exercise and aims at presenting the current state of the design, providing insight in the design process, drawing conclusions on the feasibility and making recommendations for further design and research. This was done by means of systems engineering tools, calculations, qualitative analyses and statistical models. These methods are applied in research of the design case, evaluation of potential designs and further detailed design of the selected concept.

This report is structured as follows: Part I focuses on the project definition. A market analysis and design case analysis are performed and the organisational aspects of the project are discussed. Part II describes the general design of the aircraft. Next to the configuration and general performance, the cost, operations, RAMS, sustainability and production plan are discussed. The design of several subsystems of the aircraft is presented in Part III. Here, amongst others, the fuselage and hull, wing and empennage and propulsion systems are elaborated upon. Part IV is the final part of the report and discusses the way forward. Attention is paid to the evaluation of the preliminary design and recommendations and planning for further design.

[1] https://www.un.org/esa/sustdev/natlinfo/indicators/methodology_sheets/oceans_seas_coasts/pop_coastal_areas.pdf Retrieved 20-06-'17

I

Project definition

The aim of this part is to inform the reader on a unique opportunity to conquer the business jet market. Firstly, through a market analysis, a quantification of customer needs and market constraints is given in Chapter 1. Together with Chapter 2, a complete picture of the design space and its constraints is obtained. In order to properly understand the design process and choices, Part I is concluded with Chapter 3. This chapter explains how the team approached the design case from an organisational point of view.

1
Market analysis

As a basis for the design, a market analysis is performed. Its goal is both to show the sales potential of the aircraft and to investigate requirements based on the current market. In general, the business jet market is a profitable market which is expected to grow, also due to emerging markets. India, for example, is expected to be the third largest aviation market by 2020, having tripled its executive aircraft industry in 2020 with respect to 2015 [39]. The novel idea of a business jet with amphibious capabilities can offer advantages in flexibility of usage, as well in reduction of travel time, as it does not rely on regular airports for operations. This really distinguishes a water business jet from other aircraft; no current aircraft offers executive transport with such a high level of flexibility. The combination of high cruise speed, long range and extensive number of possible landing locations on both water and land, gives this aircraft its unique selling point.

1.1. Current market

The current long range business jet market is dominated by three players: Gulfstream, Bombardier and Dassault, accounting for 48%, 30%, and 22% of the market, respectively. An average annual increase of 2.7% in deliveries is expected for the coming ten years, resulting in 1,871 units sold, which generates a total segment revenue of 143,885 million USD [26]. The low fragmentation of the market provides a high entry barrier, since these established companies have access to distribution networks and other complementary assets. They can also profit from economies of scale. An overview of several reference aircraft can be found in Appendix E.

However, the products produced by these three companies are quite similar since differentiation is limited. A business jet with amphibious capabilities would definitely be advantageous over the other available jets in this sector, of which none have such capabilities.

The advantage of amphibious capabilities is evident when looking at the top 10 most used business routes. Nine out of ten of these routes allow for utilisation of large bodies of water for takeoff and landing [35]. Landing on water offers a reduction in travel time compared to airports located further away from the city centre. Furthermore, flexibility is greatly improved by removing dependency on busy airports which may not have slots available. As an example, Figure 1.1 shows the potential time saving by landing on water in Vancouver. Imagine a group of businessmen having an emergency meeting in Vancouver. The airports are busy, so only the airport located further away has a slot available. However, this slot is only available later in the day. The benefits of a water business jet that can land close to the city centre at any time of the day are apparent in this scenario.

Being the first to bring a business water jet to the market imposes a large first mover advantage, based both on reputation and knowledge. It would allow Jaeger to instantly gain a large share in the water aircraft market, strengthening its position for the years to come.

1.2. Stakeholders

A business jet is a complex system which involves many different persons and parties. Getting an overview of these stakeholders and their interests allows to create a positive relationship with the relevant stakeholders. These stakeholders also impose new requirements on the design which should be met.

A general approach to a stakeholders analysis is presented by Bryson [2], where the stakeholders are divided in four categories based on their interest and influence. Figure 1.2 maps these categories. Key players

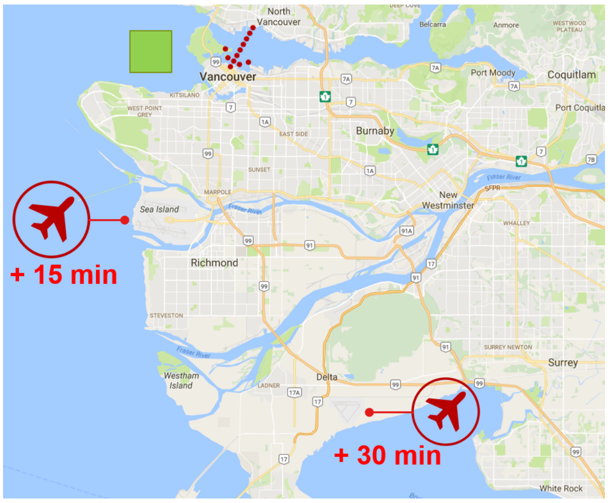

Figure 1.1: The potential time advantage of landing on a body of water as compared to at an airport

require the most attention since they are crucial to the project, so this section focuses on identifying these key stakeholders. The key stakeholders are the investor(s) and the governmental authorities. As financiers, the investors have a large influence on the project, and with their money at risk their interest is also high. Regular meetings should inform the investors on the progress and supply the engineers with feedback on the design. Governmental authorities, like airworthiness and seaworthiness authorities also have a large influence on the project. Their legislative power could prevent the aircraft from being able to operate. Updates on the design and operations plan should be given. This is of extra significance for this project since it may require new legislation due to its unique operations. Including authorities in an early stage allows for the design to be adjusted to possible new legislation.

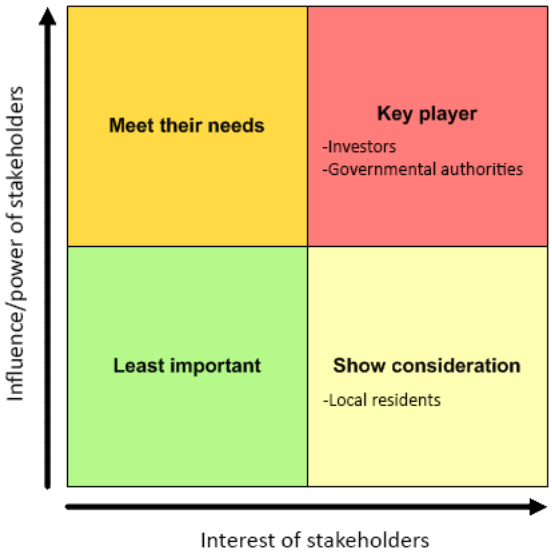

Figure 1.2: Schematic map of stakeholder ranked on interest and influence. [1]

Less influential stakeholders include the local residents. Residents living near landing sites are mostly concerned with the noise emission of the aircraft. Landing on water allows for approach route optimisation over

[1] https://www.stakeholdermap.com/images/stakeholder-analysis.gif Retrieved 27-06-'17

water, this way limiting the community noise impact. Subsection 6.1.4 elaborates on the community noise impact of the aircraft.

Future passengers are also considered important stakeholders. Although not very influential in the design phase they determine the ultimate success of the aircraft. Their needs should therefore be addressed throughout the design process, for example through market research. In every design step the customer wishes should be a design consideration to fully address these stakeholders.

1.3. Range and cost

In order to make the aircraft competitive, proper requirements on range and cost should be set. These initial requirements are based on reference aircraft and further analysis.

A range of 4500 NM was selected as requirement[36]. As can be seen in Figure 1.3 the range fully covers the emerging market of Asia. It also covers all top ten business routes [35], and easily covers the average flight distance of the Falcon 7X, which equals 1100 NM [14].

Figure 1.3: Range of 4500 NM covering the Southeast Asian market flying from Kuala Lumpur[2].

A sales price of 60 million USD was set as a requirement [36]. Figure 1.4 shows that this sales price is comparable to reference aircraft. The amphibious capabilities are expected to impose a cost penalty on the aircraft, while on the other hand new production techniques are expected to lower the cost. These effects are assumed to cancel out and result in a sales price similar to reference aircraft. Analysis on the costs can be found in Chapter 5.

1.4. Takeoff and landing performance

In order to remain competitive and increase the flexibility in usage, the aircraft should have a takeoff and landing length suitable to its potential operating locations. Looking at the 50 most visited business airports around the world [36], a balanced field length (BFL) of 2000 m allows usage of all of them. In order to arrive at a preliminary BFL on water, a water drag penalty of 40% was added, based on the Beriev BE200 [3]. The resulting BFL of approximately 3000 m was found small enough to be applied in several business-centric cities like New York, Vancouver, Singapore and San Francisco. Chapter 6 elaborates on this.

1.5. Spinoff possibilities

In order to improve the marketability of the aircraft even further, spinoff possibilities can be thought of. This section aims at presenting ideas on this topic. Additionally, some design considerations for improving the marketability through spinoffs are discussed here.

[2]Made with `freemaptools.com/radius-around-point.htm`

[3]`http://www.beriev.com/eng/Be-200_e/Be-200_e.html` Retrieved 20-06-'17

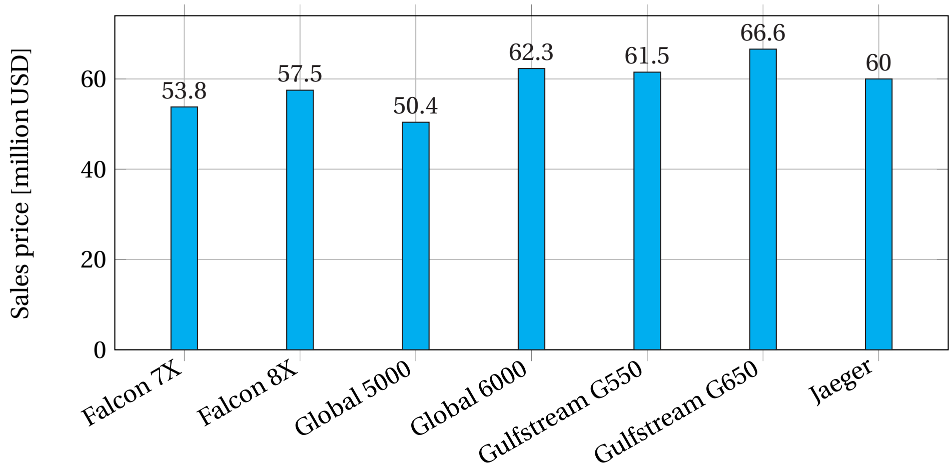

Figure 1.4: The sales prices of selected reference aircraft as compared to that of the Jaeger. [24]

The potential time benefit gained by landing the water business jet on water is percentually greatest when making short flights. Because of the ability of the aircraft to land at a greater variety of landing sites, exploiting its point-to-point transport capabilities is a logical consideration. Not only would this point-to-point transport result in passengers' travel comfort being increased through shorter travel times, but replacing the traditional hub-and-spokes system may also reduce the environmental footprint of the aircraft. An analysis of the potential sustainability gain is given in Section 8.2.

This regional, high speed transport would then be most optimally used by allowing more payload or more passengers aboard. Therefore, a fuselage configuration allowing for a larger amount of passengers should be possible within the available cabin space. It was therefore chosen to widen the fuselage somewhat, to 2.7 m, such that a two abreast seating is possible. Consequently, 60 passengers can be taken aboard instead of the usual 16 passengers in VIP seating configuration. The range corresponding to this payload is approximately 3000 NM, as will be elaborated upon more in Section 4.2.

On a different note, the spinoff possibility of using the aircraft as cargo aircraft was investigated. However, it was found that this spinoff is not effective, because of the difficult loading of cargo. In this sense, the aircraft cannot compete with other cargo aircraft which, for example, have nose loading possibilities such as the Boeing 747-400 freighters. Applications are limited to remote areas, disaster areas or other locations where no regular airport exists and the amphibious capabilities offer explicit advantages.

2

Design case analysis

Having identified the main focus points the design in Chapter 1, it is key to completely define the design space of the aircraft. Therefore, a thorough analysis of the system's critical functions and design parameters was performed. This forms an addition to the market analysis, which focused on market drivers, instead of functional drivers. In Section 2.1, the required functions of the system, discovered through a functional analysis, will be presented. Section 2.2 then presents a synthesis of the most important functional requirements and of the market requirements as obtained in Chapter 1. Subsequently, the influence of uncertainty on certain design parameters on the overall aircraft performance will be investigated in Section 2.3. Finally in Section 2.4, several sustainability elements on which the aircraft is thought to be critical will be addressed shortly.

2.1. Functional analysis

In order to investigate which functions the aircraft should perform, a functional flow diagram and functional breakdown structure have been set up. These tools offer a way to systematically order and group the functions. This systematic approach ensures that all functions are considered.

Figure 2.1 presents the functional flow on top level. This is a very general flow, which applies to most conventional aircraft. An elaboration on this functional flow was presented in the baseline report [35]. The functions specific for operations on water were considered most critical for the feasibility of the project. These functions are therefore presented in more detail in Figure 2.2. The functional flow has been updated several times as the design progressed. Figure 2.2 shows the latest version of this flow where already several design choices are implemented and reflected in the functional flow. In Chapter 6 the argumentation behind these design choices can be found.

During the design the identified water specific functions require extra attention. The novelty of the design comes down mostly to these points, and a proper functional flow greatly helps at identifying possible requirements and other design considerations. Examples of water specific functions the aircraft should perform include providing buoyancy and taxiing on water. The requirements that follow from the functional flow are discussed in Section 2.2.

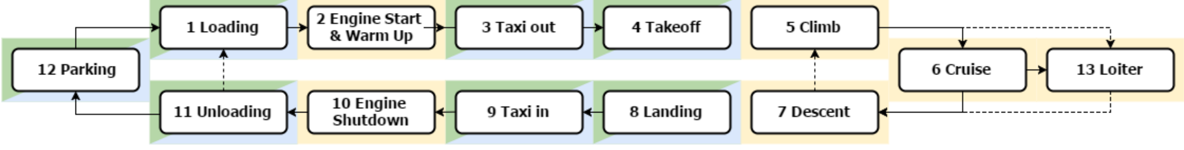

Figure 2.1: Top level functional flow for the water business jet (green/blue background indicates a difference on land and water).

For a complete overview the functions are also grouped in a functional breakdown structure, which is presented in Figure 2.3. Grouping the functions in the functional breakdown structure provides new insights in the functions of the aircraft. Some functions, for example, are clearly present in the functional breakdown structure while they do not appear in the functional flow diagram. Combining both tools gives a good

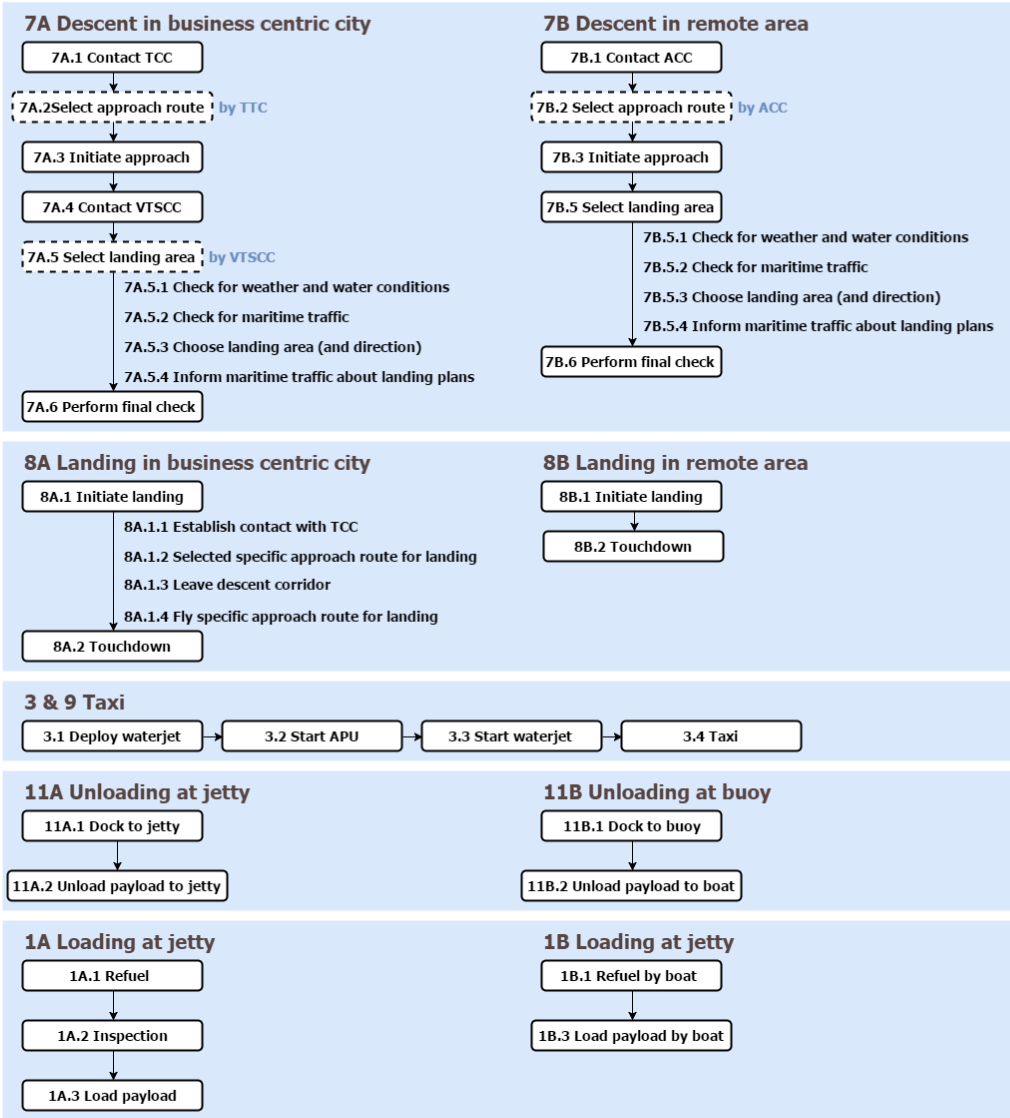

Figure 2.2: Detailed functional flows for operations on water.

overview of all functions, which form the basis of the system and subsystem design performed in the weeks after. In the end, the customer wants functions, not systems. Therefore it is of importance to keep the functions in mind throughout the design process, and this functional analysis fulfilled this purpose.

2.2. Requirement analysis

As a means of summarising the foregoing analyses, the previously discussed characteristics of the aircraft are translated into requirements. The functions that the aircraft needs to perform as discussed in Section 2.1 are translated into requirements, whilst the requirements as discussed in Chapter 1 will be repeated here in a more formal manner. Additionally, it will be indicated in which section the requirement is dealt with through research and design effort. Some requirements come from the market analysis as performed in the midterm report, and are cited accordingly.

The requirements obtained through the quantification of market needs (Chapter 1) are the following.

- The aircraft shall have a minimum range of 4500 NM taking into account the NBAA IFR reserve fuel conditions. (Analysed in Subsection 4.2.1)
- The aircraft shall be sold for a price of 60 million USD. (Analysed in Chapter 5)

- The aircraft shall provide enough lift to not stall at 41 $m\,s^{-1}$ in water landing configuration at MLW [36]. (Analysed in Subsection 11.1.1)
- The aircraft shall provide enough lift to not stall at 41 $m\,s^{-1}$ in land landing configuration at MLW [36]. (Analysed in Subsection 11.1.1)
- The aircraft shall have a balanced field length on land of 2000 m. (Analysed in Section 4.2)
- The aircraft shall have a balanced field length on water of 3000 m. (Analysed in Section 4.2)

As for the requirements that come from the functional analysis, only few will be stated here. This is done partly because there is overlap between requirements coming from the market analysis. However, some obvious requirements coming from the functional analysis , such as the aircraft's being able to land on water, are omitted for the sake of clarity. A full list of requirements can be found in Appendix L. The following requirements come from the functional analysis done in the midterm report:

- The aircraft shall have a resistance from corrosion by (sea)water [36]. (Analysed in Chapter 7)
- The aircraft shall have a MLW equal to its MTOW [36]. (Analysed in Subsection 11.3.1)
- Spray during takeoff and landing shall not be directly ingested into the engines [36]. (Analysed in Subsection 10.1.4)
- The aircraft shall provide the required movements during taxi on water [36]. (Analysed in Section 13.2)

2.3. Most Important Design Parameters

Defining the parameters that are most influential on the Jaeger's performance with respect to the most important requirements as analysed in Section 2.2, aids in making choices and trade-offs between concepts, and furthermore gives an indication which areas should be analysed with the highest priority. In this section a sensitivity analysis is performed with respect to takeoff weight (W_{TO}) and range, which showed that lift-over-drag and range were the most influential on the overall performance.

Table 2.1 shows the influence of the most important design parameters to two main requirements. This table only shows how a 1% change in lift over drag, engine efficiency, payload weight and range percentually influences the takeoff weight and range.

Table 2.1: Relative change in W_{TO} and Range because of a 1% change in important design parameters.

Parameter which is increased by 1%	Initially assumed	WTO (% increase)	Range (% increase)
SFC [$kg\,N^{-1}\,s^{-1}$]	0.55	+3%	-1.1%
LD [-]	13	+6.9%	+1.1%
Payload (16 pax) [kg]	2000	-	-0.11%
Payload (max cargo) [kg]	15000	-	-0.70%
Range [NM]	5000	+8.8%	-

Although the choice of design parameters and characteristics seems limited, it actually is very useful to know the influence of aerodynamic performance, thrust performance, payload weight and range on the ability of the aircraft to meet important requirements. Furthermore, takeoff weight is correlated with stall speed, field performance and cost of the overall design. Therefore, parameters that are more influential on the takeoff weight, are also more influential on the requirements regarding these characteristics. The results of this analysis thus actually do provide a good sense of the relative importance of design parameters.

In order to arrive at the relative sensitivities, it was necessary to use some sort of numerical model to judge the influence of specific parameters. A Class 1 weight estimation of the aircraft, was applied, combining statistical data from business jets and seaplanes to arrive at a reliable approximation. Furthermore, considering range, Breguet's range equations were applied as an early estimate. It was found that these preliminary approximations were sufficient to gather an indication on which parameters are the most important to meet the requirements that were found critical.

It can be concluded that by means of preliminary analyses, lift over drag and engine specific fuel consumption seem to be the most important parameters. It thus logically follows that when doing tradeoffs, aerodynamic lift and drag properties of several concepts should be of high importance. Furthermore, design tasks regarding the development of an efficient propulsion system and the development of methods to reduce drag,9 should be given a high priority. However, due to the preliminary analysis of this model, not all parameters were considered, and

2.4. Sustainability analysis

From the functional analysis, it is clear that most critical functions of the aircraft are related to its operating on water. However obvious this may seem, it does have implications on the aircraft's performance in terms of sustainability. Therefore this section will briefly mention the most important aspects for the design case in terms of sustainability.

The most obvious example of the aircraft's environmental impact due to its water operations, is the impact on the aquatic environment. As the aircraft is partially submerged under water and aircraft fuselages are normally made of metal alloys, corrosion may pose a serious threat for performance in terms of sustainability. In contrast, the aircraft operating on water might reduce its environmental footprint by reducing emissions through shorter travel times, as discussed in Section 1.5.

Additionally, the development of a water business jet opens up new possibilities for flexible modes of transportation. It could lead to a large scale distributed transport network in contrast to the current hubs-and-spokes network. Such a system can prove to be more effective by ensuring a higher degree of aircraft capacity utilisation and reducing the total distance travelled of all aircraft. As an overall result less fuel would be consumed which increases the industry's sustainability as a whole.

Finally, more conventional measures of sustainability will be researched, such as community noise impact and NOx and CO_2 emissions during nominal usage. All elements mentioned above will be discussed in more detail in Chapter 8.

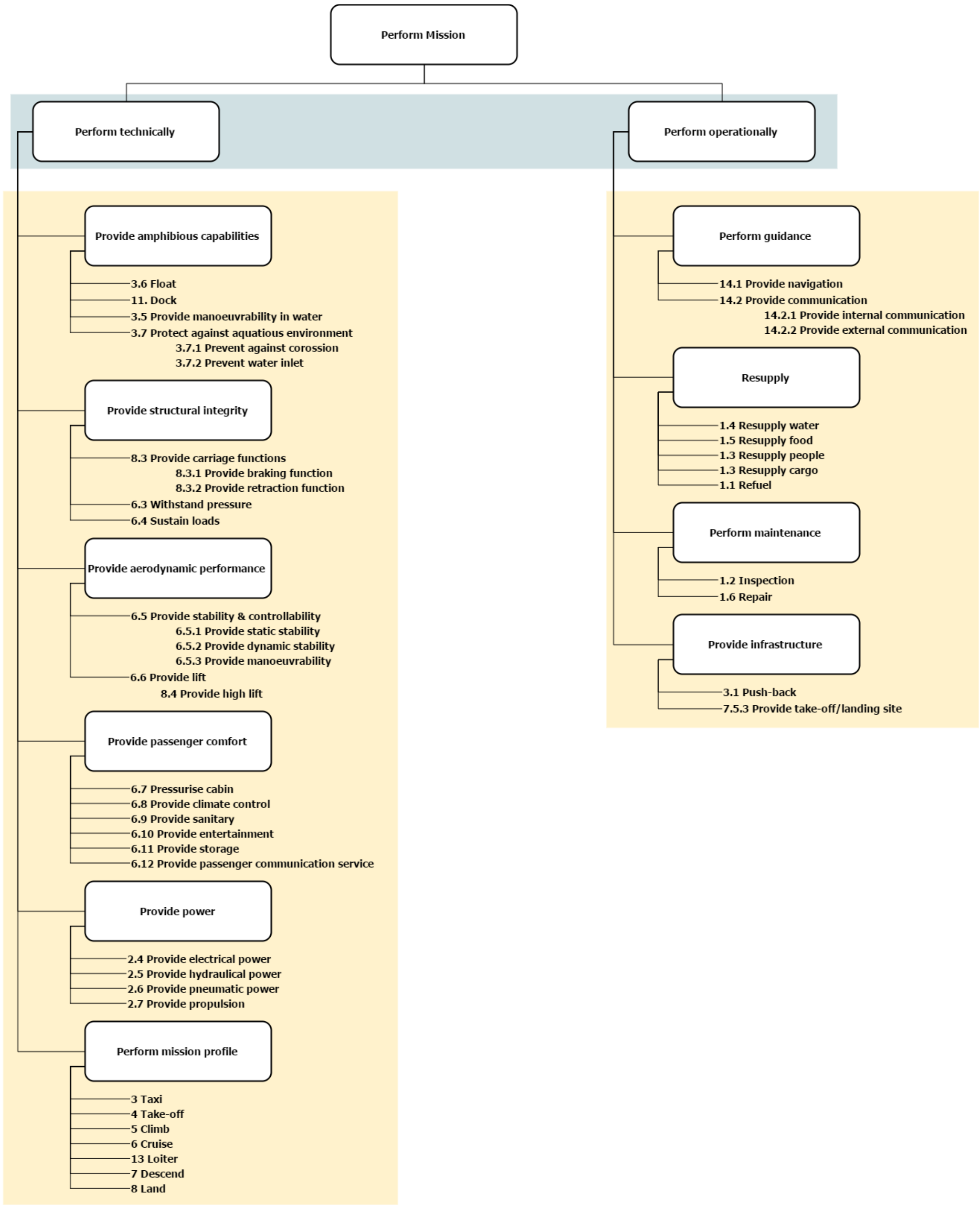

Figure 2.3: Functional breakdown structure of the aircraft.

3

Project organisation

In order to give the reader insight in the design flow, this chapter will elaborate more on the organisational approach of the group in terms of two specific fields. These fields are organisation, elaborated upon in Section 3.1, and procedures, which is discussed in Section 3.2. With this information, the design process and its different phases are finally discussed in Section 3.3.

3.1. Organisational approach

In organising itself, the group adhered to a philosophy of rather taking a step back than doing work that becomes obsolete. In order to achieve this, more time has to be put into planning and organisation. As a result, however, technical work may be done more effectively, rendering the overall group performance better.

Exemplary hereof is the flexible planning the group adhered to. Up to and including the conceptual design phase, the group performed weekly updates on the Gantt chart and work flow diagrams, such that a sufficient level of detail was obtained to work effectively. This way, it was prevented a planning for four weeks had been made, which ultimately would not have been adhered to. From the detailed design phase onwards, the group adhered to a system of setting weekly design goals and planning accordingly, as will be discussed in more detail in Section 3.3.

In the same way, design roles were assigned flexibly and updated weekly. Although in the beginning of the project several engineering departments and functions were formed, it was found that using these departments work effectiveness was compromised on. Instead, resources were allocated based on the design goals set for that week, their importance, and their subject matter difficulty.

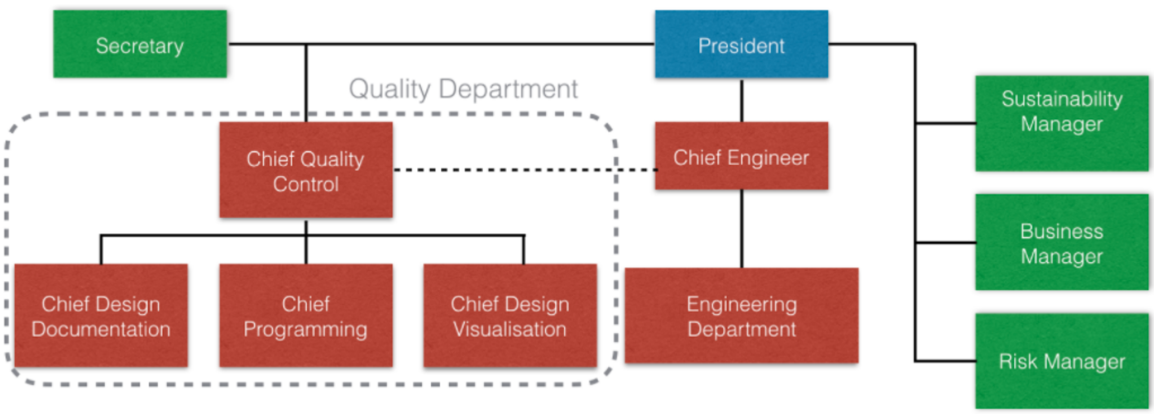

Figure 3.1: The organisational hierarchy and task divisions. Red and green blocks indicate tasks requiring and not requiring managing of other people, respectively. The blue block indicates carrying final responsibility over the team.

In contrast, the organisational roles that were divided amongst group members remained fixed throughout the project. Namely, contrary to the engineering tasks, the organisational tasks are performed most effectively when they are mastered by one person. As a result, this person can develop procedures and personal insight into what works most efficiently for the group. For example, the Chief Design Visualisation developed procedures such that all part designs were compatible and he was able to enforce these procedures throughout the project. A total overview of the group members' organisational roles and the organisational hierarchy can be seen in Figure 3.1.

For more insight into this working philosophy being brought into practice, the reader is referred to the midterm report [36]. This report contains more detailed examples of the updating of Gantt charts, work flow diagrams, and the flexible planning and engineering task division.

3.2. Procedures

In order to attain smooth integration of the different subsystems and design efforts, it is required the group works uniformly and consistently. Therefore, procedures were set up, which will be elaborated upon shortly in this section.

3.2.1. General procedures

As mentioned before, part of the team effectiveness was ensured through solid conventions and procedures. These clear guidelines on technical and management aspects of the project removed ambiguity on for example LaTeX use. For specifics on these conventions and procedures, the reader is referred to the project plan [37].

As a result, a high level of uniformity is obtained for the technical work, the reporting, and visualisation. Additionally, having clear conventions on programming ensured a smooth integration of different working environments, also allowing for retrieving the right current engineering values at any point in time. As a result, the potential organisational difficulty of concurrent engineering was mitigated properly.

In the same way, group meetings were found to be an effective means of ensuring good working relations. Having weekly meetings on not only the group progress and functioning, but also on the performance of peers ensured any internal conflicts were prevented.

3.2.2. Verification and validation procedures

Additionally, verification and validation procedures were set up so that, where possible, verification and validation could be executed. Verification consists of two parts. The first of which is code verification, serving to check whether the model works consistently and precise enough, as intended.

Code verification is done in two parts by first verifying units of code, after which the whole system is verified. For example in the cost breakdown program explained in Chapter 5, first it is verified that the engineering man hours block works. Afterwards, converting the engineering man hours into engineering cost is checked. Finally, the integration of the two blocks is verified by a system test. Additionally, programs are tested on whether they give logical outputs to certain inputs. Using the same example, giving a zero airframe weight as input to the cost program should give a zero cost output.

Afterwards, calculation verification is performed in order to check whether the model gives a logical output. This is done by checking whether the results agree within acceptable limits with the results obtained through a different model.

Finally, validation is performed whenever real-life data is available. Generally, these data are then used as inputs in the available model. By checking the model outputs against their known real-life equivalents, it can be seen whether the used model agrees with reality. As little design specifications are normally disclosed by aircraft companies, procedures were also developed for the case when no real-life data are available. When this is the case, it is attempted to present a method through which these data can be obtained.

3.3. Flow of activities and major design phases

Insight in the process is needed to supply confidence in the design choices made, which serves as background to the technical work done. This section presents the project flow of the Design Synthesis Exercise of group 07. Its aim is to inform the reader on the road taken towards the final design. Figure 3.2 provides a visual representation of the flow of activites and major design phases.

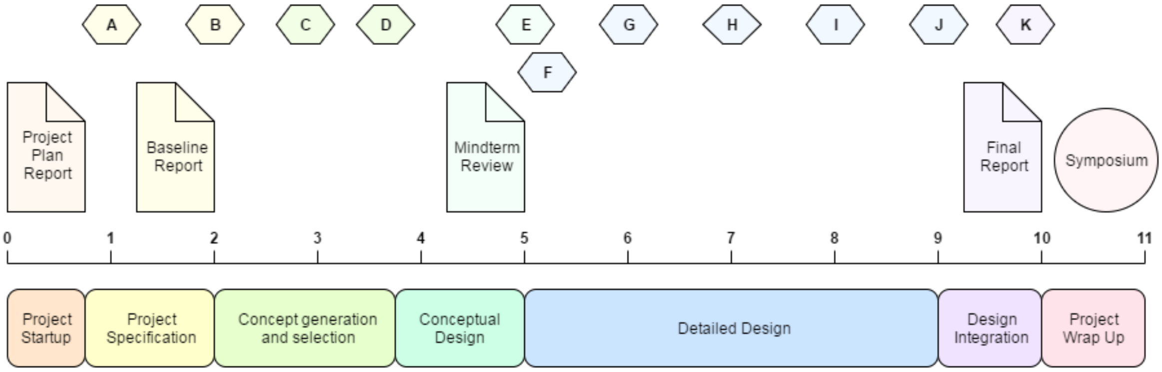

Figure 3.2: Timeline of the project flow including (from bottom to top) project phases, week numbers, deliverables and milestones.

The following milestones are indicated in Figure 3.2:

A. Initial requirements have been set up
B. Design options have been generated
C. All concepts have been generated
D. A concept is selected
E. The conceptual design is finished
F. Configuration had to be changed from canard to T-tail due to risk analysis based on the conceptual design
G. Iteration 1 has been performed
H. Iteration 2 has been performed
I. Iteration 3 has been performed
J. Iteration 4 has been performed
K. The design is integrated to check the final feasibility

Many of these major milestones have been planned beforehand, especially during the project startup phase. A few milestones were not planned and can only be considered as milestones in hindsight. Milestone E. is good example of this. Obviously, a change in configuration was not planned, but the technical risk analysis at the end of the conceptual design pointed out that the canard configuration had to many limitations. The centre of gravity range required for a beneficial trim angle was hard to match to the centre of gravity range required for in flight stability. It was therefore decided that changing to a T-tail configuration would benefit the design the most, and therefore this design change was implemented.

Each design phase will be shortly discussed, explaining its methods and goals for the project. The **project startup phase** was mainly focused on getting organised. Most of the content from Section 3.1 and Section 3.2 was created in this phase. The project plan report [37] was the deliverable concluding this phase and gives an elaborate overview of the original planning and organisation. The **project specification phase** had as goal to provide a clear overview of the design problem. It consisted of determining the functions and requirements of the system, based on an elaborate design case analysis. The baseline report [35] documents this and served as a basis for further design.

During the **concept generation and selection phase** four top level concepts were generated from which one was selected. The four concepts were combinations from the many design options generated, with the infeasible options and combinations eliminated. An extensive tradeoff was performed based on the following criteria: hydrodynamic performance, aerodynamic performance, structural performance, development risk, passenger comfort, spinoff possibilities, cost and sustainability. From the tradeoff table as presented in Appendix J it can be seen that the canard configuration with side floats was considered the best option to proceed with. This concept was further designed during the **conceptual design phase**. Here the groundwork was laid for further design iterations. The midterm report [36] extensively describes the concept generation and selection phase and conceptual design phase.

At the start of the **detailed design phase** it was decided to change the organisation to a more team based structure, were the teams consist of two or three people and focus on smaller design goals. Every week will consist of a new iteration with new design goals. These design goals were set, based on a weekly technical risk assessment and the general progress. Basically every iteration should address the aspects most critical to the feasibility of the project. Figure 3.3 provides a schematic visualisation of the work flow for each iteration.

The technical risk assessment at the beginning of this phase indicated that the canard configuration imposed too high of a risk on the project. The high trim angle, caused by the aft location of the centre of gravity, combined with stability limitations associated with this configuration made this design too risky to continue with. The higher efficiency and good performance of the canard configuration do not compensate for this higher risk, and it was therefore decided to change concept. It was chosen to pivot by advancing the design process with the T-tail configuration with side floats. Although the cruise performance is slightly inferior to the canard configuration, the T-tail configuration has better stability characteristics and more favourable centre of gravity location.

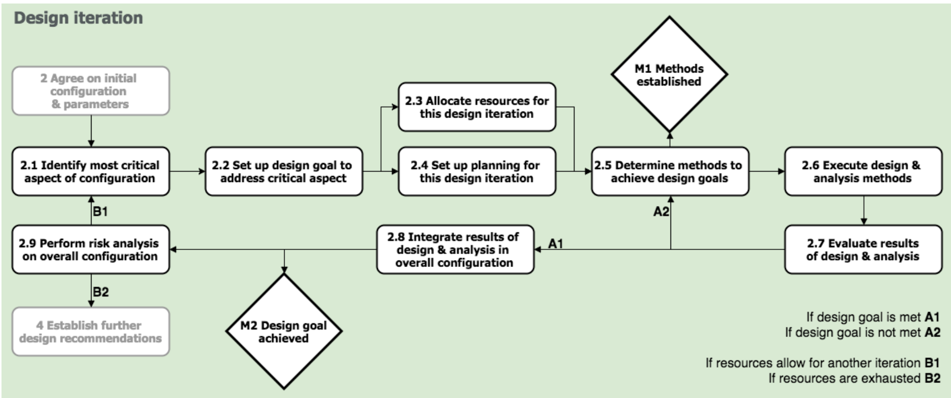

Figure 3.3: Work flow diagram for every iteration.

After these four iterations, effort was put in integrating the design in the **design integration phase**. This report, the final report, shows the final result of many weeks of designing and concludes on the feasibility of a water business jet. All design choices and specifications can be found in Part II and Part III.

II

General design

The water business jet and the operation of it are feasible to a certain extent. The design that comes with this feasibility must be shown in order to prove and understand that. Also, the design described here is critical for the understanding of the next part. Part III describes the aircraft design in further detail, as all subsystems are treated there. This part comprises of the results of different elements of the feasibility study, including aircraft characteristics, costs, operations, quality assessment, sustainability and is concluded with a manufacturing plan. Chapter 4 presents the general design of the aircraft together with a performance analysis. In Chapter 5 an overview is given of the actual costs of the aircraft and is shown that the aircraft is economically feasible. How operating the aircraft would work, is described in Chapter 6. Special attention in that chapter is paid to operations on and from water, which is the novelty of this aircraft. With the reliability, availability, maintainability and safety analysis from Chapter 7, the quality of the design is assessed. Chapter 8 discusses the impact on the environment of the water business jet, including the effect on the aquatic ecosystems. Finally, Chapter 9 shows what the manufacturing and assembly of the aircraft would look like.

4

Configuration and performance

The design for the water business jet that is analysed into further depth is a two-engine T-tail aircraft with a hull-shaped fuselage. The importance of this chapter is evident, as it gives the framework for all of the coming chapters in which the design is further explained by discussing the general performance characteristics of the Jaeger. In the following sections of this chapter, first a description of the general layout of this design is given together with the most important dimensions. After that, several subsystems are presented. The interrelations between the subsystems are discussed in Subsection 4.1.2. Characteristics of the performance of the aircraft can be found in Section 4.2.

4.1. Design configuration

The general layout of the designed aircraft is a two-engine T-tail aircraft with a hull-shaped fuselage as stated in the above. Another feature worth mentioning is that the side floats are retractable during flight and land operations. What this design looks like can be seen in Figure 1, which shows the general layout. The side, front and top views with important dimensions can be found in Figure 4.1. In these figures, the landing gear, water jet propulsion system and the retractable side floats are extended. Normally this does not happen concurrently, but here it is presented this way to make the visualisation as complete as possible. More dimensions and weights are found in Table 4.3 and Table 4.4 respectively. How the subsystems are defined and how they interrelate, can be read in Subsection 4.1.1. The interrelations given there are important to keep in mind when designing or trying to understand the design, because it can change the design of a system in a way that may not seem obvious.

Table 4.1: Jaeger fact and performance sheet (1).

Dimensions		
Length	27.3	m
Height	7.10	m
Diameter	2.70	m
Span	30.0	m
Cabin length	12.84	m

Weights		
Maximum takeoff weight	31,750	kg
Operational empty weight	16,941	kg
Max fuel weight	12,913	kg
Maximum landing weight	31,750	kg
Max payload weight	10,000	kg

Propulsion		
		Engines
Manufacturer	Safran	
Type	Silvercrest 2C	
Takeoff thrust	12,000	lbf
		Water jet
Power	37.0	kW
Taxi speed	6	m/s

Table 4.2: Jaeger fact and performance sheet (2).

Performance

Takeoff & Landing			Cruise		
	Water		Approach speed	45	m/s
BFL @ MTOW	2610	m	Maximum operating altitude	12497	m
TOFL	1980	m	Cruise speed	0.85	M
	Land		Maximum operating speed	0.9	M
BFL @ MTOW	1932	m	Maximum range - no payload	6700	NM
TOFL (sea level)	1618	m	Range - 0.85M, 16 VIP + carry-on luggage (2000 kg)	6000	NM
			Range - 0.85M, 4000 kg PL	4500	NM

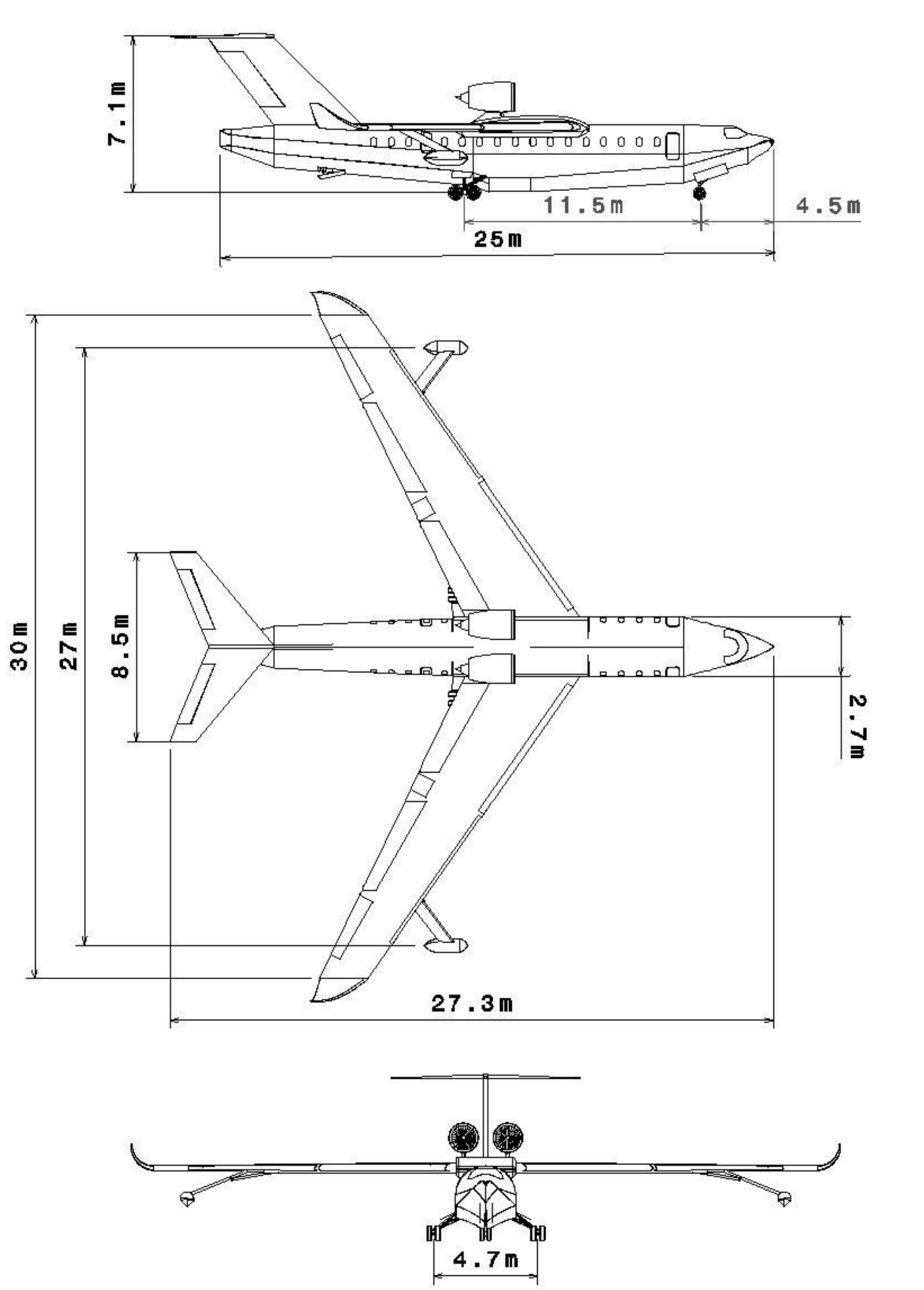

Figure 4.1: Side, top and front view of the aircraft.

Table 4.3: Dimensions of the aircraft.

Parameter	Value	Unit
Overall length	27.3	m
Overall height	7.10	m
Fuselage length	25.0	m
Fuselage diameter	2.70	m
Maximum fuselage height	3.07	m
Wing span	30.0	m
Wing surface area	115	m^2
Wing sweep angle	35.0	°
Root chord	6.39	m
Taper ratio	0.20	
Wing thickness	0.12	% chord
Horizontal tail span	8.50	m
Horizontal tail area	11.8	m^2
Horizontal tail sweep angle	40.0	°
Horizontal tail aspect ratio	0.40	
Vertical tail surface	14.0	m^2
Size main door	122 × 61.0	cm
Location main door	4.30	m from nose
Size aft door	91.4 × 50.8	cm
Location aft door	15.4	m from nose
Location water jet	19.9	m from nose
Span of extended side floats	27.0	m

Table 4.4 and Figure 4.2 show the mass budget of the aircraft. In Table 4.4, the sensitivity of each mass group is added to know which masses are likely to change. Mass groups with low sensitivity are indicated by green and with a high sensitivity by red. As can be seen in the table, six mass groups are sensitive. Their reason of sensitivity is also included in Table 4.4. The mass groups with a low sensitivity have a low sensitivity, since the dimensions that influence these mass groups are unlikely to change significantly. However, the mass of several components has changed significantly between the midterm and final values. This change can be explained by the fact that the values presented in the midterm report were based on preliminary values, which currently have been replaced by values based on more elaborate en accurate calculations. The source of the masses can be found in the last column.

4.1.1. System description

In the system description all the systems and subsystems for an entire aircraft operation are defined. This includes both the subsystems mounted on the aircraft, as well as those required for the operation of the aircraft. Outside the system boundary, elements are defined that are not part of the system, but do influence it. While designing the relevant subsystems the full system description is kept in mind in light of integration. These subsystems are not totally stand-alone, which means they do interrelate. These relations are discussed in Subsection 4.1.2.

Figure 4.3 is a visual representation of the system description. Within the system boundary, a distinction is made between the aircraft element and the operational element. The aircraft element comprises of basically all the hardware of the aircraft, whereas the operational element consists of actions that need to be done to make the aircraft fly. Outside the system boundary, the stakeholders are the most influential parties on the design of the aircraft. They drive the design while not being part of it. Other design drivers, that drive the design to a lesser extent than the stakeholders are put in the category ’other.’

When looking at the aircraft element in more depth, one can see that the element is subdivided into several sub elements. The reason for subdividing into these groups is that the subsystems in the groups have to be designed individually, while they are part of the same expertise within the design of aircraft. The airframe element consists of all structural items such as the wing, empennage and the fuselage with its hydrodynamic hull. This hull is an important item as it makes water operations possible, and it potentially may have a significant contribution to aerodynamic drag. The propulsion group has the standard items as engines, fuel

Table 4.4: Mass budget, including sensitivity. Red is sensitive and green is not sensitive.

Group mass	Midterm [kg]	Final [kg]	[%OEW]	[%MTOW]	Sensitivity	Source
MTOW	31750	31750		100	Wing and fuselage masses uncertainty	II
OEW	16941	16941		53.4	Wing and fuselage masses uncertainty	II
Max fuel	12913	12913		40.7	Uncertain MTOW/OEW	IV
PL@maxfuel	1896	1896		6	Depends on max fuel	III
Max PL	15000	10000	-	31.5	Market analysis	V
Wing	3660	3147	18.6		Side float weight and wing reinforcement not included	I
Fuselage	4180	4173	24.6		Uncertain hull weight	I
Horizontal tail	265	117	0.7			I
Vertical tail	695	312	1.8			I
Main landing gear	1780	1258	7.4			I
Nose wheel	350	219	1.3			I
Waterjet		43	0.3			II
Engines		2078	12.3		The amount of thrust is unlikely to change	II
Other		5594	33.0			III

I = Raymer II = Fuel fraction and reference aircraft
III = Available weight left IV = Fuel tank volume V = Market analysis

storage and fuel supply systems, but also a water jet propulsion mechanism that is meant to be able to taxi on the water without having the noise from the main engines. The group mechanisms exists for several big systems that are too important to place into another group or have more features than described in another group. For example the side floats are connected to the wing and are part of the structure. However, it was chosen to place it in the mechanisms group because of the retraction mechanism it has. It is movable which requires some extra design effort. Finally, all other subsystems of the aircraft are put into interior, avionics or support.

In the operation element a category ground support can be found that comprises the loading and unloading of the passengers and if applicable, the cargo and the refuelling of the aircraft. This loading and unloading requires special attention in this design, as it must also be possible to operate on water. The other operations that are part of the aircraft element are maintenance, flight operations, development, manufacturing and infrastructure. This infrastructure includes the airfields, water, communications and navigation used by the aircraft. These items are also included in the elements outside the system boundary, and there is a direct link to the operation of the aircraft.

The stakeholders are not part of the system, but influence the design to a notable extend. The most important one is the customer, whose demand is the whole reason for developing this aircraft. Another stakeholders is the air traffic control. The regulations introduce important requirements on the fields of environment, safety and seaplane operations. Also included in the stakeholders group are maritime traffic and the harbour. These are important when landing or taking off the aircraft from a location where no other infrastructure such as an airport or seaplane base is available.

Finally, identified as items that must be kept in mind during the design, the ’other’ group consists out of the following. First, the airports, seaplane bases and other potential landing locations. The aircraft must be designed to be able to operate from all these locations and must be allowed to do so. The weather influences the Jaeger more than other aircraft, as the wave height determines whether a landing on water can be performed or not. Moreover, information about current wave heights is less easily available. The environment is also assumed to be a design driver. During the design, sustainability, noise and the foreseen effect on the aquatic environment are also taken into account.

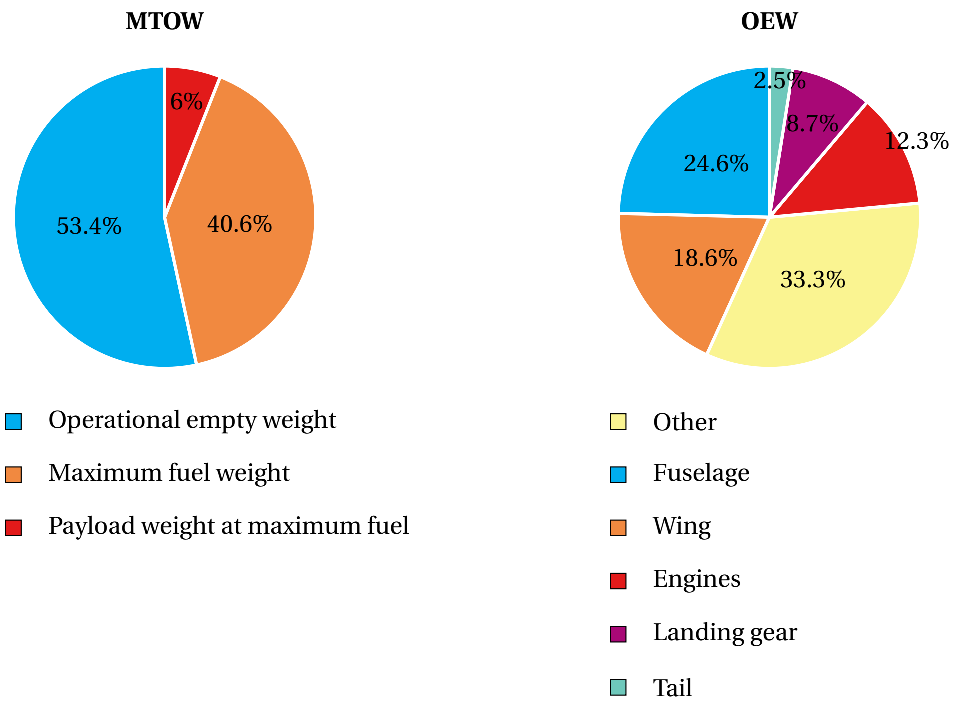

Figure 4.2: Mass budget.

4.1.2. System interactions

The separate subsystems described in Subsection 4.1.1 must be integrated to operate the entire system. These subsystems depend on each other and influence the design of other subsystems. Also, the subsystems are (partly) designed simultaneously and therefore it is important to understand the interrelations between the systems. To make sure all the elements fit upon integration of the subsystems, all designers must be up to date about the design of the other systems that influence their system. To increase the efficiency of this communication and to promote the thorough understanding of the interrelations, an N2-chart is created that can be found in Appendix H. This chart shows the inputs and outputs of the subsystems and also the possible design loops that must be dealt with correctly.

4.2. Performance characteristics

In order to accurately evaluate the feasibility of the design, its performance characteristics shall be evaluated. First, the mission profile in terms of payload/range and optimum cruise altitude is discussed in Subsection 4.2.1. Then takeoff and landing performance is discussed for both water and land operations in Subsection 4.2.2. For all the applied analyses, verification was performed according to the conventions as described in Section 3.2. Validation was performed based on an exhaustive data set of the Gulfstream V. [1 2]

4.2.1. Payload versus range

When assessing the feasibility of any aircraft, it is desirable to know possible combinations of payload, range and speed. Figure 4.4 shows the relation between payload and range for Mach 0.8, Mach 0.85 and Mach 0.9 including both all fuel reserves required by regulations, including the required fuel reserves per regulations for diversion to an airport 200 NM off course. Note-worthy is that when flying at Mach 0.85 with 16 persons capacity with only carry-on luggage, a range of 6000 NM could be achieved. Furthermore, it is seen that a payload above 10 000 kg will result in almost no range. Therefore, the requirement for a cargo payload of 15 000 kg cannot be satisfied, having 10 000 kg as the highest possible payload instead.

[1] `http://www.lissys.demon.co.uk/samp2/` Retrieved on 25/06/’17
[2] `http://www.airliners.net/aircraft-data/gulfstream-aerospace-g-v-gulfstream-v/239`. Retrieved on 25/06/’17

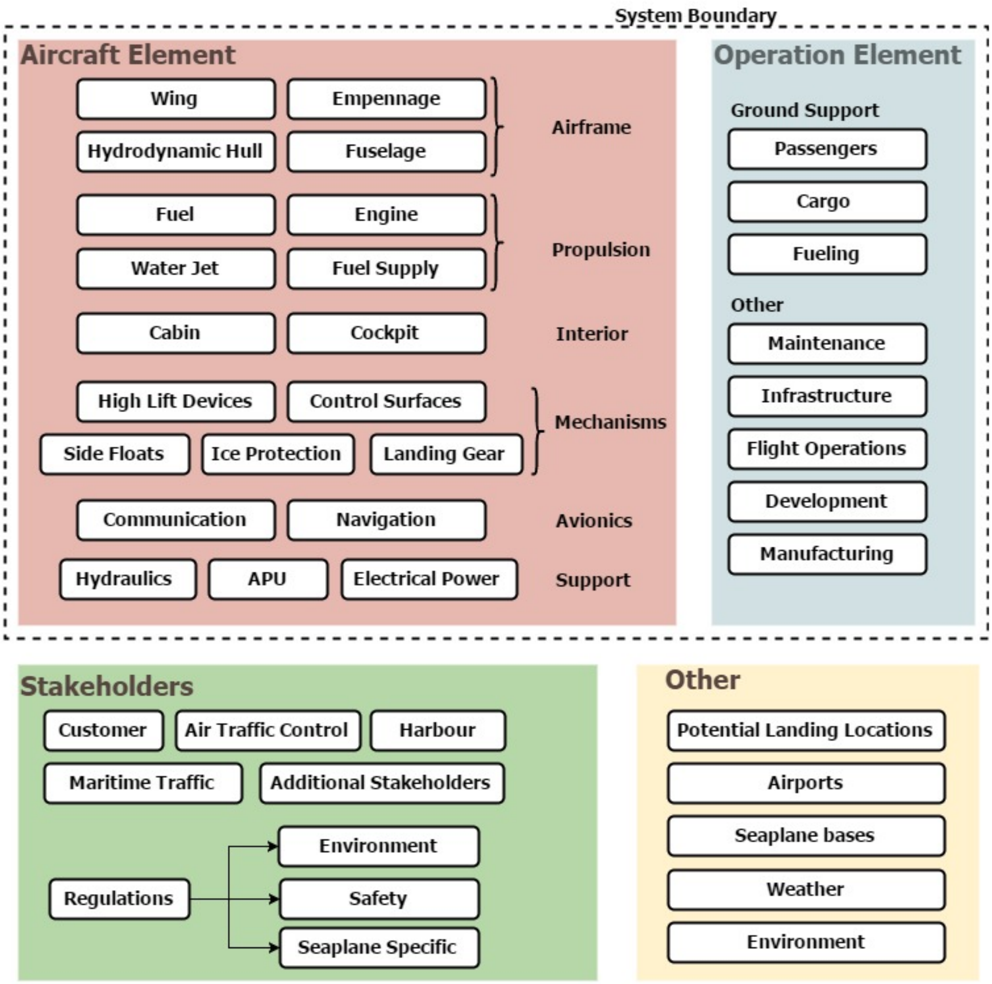

Figure 4.3: System description.

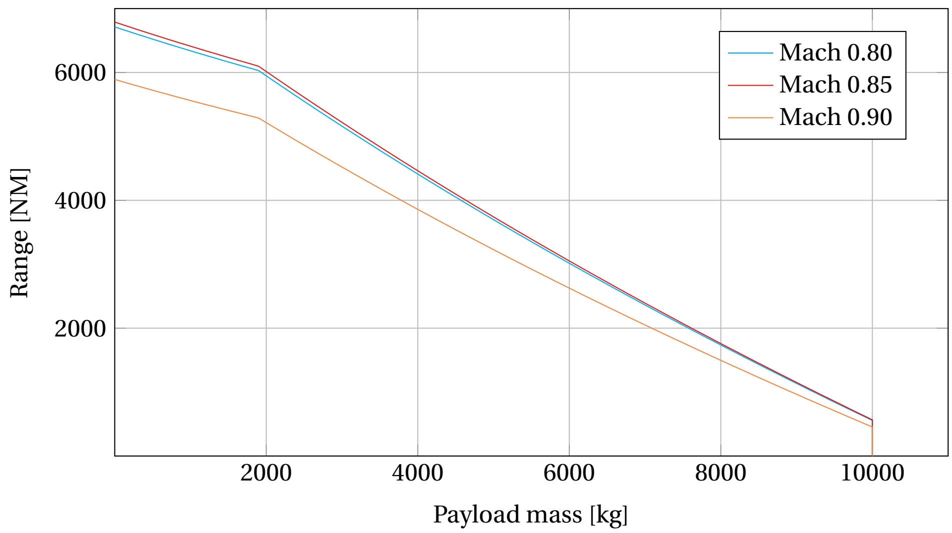

Figure 4.4: Payload-range diagram.

However, the model is not fully accurate. Firstly, it should be noted that this method ignores weather conditions, assumes that L/D does not change with weight, and that the drag polar $\frac{C_L^2}{C_D}$ is linear. Furthermore, the method is performed based on preliminary estimates, and therefore its result is in itself nothing more than a preliminary estimate. Lastly, partial loss of lift due to shock waves is an effect that may occur, but was neglected in this analysis.

In order to increase the reliability of this model, code verification was performed according to procedures described in Section 3.2. In order to assess the impact of the assumptions laying at the foundation of this model, preliminary validation was performed using the data of the Gulfstream V. A large difference is that for this Gulfstream, the maximum payload is constant up to a range of approximately 5000 NM, while the Jaeger's payload range diagram starts declining from a range of 1000 NM onwards. This effect however, is because the Gulfstream V is constrained to a maximum payload of 3000 kg, while the Jaeger is constrained to a maximum payload of 10 000 kg. Considering this, the payload range diagram considered in this section would also show a constant maximum payload until approximately 5000 NM, when the Gulfstream's payload constraint would have been adhered to. Using the Gulfstream's data, it was found that the payload range diagram was accurate, being too conservative in a boundary between 2 % and 10 %. This indicates that the model that was applied, is at least moderately accurate. In order to improve the accuracy of the Jaeger's payload range estimation, it is recommended to perform a more accurate drag analysis.

A sensitivity analysis was performed to see how the relation between payload and range would change if some of these preliminary parameters would change. Noteworthy results are that the range is most sensitive to engine efficiency, with a decrease in engine efficiency of 10 % causing an equal decrease in range. Furthermore, it is seen that the range is (slightly) larger at Mach 0.85 than at Mach 0.8. This is for the fact that the relative reduction in L/D is fully compensated by the increase in speed. One could doubt whether an increase in speed increases range is still sensible, especially in this Mach range. Verification of the drag analysis, as proposed in Subsection 10.2.1, is the way to answer that question and thus improve the reliability of this analysis as well. The sensitivity analysis showed that a 10 % increase in C_{D_0}, would decrease the range with 5 %. It is thus concluded that although the model shows promising results that are moderately reliable, the assumptions and most importantly the fact that the model is only as reliable as its input parameters, should not be forgotten.

4.2.2. General takeoff and landing performance

The market analysis has showed that a balanced field length (BFL) of 2000 m is required for land operations. Table 4.5 shows that this is indeed met by the current configuration, except for takeoff at extreme heights and temperatures, where a longer field would be needed. These values already include a 15 percent penalty for wet runway operations. Furthermore, landing distance during sea-level operations was found to be 680 meter. Regarding water operations, a BFL of 3000 m should be achieved. Based on the hydrodynamic drag analysis performed in Subsection 10.1.2, which found the BFL on water to be 2610 m, this requirement is met, as well. The remainder of this section discusses the methodology that lays at the foundation for the determination of these lengths for operations on land. The analysis behind field length on water is treated extensively in Subsection 10.1.2.

Table 4.5: Balance Field Length (BFL) and Takeoff Length (TOFL) on land during wet conditions.

Configuration	TOFL	BFL
(MTOW, 0 ft, 15°)	1618	1932
(MTOW, 5000 ft, 29°)	2002	2390
(MTOW, 5000 ft, 40°)	2180	2603

Method for field length on land

Ultimately it is desired to know the length of the smallest runway from which the Jaeger can operate safely. This runway length is the largest between the Balanced Field Length (BFL), and 115 % of the Takeoff Field Length (TOFL). TOFL is defined as the distance to accelerate and clear a screen of a height of 11 m at speed V_2. However, usually BFL is the larger of the two. Therefore, this analysis will start off by analysing the BFL, to then verify that it is indeed larger than 115 % of TOFL.

Balanced field length (BFL) is of foremost interest, as it is the minimum runway length that should be used for takeoff. Regulations define this length as the sum of acceleration to V_1, switching off the engines, and then after two seconds applying braking until the aircraft has again come to a full stop. This model depends mainly on thrust and drag, both caused by aerodynamics and ground friction, and lift to find the final distance. Because all these values are prone to change due to speed, a time-step model is used to account for this effect.

At every instantaneous moment in time, the acceleration is calculated using equilibrium of forces. Ground drag is a function of speed as well both during takeoff and braking, and was calculated using a fourth-order polynomial by CS25.109 dependant both on tire pressure and velocity. Furthermore, the aerodynamic drag is calculated relying on the lift-drag polar to calculate C_D. This acceleration is continued to the moment where V_{rotate} is achieved, which is defined as 113 percent of the stall speed for any combination of atmosphere conditions and takeoff weight. Applying this method leads to an accurate estimation of the ground run, and can be used both during braking, during rejected takeoff or landing, and acceleration towards takeoff.

Furthermore, both takeoff and landing requirements require the aircraft to pass a screen at a regulated height, respectively at the start, in case of landing, and at the end of the runway, in case of takeoff. This is at speed $V_{approach}$ and V_2 for respectively landing and takeoff. Assuming steady climb and a constant thrust and drag, the lateral distance covered between the point of takeoff and clearing the screen, is given by Equation 4.1.

$$s_{\text{airborne}} = \frac{\frac{1}{2g}V_2^2 - \frac{1}{2g}V_r^2 + h_{scr}}{\sin\gamma_{scr}} \tag{4.1}$$

There are certain drawbacks to this model. The model assumes that full thrust is instantaneously available, which causes a positive bias of the field distance, but contrarily the ground effect is neglected in its input parameters, causing a negative bias because lift and drag are respectively under- and overestimated. Furthermore, the model relies on preliminary estimates of thrust and drag as input parameters, which may be prone to change. A ten percent reduction in either C_L or thrust has the same effect on field length. Contrarily, a 50 % increase in C_{D_0} only leads to a 7 % longer takeoff distance. One can conclude that although the model shows positive result, changes in lift or thrust performance have a large influence on field performance.

In order to further assess the impact of the mentioned assumptions on the model, it is validated by using the Gulfstream V's data set as an input in the used model. Determining V_{rotate} as per CS25 for the Gulfstream V, the model used in this analysis gives for a takeoff at MTOW at sea level, a BFL of 1732 m, while Gulfstream quotes a BFL of 1801 m. Therefore, the model is 4 % too optimistic for this dataset. While it is difficult to trace the specific cause of this bias, inaccurate determination of aerodynamic parameters cannot be the cause, as the model merely gives a relationship between amongst others these aerodynamic parameters and field lengths. What certainly causes an optimistic bias is that it is assumed that full thrust is instantaneously available, just as that the brakes are applied without delay during a rejected takeoff.

Considering all, it can be concluded that this model indicates that all requirements regarding field length are complied to, for most atmospheric conditions. During future design, in order to monitor the development of the field length, one should pay caution to the development of takeoff weight, and both engine and overall lift performance, but not so much to aerodynamic drag, as it was found that the field length is most sensitive to these first three parameters, and not so much to the latter.

4.2.3. Climb performance

This subsection presents the climb performance characteristics for the preliminary design. The used methods with corresponding assumptions and limitations will be discussed first. Then the results and sensitivity analysis will be discussed. This discussion includes the thrust performance as shown in Figure 4.5, rate of climb at different altitudes as shown in Figure 4.6 and climb time as shown in Figure 4.7. Additional information in the form of power performance diagrams and a visual representation of the energy height method can be found in Appendix P.

Methods, assumptions, limitations and validation

One of the most important input parameters for the climb performance model is the engine thrust. Therefore a solid thrust model was set up first. Although engine thrust is dependant on a large number of parameters, it is generally accepted that as a rough first-order approximation, engine thrust can be described as a function of density ρ and true airspeed V [42] [5]. Equation 4.2 shows this relationship, where T_{max} is the maximum thrust, often taken at standard sea level conditions, and N is the thrust setting in a range from 0 to 1.

$$T = NT_{max}\left(\frac{\rho}{\rho_{sl}}\right)^m \left(aV^2 + bV + 1\right) \tag{4.2}$$

$$m = \begin{cases} 0.75 & h < 11.0\,\text{km} \\ 1.0 & h > 11.0\,\text{km} \end{cases} \qquad a = 4.00 \cdot 10^{-6} \quad b = 2.52 \cdot 10^{-3} \tag{4.3}$$

The density exponent m is an empirical coefficient derived from real data [51], and was taken as 0.75 for the troposphere and 1.0 for the tropopause [54]. The coefficients a and b are dependant on the engine type, with the bypass ratio as dominant factor. These can be determined by curve-fitting Equation 4.2 to known data points of the engine thrust performance. Since only the maximum thrust is known for the selected engine for the preliminary design, curve-fitting had to be performed based on data points of a similar engine. The search for an engine with similar characteristics and which had enough data available was challenging. Eventually the Rolls-Royce BR700 was selected, which is the engine used for the competitor aircraft Gulfstream GV/G550 and Global 6000 [25]. The Gulfstream GV has ultimately been used for validation of the entire climb performance model as a whole, which will be presented later on. The curve-fitting approach resulted in values of $4.00 \cdot 10^{-6}$ and $2.52 \cdot 10^{-3}$ for the coefficients a and b respectively.

Figure 4.5 shows the aircraft thrust as calculated via the above mentioned method. One can observe that the variation of thrust with true airspeed is larger at low altitudes and low velocities (or Mach numbers). It is visible that in cruise conditions thrust is relatively constant for a given altitude. This is the reason why often in first-level analysis of aircraft performance in the cruise range, constant thrust is assumed for a given altitude. For the climb performance model however this simplification was not applied. The taken approach seems sensible as a similar trend can be seen in other thrust performance diagrams [3]. However as mentioned before, validation of the entire climb performance model as a whole will be discussed later on.

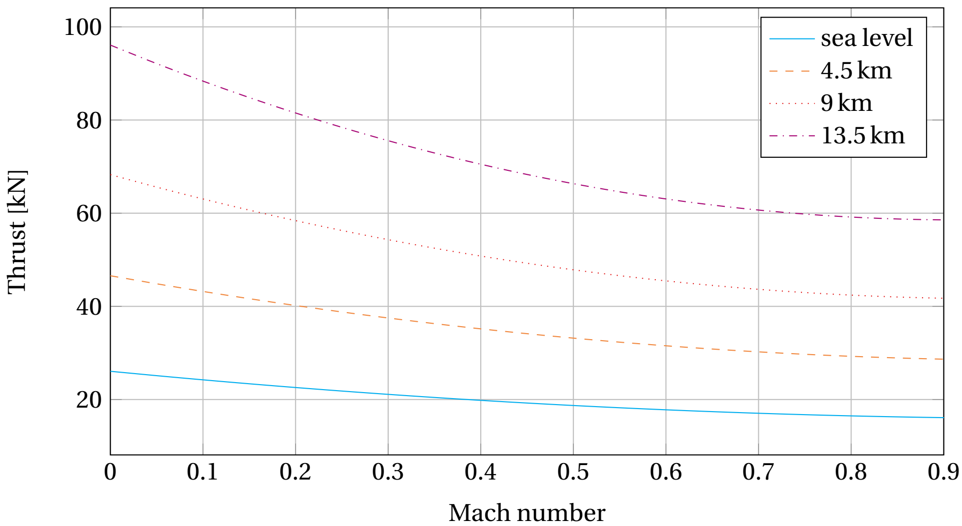

Figure 4.5: Thrust as function of true airspeed at different altitudes (Thrust setting = 90%).

The next step which the model performs is calculating the rate of climb at different velocities and altitudes. This is done based on first-order performance equations [54]. Herein it is assumed that all excess power is used for either climbing or accelerating in terms of true airspeed. Finding the optimum climb path, i.e. the climb path which results in the minimum time to climb, is done based on the energy height method [54]. The power performance diagrams and a visual representation of the energy height method can be found in Appendix P.

In the model, the following major assumptions were made:

- The used value for the zero-lift drag C_{D_0} is the one obtained at cruise conditions, FL410 and Mach 0.85. In reality this value is dependent on velocity and altitude due to compressibility effects, however it was found that a large increase in C_{D_0} occurred just after Mach 0.85 in Subsection 10.2.1. Using this value for C_{D_0} furthermore is a conservative estimation as it is not expected that this high Mach number will be reached during climb phase.
- The weight is assumed to be constant. In reality, aircraft weight decreases during climb as a result of burnt fuel. The weight reduction during climb phase however is generally low, in the order of 2 % [40].

[3] `http://128.173.204.63/courses/Nextor_SC08/Aircraft_perf_notes1.pdf`. Retrieved on 25/06/'17

Table 4.6: Climb performance of the preliminary design compared to competitor aircraft.

	Preliminary design	Gulfstream G550	Falcon 7X	Global 6000
Rate of Climb [ft/min]	4,280 [6]	3,650 [7]	3,000 [7]	3,350 [7]
Ceiling [ft]	47080 [8]	51000 [9]	51000 [9]	51000 [9]
Climb time to FL370 [min]	16 [10]	18 [9]	18 [9]	19 [9]

Also this assumption results in a conservative estimation for climb performance as a higher weight generally results in less favourable climb performance.

- The thrust setting is assumed to be at 90 % of maximum thrust. This high setting is assumed to obtain the best possible climb performance. A higher thrust setting however is viewed as not viable to sustain for a longer period of time.
- For calculating the climb time, it was assumed that the rate of climb is constant within a certain height step of the model. This height step was taken as 10 m, which is considered a high enough resolution on a height range of 16000 m. It therefore is expected that this assumption will not largely influence the results.

The model was validated by substituting data for the Gulfstream GV and comparing the modelled maximum rate of climb with the real life data.[4][5]. A difference of 1.59 % was found, which implies validity of the model. Of course it would be preferable to validate the optimum climb path and time as well, and using multiple validation inputs in the process. However it is challenging to obtain clear reference data. For this first-level performance estimation therefore this validation approach seems reasonable.

Results, sensitivity analysis and discussion

Table 4.6 presents the climb performance of the preliminary design compared to competitor aircraft. The first remarkable observation is that the calculated ceiling for the preliminary design is considerably lower than those of competitor aircraft. In addition the model calculated absolute ceiling, while the reference values concern Certificated Service Ceiling and thus could be even higher theoretically. A first explanation for this result would be a difference in thrust with reference aircraft. This however seems not sensible when noting that the preliminary concept has more thrust than the Falcon 7X (19206 lbf), but less than the Global 6000 (29 500 lbf) and Gulfstream G550 (30 770 lbf) . A more logical explanation would be a difference in the configuration at which the ceiling is calculated. The model finds the absolute ceiling at MTOW, but it is unclear in what configuration reference aircraft certify the service ceiling.

Furthermore it can be seen that the climb time is somewhat lower than competitor aircraft. An important side note must be mentioned. The model assumes unrestricted climb for calculating the climb time. However speed limits for aircraft often exist up until a certain height, as instructed by air traffic control. It is not clear whether this was taken into account in establishment of the reference data. But it is plausible since it resembles actual operational more closely than the case of unrestricted climb. This could explain the difference between the modelled and reference values.

The difference in climb time could be the direct result of a difference in rate of climb as well. The calculated value for the preliminary design is significantly higher than those of competitor aircraft. Such a large difference is most probably the result of how the rate of climb is defined or measured. The model takes the rate of climb as maximum, instantaneous rate of climb. For the references it is plausible that the rate of climb is measured as a time averaged rate of climb for a certain phase of climb, to obtain a more suitable value for operational comparison.

Figure 4.6 shows the steady rate of climb as function of true Mach number at different altitudes. It is clearly visible that the optimum climb path follows the maximum values of the steady rate of climb curves. A kink in this optimum climb path can be seen, at the transition from troposphere to tropopause. The decrease in thrust occurs more quickly in the troposphere according to Equation 4.2 and Equation 4.3. This results in a quicker decrease in steady rate of climb from this point as well.

[4] `http://www.lissys.demon.co.uk/samp2/` Retrieved on 25/06/’17

[5] `http://www.airliners.net/aircraft-data/gulfstream-aerospace-g-v-gulfstream-v/239`. Retrieved on 25/06/’17

Figure 4.6: Steady rate of climb as function of true Mach number at different altitudes.

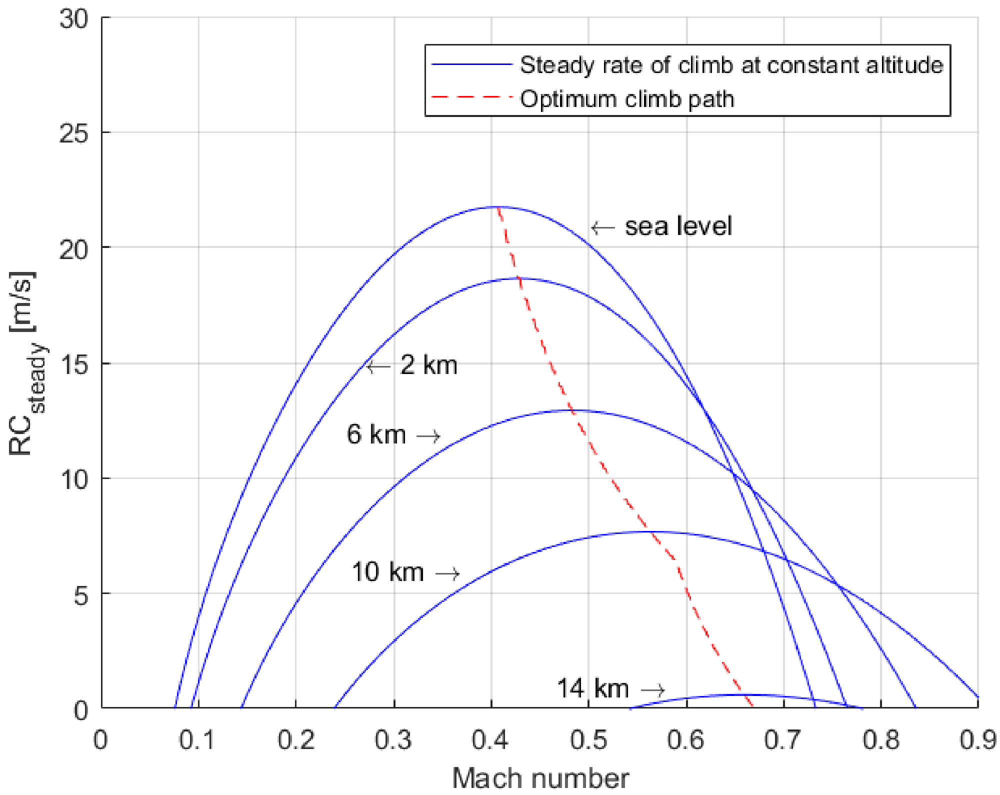

Table 4.7 presents the results of the sensitivity analysis, whereas Figure 4.7 shows the climb profile as a function of time including sensitivity analysis. This analysis was done with respect to the three input parameters on which certain assumptions were made when establishing the model, namely C_{D_0}, weight and thrust. It can be seen that the thrust and weight have the largest influence on the climb performance parameters. This supports the finding that it is critical to be certain on the configuration selected in determining climb performance parameters. In addition it shows the importance of having a detailed mass estimation, which is unlikely to vary more than 10 %.

A variation in thrust would be the result of either a changed engine selection or an adjustment of the thrust model. A change in engine selection however is not likely to occur after this design phase. In addition the thrust model has been validated and is not expected to be subject to major adjustments during refinement efforts.

The model does not show a large sensitivity with respect to zero-lift drag. In Subsection 10.2.1 however it is argued that the zero-lift drag is subject to a high degree of uncertainty, and has the risk of increasing to a large extent. A large increase of C_{D_0}, say 20-30 %, would lead to a considerable decrease in climb performance. Therefore it is desirable to obtain an estimation of C_{D_0} with a higher certainty.

[6] Maximum rate of climb at MTOW

[7] `https://www.paramountbusinessjets.com/aircraft/`. Retrieved at 26/06/'17.

[8] Absolute ceiling at MTOW

[9] `http://jetav.com/`. Ceiling is Certificated Service Ceiling. Retrieved at 26/06/'17.

[10] Unrestricted climb

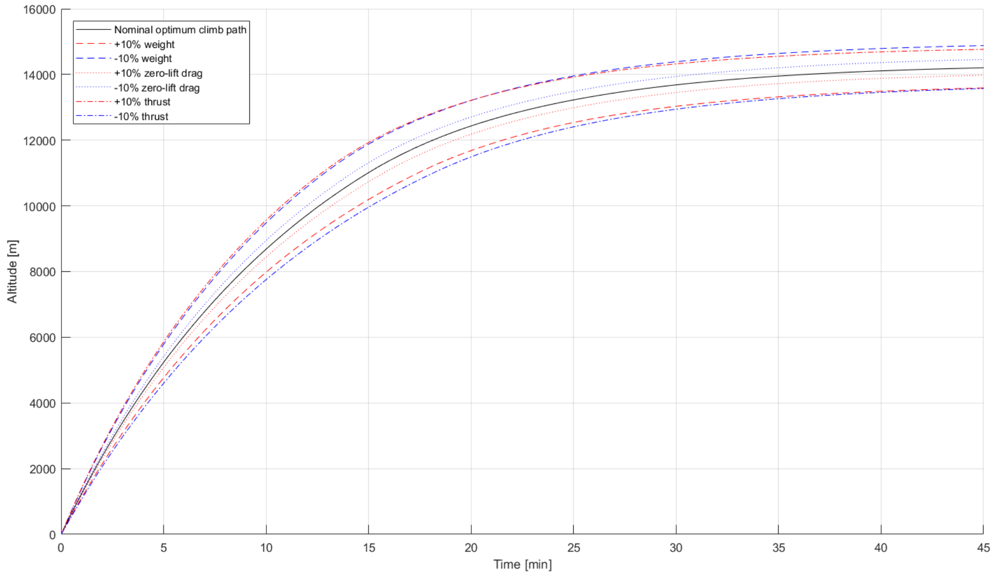

Figure 4.7: Climb time performance including sensitivity analysis.

Table 4.7: Sensitivity analysis of the climb performance.

	Nominal value	Weight		Zero-lift drag		Thrust	
		-10%	+10%	-10%	+10%	-10%	+10%
Maximum Rate of Climb [m/s]	21.7	+12.4	-10.3	+3.97	-3.53	-14.2	+14.6
Theoretical ceiling [m]	14350	+4.67	-4.18	+1.81	-1.60	-4.04	+3.76
Climb time to FL410 [min]	20.3	-16.6	+21.3	-6.4	+6.4	+26.2	-17.2

Conclusion and recommendations

The used climb performance model uses aircraft geometry, flight altitude, true airspeed, thrust and zero-lift drag as most important input parameters. The made assumptions were shown to be reasonable for the first-level estimation of climb performance parameters, as the model was validated with data of the Gulfstream GV. In general the results for the climb performance parameters seem sensible. Notable differences with competitor aircraft are present. These differences however are most probably the result of a difference in configuration when establishing the values. Therefore it is considered unwise to use the currently established data for making a business case. Sensitivity analysis showed that it is important to have a high certainty on values for weight and zero-lift drag.

It is recommended to further research how competitor business jet manufacturers establish performance data. These findings then could be used to calculate values for climb performance data which are more comparable to reference aircraft. Refining the used thrust and climb performance models is advised after a more detailed estimation on weight and zero-lift drag have been done.

5
Cost breakdown

Aircraft cost estimation is notoriously difficult, especially in the early stages of aircraft design, because a lot of design parameters are still uncertain or undetermined. In order to assess the feasibility of a concept, however, cost is one of the - if not the - most important parameters for the marketability of the concept. As a result, research has been conducted on developing cost estimating relationships (CERs), for example by Eastlake [9]. Eastlake adapted a military aircraft CER for predicting general aviation (GA) aircraft cost based on few design parameters. This model has later been adapted for executive aircraft by Gudmundsson [18], such that this model will be used.

This chapter first elaborates on the assumptions and limitations of the model. Then, the results of the cost estimation will be given in Section 5.2. Afterwards, a verification and validation procedure and a sensitivity analysis will be performed in Section 5.3.

5.1. Assumptions and limitations

It should again be stressed that due to the early design stage of the project, the cost estimation is only that, an estimation. Therefore, the underlying assumptions used in the model should be elaborated upon and its limitations should be clarified. The model used is an adaptation of the development and procurement cost of aircraft (DAPCA) IV method, fitted to business aircraft and may be found in reference [18]. The original DAPCA IV method is a method developed for estimating military aircraft costs; it was based on data of practically all US military aircraft in service at that time [18]. As a consequence, this model tends to overpredict civil aircraft cost. In an attempt to better reflect GA aircraft, Eastlake adapted DAPCA IV in such a way that as a means of validation it correctly estimated the sales price of a Cessna 172 [9].

For the timewise estimation of the production process, which is an input to the model, the development and manufacturing times are estimated. Looking at reference aircraft, a development time of approximately five years is commonly found [24]. This development time will therefore be used in further analyses. In this phase, production and certification of aircraft parts already commences, but are considered part of the development phase. Consequenlty, aircraft assembly begins in 2022.

Moreover, the number of aircraft that is expected to be produced in the first five years after development needs to be estimated. This number is needed in order to assess not only the aircraft cost, but also the production time. It is found that reference aircraft often have more than 200 aircraft built in this time span of five years [24]. However, to remain somewhat conservative in estimating, the number of aircraft produced in the first five years will be set to 100 to account for possible disappointing sales numbers, a number comparable to, but lower than that of the Falcon 7X [24]. Again, it is assumed that first all development cost, and from the start of production, all procurement cost are made uniformly over time and interest is paid accordingly.

Furthermore, some input parameters of the model have either been estimated or taken from other sources, such as Gudmundsson. For example, the hourly rates of working forces have been taken from Gudmundsson [18]. The monthly interest and inflation rates have been taken from the World Bank database, which are used for calculating loan cost and correcting for cost-push inflation, respectively.[1]

Moreover, because of the novelty of the concept of the aircraft, some contingencies have been taken into account in using the model. Namely, because the research, development and certification of the aircraft will

[1] `http://data.worldbank.org/indicator/FP.CPI.TOTL?locations=US`

be more cumbersome, it is assumed that the aircraft needs six prototypes for development. This is twice the amount of prototypes the Falcon 7X has [24]. What's more, the engineering, development support, and flight test operations costs were multiplied by a factor of 1.2 to account for the more difficult development and certification of this novel concept.

In addition to these contingencies, the model has some small deficiencies that make for a more conservative result. Namely, the model does not account for a learning curve. As a result, the increase in labour effectiveness, and thereby a decrease in manufacturing cost is not accounted for. Additionally, the airframe weight is calculated as the OEW less the engines. However, the airframe weight is usually even lower, because avionics, wiring, and control mechanisms should also be subtracted from this weight. These two deficiencies make the model more conservative. Finally, as a conservative input, no quantity discount factor was applied in for example estimating the engine cost, because no quantification of this discount could be found.

5.2. Results

In Table 5.1, the cost breakdown of the aircraft is given in terms of its development and procurement costs. Again, it is assumed a total of 100 aircraft is produced in the first five years of production. If the production were to disappoint and were 10 % lower, the aircraft unit price would rise to 59.1 million USD.

Table 5.1: Project cost analysis, hourly rates taken from Gudmundsson [18]. As stated in the text, a total of 100 aircraft produced over five years is assumed.

Division	Man hours	Rate [$/h]	Total cost [million $]
Engineering	903,800	92	223
Development support			3413
Flight test operations			218
Tooling	9,753,111	61	1332
Certification cost			5186
Manufacturing labour	15,814,209	53	1876
Quality Control			389
Materials/equipment			806
Engines			567
Avionics			10
Total cost to produce			5762

From the previous breakdown, an aircraft sales price of approximately 57.6 million USD would ensure a cost break-even. This implies that if the aircraft is sold for a price of 60 million USD, a profit of approximately 2.4 million USD is made per aircraft. Figure 5.1 shows the relatively large cost made in manufacturing the aircraft. Therefore, the importance of a setting up a proper production line is evident. A set-up for this will be given in Chapter 9.

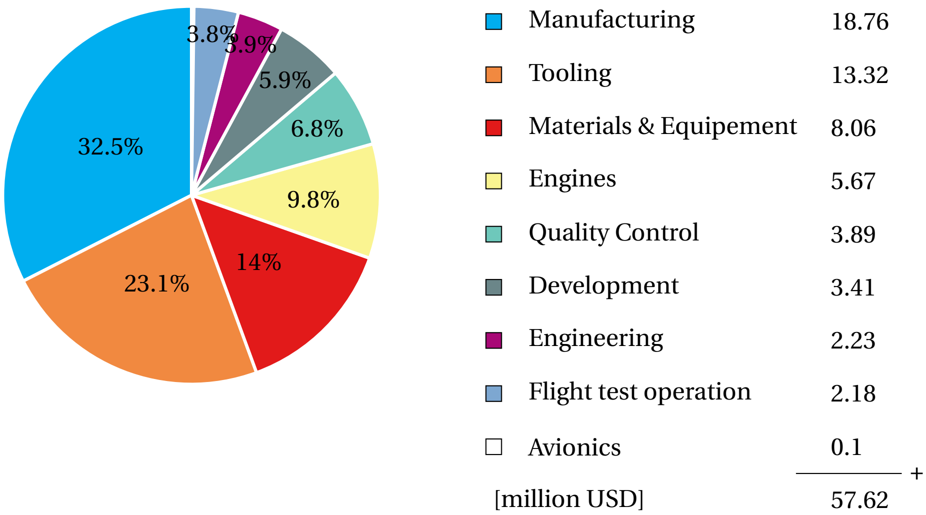

Figure 5.1: The different cost components of a single aircraft, assuming a 100 aircraft production run.

If the aforementioned development and production times are imposed on this production process, the cash flow can be seen in Figure 5.2, where interest is only paid over cash outflow (negative cashflow). For the production of this figure, it was assumed that the development and certification costs of the aircraft are one-time expenses, whereas the manufacturing and tooling costs are per aircraft. For simplification, it was also assumed that five aircraft are produced every two months and that every finished aircraft is instantly sold. It can be seen that if the aircraft is sold for a price of 60 million USD, the break-even point is in month 112. From a different perspective, a cost break-even occurs when 90 aircraft are sold, if the original production times are adhered to.

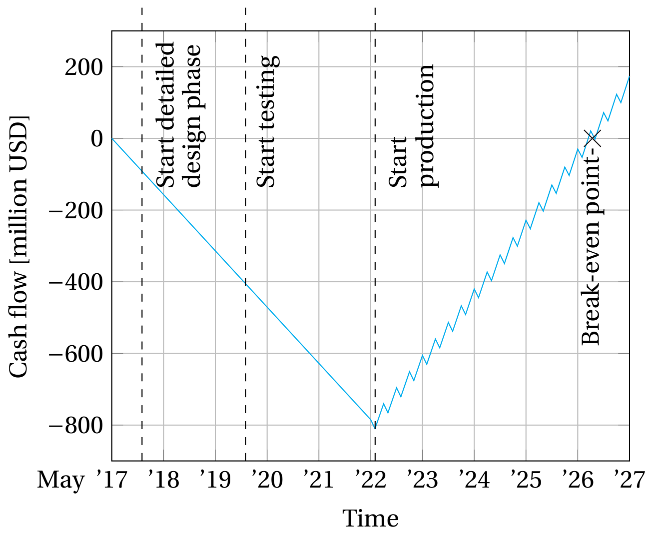

Figure 5.2: The flow of cash over time; the break-even point is found in month 112.

As for the operational costs of the aircraft, one hour of flight costs approximately 2000 USD. The operational cost breakdown can be seen in Table 5.2 for which the cost of a typical business jet is taken from Gudmundsson[18]. In calculating these values it was assumed that the engines' time between overhaul (TBO) is 6000 h. This TBO is taken from Pratt & Whitney turbofan engines with a similar thrust rating [24]. Furthermore, it was assumed that an engine overhaul costs 40 000 USD. The last major assumption is that a total of 4000 flight hours are made annually.

Table 5.2: Variable and fixed-cost analysis assuming 4000 flight hours per year.

Element	Hourly rate [thousand $/h]	Annual cost [thousand $]
	Hourly variable costs	
Fuel	1.6	6205
Engine overhaul	0.02	53
Maintenance	0.23	911
Subtotal	1.8	7170
	Annual fixed costs	
Storage		18
Insurance		23
Inspection		5
Captain		161
Co-pilot		94
Cabin attendant		89
Subtotal		390
Total	-	7560
Flight hour cost	2	

5.3. Reflection

In order to have a critical reflection on the model outcomes and on its reliability a verification and validation procedure is executed. Subsequently, a sensitivity analysis of the cost of the aircraft to its OEW is performed.

As a means of verification, the DAPCA IV method is compared to the sales prices of reference aircraft. The data in Appendix E roughly shows linear relations between range, Mach number, MTOW and on the other hand sales price. This led to the idea that the sales price can be estimated as a linear combination of these three parameters. A three dimensional least square regression gave an estimation for the sales price as described in Equation 5.1. In this equation R is the maximum range in NM, M represents the maximum Mach number, MTOW is the maximum takeoff weight in kg and P equals the sales price in million USD. The fit has a R^2 value of 0.983, suggesting that the linear fit is suiting.

$$P = 0.00897 \cdot R + 27.0 \cdot M + 0.000167 \cdot \mathrm{MTOW} - 26.1 \tag{5.1}$$

A cost penalty due to the amphibious capabilities was considered, but not applied. A weight penalty is already included in the preliminary calculation of the MTOW which also translates to the costs. Applying a separate cost penalty as well would therefore include the amphibious capabilities double. Inserting the values for the water business jet in Equation 5.1 provides an estimated sales price of 61.9 million USD. This is very close to the sales price of 60 million USD calculated in this chapter, thereby verifying the used model.

Subsequently as a means of validation, the data of several existing business jets are used as input for the model and its results are presented in Table 5.3. It can be seen that although the errors in estimating the sales prices of the Falcon 7X and the Global 6000 are relatively low, the errors are generally quite large. This is illustrative for the earliness of the stage in which the cost analysis is performed. Therefore, care should be taken in drawing conclusions from the DAPCA IV model.

Another observation from the validation comparison is that the DAPCA IV model tends to overshoot the actual aircraft cost rather than to estimate a lower sales price. This agrees with the observation made earlier that this is due to the military origin of the DAPCA IV method. Therefore, the outcomes of this analysis are more readily interpreted as a somewhat vague upper limit of the aircraft cost.

Table 5.3: Comparison of actual aircraft sales prices [24] to model outputs.

	Sales price million US$			Development cost million US$		
Aircraft	Actual	Model	Error	Actual	Model	Error
Falcon 7X	53.8	52.1	−3.2 %	600-700 (est.)	902	28.8-50.0 %
Global 6000	62.31	66.3	6.4 %	600	839	39.8 %
Gulfstream G550	61.5	56.9	−7.5 %	N.A.	N.A.	N.A.
Challenger 600	32.35	40	23 %	N.A.	N.A.	N.A.

Finally, in order to assess the sensitivity of the aircraft to the operational empty weight, a sensitivity analysis is performed. This sensitivity analysis is of particular importance, because the final OEW tends to have grown with respect to the design OEW. For example, if the OEW budget of the aircraft is overshot by 10 %, the aircraft sales price increases by approximately 4 million USD, or 7 %. Although this percentual increase is not extraordinarily large, it does cause the cost to grow above the sales price of 60 million USD.

Taking into account all the above, it may be concluded that for a sales price of 60 million USD, the aircraft design is economically feasible. However, it should be noted that due to the measure of uncertainty induced by the cost model and its dependency on the OEW, an accurate cash flow prediction is not easily obtained. It is therefore of great importance the cost estimation be performed in a more detailed manner in a later stage of the project.

6 Operations

The operations of an aircraft form an important contribution to the feasibility of the design as a whole. An aircraft which has excellent technical specifications but cannot be operated in a desirable manner will not attract potential customers. The market analysis in Chapter 1 shows that several long-range business jets for 12 to 16 passengers currently exist. For regular land operations it can therefore be assumed that the design is feasible when operating in a similar fashion to current long-range business jets. The presence of amphibious capabilities, in contrast, is a novel concept and poses several operational challenges as identified through functional and risk analyses in Chapter 2. Therefore it was chosen to address the following challenges early on in the design process and feasibility study. Section 6.1 presents an operational plan for landing and takeoff on water, which was considered as the most critical aspect of the operational feasibility. Section 6.2 discusses different scenarios for (un)loading and refuelling on water. Section 6.3 finally deals with emergency procedures related to water operations.

6.1. Landing and takeoff on water

Being able to land and takeoff on water is critical to the feasibility of the design. Throughout several risk assessments it was found that multiple operational challenges arise when aiming to land and takeoff on water. This section presents an operational plan which has taken those challenges into account and proves that landing and takeoff on water is operationally feasible. This plan then will be followed by the analyses performed on the different challenges. In this way one can easily see how the landing and takeoff operations has been designed for these challenges. Subsection 6.1.2 elaborates on the geographical and infrastructural aspects; Subsection 6.1.3 presents the results on the research on maritime traffic near major business-centric cities; Subsection 6.1.4 addresses the requirements on community noise in densely populated urban areas; Subsection 6.1.5 treats the regulations involved with landing and takeoff on water; and finally Subsection 6.1.6 touches on the subject of weather. Throughout this section, only the situation of landing has been considered. Therefore from now on the terminology landing on water will be used. This choice was made since the flexibility of the concept is a result of the possibility to land at either an aircraft or a large body of water. Furthermore, landing is considered to be a more critical situation than taking off. At last it is safe to assume that if an aircraft can land on water, it can take off at that location as well with similar operations. Of course the fact that takeoff distance generally is longer than landing distance should be taken into account. One should keep in mind however that takeoff would require operations similar to landing.

6.1.1. Operational plan for landing on water

In setting up the operational plan for landing on water, two scenarios are distinguished: operations near business-centric cities, and operations at remote areas. These are identified in Subsection 6.1.2 as the most important scenarios to develop an operational landing plan for. Figure 6.1a and Figure 6.1b visualise the operational landing plan for both business-centric cities and remote locations respectively. Figure 6.2 provides the functional flow diagrams corresponding to the operational plan.

A large amount of business-centric cities are located near bodies of water which provide enough space for landing. At these locations maritime traffic does not pose constraints on landing operations. The majority even provides the possibility of having a designated area for landing aircraft, which would make landing

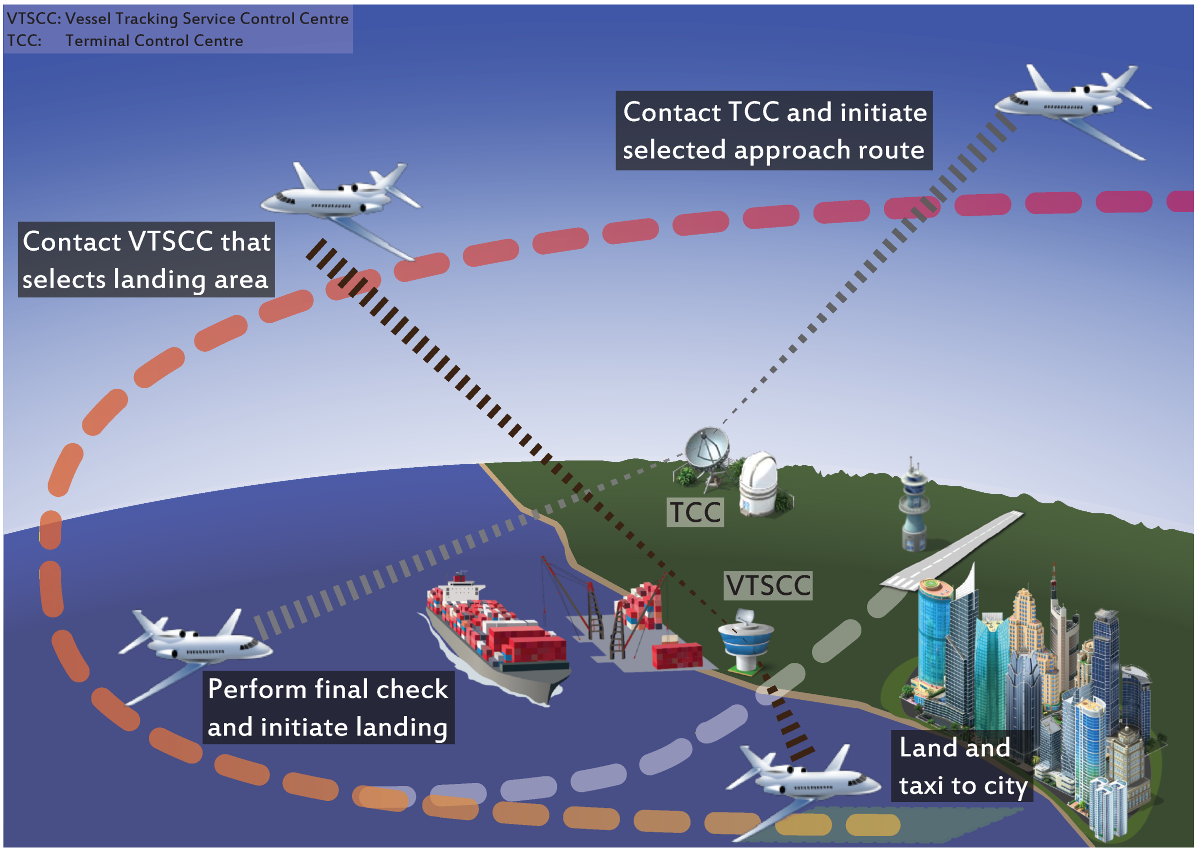

(a) Landing near major business-centric cities. Regular descent corridors are followed until initiate landing.

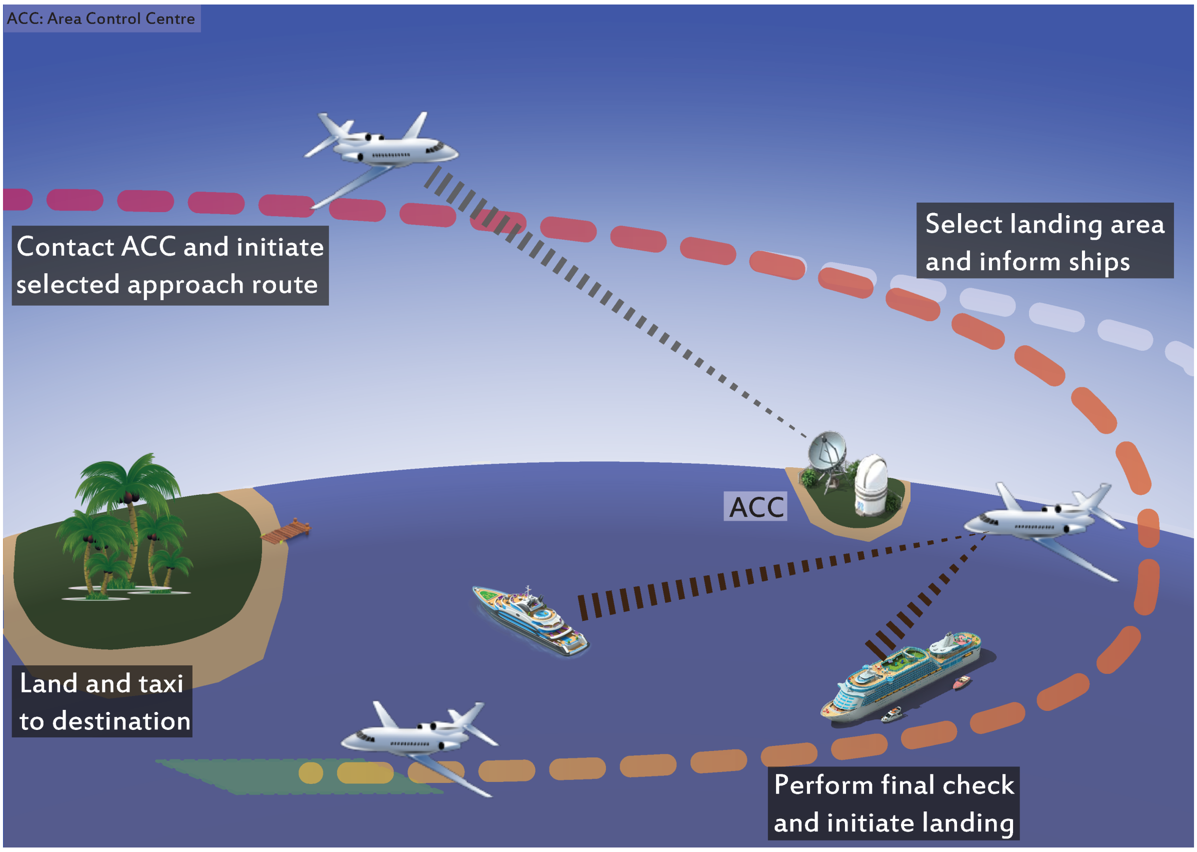

(b) Landing at remote locations. Landing area selected by pilot based on visual inspection.

Figure 6.1: Visualisation of operational plan for landing on water

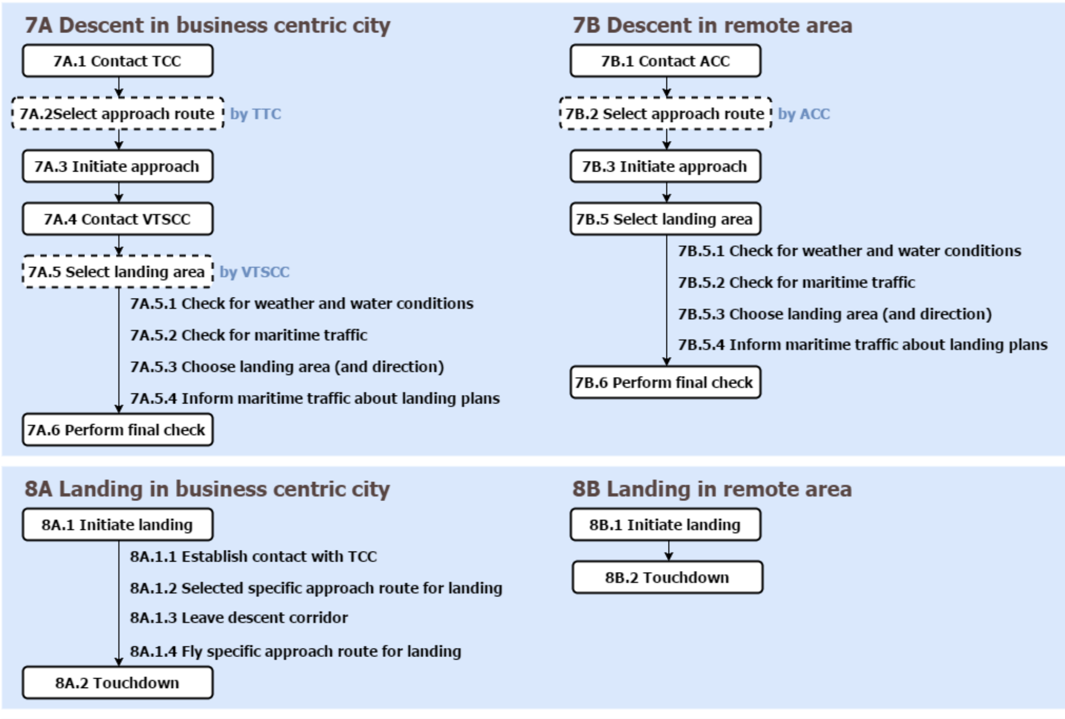

Figure 6.2: The functional flow representation for the operational plan for landing on water.

in dark conditions possible as well. More detail on maritime traffic can be found in Subsection 6.1.3. The landing site has to be at least 5 km outside the coast due to noise constraints posed in REQ-14.0F. At a taxi speed of 21.6 km/h this off coast distance translates into a taxi time less than 15 minutes, which is comparable to regular taxi times at airports. The out of coast distance is a very conservative estimation and has a high probability of decreasing when more detailed noise research can be performed. More on this topic can be found in Subsection 6.1.4. In addition, weather will not have a large impact on landing operations near major business-centric cities. Landing would be possible at least 90% of the time throughout the year when considering wave forming due to wind in rough weather. Subsection 6.1.6 presents the analysis preceding this conclusion.

The major advantage of the proposed plans is the fact that no new infrastructure has to be developed. This saves a lot of costs as no large investments have to be made to facilitate landing at a large number of locations. In addition this ensures the flexibility character of the design is guaranteed and enhances marketability of the aircraft. Scenario 1 combines existing infrastructure for aircraft and vessels. Vessel Tracking Service Control Centres (VTSCC) can provide services for landing operations, such as checking maritime traffic and weather and water conditions and selecting a landing site. Since no Air Traffic Control Tower (ATCT) is present, the pilot will have to directly submit the flight plan into the central Air Traffic Control System (e.g. the FAA host computer) and initiate contact with the Terminal Control Centre (TCC). The most important consequence is that the aircraft needs two separate VHF transmitters to ensure an easy transition between air and marine communication, for example when leaving the regular descent corridor. In scenario 2 landing will be done based on pilot visuals. At such remote locations the pilot will have the time and space to do such a landing. To do so, pilots are required to follow additional training which can be included within the type rating of the aircraft. Subsection 6.1.2 elaborates more extensively on the infrastructural aspects of the operational plan for landing.

Regulations on landing on water highly differ on a country or even state level. These regulations range from being allowed to land everywhere on the one hand to being restricted to designated seaplane bases on the other hand. In the presence of existing seaplane bases operations are possible after modification of the runway length. For other locations is in general allowed to operate on water. Subsection 6.1.5 further elaborates upon regulations.

6.1.2. Geographics and Infrastructure

The geography and infrastructure at locations of interest are important factors for operating a business jet. In geographical terms, the main concern is whether enough physical space is present to land reasonably close to city centres. For infrastructure it is necessary to investigate into what extent air traffic control is available or possible for landing on large bodies of water.

Geography

The question of whether landing and takeoff would be possible in terms of physical space was addressed by checking locations of interest for a possible landing site of 3 km as imposed by REQ 12.0-B. The choice of these locations was based on their market importance and includes the cities from the top 10 (emerging) business routes, large Asian cities and cities which are considered to be the part of the most economically powerful cities in the world. It was found that the majority of this selection provides enough space for landing and takeoff on water. For example, 5 of the top 10 routes provide the possibility of both landing and taking off on water within one trip, whereas another 4 routes provide the possibility of either landing or taking off on water at one location. Appendix C lists the 28 locations which provide enough space for landing and takeoff on water. The presented table also includes the results from the research on maritime traffic near major business-centric cities for which the reader is referred to Subsection 6.1.3.

Infrastructure

At regular airports, landing operations are mostly accompanied by a high degree of air traffic control. Therefore it is important to investigate into what extent this is available or possible for landing on large bodies of water.

Appendix B shows a schematic overview of Air Traffic Control system, specific to the United States of America. Such systems are identical throughout the entire world however, with certain terminology being the only difference [1]. The main difference between landing on water and landing at an airport, is that regular Air Traffic Control Towers (ATCT) cannot be used. The other elements of the system such as the Terminal Control Centre (TCC, USA: TRACON) and Area Control Centre (ACC, USA: ARTCC) can still be made use of since no difference is present between landing at airports or on water here in terms of flight profile. Landing near business-centric cities means that it for sure is within a TCC area and thus can make use of that infrastructure. TCC directs aircraft to follow regular ascent and descent corridors within an area. This already starts quite a distance away from the airport ($\tilde{5}0$ miles), so when landing on water, these corridors can still be made use of.

Services that normally are provided by ATCT and thus what is also required for the landing procedures on water include integration of flight plan into FAA host computer; checking (maritime) traffic at landing location; check weather (and water) conditions at landing location; and directing aircraft from takeoff and landing flight path to regular ascent and descent corridors respectively.

Potential landing locations can be grouped into four categories according to available infrastructure:

1. Sea plane basis. Provides the required infrastructure for seaplanes. Has a sea lane designated for landing of seaplanes.
2. Major business-centric city. High probability of harbour or infrastructure for vessels. Vessel Tracking Service Control Centre (VTSCC) available.
3. Smaller city. Small probability of harbour or infrastructure for vessels. No VTSCC available.
4. Remote location. No infrastructure present here.

Categories 2 and 4 are of main interest when setting up the operational plan for landing on water. Being able to land near major business-centric cities is key to attract target customers. The possibility of landing at remote locations in addition provides a high degree of flexibility which distinguishes the concept from other competitors in the market. At last, the amount of seaplane bases at interesting locations is very small. Only 4 of the 490 seaplane basis currently in use in the United States are located near major business-centric cities. Designing the operational plan for landing on water based on the infrastructure of seaplane bases is therefore considered not effective.

In category 2, the VTSCC could take over some of the required services for landing operations. This includes checking maritime traffic and weather and water conditions at the landing location and selecting a landing site. To make this possible, means of communication between the aircraft and VTSCC should be provided. Both air and marine communication is done over VHF frequency, however different bands are used

[1] `http://science.howstuffworks.com/transport/flight/modern/air-traffic-control2.htm`. Retrieved 31-05-'17

for boats and aircraft: 108 – 137 MHz, and 156 - 174 MHz, respectively. Two separate VHF transmitters should be present in the aircraft to ensure easy transition between air and marine communication.

In category 4, the pilot would have to be able to land on visuals only due to the lack of ATC infrastructure. It is safe to assume that the pilot has the time and space to do such a landing at remote locations. For such landing operations, pilot are required to follow additional training which can be included within the type rating of the aircraft.

6.1.3. Maritime traffic near major business-centric cities

One of the possible constraints that comes to mind when thinking about landing on water is interference with maritime traffic. This is especially the case with major business-centric cities which often function as trade hub and have large ports. Therefore it is necessary to analyse the intensity of maritime traffic and see how this affects the possibility of landing on water.

A total of 28 locations have been researched on their maritime traffic. This selection was based on their market importance and includes cities from the top 10 (emerging) business routes, large Asian cities and cities which are considered to be the part of the most economically powerful cities in the world. The intensity of maritime traffic then could be viewed with the use of live open source data. Attention was paid to both routes and anchoring areas of vessels.

Figure 6.3 summarises the results of the research conducted whereas the full results can be found in Appendix C. The majority of the cities researched have a low intensity of maritime traffic. In addition these cities are often located immediately next to an ocean or large lake and have no lagoons or other water entries. A runway length of 3 km is easily feasible and thus an aircraft could almost certainly always land at these locations. Furthermore they provide the possibility of having a designated area for landing for aircraft, restricted for regular vessels. With proper lighting, this would make landing in dark conditions possible as well.

Three locations have a high amount of maritime traffic which is properly organised. Specified routes and anchoring locations are present for vessels. This means that there are specific areas with a low density maritime traffic which provide the opportunity for landing. Since these locations are not entirely traffic free, good communication with vessels is required in order to safely operate at these locations. Designated areas for landing however seem not feasible. As a consequence landing at night would be too large of a risk due to the limited visuals of the pilot. At last three locations show a high amount of maritime traffic which is not organised. Vessels take seemingly random routes and thus landing here is not feasible. These locations are medium sized lakes or bays.

It should be taken into account that the intensity of maritime traffic has been researched at a certain time instance. The results are sensitive to the time instance at which the intensity has been checked. Maritime traffic will show a higher intensity at day than at night and can vary over a longer period of time as well. The used method however is considered as adequate for a first feasibility assessment with regard to the introduced challenge.

It can be concluded that maritime traffic in general poses no constraints on landing operations on water near major business-centric cities. Approximately 80% of the researched locations have a near certain possibility of landing, whereas another 10% show a good possibility to do so. For this good communication with vessels is required for safe operations.

For further research on this specific topic it is recommended to do a long-term tracking of maritime traffic at the locations presented in this analysis. Focus points herein should be the distribution of maritime traffic intensity over time in general, and the specific amount of time available for a certain landing area to be entirely vessel free. In addition, it is advised to obtain more information on smaller boats or ships which are not included in automatic tracking systems.

6.1.4. Community noise in densely populated urban areas

Operating near major business-centric cities poses a challenge in terms of community noise. This challenge was translated into a top-level requirement of 70 dBA community noise. To check the feasibility of meeting this requirement without compromising on marketability, a qualitative analysis is done.

This qualitative analysis was performed using the FAA's integrated noise model (INM). This model is based on measurements and thus provides valid data. For obtaining noise values the takeoff situation was selected, since this is the most critical case in terms of noise impact. From a database of reference aircraft, the Gulfstream GV was chosen. The main reason is that this aircraft has engines from the same family as those used

[2] https://www.marinetraffic.com/nl/

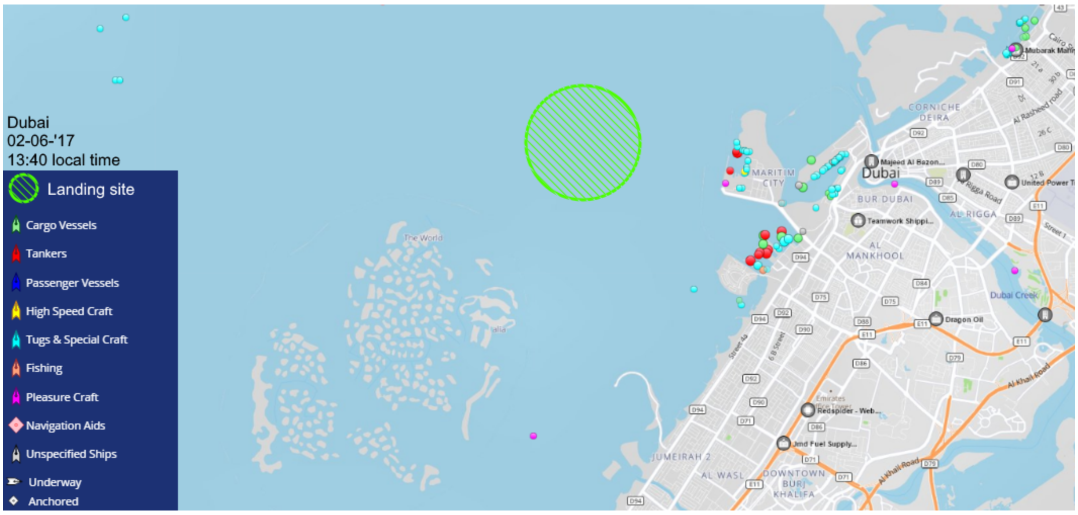

(a) Category 1: Low intensity maritime traffic. Locations: Amsterdam, Boston, Buenos Aires, Chicago, Côte d'Azur, Dubai, Dublin,Florida (Southeast coast), Geneva, Helsinki, Lagos, Los Angeles, Mumbai, New York City (Lower Bay), Oslo, San Francisco, Sydney, Tel Aviv, Toronto, Vancouver, Washington DC, Zurich.

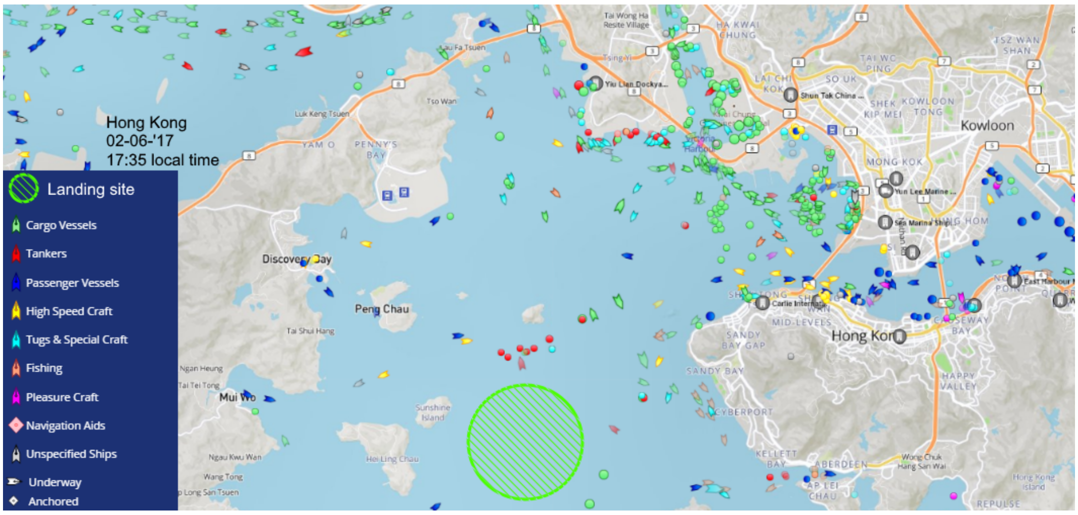

(b) Category 2: High intensity maritime traffic, organised. Locations: Hong Kong, Shanghai, Singapore.

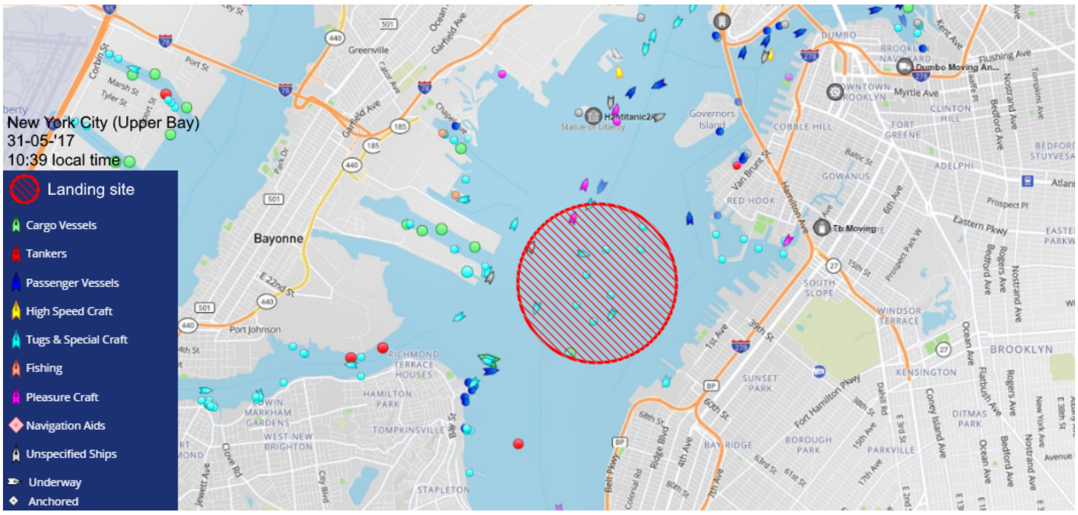

(c) Category 3: High intensity maritime traffic, unorganised. Locations: New York City (Upper Bay), Osaka, Tokyo.

Figure 6.3: Maritime traffic at major business-centric cities. Live data obtained from online marine tracking service[2]

on the Global Express and Gulfstream G550. In addition, the INM uses data for a twin-engine takeoff with 12900 lbf of takeoff thrust and 100% throttle from the start, whereas we use twin-engine takeoff with 12000 lbf with throttle going from 25 ro 95% in the first 10 seconds. Therefore our engine takeoff thrust is similar, but lower, making this a conservative estimation. For reference on how the programme is used, see reference [1].

From this analysis, it was found that water takeoff (and landing) should be performed at least 5 km off coast. At this distance, the most critical noise level (SEL) is less than the required 70 dBA as illustrated in Figure 6.4. For reference on the different noise weighting methods the reader is referred to reference [1]. At a taxi speed of 21.6 km/h this off-coast distance translates into a taxi time less than 15 min, which is comparable to regular taxi times at airports.

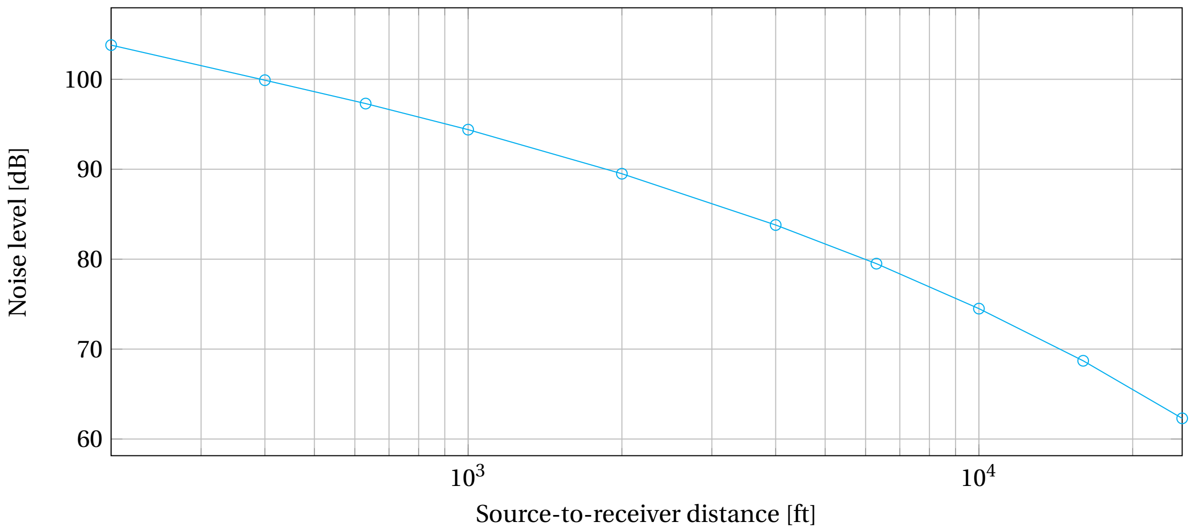

Figure 6.4: The relation between community noise and source-to-receiver distance for noise ID BR710.

It should be taken into account that nowadays improved engine technology makes significant noise reduction possible as compared to the reference aircraft used in this analysis. Implementation of chevrons on the engine nozzles for example reduces the noise level by up to 3 dBA [55]. In addition, the engine placement above the main wing results in noise shielding further reducing community noise levels. As such a takeoff and landing location 5 km off coast is a conservative estimation. It is highly probable that taking off and landing closer to the coast will be possible. This would reduce taxi time even further.

It can be concluded that noise requirements will have no large impact on the feasibility of the landing and takeoff on water operations. Even with such a conservative estimation, taxi time is acceptable and no compromise on marketability has to be made. For further research on this specific topic it is recommended to perform a more elaborate analysis for the selected engines which are presented in Chapter 13. This way, a more detailed value can be obtained for out of coast operations distance and consequently taxi time. Furthermore, this could contribute to research on climb and descent routes near densely populated urban areas.

6.1.5. Regulations

To be able to operate an aircraft on the water, one should be allowed to takeoff and land at the selected area. In the case of a water business jet, the question whether this is allowed is even more essential, as air traffic is highly regulated around big cities. Furthermore, a landing or takeoff from water is quite a special operation, which poses risks at both the aircraft as other vessels and persons in the water. The operations also influence the environment and surroundings. For these reasons it is likely that seaplane operations are restricted at the locations one wants to fly to. This subsection describes the research that was done to prove that the aircraft can and is (potentially) allowed to operate from a lot of places, which makes the idea of a water business jet even more attractive to potential customers. To limit the duration of the research and make it feasible for this project, an overview is given by focusing on six cities around the world. These cities are located in different continents and countries, to create a diverse view.

The cities chosen are the following:

- Chicago
- New York
- Amsterdam
- Hong Kong
- Dubai
- Buenos Aires

Because regulations for some of the above mentioned cities are not accessible or non-existent, the research mainly focused on already existing laws, current or historical seaplane operations and operations nearby. The results per city are described below.

Starting with the United States, it was found out that seaplane regulations differ extremely per state and owner of the water, from restricted to seaplane bases in New Jersey to basically everywhere allowed in Oregon. [3] Chicago is located in Illinois where the use of seaplanes is not restricted to bases, so it is probably possible on lakes. It might be needed to get a permission to land or to create a base, depending on the exact laws. For the case of New York it is simpler, the city already has a seaplane base with a 10000 feet runway, from which the aircraft will be able to operate.[4] In Amsterdam and the rest of the Netherlands, aircraft operations are only allowed from and to designated airfields.[5] However, an exception is made for three seaplanes in the province of Flevoland,[6] that are allowed to take off and land on the waters of that province, of which the closest point is located only ten kilometres from Amsterdam. It is likely that a fourth aircraft can be added or that permissions can be given for another province. In Hong Kong, the aviation laws explicitly mention seaplanes[4], which make it likely that operations are allowed. Dubai already has seaplane operations at the moment,[7] making it likely to operate this business jet as well. Finally, Buenes Aires had seaplane operations in the past.[8]

From this research, the conclusion can be drawn that regulations differ extremely for different states and countries, from allowed to land and takeoff everywhere to restricted to designated seaplane bases. Where seaplane bases are already existent, operations are possible, or will be allowed after modification of the runway length. For other places either a seaplane base can be created or it is allowed to operate on other waters. This means that the aircraft is likely to be usable in an enormous set of locations.

6.1.6. Weather

Weather places a significant role when landing on water. Rough weather makes landing difficult due to the waves, while ice would make landing impossible. Weather is a very local phenomena, but an attempt is made to plausibly indicate how often weather conditions would prevent the aircraft from operating. This is done based on the analysis of three large business-centric cities: New York, Vancouver and Hong Kong.

Firstly the forming of ice is investigated. Partly or fully frozen bodies of water ask too much of the structure of the aircraft while landing, risking leakage of the hull. Appendix D shows the climate for New York, Vancouver and Hong Kong. The average temperatures of these cities are almost always above 0 $°C$ throughout the year. In combination with the fact that these large (salt) bodies of water require low temperatures for a long time before freezing, it is made plausible that freezing does not pose a large problem for the operations of aircraft.

Secondly, the wave forming due to wind is considered. The aircraft can operate up to waves of 1 m, as described in Subsection 12.2.1. According to the Beaufort scale, this corresponds to a wind force of 4 Bft (around $20\,\mathrm{km\,h^{-1}}$), described as a moderate breeze [9]. However, these wave heights refer to fully developed waves at open sea. For more sheltered locations, like a city in a bay, higher wind speeds are required to form waves of 1 meter. When looking at the average and 90^{th} percentile wind speeds for these three cities as shown in Appendix D, it can be concluded that landing is possible at least 90% of the time, since the 90^{th} percentile wind speed is below $20\,\mathrm{km\,h^{-1}}$ for every city in every month.

In general it can be concluded that weather will not highly limit operations in cities with temperatures and wind speeds comparable to New York, Vancouver and Hong Kong.

[3] https://www.seaplanepilotsassociation.org/resources/faq/facilities-landing-areas/
[4] https://nfdc.faa.gov/nfdcApps/services/airportLookup/airportDisplay.jsp?airportId=6N7
[5] http://wetten.overheid.nl/BWBR0002267/2014-01-01#HoofdstukIV
[6] http://decentrale.regelgeving.overheid.nl/cvdr/xhtmloutput/historie/Flevoland/119298/119298_1.html
[7] https://seawings.ae/
[8] http://www.histarmar.com.ar/AVIACION/SundringhamsAA/LadiesoftheRiverPlate.htm
[9] https://www.britannica.com/science/Beaufort-scale. Retrieved 20-06-'17

6.2. (Un)loading and refuelling on water

Loading and unloading of a regular aircraft is straightforward as an airport provides loading and fuelling infrastructure. But the water business jet is not always operative on a regular airport but on the sea or at seaports which are not (always) equipped with the proper infrastructure. This section is thus dedicated to the loading, unloading and refuelling of the aircraft when docked on water. First of all four docking methods have been selected followed by a door selection. Afterwards, refuelling of the aircraft will be addressed.

6.2.1. (Un)loading

The first concept, as shown in Figure A.3, is a big horseshoe dock. It allows accessing the aircraft on both sides which makes it comfortable for passengers and allows for easy loading, fuelling and maintaining. Due to the wide placed side floats, the possible wideness of the platforms could allow for eventual vessels that help during loading or maintenance. That the aircraft is easily accessible from both sides is very useful for the potential spinoff case as up until 79 passengers will have to enter the aircraft.

Figure A.4 shows the second (un)loading option which consists of a pier width extendable platforms to reach the aircraft doors. It is still very doable to perform the necessary actions when docked, however it could cost more effort to load the aircraft as vehicles won't be able to reach the doors.

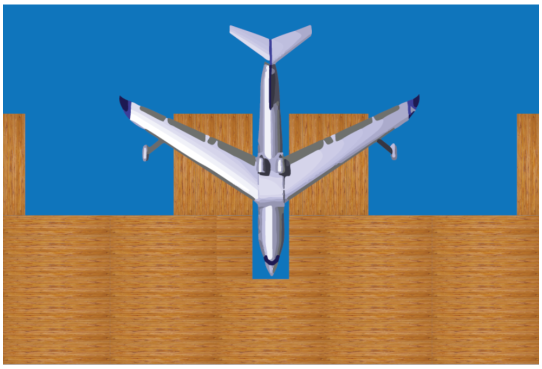

Figure 6.5: (Un)loading concept 1.

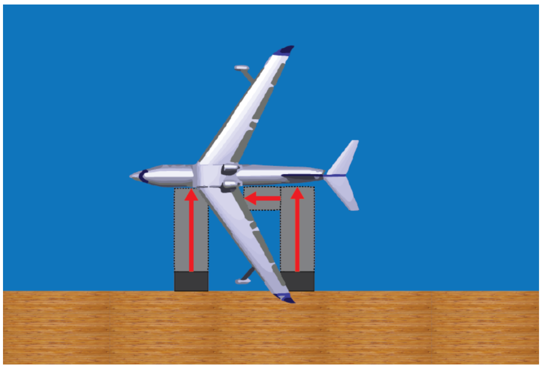

Figure 6.6: (Un)loading concept 2.

The next option is towing the aircraft out of the water by the means of a tow truck as can be seen in Figure 6.7. For this, the aircraft will need one or more reinforcements on the fuselage to attach the rope to. Also, as will be explained in Section 14.1, the landing gear will have to be opened in the water to be pulled up the ramp. Therefore, sealing the fairings should be taken care of and maintenance against water is very important to extend the life of the landing gear. Loading and maintenance can be done in a regular way and this option allows for easy storage of the aircraft inside a hangar.

The fourth and final option is docking the aircraft in the water by the means of an anchor. A boat can then reach the aircraft and be attached to the stairs of the aircraft so that entering the aircraft does not become an issue, this is shown in Figure 6.8. The anchor should, in the best scenario, be provided by the port and it should be easily attachable to the aircraft. This attaching point could be the reinforced point(s) for towing. When one wants to travel to a certain location, one should be aware of the docking options and facilities so that an anchor could be taken along if needed. This anchor should be able to be stored in the cabin and to be easily moved in or out of the aircraft.

Figure 6.7: (Un)loading concept 3.

Figure 6.8: (Un)loading concept 4.

When the aircraft would be needed to be docked for a longer time, concept 3 would be the most evident solution as already existing hangars could be used for storage. Another option would be using hangars for the first concept as these already exist for smaller seaplanes (Figure 6.9). A hangar like this could be designed for the Jaeger with the appropriate dimensions and could still be used to store 2 or more small sea planes.

Doors

For regulatory reasons, as specified in CS25 and considering the spinoff, the doors will be a type 1 and a type 3 door on both sides of the aircraft. With this door configuration a maximum of 79 passengers is allowed to transport. When using the Jaeger as business jet, only doors at 1 side will be used for making more space available inside the aircraft, this is allowed as for 10 to 19 passengers only 1 type III door is required at each side of the aircraft [8]. The type 1 door is placed in the front of the fuselage at 4.3 m and the type 3 door is placed just after the wing at 15.45 m, they are respectively 1.22 mx0.65m and 0.6mx1m. The front door seems small but as it is placed relatively high (1.58 m from the lowest point of the fuselage), there is space enough so no one hits their head against the fuselage due to the curve it makes. The aft door is very small but this one will mainly function as emergency exit or as cargo door. The doors are positioned so that when the aircraft floats in the water, the water line does not interfere with the doors.

Figure 6.9: Sea plane hangar concept. [10]

6.2.2. Refuelling

Refuelling the aircraft can mostly be done when the aircraft is docked in the ways presented in this section. However, fuelling on water (loading concept 3) should only be done when no other options are available as this increases the risk of leaking fuel into the water due to not lying stable in the moving water compared to almost lying still when being docked to land. This could be done by a boat containing fuel tanks but extra care should be taken so that no fuel is spilled into the water.[11]

General refuelling of the aircraft also requires some attention but regulations can vary between different areas. Just like regular aircraft, seaplanes and the equipment needed for fuelling need bonding. This is because aviation fuels generate electrostatic charges which could be potential ignition sources for fuel vapours and cause fire. By bonding the fuelling system with the aircraft, this charge can be neutralised. Other precautions should be taken as well. These include for example smoking, passengers, electronic devices not to be inside a safety zone of 3 meters from where the fuelling occurs. Not involved vehicles should even be 15 m away of the source. In case of thunderstorms, when lightning is observed within 8 km, fuelling operations will have to be stopped and bonding cables have to be removed. [12]

[10] http://www.dougronan.com/ontario/images/members/strickerhangar2.jpg
[11] https://www.sa.gov.au/__data/assets/pdf_file/0012/12126/Safety-on-the-Water.pdf
[12] https://www.tc.gc.ca/eng/civilaviation/publications/tp185-2-04-564-2851.htm

6.3. Emergency procedures

As emergencies can occur anytime, each aircraft should have emergency procedure during flight as well as during landing and takeoff. This procedure is rather general and straightforward. First of all the pilot should configure the aircraft for the best gliding speed, this speed allows for having maximum range and thus allowing for having more time to prepare for the landing. After this, a landing area has to be selected. This is not a really big problem as the Jaeger allows landing on water and land and thus having more area options (not taking into account maritime traffic and impact on aquatic ecosystems). The next step is to go through the emergency checklist depending on the kind of emergency. Then the control tower should be contacted so they can provide emergency services. Finally the landing will have to be performed.
The best gliding speed can be obtained by flying at the minimum descent angle. For the Jaeger, at cruise height, this speed is 167 $\mathrm{m\,s^{-1}}$ and at landing configuration, a sea level, 53 $\mathrm{m\,s^{-1}}$. Despite the advantage of having more landing area options, problems could arise with one of the gears so that some landing options could be restricted. Gear problems are considered being the critical emergencies as this is the sole difference with regular aircraft.
It should be noted that an aircraft must have emergency means to extend the landing gear (or side floats) in case of any probable failure in the normal extension and retraction mechanism or the failure of an hydraulic or electric source [8]. Considering the Alitalia A320 in Rome (29/09/2013) or the LOT Polish airlines (01/11/2011), problems can still occur with the landing gear and thus emergency procedures have to be considered.
When only the landing gear would fail it is still possible to land on water if this is still reachable. But imagine water is too far away and the aircraft therefore has to land on land. It is possible to make an emergency landing on land while doing little or no damage to the hull or side floats. This can be done by keeping the keel of the hull (and side floats) as nearly parallel to the landing surface as possible during touchdown. After touchdown, to prevent nose-over tendency and reduce the deceleration, the elevators must be fully deployed and additional power must be applied for the effectivity of the elevators. [13]
When the side float mechanism would fail, both water and land landing are still possible. When landing on water, only the stability would be affected and the wing could hit the water but this can be tackled by using the ailerons to keep in control of the aircraft and keep the wings horizontal. When both the landing gear and side floats fail, one of two above mentioned methods can be performed.
What the checklist concerns, there are several checklist for different emergencies. These can include checklists for engine failure, electrical failure or checklist in case of fire. This checklist will look like something in the form of 'Aviate - Navigate - Investigate - Communicate - Secure' as presented in the following bullet points:

- Set configuration for best glide performance
- Navigate to the best landing area
- Investigate mixture, fuel, tanks, seat belt signs,...
- Communicate to control tower
- Prepare for landing: gear down, throttle,...

Considering emergencies during takeoff, more specific engine failure, a margin has been taken for the required takeoff distance. If the aircraft would not be able to land anymore within this margin, the pilot can decide whether it is possible to turn around and perform an emergency landing on the runway or to perform an emergency landing off the runway.
So in general, the emergency procedures are the same as in regular aircraft with an advantage in selecting a landing area for emergency landings. The most critical emergencies were considered to be a landing gear and/or side float failure as these could restrict landing area options. However both these failures are tackled by the amphibious capabilities of the aircraft.

[13] `http://www.pilotfriend.com/training/flight_training/seaplanes/landings.htm`

7 RAMS

To control and monitor the quality and performance of the aircraft, a reliability, availability, maintenance and safety analysis is conducted. To research the reliability and safety, a failure mode effects and criticality analysis is used for the entire aircraft. With a fault tree analysis, the side float mechanism is looked into, as this new concept is thought to be more sensible to failure. For availability and maintainability, the focus lies on differences from a non-seaplane. With this, the most critical failure modes of the aircraft and with special attention the side floats are found. With the knowledge of the weak points, risks imposed by them can be mitigated is some cases. The maintainability and availability, which are highly linked to each other, do not pose any problems to the aircraft, because the extra maintenance resulting from the harsh aquatic environment can be done in the many hours a business jet is normally not used.

7.1. Reliability

Table 7.1 shows the failure mode, effects, and criticality analysis (FMECA) of the significant subsystems. The analysis helps to identify the interrelations between the failure modes of different subsystems. Some paths can still change in later design phases. For example, the cabin pressure is now provided by bleed air, while some recently released aircraft, like the Boeing 787 Dreamliner, use electrical system for this function. The coloured circles indicate the criticality of the failure mode which go from rather insignificant (yellow) to catastrophic (red). The FMECA shows that especially the support system have a highly indirect influence as expected. The aircraft differs a lot from conventional aircraft due to its amphibious capabilities. This can be seen in most of the mechanisms and the hull where, in case of failure, choose between ground and water landing. When the landing gear fails to deploy at a conventional aircraft a belly landing is the result. In the case of an amphibious aircraft this can be avoided by landing on water.

Table 7.1: Failure mode, effects, and criticality analysis (FMECA).

	Subsystem	Failure	Effect		Mitigation
1	**Cabin**				
1.1	Entertainment		Passenger discomfort	●	
1.2	Cabin temperature		Passenger discomfort	●	
1.3	Cabin lighting		Passenger discomfort	●	
1.4	Cabin pressure		Emergency	●	Oxygen masks
2	**Avionics**				
2.1	Navigation		Emergency	●	
2.2	Communication		Emergency	●	
3	**Mechanisms**				
3.1	Ice protection	Accretion	→ 3.2, 3.3, 3.4, 3.5, 4.1		
3.2	Control surfaces	Immovable	Catastrophe	●	
3.3	Lift control devices	Failure to deploy	Increased landing distance	●	
		Failure to retract	Increased drag	●	
3.4	Landing gear	Failure to deploy	Emergency	●	Diverge to water landing
		Failure to retract	Increased drag	●	
3.5	Side floats	Failure to deploy	Emergency	●	Diverge to ground landing
		Failure to retract	Increased drag	●	
4	**Propulsion**				
4.1	Engine		Emergency	●	Redundant thrust
4.2	Fuel		→ 4.1		Redundant pumps
5	**Support**				
5.1	Electrical power		→ 1.1, 1.2, 1.3, 2.1, 2.2		Emergency Power Unit (EPU)
5.2	Hydraulics		→ 3.2, 3.3, 3.4, 3.5		
5.3	Bleed air		→ 1.4, 3.1		
6	**Airframe**				
6.1	Hull	Leakage	Reduced buoyancy	●	Redundant compartments; Diversion to ground landing
6.2	Fuselage	Leakage	→ 1.4		
		Disintegration	Catastrophe	●	
6.3	Wing	Disintegration	Catastrophe	●	
6.4	Empennage	Disintegration	Catastrophe	●	

7.2. Availability

This section describes the availability analysis on the aircraft. It mainly focuses on the unavailability due to maintenance, as other forms of unavailability were assumed to be not different from other aircraft. The conclusion of availability analysis is that the availability is not less despite the extra maintenance the aquatic environments requires. The reason for this is that a business jet is used less often, so more time is available to carry out the maintenance.
Most of the time an aircraft is unavailable due to maintenance, it is due to a scheduled check. Different types of checks are done, with different time intervals.[1] Generally, four types of checks can be distinguished. The type A check is a minor check that can be done in several hours, while the B check consists of a more complete check. The type C check is way more extensive and for the D check the aircraft is basically completely taken apart. A quick overview of these checks for passenger aircraft is given in Table 7.2.

Table 7.2: Standard maintenance checks.

Type check	Incidence	Required time
A	400-600 flight hours or 200-300 cycles	Minimum of 10 hours
B	Every 6-8 months	1-3 days
C	20-24 months	1-2 weeks
D	4-6 years	2 months

The type A check is done every 400-600 flight hours normally, for a passenger jet. However, a business jet has far less flight hours per year, around 365 hours a year [31]. This makes the B check more frequent than the A check if the schedule shown above is stuck to. However, the A check is included in the B check. This makes the A check obsolete.
Moreover, business jets are not as frequently used as passenger aircraft. Therefore, maintenance has less influence on the availability when scheduled properly. This is because the availability does not decrease when the aircraft is unavailable and one does not want to use it at that instant. It is important though, in case of C and even more in the case of D checks, that the time it takes to perform the maintenance is quite long and in those cases it is likely that operations must be cancelled for the maintenance, limiting the availability. Due to the hostile environment the aircraft operates in, namely the aquatic environment, it is likely that maintenance is more intensive and thus takes more time. For example one wants to check for degradation due to corrosion more often. This increases maintenance times. However, the effect on the availability when smaller checks are carried out is probably negligible.

7.3. Maintainability

The maintainability analysis that is described in this section mainly focuses on the differences between a normal business jet and the water business jet. This is because the analysis would be too extensive when also focusing on the common points. The main finding of this section is that the water business jet requires more extensive maintenance and more frequently reparations, due to the aquatic environment and the configuration that results from that. This requires more expertise from the people that maintain the aircraft, increasing costs. Also, due to more frequent and extensive maintenance, both costs and required time increase. The differences that are found and their influence on the maintainability of the aircraft as described above are listed below.

Corrosive environment
Due to the corrosive environment, maintenance has to be conducted more frequently and is more extensive. Parts that can be difficult to detach must be replaced more frequently, as they have a lower life time due to corrosion. This increases the maintenance time and costs.

Leakage of water
More maintenance and inspection is required on the sealing of the hull, especially where cut outs are made in the hull, to prevent leakage and potential sinking of the aircraft. Cut-outs are for example made for landing gear and the water jet. Mitigation can be done by making sealing easy accessible if possible and limiting the amount of cut-outs.

[1] `https://www.lufthansa-technik.com/aircraft-maintenance`

Side float mechanism
The addition of the retractable side float mechanism, simply increases the amount of systems present on the aircraft. Just like other parts, it requires maintenance. An advantage is that the float mechanism is easily accessible from below the wing.

Engine location
In the chosen configuration, the engines are located on top of the wings and fuselage, making them harder to access. This decreases the safety and efficiency of the maintenance, compared to a fuselage-podded or wing connected engine. Service engineers now have to climb on top of the aircraft to be able to reach the engines. However, no other locations for the engines are possible. Supportive structures as a ladder are be needed for the engineers, together with safety measures.

Waterjet system
The waterjet system uses the salty water and is therefore a maintenance intensive system. Also, more knowledge of the waterjet system is required which is normally not used on aircraft. The accessibility of the system is however increased by the placement of the waterjet at an easily accessible location in the hull. e

Materials and coating
Protection against corrosion requires other materials and coatings. Experience and knowledge about these materials can be on a different level from a normal business jet, making maintenance less easy.

Manoeuvring on water
When manoeuvring on the water, small floating objects can be overlooked. This is very different from a runway on land, that is always clean. For this reason, bumps and leakages can initiate in the hull. This is easy to check when out of the water, only repairing takes considerably more time.

Systems for vessel operations
The systems needed to operate on the water, such as the VHF transmitter and radar, need maintenance as well. However, this is assumed to be not much more than for other systems in the cockpit and does not really change maintainability.
The differences explained above make the maintainability of the aircraft different compared to normal aircraft. As a final remark, for accessibility all maintenance is to be conducted on land, except for minor repairs that can be done on the water. The conclusion of this section is that maintenance is slightly more time consuming and more expensive. This must be kept in mind when operating the water business jet.

7.4. Safety

Section 7.1 is highly related to the safety of the aircraft. Strong interrelations between the subsystem failures makes the aircraft less safe. Because of this gives the FMECA already a good impression of the safety.
However there are some points to address in terms of safety concerns. The concept is new and therefore not similar to other projects. This could cause a high infant mortality failure rate because technologies are used that have not been used in this combination before. Secondly, there is the aggressive environment in which an amphibious aircraft operates. This will increase failure due to wear out.
Specifically the retractable side floats can impose new safety issues to the aircraft. Therefore a fault tree analysis (FTA) is applied to this subsystem. This helps understand how the subsystem can fail, to identify the best ways to reduce risk. This is displayed in Figure 7.1

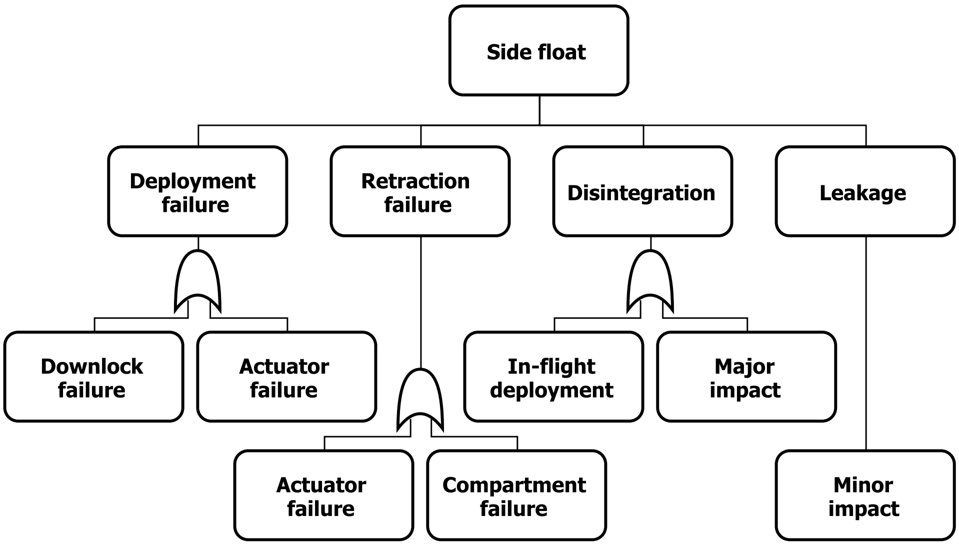

Figure 7.1: Fault tree analysis of the side floats.

Downlock is the mechanism that hold the side float down when it is deployed. When this component fails the side float can not cope with the force and is practically useless. Compartment failure can be caused by, for example, ice accretion in the compartment which makes it impossible for the side float to retract. Icing in general is a large problem for the mechanism. Local heating can be used to mitigate this risk. When the side floats deploy in-flight, which could mean Mach 0.9, this will probably cause disintegration of the side floats, but maybe also the wing due to the aerodynamic forces. It also affect the stability of the aircraft. This can be mitigated by using a warning system in the cockpit to prevent pilots from accidental deployment. The side floats can also disintegrate by major impact by, for example, a boat of rock. This could also be a minor impact which causes leakage and eventual loss of buoyancy.

8 Sustainability

Although the operation of business jet aircraft may not be seen as a very sustainable mode of transportation, the reality remains that a market for business jets exists and they will be operated. Thus, providing a product that improves upon the sustainability aspects of existing business jet aircraft can have a positive impact on sustainability. For the Jaeger amphibious aircraft, this was done in terms of emissions, noise and the potential for decentralised transport. However, due to the amphibious capabilities, a negative impact on the aquatic environment is created. To minimise this impact, mitigation strategies were made and can be found in Section 8.3.

8.1. Emission performance

The emissions, both in terms of chemical pollutant and noise, of an aircraft are critical measures for evaluating the impact of a design on its environment. Table 8.1 summarises the three major emission types examined in the preliminary design of the Jaeger amphibious business jet. As can be seen in Table 8.1, the Jaeger aircraft excels in all three emissions compared to competitors and therefore creates a positive impact on the sustainability. The remainder of this section details how these values were obtained.

Table 8.1: Emission performance.

Emission	Value	Unit	Remarks
NOx	4.1	kg/LTO	50% below CAEP/6 and well below competitors
CO2	2743	kg/hr	15% below competitors
Noise	20	EPNdB/engine	Well below stage 4 noise requirement

8.1.1. NOx emission

The NOx emission discussed in this subsection does only deal with the emissions below 3000 feet, since this is the main concern of the ICAO. The SC-2C engine installed onto the aircraft has an outstanding performance on NOx emissions. It has a NOx emission of 50% of the CAEP/6[48] , where the CAEP/6 states the limit of NOx w.r.t. the overall engine pressure ratio set by the ICAO. The limit of NOx of the CAEP/6 is based on the following Landing Takeoff (LTO) cycle:

- **Takeoff**: 100% available thrust for 0.7 minutes
- **Climb**: 85% available thrust for 2.2 minutes
- **Approach**: 30% available thrust for 4.0 minutes
- **Taxi**: 7% available thrust for 26 minutes

The amount of NOx can be calculated using Figure 8.1. On the vertical axis the amount of NOx per g/kN can be found. Since the SC-2C has an engine overall pressure ratio of 38.5[10] and 50% less NOx than CAEP/6, the aircraft has a NOx emission of 38 g/kN times the maximum thrust of the engines. This results in a NOx emission of 4.1 kg during the LTO cycle. As can be seen in Figure 8.1, this is well below other engines shown in the figure and this means that the SC-2C engine is more sustainable regarding NOx emission than similar aircraft engines.

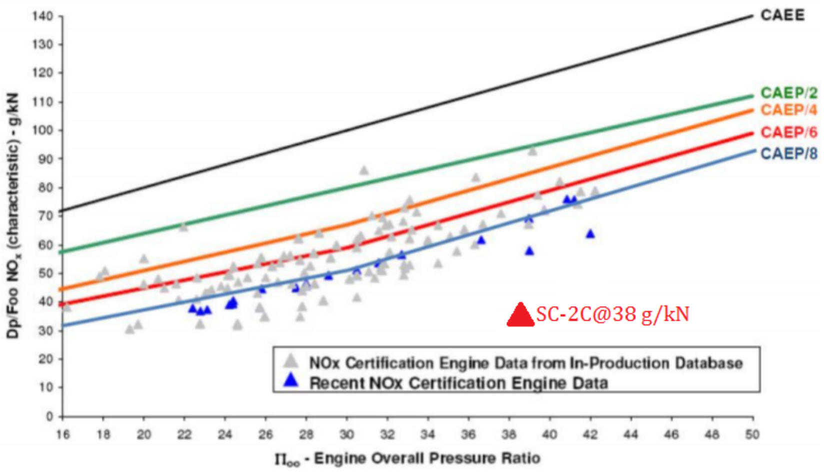

Figure 8.1: Allowed NOx production according to CAEP[7].

8.1.2. CO_2 emission

Having a 15% better fuel efficiency than similar engines in the 12 000 lbf category, the CO_2 emission of the SC-2C engine is better as well. The CO_2 emission can be calculated by knowing the fuel mass flow shown in Equation 8.1. Since the fuel efficiency is 15% lower than similar engines, a SFC of 0.57 during cruise is used which is 15% less than the similar CF34-8C engine. The thrust at cruise to calculate the fuel mass flow was calculated using Equation 8.2 and Equation 8.3 and is equal to 23020 N in average during cruise. Knowing the fuel flow $\dot{m}_f$ of 1338 kg h^{-1}, the CO_2 emission can be calculated using a conversion factor of: 1 kg fuel produces 2.05 kg CO_2. This results in a CO_2 emission of 2743 kg h^{-1}.

$$SFC_{cr} = \frac{\dot{m}_f}{T_{cr}} \rightarrow \dot{m}_f = SFC_{cr} \cdot T_{cr} = 0.0581\,\mathrm{kg/(h\,N)} \cdot 23\,020\,\mathrm{N} = 1338\,\mathrm{kg/h} \tag{8.1}$$

$$C_D = C_{D_{0cr}} + \frac{C_{L_{cr}}^2}{\pi A e} = 0.01982 + \frac{0.23^2}{\pi 7.830.95} = 0.0221 \tag{8.2}$$

$$T_{cr} = D_{cr} = \frac{1}{2} C_D \rho V_{cr}^2 S = \frac{1}{2} 0.02210.288250.8^2 115 = 23\,020\,\mathrm{N} \tag{8.3}$$

8.1.3. Noise

In Chapter 6 noise is covered w.r.t. to the noise requirement of 70 dBA. In this subsection the focus is on the noise performance of the SC-2C engine.
Aircraft engines have to comply with noise requirements. These noise requirements are divided into stages with stage 1 the least strict and stage 4 the most strict stage. For the SC-2C engine, the noise performance is well below the stage 4 noise requirements[48]. This means that the SC-2C noise performance are excellent and contribute to a better noise environment around airports[48] [15].

8.2. Potential for distributed transport

Imagine having a company with a lot of connections all over the world but with one problem; the company is situated on an island without an airport or infrastructure to land an aircraft. This means that to reach the company, from a far location, one has to first travel to a nearby airport to then take a boat to reach the island. This is were distributed transport comes in useful.
With distributed transport, in this sector, it is intended that instead of having to land at an airport to reach a certain location, one can reach that location directly.
Distributed transport has a lot of advantages. A lot of time is saved as one does not have to pass by the airport and does not have to take a boat, instead one can directly land and taxi to their destination. Another advantage is the reduced emissions which follow from the possible loitering and from the boat due to the same reason as saving time. This causes this concept to be very sustainable and thus being a concept which should be considered further on.
The Jaeger makes it possible to directly land at the location, the island in this case, and use its water jet to taxi to the shore or port. It has to be noted that the water jet does not cause extra emissions as it is driven by the APU and thus causing significant differences with respect to using a boat.
However, some extra systems will have to be installed as some risks are associated with this concept as boats have to be evaded while landing on water. Therefore the following procedure should be used. To select a landing area , first of all the area control centre (ACC) should be contacted. When the area is decided upon, this should be communicated to the vessels present in that area to check whether it is possible to land. In order to be able to communicate with these vessels an extra system is needed, Vessel Tracking Service (VTS). Finally when all involved parties are informed and clearance is given, the aircraft can land and taxi to its destination.

8.3. Impact of the aircraft on aquatic ecosystems

Landing on water is a unique aspect of this project. Unfortunately the effect of aircraft on aquatic ecosystems has not been investigated before. This section will discuss a number of potential risks for the environment. In addition, appropriate mitigation strategies will be given whenever possible.

Fuel spills

Large scale fuel spills pose a significant threat to the marine environment. Annually, several hundred thousands of bird die due to oil and fuel spills.[1] In addition, toxic additives in the liquids will be absorbed by the water, causing untold amounts of damage to the population of fish.
Jet fuel is a category of oil products that can not be cleaned of the water. [2] This means that no matter what, a spill will exert its full effect on the surrounding environment. Although fuels evaporate from the water surface in 24-48 hours, they do have very high concentrations of toxic additives that do not evaporate. These additives will be permanently introduced into the ecosystem.
Because refuelling on the water is an option for the aircraft, there is the possibility of fuel spills of up to 0.5 tonnes (assuming fuel flow gets shut down after that amount of spillage). The primary assumed cause for these kinds of spills is refuelling equipment failure or human error. This means that mitigation will focus on minimising the chance of human error.

[1] `http://www.sibleyguides.com/conservation/causes-of-bird-mortality/`
[2] `http://response.restoration.noaa.gov/oil-and-chemical-spills/oil-spills/oil-types.html`

Since the impact of the fuels itself can not be lessened, mitigation strategies focus on reducing the chance of fuel spills. This is achieved using two measures; Firstly, there will be strict procedures for refuelling on water. These procedures will focus on ensuring a proper, liquid tight, connection is made between the fuel tank and the refuelling system. In addition; the fuel system on the aircraft should be design such that spill can only happen due to gross negligence. This can be achieved by implementing spill preventing fuel caps and by selecting the amount of fuel to be pumped in advance.

Lubricant spills
Lubricant spills encompass large scale leakage of primarily engine lubricants into the water. Due to the nature of lubricants, they are significantly more damaging to the environment per litre of spilled liquid. However, because the leaks are orders of magnitude smaller than fuel spills, the overall impact is smaller. Lubricant spills are caused by failure of engine components. In addition, human error during maintenance of the engines can cause spills.
The impact of spill can not be lessened. Therefore mitigation focuses on reducing the chance of spills. Since engine failures can not be timed, nothing can be done about that. However, engine maintenance can be restricted to land only. Not only would it prevent human error based oil spills, land is also a lot more convenient a environment for maintenance.

Lubricant sweating
All engines 'sweat' a small amount of oil. This is simply due to the nature of the design, where oil is used close up small gaps and lubricate small gaps between moving parts. This type of sweating is universal for both jet engines and reciprocating engines and can not be stopped. The amount leaked is in the order of millilitres per week.
The only way to prevent this lubricant from entering the surrounding ecosystem, is by catching it in a special reservoir build into the engine cowling. This reservoir needs to be emptied on a regular basis, preferably during B-checks. This means that the reservoir needs to be large enough to contain the amount leaked between B-checks.

Collision with fragile, stationary, ecosystems
In addition to the structural risks associated with collisions, stationary ecosystems like reefs recover only slowly from major disturbances like that. Tropical coral only grows 0.3-2 centimetres per year. [3] This means the destruction caused by impacts will take centuries to recover.
The risk of collision with reefs can be minimised by selecting and scouting a landing site before arrival with the aircraft. In addition, the coastguard is able to assist in selecting an appropriate landing site. The impact of the collision can not be lessened for both the aircraft and the reef. Therefore preventing collisions is of the utmost importance.

Disturbance of fragile ecosystems
Just like humans, animals dislike excessive noise pollution. Especially birds who have their nesting grounds at the coast are negatively impacted by loud noises. A common effect is that the reproductive success declines significantly.
This can easily be mitigated by applying the same rules for takeoff, landing, and taxi that apply near inhabited areas as described in Subsection 6.1.4 to areas known to be bird nesting grounds.

[3] http://oceanservice.noaa.gov/education/kits/corals/coral04_reefs.html

9 Production plan

This chapter will present a basic set up for the general manufacturing and assembly of the aircraft. In this phase of the design any attention to part manufacturing is considered premature and therefore this section will focus on the assembly and the general production method.

9.1. Assembly

The aircraft will be assembled from parts and subassemblies at an assembly line, as is standard in the aircraft industry. This is done for several reasons, including production efficiency, ease of production, size of the product, operations and maintenance. The assembly line, with several branches feeding into the final line, will consist of several stations where the same crew performs the same task in a fixed amount of time. This time should be the same for each station and equals the delivery time. Figure 9.1 shows a schematic representation of the assembly line and its stations.
The order of assembly is not only based on convenience, but also financial considerations play a role. The engines, for example, are integrated at the last station to save interest costs on such expensive parts. Figure 9.2 gives a visual representation of the assembly sequence of the aircraft. Letting the same crew perform the same task at every station will lead to a learning curve, meaning less man hours will be required for the same tasks. This will reduce production costs or time as more aircraft are produced.

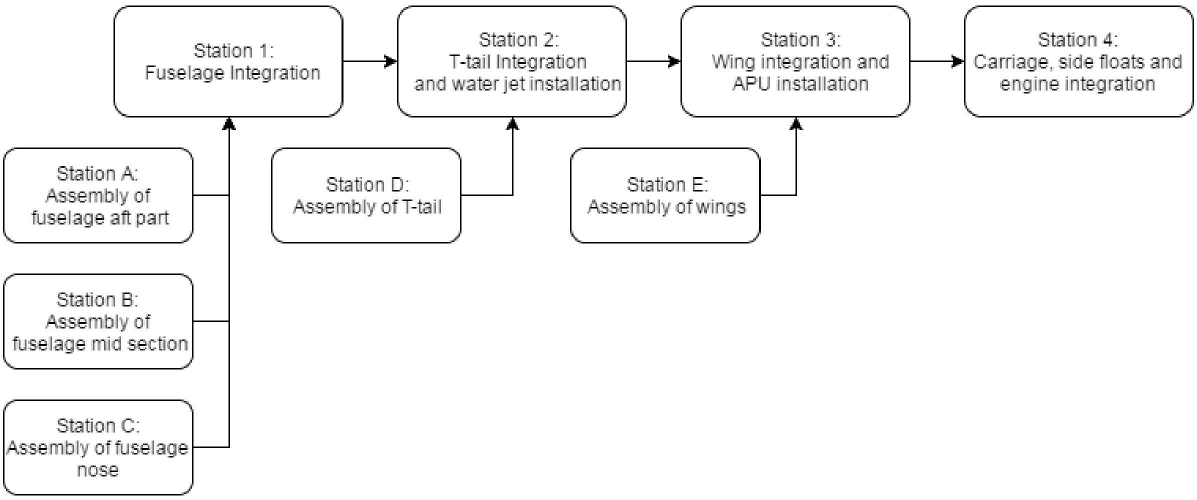

Figure 9.1: Schematic representation of the assembly line.

In the market and cost analysis it was determined that in the first 5 years of production around 100 aircraft will be produced. This comes down to a delivery time of 0.6 months, or approximately 13 working days. The workload and people should therefore be accordingly divided over the stations, to ensure each station has the same throughput time. The cost estimation method from Chapter 5 estimated a required number of man hours of 158.000 per aircraft. This will lead to around 1.500 people working full time on the manufacturing of the aircraft. This includes the full production of the aircraft, including all its parts. However, it is likely that many parts will be supplied by external parties, thereby reducing the number of people directly employed in the assembly process.

9.2. Lean manufacturing

In order to reduce the production costs, increase the sustainability, and increase the marketability of the aircraft, the principle of lean manufacturing will be applied throughout the whole production process. Lean manufacturing is a customer focused production philosophy based on a pull market and reducing waste. Lean manufacturing is not a clear method that can be implemented, but a way of thinking that should be applied throughout the whole process.
The business jet market is a pull market, where customers display a demand for customised products, in contrast to a push market where companies push their generic products to the market. Customer focus can be achieved by reducing lead times and offering personalised products. Reducing lead times is not only valued by the customers since it is directly related to their waiting time, but also reduces storage and interest costs. Offering, to some extent, custom products is a must for the business jet market, where many customers have unique wishes.
Next to material waste, lean manufacturing focuses on reducing other kinds of waste as well. Waste is defined as anything that does not directly add value to the product. Examples are transportation, rework, waiting time and storage of inventory and work in progress. These forms of waste will be minimised by an efficient factory lay out, minimal stock and no overproduction. Reducing all these kinds of waste saves costs and also increases the sustainability of the aircraft.

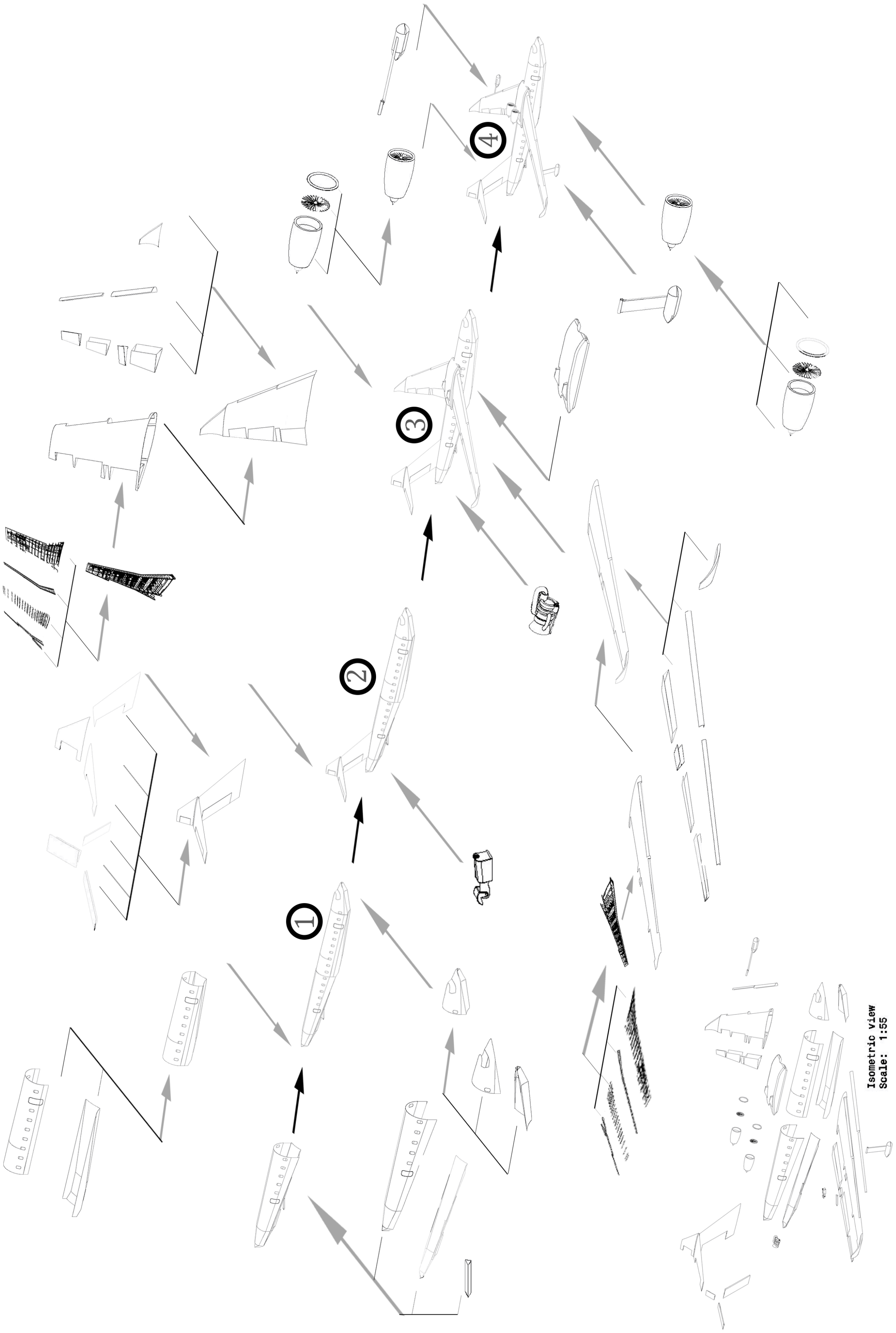

Figure 9.2: Assembly sequence chart for the aircraft.

III

Subsystem design

In order to address the feasibility of the aircraft, critical subsystems unique to the Jaeger aircraft are designed and their integration into the overall system are looked into. The main purpose of this part is to give a detailed overview of these subsystems. Each chapter addresses the state of the design. Firstly, Chapter 10 focuses on the design of the fuselage and hull with special attention to the hydrodynamics, since the hull is the major contribution to the amphibious capabilities. Secondly, Chapter 11 discusses the wing, empennage, and high-lift devices. They are all highly dependent on aerodynamics and crucial to the design of an aircraft. Thirdly, Chapter 12 is about the revolutionary design of retractable side floats. Chapter 13 considers the regular propulsion system, but the waterjet as well. The latter is a key aspect in the design in order to taxi in a more sustainable way. Finally, Chapter 14 explains the state of the supportive subsystems such as the landing gear, auxiliary power unit, avionics, and hydraulics. The interior is the discussed in that chapter too. The way the earlier discovered design challenges were treated and to what this lead will be given. After this chapter the reader will have an impression of the presented design up to the details reached at this point.

10
Fuselage and hull

The fuselage and hull form a critical subsystem of the aircraft due to its water operations. The hull shaped fuselage will need careful design to meet the conflicting aerodynamic and hydrodynamic requirements. An optimal hydrodynamic shape is not aerodynamically optimal, so a balance between the two needs to be struck. Section 10.1 elaborates on the hydrodynamic performance of the hull. This includes the trim angle, drag calculations, dynamic stability and spray characteristics. Section 11.1, on the other hand, discusses the aerodynamic performance of the hull, with special attention to the drag in cruise. Lastly Section 11.3 deals with the structural performance of the hull.

10.1. Hydrodynamic performance

Due to the amphibious nature of the aircraft, the hull design has an extra dimension that needs to be taken into account. The aspects of the hull discussed in this section are vital for the ease of operation and the comfort of the ride. More importantly, the feasibility of the entire concept will have to be put in question when the performance of the hull is not up to standards. A short recap on flying boat nomenclature is given in Appendix Q.

Subsection 10.1.1 will discuss the effect of trim on the aircraft, in addition to the extreme values obtained during operations. Subsection 10.1.2 will discuss the hydrodynamic drag that the aircraft experiences during several stages of operations. Subsection 10.1.3 will discuss the aspect of dynamic stability on the water, in so far that is possible. Subsection 10.1.4 will discuss the relevant aspects of spray on the aircraft.

10.1.1. Trim angle at rest

The trim angle is the angle that a horizontal line of the boat (usually the design waterline) makes with the water surface (in the absence of wave). In boats there is some room for varying trim angles due to the distance between the water surface and the deck of the ship, or freeboard. Unfortunately, limits on the placement of doors restricts the extreme values of the trim in this case. The trim angle can vary from the design value due to shifting load cases and waves.

Trim occurs when the centre of gravity of a vessel is not lined up with the centre of buoyancy. There will be a resulting moment that rotates the vessel. The rotation changes the underwater shape of the vessel such that the centre of buoyancy moves closer to the centre of gravity. At a certain trim angle the two centres will line up, and an equilibrium position is reached.

To calculate the shifting centre of buoyancy position, an ever changing volumetric integral needs to be solved until an equilibrium is found. The most accurate way of describing the underwater shape of the hull is by using a number of poly surfaces. Unfortunately, these surfaces are not easily expressed in terms of a analytic integral.

To solve the problem of obtaining accurate indications of trim, the program MAXSURF has been used. MAXSURF is a maritime-industry standard program used to get a prediction of various hull parameters and lateral stability. The result of the analysis performed can be seen in Figure 10.1.

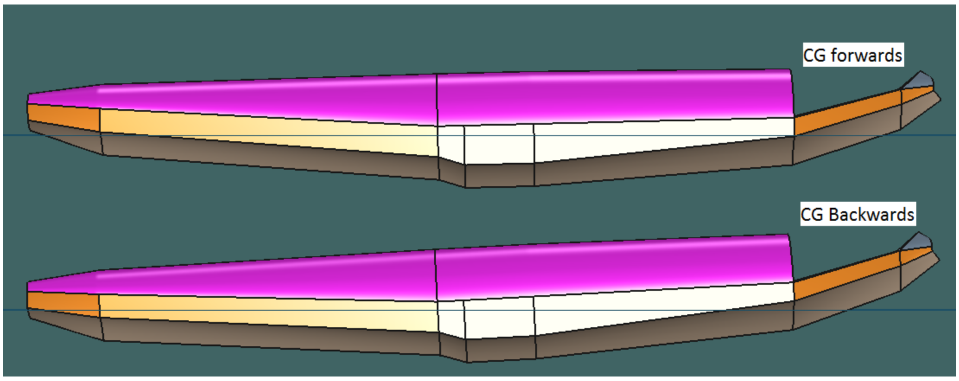

Figure 10.1: Trim angles with centre of gravity locations of 15.0 and 13.5 m behind the aircraft nose.

For the designed hull, the maximum trim angle during operation is between 1.4° and 3.1° when the aircraft stays within the design limits of centre of gravity. As a result, there is enough space for a type I door at the front of the aircraft, and a type III door at the back.
Although operationally it is not possible to load and unload the aircraft, the maximum trim in the condition of 1.5 m waves (height explained in Subsection 12.2.1) should still be considered to make an assessment of the comfort of the ride in heavy seas. Figure 10.2 shows the effects of waves on the trim behaviour of the aircraft. Although the trim angle stayed between 7° and −2.5°, those numbers should just be taken as an indication, as the stochastic nature of waves means that wave height and shape can differ wildly between them. Therefore the exact trim angles for specific wave conditions are impossible to predict.

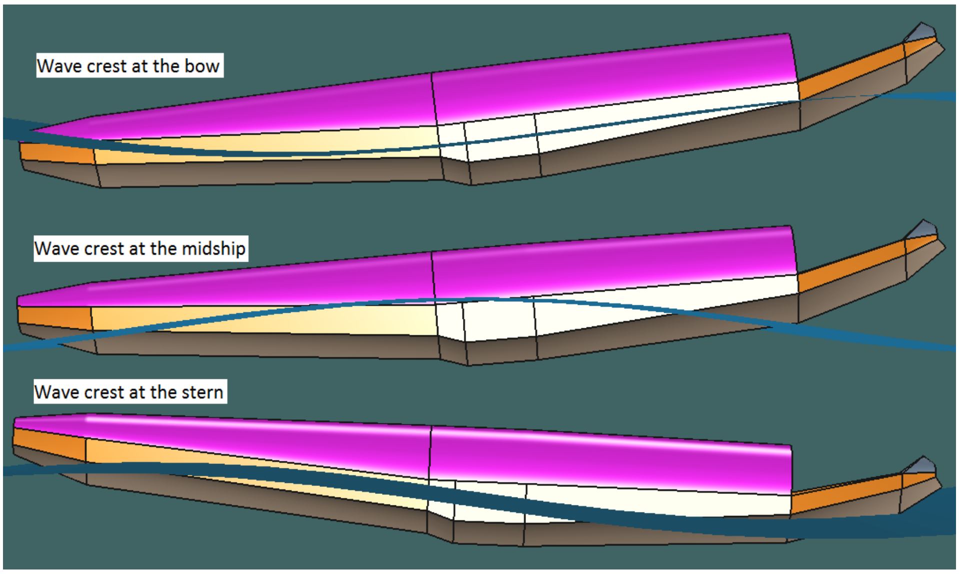

Figure 10.2: Trim angles with a 1.5 m wave along several points of the fuselage.

10.1.2. Drag during taxiing and takeoff

To support the takeoff length as presented in Subsection 4.2.2, calculations on the hydrodynamic drag are presented in this subsection. Hydrodynamic drag is ill-defined and little theory is available on the subject. The calculated drag is therefore based on equations fitted to empirical data gathered from systematic series of hull shapes tested in towing tanks. In particular, a fit from Keuning and Katgerd [28] to 'the Delft Series' for the lower speeds regimes and equations from Savitsky [43, 44] for higher speeds were used. These equations use several geometric parameters of the hull in combination with its water displacement as input. These hydrodynamic equations were combined with aerodynamic lift and drag to complete the model for predicting the water takeoff performance of the aircraft. The model was verified by comparing the results to the results of the MAXSURF computer programme. At the end of this subsection a towing tank test is proposed to validate the calculations.

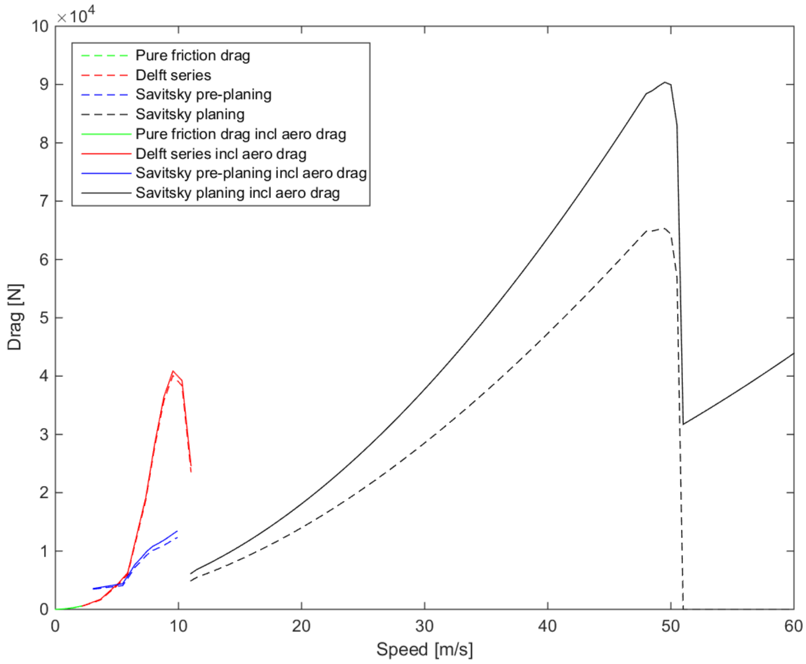

Figure 10.3: Drag as a function of speed for takeoff and landing on water.

The drag associated with a certain velocity is shown in Figure 10.3. Four speed regimes can be indicated. For very low Froude numbers wave drag is negligible and only friction drag is present, which is described using the ITTC '57 equation [23]. For Froude numbers above 0.15, next to the friction drag, wave drag occurs as described by the Delft Series. For higher speeds pre-planing and planing phenomena occur, for which the total drag is described by Savitsky.

Additionally, aerodynamic effects were added to all regimes which influences the drag in two ways. Firstly, aerodynamic drag adds to the total drag. Secondly, the aerodynamic lift reduces the displacement of the hull, this way reducing the hydrodynamic drag. The constructed curve is shaped as can be expected for a water plane. The drag hump around $9\,\mathrm{m\,s^{-1}}$ is typical for speeds below aquaplaning velocity. Furthermore, it can be seen that the hydrodynamic drag disappears at approximately $51\,\mathrm{m\,s^{-1}}$, while the aerodynamic drag increases. This corresponds to the rotation speed: the moment the aircraft increases its angle of attack and lifts off the water.

The geometric parameters that serve as input for these calculations (like the length of waterline and beam of waterline) were found from the MAXSURF model of the hull shape for different trim angles and displacements. The aquaplaning buoyant displacement was found using Equation 10.1. For lower speeds, where the aircraft serves as a displacement hull, these values are representative, but at higher speeds the aircraft starts aquaplaning and different assumptions need to be made. No theory is available to determine these geometric parameters for an aquaplaning body, so assumptions were made based on estimations. For example, it was assumed that the planing surface only consists of the after body.

$$\Delta = \mathrm{MTOW} - \frac{L_{hydro} + L_{aero}}{g} \tag{10.1}$$

This drag was used to determine the liftoff length at water, which served as an input in calculating the takeoff length in Subsection 4.2.2. It is assumed that 95 % of the maximum thrust is utilised during takeoff and that the thrust increases linearly from 25 % to 95 % in the first 10 s [18]. The liftoff distance equals 1250 m using the engines as selected in Subsection 13.1.1, as can be read from Figure 10.4. In a similar fashion a stand still distance (i.e. the distance from rotation speed to stand still on water) of 1360 m was found. This distance, however, was calculated without the effects of spoilers or other air brakes, so the actual distance will be shorter.

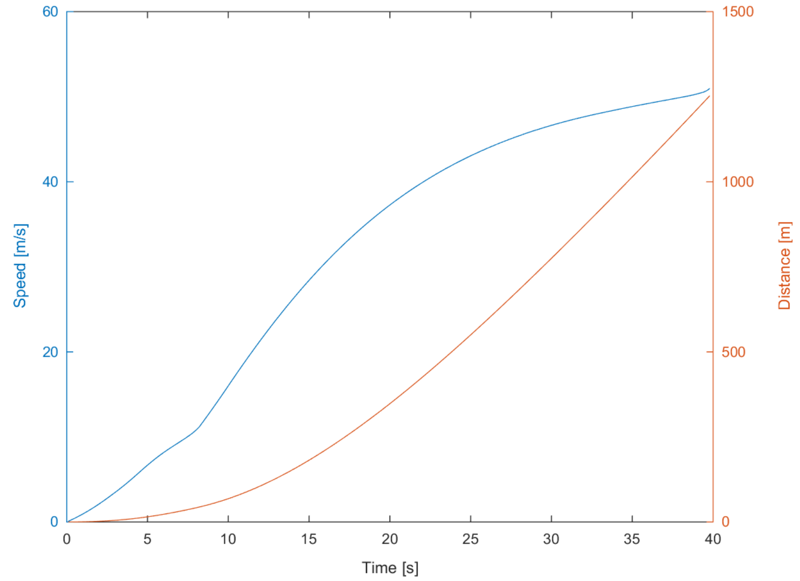

Figure 10.4: Liftoff distance of the aircraft on water.

Sensitivity analysis

The sensitivity of certain parameters which served as input to the model were analysed to guide further design. The results of this analysis are presented in Table 10.1. The maximum takeoff weight has the largest influence on the maximum drag. This is partly because of the increase in drag due to the displacement, but mostly due to the difference in stall speed, and therefore rotation speed. A lower maximum takeoff weight allows for a lower rotation speed, which corresponds to a lower maximum drag.

The width and length of the fuselage also influence the maximum drag significantly. The deadrise angle is of less influence and should therefore be driven by other design considerations. The current design meets the takeoff requirements, but changes of more than 5 % in the beam waterline, length waterline or maximum takeoff weight will require new engine selection, unless the drag is compensated by changing other parameters.

Table 10.1: Sensitivity analysis of several inputs to the model compared to the change in maximum drag.

	Percentual change	Change in maximum drag
BWL	+10%	+7.3%
	+5%	+3.6%
	-5%	-3.7%
	-10%	-7.3%
LWL	+10%	+7.3%
	+5%	+3.7%
	-5%	-3.7%
	-10%	-7.3%
Deadrise angle	+10%	+1.7%
	+5%	+0.8%
	-5%	-0.8%
	-10%	+1.5%
MTOW	+10%	+9.6%
	+5%	+3.8%
	-5%	-5.5%
	-10%	-9.2%

Verification and validation

In order to verify the model the calculated drag was compared to the drag provided by MAXSURF. Since MAXSURF is a computer program for the analysis of ships the aerodynamic influences were taken out of the model. It was also noted that MAXSURF does not account for the reduction in displacement at planing speeds, so the hydrodynamic lift was also omitted. This way the model was based on similar assumptions as the MAXSURF program, allowing for comparison.

The results of this verification are plotted in Figure 10.5. The Delft series shows some differences, but the largest discrepancies are seen in the planing phase. The differences for the Delft series can be explained by the fact that MAXSURF uses an older fit to the Delft series where less hulls are included. The differences at higher speeds are probably due to small changes in assumed geometric parameters, that have large effect at high speeds. However, the general shape and order of magnitude is comparable to the data gathered from MAXSURF and supplies confidence in the correctness of the calculations.

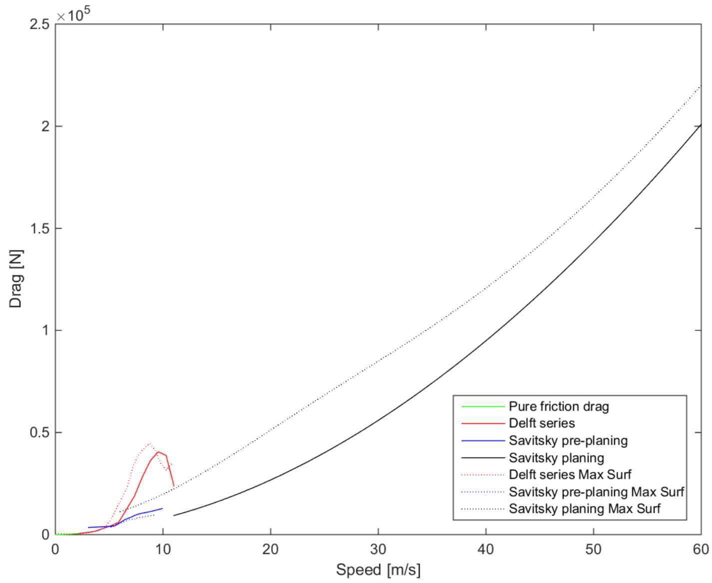

Figure 10.5: Drag versus speed without aerodynamic effects with data from the model and MAXSURF.

In order to validate and update the model, it is suggested to execute a towing tank test. The methods used for the model impose some limitations which can only be resolved by performing towing tank tests. The first limitation is that existing test have been performed with less slender hull shapes than applicable for aircraft. For example, the most slender hull tested in the Delft series has a length waterline over beam waterline ratio of 5.88, in contrast to 8.26 for the water business jet. Moreover, all theory is based on tests performed at lower speeds than required for the takeoff of an aircraft. This means that the calculations are extrapolations of the test data, making them in general less reliable. A custom towing tank test resolves this issue, providing more accurate data for determining the hydrodynamic performance.

A towing tank test consists of an elongated water basin through which scale models of hulls are towed while measuring, amongst others, the total resistance. When scaling results of a test, two non-dimensional parameters are of interest: the Froude number (which is related to wave forming) and the Reynolds number (which is related to viscous effects).

When looking at these two parameters as described in Equation 10.2 it is evident that when scaling a test (i.e. changing the characteristic length L) it is not possible to keep both the Reynolds number and Froude number equal to the full scale value. Since the Froude number describes the forming of waves, which influences the wetted area, it is common practice to let the Froude number correspond to full scale model and correct for the difference in Reynolds number. Froude's hypothesis is commonly used for this, which states that the total drag consists of frictional drag, which is only dependent on the Reynolds number, and residual drag, which is only dependend on the Froude number. Froude's hypothesis is described in non-dimensional parameters in Equation 10.3.

$$Re = \frac{VL}{\nu} \qquad\qquad Fr = \frac{V}{\sqrt{gL}} \tag{10.2}$$

$$C_T = C_F(Re) + C_R(Fr) \tag{10.3}$$

Equation 10.4 is used to determine the full scale drag coefficient of a hull, based on measurements of a scaled model at a corresponding Froude number. The friction coefficient is determined as a function of the Reynolds number by the ITTC '57 frictional correlation line in Equation 10.5 [23].

$$C_{T\,hull} = C_{T\,model} - C_{F\,model} + C_{F\,hull} \tag{10.4}$$

$$C_F = \frac{0.075}{\left(log_{10}(Re) - 2\right)^2} \tag{10.5}$$

The towing tank test is designed for usage of the large Delft University of Technology towing tank test facility. Its dimensions are 142 by 4.22 by 2.50 m with a maximum towing speed of $8\,\mathrm{m\,s^{-1}}$ [1]. To avoid wave interference with the walls, towed models should not be larger than on fifth of the tank width [29]. For the Delft towing tank this results in a maximum model width of 0.84 m.

In order to maintain the same Froude number as at $50\,\mathrm{m\,s^{-1}}$ and adhere to the maximum towing speed a model sized 0.069 by 0.596 is required. However, at a towing speed of $8\,\mathrm{m\,s^{-1}}$ the corresponding Reynolds number of the model will be 244 times smaller compared to the full scale value. Using a larger test model reduces this difference in Reynolds number, but requires a larger towing speed to reach the required Froude number.

For this reason it is proposed to perform the towing test with two models. One smaller model is used to acquire the drag coefficients for the higher speeds, and one slightly larger model to determine the drag more accurately at lower speeds. The other model will have dimension of 0.192 by 1.59 m, leading to a maximum Froude Number of 2.03 (equivalent to a $30\,\mathrm{m\,s^{-1}}$ full scale speed). The Reynolds number at a towing speed of $8\,\mathrm{m\,s^{-1}}$ is in this case 'only' 54 times higher than for the full scale hull. Appendix G shows the proposed testing speeds for both models.

Summarising, the towing tank test will consist of the following steps:

1. Both models are towed trough the tank at speeds as indicated in Appendix G.
2. The total resistance is measured for each speed and converted to non-dimensional coefficients.
3. The resistance coefficient is corrected for the deviant Reynolds number using Equations 10.4 and 10.5.
4. The full scale drag is plotted versus the velocity and compared to Figure 10.3 as final step in the validation.

10.1.3. Dynamic stability during high speed operations

For planing hulls, porpoising may impose a problem for the handling, structural integrity, comfort and speed of the aircraft. Porpoising is defined as the oscillating motion of a boat in both pitch and heave of sustained or increasing amplitude, mostly occurring at higher speeds.

Savitsky [43] provides a preliminary method, mostly based on reference [6], to evaluate the porpoising behaviour based on the basic planing coefficients C_V, C_L and τ. For a given deadrise angle, a relation between C_L, τ and the porpoising stability exists. In general, a higher C_L, lower trim angle and higher deadrise are beneficial for porpoising stability. In the planing phase, the water business jet has a trim angle of 4°, a $\sqrt{C_L/2}$ ranging between 0.19 and 0.34 and a deadrise angle of 25°. Figure 10.6 indicates that stable planing should occur in this situation.

[1] `http://www.3me.tudelft.nl/en/about-the-faculty/departments/maritime-and-transport-technology/research/ship-hydromechanics-structures/research-facilities/towing-tank-no-1/` Retrieved 21-06-'17

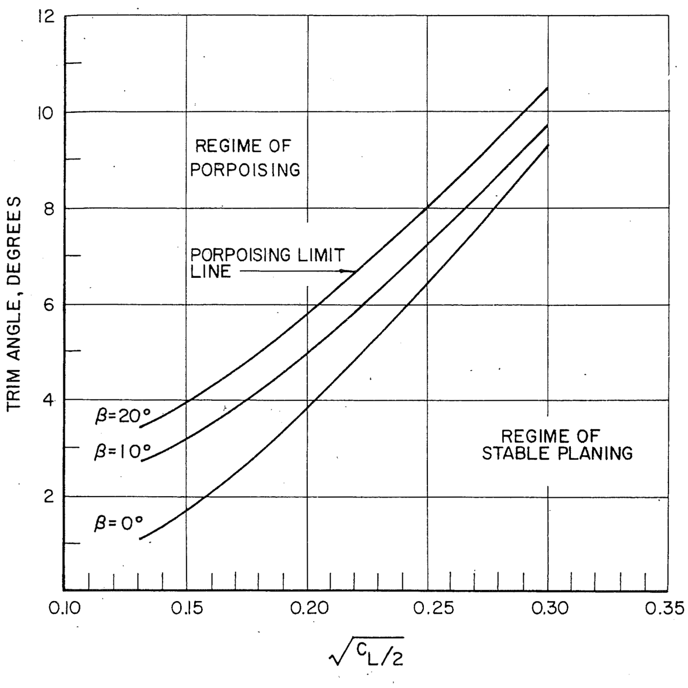

Figure 10.6: Porpoising limits for prismatic planing hulls [43].

10.1.4. Spray characteristics

The spray characteristics of the hull at higher speed play a significant role in the performance of the hull and should therefore be addressed. Firstly the amount of spray should be minimised to avoid, for example, water ingestion into the engines. Moreover, the forward component of spray causes additional drag, which is undesirable. Attention should also be paid to the visibility of the pilots, which should not be blocked by the spray.

Thurston [49] presents a preliminary estimation of the spray characteristics via a spray coefficient K, as defined in Equation 10.6. $K = 0.0525$ corresponds to light spray, while $K = 0.0825$ is defined as acceptable for overload and $K = 0.0975$ indicates excessive spray. A spray coefficient of $K = 0.0718$ was found for the water business jet, indicating acceptable spray.

$$K = \frac{\Delta}{B \cdot \rho_{\text{water}} \cdot L^2_{\text{forebody}}} \tag{10.6}$$

While negligible at lower speeds, whisker drag becomes a larger contribution at higher speed of up to 15 %. Spray rails can be installed to reduce this drag up to 6 % at high speeds. Savitsky [45] provides some design considerations for the strips. Looking from the side the strips should be short with the backward parts just over the stagnation line. Looking from the front a triangular shape is suggested with sharp edges. Savitsky provides several test results which show that spray strips reduce the drag at high speeds, without increasing the drag at low speeds or other characteristics of the hull.

However, the direct effects of spray strips on the aerodynamic performance is not known. It is suggested that the spray characteristics are also investigated in the towing tank test as described in Subsection 10.1.2. With more information on the effects of spray rails on the hydrodynamic and aerodynamic performance a tradeoff can be made whether spray rails are needed or not.

10.2. Aerodynamic performance

This section treats the aerodynamic performance of the fuselage. Specifically, two aspects are looked into. First, Subsection 10.2.1 elaborates upon the drag performance, which is part of the drag performance estimation for the full aircraft. This analysis was given priority in this phase of the design, since the drag highly affects the attainable range of the concept, which is one of the most important requirements. In an earlier design phase, it was identified that the step in the fuselage hull introduces a high risk of shock wave formation. Therefore a qualitative assessment on the effect of the hull geometry on the airflow at high Mach numbers was performed, of which the findings are presented in Subsection 10.2.2.

10.2.1. Drag performance estimation

In this phase of the design a drag performance estimation of the full aircraft was performed. This subsection presents the aspects of this analysis which are of relevance with respect to the fuselage.

Method, assumptions and limitations

The method used to estimate the zero-lift aerodynamic drag for the fuselage is presented in Appendix I. The method is presented as a parametric drag estimation which can be applied to non-conventional fuselage shapes. However, it was found that it is hard to take the hull shape into account. This was due to the fact that the proper fineness ratio is rather ambiguous for boat shaped bodies [50]. Therefore, the fineness ratio was determined as if the fuselage would have a conventional shape. To account for the hull shape fuselage, a drag penalty based on statistical data was used. The used reference states that the hull accounts for 21 % of the total zero-lift drag [46]. Important input parameters include fuselage length, maximum fuselage diameter, fuselage base area, maximum frontal area and Mach number.

Results and sensitivity analysis

Table 10.2 presents the results for the zero-lift aerodynamic drag estimation. This estimation was done for relevant Mach numbers: 0.80 for slow cruise speed, 0.85 for design cruise speed, and 0.90 for maximum operating speed. Table 10.3 and Table 10.4 present the results of the performed sensitivity analysis.

Table 10.2: Zero-lift drag coefficient for fuselage and aircraft in cruise configuration at FL410.

Mach number		0.8	0.85	0.9
Fuselage	Friction [-]	0.003 00	0.002 96	0.002 91
	Wave [-]	0	0	0.000 202
	Penalty due to hull [-]	0.002 56	0.002 83	0.004 16
	Total [-]	0.005 56	0.005 79	0.007 28
	Percentage of full aircraft [%]	45.6	42.9	36.7
Full aircraft	Friction [-]	0.008 61	0.008 59	0.008 56
	Wave [-]	0.001 03	0.002 07	0.007 09
	Total [-]	0.0122	0.0135	0.0198
	Difference with design cruise Mach [%]	−9.50	0	46.9

The first observation is that the found value of 0.0135 for the zero-lift drag at the aimed operating cruise Mach number of 0.85 is comparable to regular business jets [33]. It is an indication that the current design configuration is feasible in terms of aerodynamic drag performance. This is further supported by the performance characteristics as presented in Chapter 4. With 43 % the fuselage has a large contribution to the zero-lift drag of the aircraft. This can be attributed to the fact that the hull shape imposes a large penalty on the drag.

Table 10.3: Sensitivity analysis of zero-lift drag coefficient for fuselage and aircraft with respect to hull drag penalty.

Change in drag penalty hull [%]	Change in zero-lift drag coefficient [%] Fuselage	Full aircraft
−50	−27.3	−11.7
−40	−22.4	−9.61
−30	−17.2	−7.39
−20	−11.8	−5.05
−10	−6.03	−2.59
0	0	0
+10	+6.36	+2.73
+20	+13.1	+5.61
+30	+20.2	+8.67
+40	+27.7	+11.9
+50	+35.7	+15.3

Table 10.4: Sensitivity analysis of zero-lift drag coefficient for fuselage and aircraft with respect to fuselage length and maximum diameter.

Change in input parameter [%]		Change in zero lift drag coefficient [%]	
		Fuselage	Full aircraft
Fuselage length	-10	-4.73	-2.03
	-5	-2.37	-1.02
	0	0	0
	5	+2.37	+1.02
	10	+4.75	+2.04
Fuselage max. diameter	-10	-12.9	-5.54
	-5	-6.7	-2.86
	0	0	0
	5	+7.1	+3.04
	10	+14.6	+6.27

The zero-lift drag shows a high degree of sensitivity with respect to Mach number above 0.85. Cruising at 0.8 Mach reduces the zero-lift drag with approximately 10 %, whereas cruising at 0.9 Mach increases the zero-lift drag with almost 50 %. Such an increase most probably results in a much higher fuel consumption. This implies that operating at a cruise Mach above 0.85 would mean cutting back on range a lot. In addition, it indicates that flying at 0.9 Mach would come be aerodynamically challenging. To correctly judge this however, it would be necessary to have a solid estimation of the total drag coefficient of the aircraft at such conditions.

Since the drag penalty imposed by the hull shape is merely based on statistical data, it is plausible that this value will turn out to be considerably far off from the actual penalty due to the hull shape. Therefore a large variation of −50 % to 50 % was considered within the sensitivity analysis for this parameter. It can be seen that in such cases, the zero-lift drag shows a large change. For the fuselage length and maximum diameter a variation of −10 % to 10 % on input values was considered. At these extremes, the maximum change in zero-lift drag is just over 6 %. However at this design stage the fuselage length and maximum diameter have a much lower probability of changing to such an extent than the drag penalty due to the hull.

Discussion, verification and validation

As mentioned in Appendix I the individual models for friction and wave drag have been validated [19] [53] [13], whereas the drag penalty due to the hull is based on statistical, real-life data. However, the combination of the models, and addition of the drag penalty, within this method as a whole have not been validated. It turned out to be too challenging to acquire useful drag data of reference aircraft with the available resources. To have assurance on the obtained results, validation methods should be established.

Firstly, the combination of the friction and wave drag models should be validated. Firstly, this can be done using data of reference aircraft as input values and comparison for output values. Then, validation should be done with the used parameters excluding the hull shaped fuselage. This could take place in a similar fashion as how this friction model combined with another wave drag model was validated by Gur, Mason and Schetz [19]. In short, this includes performing a wind tunnel test in which special attention should be paid to match the model and test values of the Reynolds number and location of transition from laminar to turbulent flow. After validation of the friction and wave drag models has been done, the hull shape should be included in the wind tunnel test. Through this, it can be assessed whether the applied drag penalty due to the hull is a good approximation. This is of great importance since the sensitivity analysis showed that the zero-lift drag is susceptible to large changes due to the large range of possible drag penalty values.

Conclusion and recommendations
The results indicate that the current design configuration is feasible in terms of aerodynamic drag performance. However, the effect of the hull was based on statistical data which did not account for the specific geometry of the hull. In addition the results showed a high degree of sensitivity to exactly this effect of the hull. On top of that, the method is a combination of different models which is yet to be validated. Therefore it can be concluded that although the results indicate feasibility at this point, a high degree of uncertainty is present.
It is highly recommended to aim future analysis and design efforts at the effects of the hull shape on the aerodynamic drag. This includes validation of the methods used, a thorough literature research on hull shaped fuselages and further exploration in full configuration drag estimations based on parametric geometry definition.

10.2.2. Effect of hull geometry on airflow at high Mach numbers

A rough estimation of the flow around the hull was performed for Mach numbers 0.8, 0.85 and 0.9 in standard ISA conditions at 41 000 ft. This rough estimate consists of a three dimensional computational fluid dynamics, CFD. The analysis was done for the step on the lower side of the hull because this is the main difference between the Jaeger and a conventional aircraft. The analysis was performed using ANSYS CFX for the analysis and ICEM CFD for meshing. The exact setup of the analysis can be found in Section A.1. The final results in Section A.2 show a shock wave being created at the step for all three conditions. The shock wave does become less intense when the Mach number goes down. The flow detaches from the surface at the step and reattaches again further downstream. Lower mach numbers cause this reattachment to occur at a further distance from the step. The opening boundary condition is not set accurately, which causes the flow near these boundaries to be inaccurate. This boundary condition gives additional errors when the flow is not attached to the wall at the opening. In this case the whole domain is effected. Mach numbers lower than 0.8 showed this effect and are therefore not included in the report. The step is modelled as an infinite plate. In real life it is a three dimensional object, causing airflow around the step that will lower the shocks created. In conclusion, the analysis show a high probability of shock waves forming around the step. The shock waves will cause an increase in drag and might cause an increase in noise levels. Both these effects have to be studied in greater detail for a three dimensional model. This model can also be used for other aerodynamic analyses This was not performed since not enough computing power was available to model a domain around the complete aircraft.

10.3. Structural performance

An amphibious aircraft design introduces challenges to the structural design of the fuselage. To perform an accurate feasibility assessment it is important to understand the pressures that act on the hull which is explained in Subsection 10.3.1. The fuselage holds the payload and brings all the structural elements together. Especially the wing applies huge loads on the fuselage. Because of this the integration between the fuselage and wing is discussed in Subsection 10.3.2.To support further design, the critical aspects for the structural design of the fuselage are addressed in Subsection 10.3.3.

10.3.1. Hull load case analysis

The structural design of the hull should specifically consider the landing and takeoff case since they are expected to differ significantly. Fortunately, the certification document for the Beriev Be-200ES-E, a similar aircraft in terms of hull shape, specifies a parametric design for the hull and main float structures [11]. This includes the bottom plating, frames, bulkheads and stringers. Local pressures can be calculated for the keel and the chine which are dependent on takeoff stall speed and the deadrise angle. Linear interpolation can be used to obtain a distribution. Figure 10.7 shows the pattern as a result of this analysis.

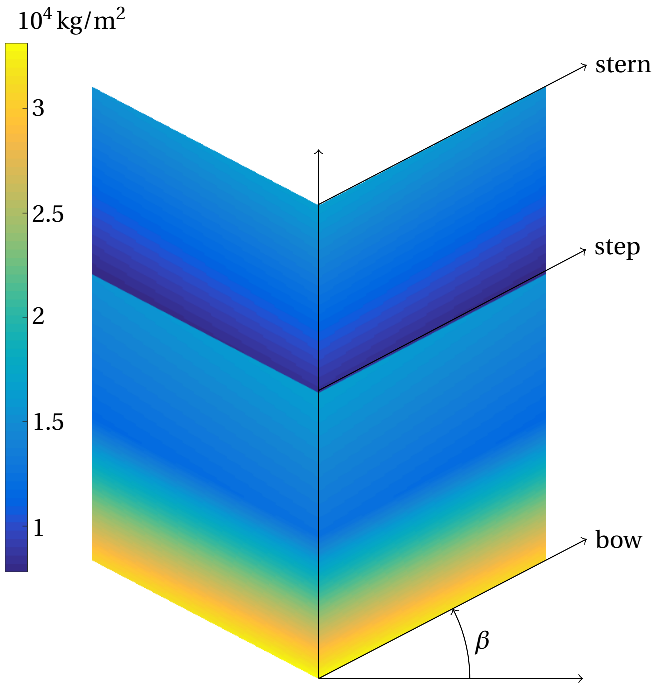

Figure 10.7: Local presssure distribution on the hull.

The pressure is the highest at the keel at the bow of the hull. It decreases in the longitudinal direction until halfway the forebody. Then it increases until a sudden drop occurs at the step, after which it increases again. The lowest value occurs at the chine at the step. The same document also gives distributed pressures to design the frames, keel and chine structure. These only vary in the longitudinal direction in a similar way to the local pressures. The landing stall speed and the deadrise angle are the main inputs for this distribution.

10.3.2. Fuselage-wing integration

When an integration between the fuselage and wing is chosen this will allow further analysis of the load path in that region and support futher design. A thesis of Supamusdisukul conducts a research on five different configuration from an aerodynamic perspective [47]. The aircraft does not use a low-wing configuration due to the amphibious capabilities and is not studies in the thesis. Aerodynamically a configuration where the wing connected to the fuselage with a plain strut at distance of approximately one chord was optimal. This configuration is very unconventional and structurally challenging due to the sharp corners which could cause high stress concentrations. For the water business jet a configuration was chosen which is displayed in Figure 10.8. The wing is basically on top of the fuselage and the fuselage rises to the wing using surface blending.

10.3.3. Critical aspects for structural design

This section explains the structural analysis for the hull. It the most critical relations, structurally, are those with the hull and wing. The obtained pressure distributions can be used for initial sizing of the hull structure. Both show that the pressure on the bow can be critical. It is, unfortunately, not specified exactly in which situation (speed and mode) these pressures occur. Load factors can be calculated which can be incorporated as safety factor. Ideally a pilot lands on the step, but there is also a load factor for the bow- or stern landing case. The latter takes the radius of gyration in pitch in account. All load factors are dependent

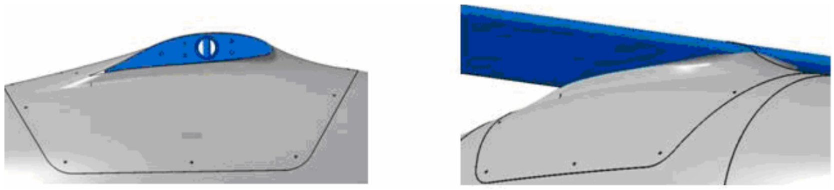

Figure 10.8: Chosen integration between fuselage and wing [47].

on the associated stall speed, design gross weight and deadrise angle. A higher deadrise angle is beneficial for the structural design because the force of the water will be more distributed. The pressures and load factors are related to the stall speed squared so when the structural design of the hull turns out to be problematic, one could invest more design effort into the high-lift devices in order to reduce the stall speed. Buoyancy provided by the hull is a critical aspect of the structural design. Regulations indicate that the aircraft should still provide sufficient buoyancy with several compartments damaged. Predicting when a compartment fails requires a sophisticated analysis which is not part of this design phase. An integration between the fuselage is wing, but mainly from an aerodynamic standpoint. Structurally this has not been incorporated in the design which should be done in later phases. The required buoyancy, the experienced hull pressures and the wing-fuselage integration provide a good starting point for the structural design, where the bow is identified as a critical point for the hull and the stall speed as most important input.

11

Wing, empennage and high-lift devices

In order to ensure proper aircraft performance aerodynamically, in cruise, takeoff, and landing, but also structurally, the wing is of course of utmost importance. First of all, in Section 11.1, the wing is sized along with the high-lift devices and a drag estimation is performed. This is followed by the empennage sizing considering the stability and controllability of the aircraft, as shown in Section 11.2. Finally the structural performance of the wing is discussed in Section 11.3.

11.1. Aerodynamic performance

This section is dedicated to the aerodynamic performance of the aircraft. Fist of all the wing sizing method is described with its result resulting from iterations including the high-lift devices sizing. Both the wing sizing and high-lift devices sizing are discussed in Subsection 11.1.1. This is followed by an estimation of the drag performance of the aircraft in Subsection 11.1.2. The behaviour of the entire aircraft at different mach numbers is assessed.

11.1.1. Wing and high-lift devices sizing for lift performance

The wing design resulted in the values presented in Table 11.1 and has the NACA 23012 as aerofoil. It can be seen that the wing has a considerable sweep angle but this is in order to not have problems with the high Mach number at which the aircraft is supposed to fly. The taper ratio was chosen to be the minimal value to avoid tip stall. As high lift devices, trailing edge double-slotted flaps and leading edge slats are used. This section first discusses how the wing was sized followed by an elaboration on the high-lift devices selection.

Wing sizing

The wing was initially sized according to Equation 11.1.

$$\frac{W}{S} = C_L \frac{1}{2} \rho V_{\text{stall}}^2 \tag{11.1}$$

A stall speed of $45\,\mathrm{m\,s^{-1}}$, which followed from the Class I weight estimation, and a maximum lift coefficient of 2.6, from reference aircraft [3], were used . This led to a surface of $97\,\mathrm{m^2}$. Later on in the design phase, this method was adapted during the sizing of the high-lift devices as this amount of lift could not be reached. The $\frac{W}{S}$ was then used for minimum thrust-to-weight ratio, being $2720\,\mathrm{kg\,m^{-2}}$, resulting in a wing surface of $115\,\mathrm{m^2}$ and leading to a smaller $C_{L_{max}}$ of 2.2.
It has to be noted that the span has been fixed at a value of $30\,\mathrm{m^2}$ which lead to a smaller aspect ratio. This value was considered to be the maximum allowed span in order to still allow for easy access to airports and waterways.

High-lift device sizing

The first step in the high-lift devices sizing was to determine which kind of high-lift devices would be used. Reference aircraft were looked into and the amount of lift required was considered, a C_L of 2.6 was aimed to reach. However, a second iteration caused this value to decrease to 2.2 as another design point was chosen, i.e. the minimum thrust-to-weight ratio. It followed that using leading edge slats and double slotted Fowler

Table 11.1: Wing parameters.

Parameter	Value	Unit
Surface	115	m^2
Span	30	m
Aspect ratio	7.83	/
Taper	0.2	/
Sweep	35	°
Root chord	6.39	m
Tip chord	1.28	m

flaps at the trailing edge were needed to reach the C_L goal. Then using the aerofoil parameters $C_{l_{max}}$ and C_{l_α}, the whole sizing process could be started. This process is the method as described in [34].
The $C_{L_{max}}$ and stall angle of attack (α_{stall}) of the basic wing could be obtained from the following formulas:

$$C_{L_{max}} = \frac{C_{L_{max}}}{C_{l_{max}}} C_{l_{max}} \tag{11.2}$$

$$\alpha_{stall} = \frac{C_{L_{max}}}{C_{l_\alpha}} + \alpha_0 + \Delta\alpha_{C_{L_{max}}} \tag{11.3}$$

Using figures Figure 11.1 and Figure 11.2, these values could be calculated. This resulted in a maximum lift coefficient, for the basic wing, of 1.42 and a stall angle of attack of 13.1°.

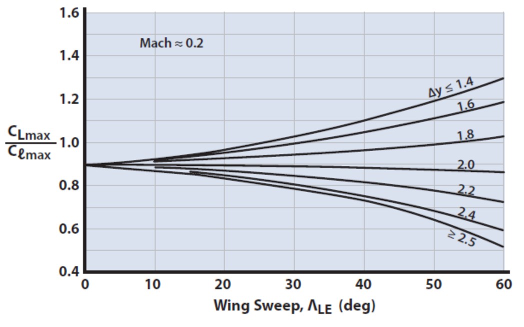

Figure 11.1: Maximum lift of high aspect ratio wings. [34]

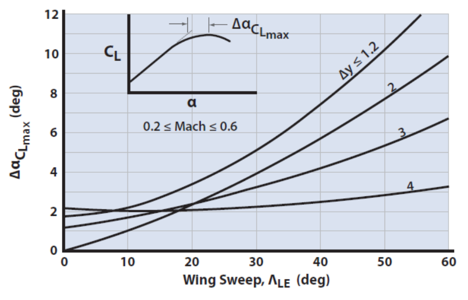

Figure 11.2: Angle of attack increment of high aspect ratio wings. [34]

For further sizing, some assumptions had to be made:

- $\delta_{\text{flap}} = 40°$
- $\frac{c_{\text{flap}}}{c} = 0.3$: This value followed from the rear spar location, which is located at 60 % of the chord, and taking into account a margin of 10 %.

- $\frac{c'}{c}_{\text{slats}}$ = 1.1: It was assumed that extending the slats would lead to an increase in chord length of 10 %.
- $\frac{S_{\text{wet}}}{S_{\text{flap}}}$ = 0.6: This value was assumed as enough flapped area of the wing is needed to generate enough lift while the area loss due to the side floats had to be accounted for.
- $\frac{S_{\text{wet}}}{S_{\text{slat}}}$ = 0.8: This value is used as the slats use almost the whole leading edge.

These assumptions lead to a ΔC_L, due to high-lift devices, of 1.28.
As mentioned, the second iteration caused the $C_{L_{max}}$ to decrease. This was because reaching the $C_{L_{max}}$ was not possible as the flapped surface did not allow for enough ΔC_L due to the integration of the side floats. Therefore it was decided to use another aerofoil (NACA 23012), with a higher $C_{l_{max}}$ of 1.89, along with a higher wing surface which would require a smaller $C_{L_{max}}$. These two changes would lead to the need for a smaller ΔC_L so that the area of the high-lift devices would suffice. The wing surface was increased by designing for the minimum thrust-to-weight ratio, being 2720 N m^{-2}.
With the current flap and slat sizes, having a wetted area ratio of 0.6 and 0.8 respectively, a $C_{L_{max}}$ of 2.7 is reached, meaning that the HLDs are oversized. However, the $\frac{S_{\text{wet}}}{S}$ ratios are rather optimistic and thus smaller flaps and slats could be used. More plausible areas would be 0.4 for the flaps as they only use the area up until 7.5 m from the centre of the fuselage due to the storage of the side float. This value also allows for ailerons to be installed on the wing. The slats can also be positioned until 7.5 m and from 10.8 m on leading to a wetted area ratio of 0.6, again due to the side float storage. Using the updated ratios, a maximum lift coefficient of 2.3 would be obtained while a value of 2.2 was needed.

Control surfaces

As control surfaces, ailerons will be positioned on the wing. Using the $\left(\frac{S_{wet}}{S}\right)_{flaps}$ of 0.4, sufficient space to place the ailerons is available. A small one, for high speed, will be positioned between the flap and the fuselage. And a bigger aileron, for lower speeds, will be placed between 10.8 m, where the side float storage stops, and the wing tip. As ailerons are normally positioned between 50 % and 90 % of the wing span [3], outboard ailerons with a width of up until 1.7 m can be used.

11.1.2. Drag performance estimation

In this phase of the design a drag performance estimation of the full aircraft was performed. This subsection presents the aspects of this analysis which are of relevance with respect to the wing and empennage.
The method used to estimate the zero-lift aerodynamic drag for the fuselage is presented in Appendix I. For estimating the friction drag, the wing and empennage planforms are divided into multiple trapezoid panels with a characteristic length for each. The number of panels were as follows: 10 for one wing, 10 for one half of the horizontal tail, and 10 for the entire vertical tail. This number of panels is similar to the values used for validation of the original model [19]. The friction drag is estimated for each individual panel and then summed to obtain the total friction drag. Important input parameters include surface area, taper ratio, span, thickness over chord ratio, sweep angle, altitude and Mach number. For estimating the wave drag, relationships based on historical data were used [13]. In this method, wave drag of the empennage is included within the wave drag calculations for the fuselage. Important input parameters include the effective thickness over chord ratio, wing camber and Mach number.
Table 11.2 presents the results for the zero-lift aerodynamic drag estimation for the wing, empennage and full aircraft. This estimation was done for relevant Mach numbers: 0.80 for slow cruise speed, 0.85 for design cruise speed, and 0.90 for maximum operating speed. It can be seen that the empennage form non-negligible contributions to the full aircraft drag.
The most notable finding is the variation of friction and wave drag with Mach number. The friction drag shows almost no sensitivity to the Mach number. However, the wave drag obviously does highly depend on the Mach number as it represents the drag due to compressibility effects. Decreasing the cruise speed from 0.85 to 0.80 results in a wave drag twice as low, whereas increasing the cruise speed from 0.85 to 0.9 would more than triple the wave drag. This has a large impact on the total zero-lift drag of the aircraft, which increases with almost 50 % when increasing cruise speed from 0.85 to 0.9. This implies that operating at a cruise Mach above 0.85 would mean cutting back on range a lot.
As mentioned in Appendix I the individual models for friction and wave drag have been validated [19] [53] [13]. However the combination of the models within this method as a whole have not been validated. To have assurance on the obtained results, validation methods should be established. The proposed approach is discussed into further detail in Subsection 10.2.1.

Table 11.2: Zero lift drag coefficients for wing, empennage and aircraft in cruise configuration at FL410.

Mach number		**0.8**	**0.85**	**0.9**
Wing	Friction [-]	0.00466	0.00467	0.00468
	Wave [-]	0.00103	0.00207	0.00689
	Total [-]	0.00569	0.00674	0.0116
	Percentage of full aircraft [%]	**46.6**	**49.9**	**58.4**
Horizontal tail	Friction [-]	0.000391	0.000401	0.000408
	Percentage of full aircraft [%]	**3.20**	**2.97**	**2.06**
Vertical tail	Friction [-]	0.000563	0.000563	0.000562
	Percentage of full aircraft [%]	**4.61**	**4.17**	**2.84**
Full aircraft	Friction [-]	0.00861	0.00859	0.00856
	Wave [-]	0.00103	0.00207	0.00709
	Total [-]	**0.0122**	**0.0135**	**0.0198**
	Difference with design cruise Mach [%]	**-9.50**	**0**	**+46.9**

11.2. Aerodynamic stability

This part focuses on the sizing of the empennage to guarantee longitudinal static stability, controllability, lateral static stability and dynamic stability. The empennage of the aircraft has been sized with deep stall risk taken into account. The final empennage sizes are as follows.

- **Horizontal tail size** 18.1 m^2
- **Vertical tail size** 11.7 m^2

11.2.1. Horizontal tail sizing

The horizontal tail was sized for stability and controllability using the methods of SEAD [17]. First, a potato plot is generated loading cargo, passengers and fuel consecutively. This gives the outer limits for the centre of gravity position. To allow the passengers to freely move around in the cabin, a margin of 0.3 m was added to the positions of both the front and aft centre of gravity. Hereafter, the minimum required horizontal tail size for stability and that for controllability were calculated. The horizontal tail size to provide stability was calculated using Equation 11.4.

$$S_{h_{min}} = \frac{(x_{cg,aft} - x_{ac}) \cdot S \cdot C_{L_\alpha}}{C_{L_{\alpha_h}} \cdot (1 - \frac{\delta\varepsilon}{\delta\alpha}) \cdot (x_{ac,h} - x_{ac}) \cdot (\frac{V_h}{V})^2} \tag{11.4}$$

As the for the T-tail the downwash ($\frac{d\varepsilon}{d\alpha}$) equals 0 and $\left(\frac{V_h}{V}\right) = 1$, this equation simplifies to Equation 11.5.

$$S_{h_{min}} = \frac{(x_{cg,aft} - x_{ac}) \cdot S \cdot C_{L_\alpha}}{C_{L_{\alpha_h}} \cdot (x_{ac,h} - x_{ac})} \tag{11.5}$$

The minimum required horizontal tail size for controllability was calculated using Equation 11.6. For $C_{m_{ac}}$ the aerofoil, flaps, fuselage and engine nacelles contribution was taken into account.

$$S_{h_{min}} = \frac{(x_{cg,front} - x_{ac} + \frac{Cm_{ac}}{C_{L_{A-h}}}) \cdot S}{\frac{C_{L_h}}{C_{L_{A-h}}} \cdot (x_{ac,h} - x_{ac}) \cdot (\frac{V_h}{V})^2} \tag{11.6}$$

Again, simplifying due to the T-tail configuration gives Equation 11.7

$$S_{h_{min}} = \frac{(x_{cg,front} - x_{ac} + \frac{Cm_{ac}}{C_{L_{A-h}}}) \cdot S}{\frac{C_{L_h}}{C_{L_{A-h}}} \cdot (x_{ac,h} - x_{ac})} \tag{11.7}$$

The highest minimum required horizontal tail surface area is the one selected for the design. An extra 15 % surface area is added to mitigate the deep stall risk that is inherent to the T-tail configuration. The main wing, including the engines and fuel, is moved forward or backward until the lowest required horizontal tail surface is found. This will allow for the lowest drag solution, and therefor lower emissions and cost. The surface area found was 18.1 m^2. Calculating the horizontal tail volume with Equation 11.8 gives a value of 0.57, which is similar to aircraft such as the JRF-6B, Martin PBM-3, G.A.-III and even the 747SP[40]. It is relatively low to most other business jets, but this can be explained by the relative high chord length of the Jaeger.

$$\mathbb{V}_h = \frac{l_h \cdot S_h}{S \cdot c} \tag{11.8}$$

11.2.2. Vertical tail sizing

The vertical tail was sized for a one engine out, full takeoff thrust at stall speed in landing configuration with the most aft centre of gravity position. This situation would cause the highest moment created on the aircraft with minimum restoring moment from the tail. The aircraft fuselage was assumed to have the height at the step throughout the entire fuselage length. The fuselage was assumed to contribute to the moment created as if it were a flat plate with a C_L that is one fifth that of the vertical tail in the critical situation.
The vertical tail is sized to obtain moment equilibrium around the most aft centre of gravity according to Equation 11.9. This condition would cause the aircraft not to spin out of control when no rudder inputs are given. When rudder inputs would be considered, the size of the tail could be decreased, since a higher $C_{L_{max_{vertical}}}$ can be achieved. The vertical tail size required is 11.7 m^2. Finally the vertical tail volume coefficient is calculated and compared to other aircraft in Roskam [40]. The vertical tail volume is calculated with Equation 11.10 resulting in 0.041. This is in the range of some other seaplanes as the P68B, J4F-1 and JRF-6B [40]. These seaplanes are all twin propeller aircraft and have their engines mounted very close to the centre line of the aircraft as well. The engine positioning is addressed in Subsection 13.1.2. The tail volume coefficient is however less than that of other business jets and transport aircraft. These business jets have their engines mounted further away from the centre line of the aircraft. The fly by wire system will provide extra stability to the aircraft since the control surfaces are actively used for stability. This could have been used to lower the tail size, however an increase in the stability limit was chosen, which leads to more safety.

$$S_v = \frac{T \cdot l_{eng} + 0.5 \cdot \rho \cdot V_{\text{landing}}^2 \cdot C_{L_{max}} \cdot l_{fus} \cdot h_{fus} \cdot (x_{cg,\text{aft}} - x_{ac,fus})}{0.5 \cdot \rho \cdot V_{\text{landing}}^2 \cdot C_{L_{max_v}} \cdot S_{vertical} \cdot (x_{cg,\text{aft}} - x_{ac,v})} \tag{11.9}$$

$$\mathbb{V}_v = \frac{(x_{ac,v} - x_{ac,w}) \cdot S_v}{S_w \cdot b_w} \tag{11.10}$$

11.2.3. Dynamic stability

No analysis of the dynamic stability of the aircraft has been performed. The fly-by-wire technology will allow the aircraft to be actively dynamically stable, however the passive dynamic stability shall be researched. This part will describe the procedure for researching the dynamic stability of the aircraft.
To analyse the dynamic stability of the aircraft, the longitudinal and lateral stability derivatives and control derivatives has to be found. After obtaining these parameters, a state-space model of the aircraft can be set up and solved for the eigenmotions of the aircraft. This model can be setup without active damping, creating the passive dynamic stability eigenmodes, or with the active damping performed by the fly-by-wire system, creating the active dynamic stability eigenmodes. There are two ways of finding the stability and control derivatives, one consists of wind tunnel tests, the other of CFD analysis.

1. **Wind tunnel test:** In the wind tunnel a model of the aircraft can be rotated around its three axes to find the induced forces and moments. From these forces and moments the stability derivatives can be calculated. Other models with control surfaces deployed should be tested separately to determine the control derivatives.
2. **CFD analysis:** The stability and control derivatives can be found by rotating the domain over all three axes and determining the induced forces and moments. From these forces and moments the stability derivatives can be calculated. A separate CFD analysis with different control surfaces deflected has to be compared to the clean configuration to calculate the control derivatives. These derivatives should be calculated for different aircraft configurations such as gears deployed, floats deployed, flaps deployed and speed brakes deployed in different atmospheric conditions like sea level and high altitude, low and high velocity and finally turbulence.

CFD analyses are much less costly than wind tunnel tests and provide accurate results. The CFD analysis should however be validated by a wind tunnel test for at least one condition to ensure correct results. For a proper CFD analysis of the complete aircraft, a lot of computing power is required. This will be part of future developments of the aircraft. Ansys, as used in Subsection 10.2.2, can be used to perform these CFD analyses.
The vertical tail size will have to be increased in case of an unstable dutch roll stability mode. The vertical tail has to be sized correctly before going into further detail on the project. It is recommended to do the dynamic stability analysis in the next stadium of the project.

11.3. Structural performance

In this section the structural performance of the wing will be discussed. First a load case analysis will be done which contains loading diagrams of the entire wing and secondly the wing-side float integration will be explained. The latter includes design options for wing-side float integration.

11.3.1. Load case analysis

To design the wing properly, loading diagrams are essential. Therefore loading diagrams were made to obtain a first impression of the loads acting throughout the wing. These loading diagrams were used to find out which location on the wing is most appropriate to install the side floats as explained in Section 12.3. Furthermore these loading diagrams will be used for the design of the whole wing which is not done for now, but will be done in the future.
The loading diagrams of the wing can be found in Figure 11.3. These diagrams were made at MTOW with maximum cargo (15 t) and 2000 kg fuel and is the most critical situation which need to be designed for. Furthermore, the loading diagrams are made at an ultimate load factor of 3.75, which is a result of a safety factor of 1.5 and the n_{max} of 2.5. The latter comes from the V-n diagram together with a V_{ult} of 140 m s^{-1} [36].

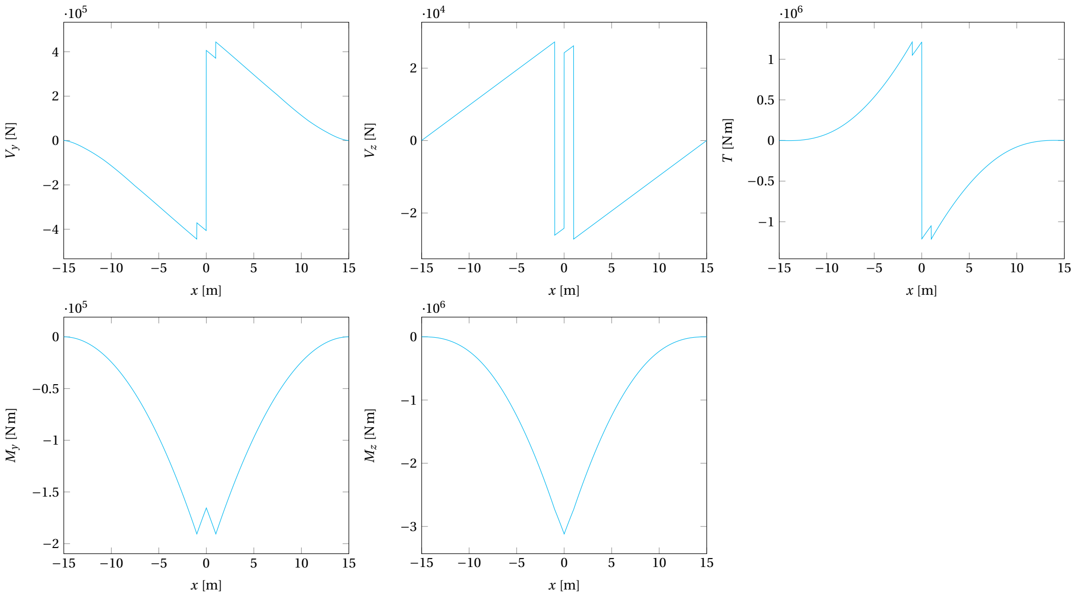

Figure 11.3: Loading diagrams of the wing at most critical situation.

As can be seen from the shapes of the graphs in Figure 11.3, the loading diagrams from each individual element contributing to the total loading diagrams were combined. The loading diagrams range from −15 m to 15 m and is in total 30 m like the wing span. The axis system for these loading diagrams can be found in Figure 12.5 and Figure 12.6. The most remarkable shape in the loading diagrams is due the weight and the thrust of the engine. The peaks caused by the engine can be found between −1 m and 1 m. The contribution of the fuel fuel weight, which should cause peaks in the loading diagrams as well is hard to see, since the contribution of the fuel weight is way less compared to the lift.
In Table 11.3 each individual element along with their responsible load is shown to get a clear overview of

each individual contribution. Also, a colour is added which can be green or red. Green means that the element has a high contribution to the total loads and determines mainly the wing box design and for red vice versa. Table 11.3 shows that the wing, drag and engine thrust have a high contribution to the loading diagram and the wing box design. This means that the sensitivity of the wing box design due to these three components is high and should be taken into account for further design.

Table 11.3: Contribution to loading diagrams of each element.

Element	V_y	V_z	T	M_z	M_y
Lift	🟢		🟢	🟢	
Drag		🟢			🟢
Fuel weight	🔴		🔴	🔴	
Wing weight	🔴		🔴	🔴	
Engine thrust		🟢	🔴		🔴
Engine weight	🔴		🔴	🔴	
Side float weight	🔴		🔴	🔴	

🔴 Low impact on wing structure
🟢 High impact on wing structure

For the construction of the loading diagrams several assumptions were made. The most important assumptions can be found below:

- **Elliptical lift distribution:** Since the aircraft has a sweep of 35 degrees and a taper ratio of 0.2, the lift distribution of the wing is close to an elliptical distribution according to Raymer [38].
- **Fuel distribution:** The fuel of 2000 kg is put as close as possible to the tips of the wing to provide maximum bending relief.
- **Wing weight distribution:** The weight of the wing is distributed according to the cross-section of the wing at each location [36].
- **One wing-fuselage attachment:** The loading diagrams show peaks or going from positive to a negative value and vice versa at x = 0 m. At this location it is assumed that the wing is attached at one point to the aircraft. At this point one vertical force,one horizontal force and one torsion moment act at this attachment and can be seen in the shape of the loading diagrams. When the wing will be designed in more detail, the diagrams change according to the wing-fuselage interference.
- **Sign conventions**: The values in the loading diagrams are according to the axis system in Figure 12.5 and Figure 12.6.

11.3.2. Integration between wing and side float: side float loads

In this subsection the impact of two critical load cases on the wing will be discussed. These two critical load cases are the maximum landing load when landing on water and the submerged loading. The maximum landing load F_y is equal to 3800 N (Table 12.5) at 11 m where the side float is connected to the wing. This landing load is just 4.7% of V_y at 11 m from Figure 11.3. Moreover when the aircraft lands on water, V_y from Figure 11.3 is much less at 11 m and therefore the wing is able to carry the side float landing load easily.
The submerged loading causes loads in three directions and are calculated in Subsection 12.3.2. However, in this case F_x and F_z are not within the maximum loads from Figure 11.3. F_z is 2150 N larger than V_z at 11 m and is 27%. However, the shear flow created by F_z is much smaller than the shear flow created by V_y, since F_z is 2.6% of V_y. Therefore it can be said that the wing is able to carry F_z, since the wing box is designed according to Figure 11.3.
Furthermore, F_x is equal to 8000 N and was not taken into account in the loading diagrams. Because F_x causes normal stresses like M_y and M_z. This normal stress can be added to these two and the wing box can be design according to the total normal stresses.

11.3.3. Integration between wing and side float: side float storage

In this subsection the change in wing box design due to the side floats storage will be discussed. As explained in Subsection 11.3.2, the loads experience by the side floats do not change the wing box layout substantially. Because of the low loads compared to the loading diagrams made for the most critical situation. However, the storage of the side floats does change the wing box layout in a certain extent. The change in wing box layout will be discussed qualitatively by proposals to guarantee stiffness and strength despite the placement of the side floats in the wing. The locations of the side floats are between the inner and outer fuel tanks shown in Figure 13.2. The design options are based on the torsion resistance and rib structure which are most influenced by the side floats. Bending is of less importance, since the spars carry mainly the bending loads and the spars do not change at the location of the side floats[20].

Torsion resistance

The main issue due to the gap in the bottom of the wing box is differential bending because of torsion shown in Figure 11.4[27]. Differential bending is caused by the front and back spar that go up or down and changes the wing in an unfavourable shape. By changing the geometry of the spars, the spars can be made stiffer and the effect of differential bending is less of an issue. However, when calculations show that this is not sufficient two wing boxes can be added before and after the front and aft spar respectively shown in Figure 11.5 and Figure 11.6. These wing boxes will add more torsion resistance to the wing and decrease the differential bending of the wing. However, the second design option makes flaps infeasible at the location of the side floats, due to the aft wing box at the location of the actuators of the flaps. Fortunately, this is not a problem, since there is still sufficient space left for the flaps somewhere else on the wing as explained in Subsection 11.1.1.

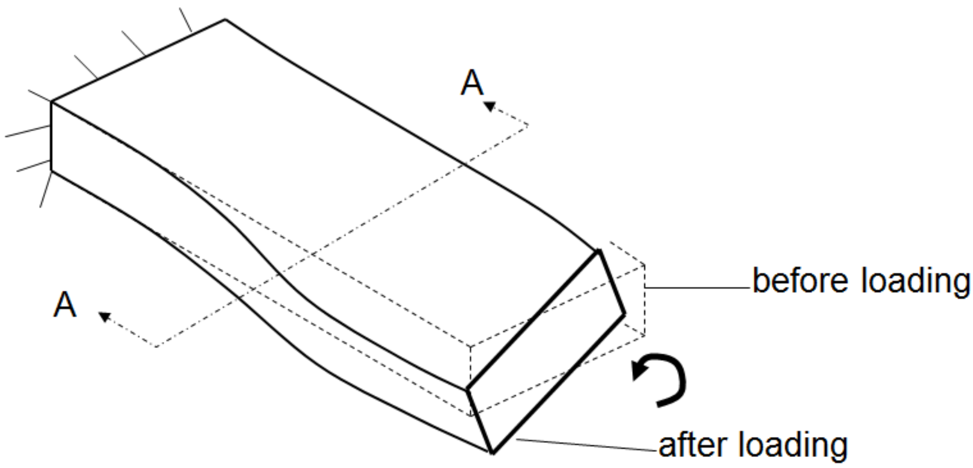

Figure 11.4: Differential bending wing due to gap bottom wing box.[27]

Figure 11.5: Cross-section wing box with front and back wing box.

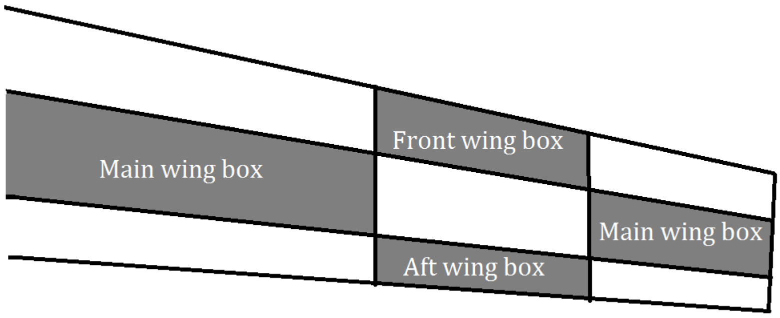

Figure 11.6: Top view wing box proposal.

Rib design

Ribs have different functions like maintaining the aerodynamic profile of the wing, providing stability against panel buckling and introducing local load into the structure. With the placement of the side floats, the ribs cannot keep the same cross-section and pitch due to the side float interference. A cross-section of the wing box with the connection, connecting the float to the hinge of the mechanism, can be found in Figure 11.5. A cutout is made in the rib to avoid interference. One thing to take into account is that the rib pitch might be lower and/or the rib thickness higher, since the rib loses its strength due to the cutout. Furthermore, there might be an uncertainty regarding the strength of the ribs at the location of the float of the side float in the wing. This is because the float has a diameter of 60 cm, while the rib pitch is generally between 20 cm 100 cm[20]. So, the rib pitch around the float might be too large, therefore special attention needs to be taken for further design to make sure that the wing is able to carry the loads at this location.

Risk and weight

To get a clear overview of the design process of the wing box at the side float storage location, Figure 11.7 was made to represent this. This flow diagram starts at 1 and 4 and flows to the right. When after a box in the flow diagram the wing box design has still not met the required performance, one has to follow the arrow with 'No' to the next box until the wing box has met the required performance characteristics. However it might be possible that box 8 is reached in the flow diagram. This would mean that the side floats are not feasible, which is a risk for the aircraft design. But this risk can be mitigated by either changing the location of the side float or going back to the design option trees and choosing the wide body configuration.
In addition, the weight of the aircraft will increase most likely due to the reinforcement of the wing. As contingency, it is expected that the aircraft weight will increase with a maximum of 10% w.r.t. the current estimated weight estimated in Table 4.4. This should be taken into account during further design.

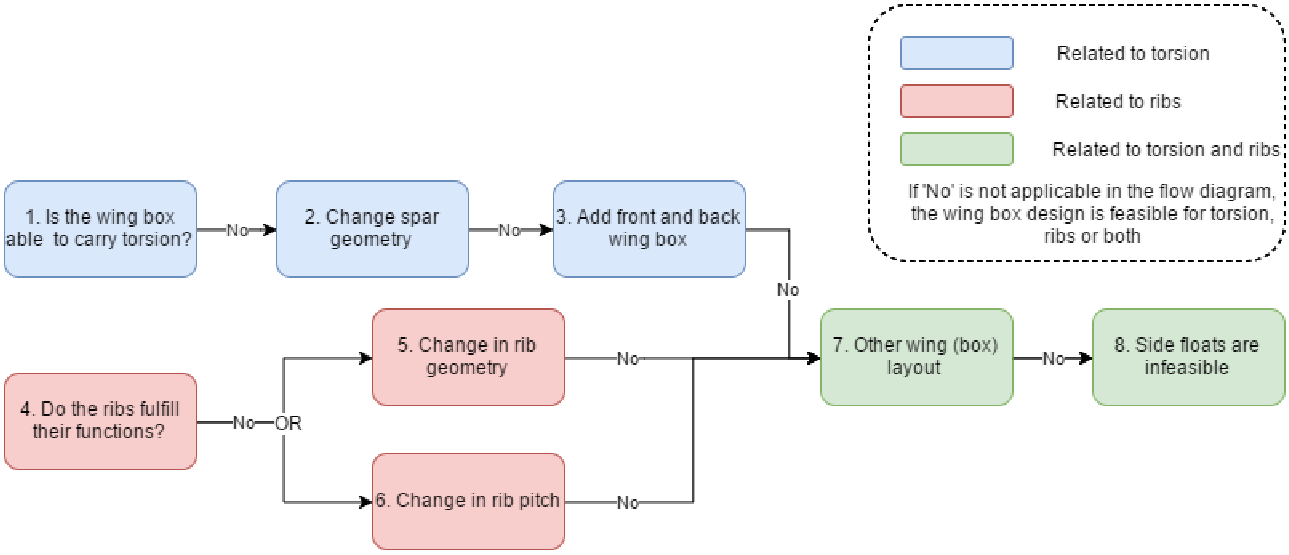

Figure 11.7: Design flow diagram for the wing box due to side float storage.

12
Side floats

Due to the aircraft's being subject to disturbing waves, the aircraft needs auxiliary floats to achieve sufficient lateral stability. Without these floats the aircraft will quickly roll on its wings. For several structural and maintenance reasons this is not a desirable situation. Therefore, the lateral stability of the aircraft needs to be augmented to ensure a long and comfortable service life of the aircraft.

Side floats (or auxiliary floats) are small flotation volumes placed significantly outboard of the aircraft to enhance the lateral stability in a number of environmental conditions. The float parameters found to provide sufficient stability are given in Table 12.1. A graphical representation of the used retraction mechanism is found in Figure 12.6.

Table 12.1: Summary of important float parameters.

Symbol	Description	Value
V_{sf}	Float volume	0.45 m^2
X_{sf}	Side float location	13.5 m
L_{piston}	Actuation piston extended length	3.7 m

An important aid in the detailed design of this subsystem was a clear inspection of its interfaces. All other subsystems with which the side float will interact, are identified by means of both an N2-chart and can be found in Section F.2. Furthermore, all parameters used as in- and output for the design process are defined in Table 12.2. The interaction with the wing box, both considering necessary storage space and induced loads, are identified as important outputs of this design. In Section 11.3 a detailed description of this integration is given.

Table 12.2: In- and outputs for the design process of the side floats.

Inputs	**Outputs**
Wave characteristics	Loads on wing box
Wind	Storage location in wing box
System weight	Stabilising moment
Regulations	Aerodynamic drag
	Hydrodynamic drag
	Weight

In Section 12.1 the stabilising concept is explained. Section 12.2 describes the required size of the float. The structural integrity of the float will be evaluated in Section 12.3. Finally, some recommendations for further design steps are given in Section 12.4.

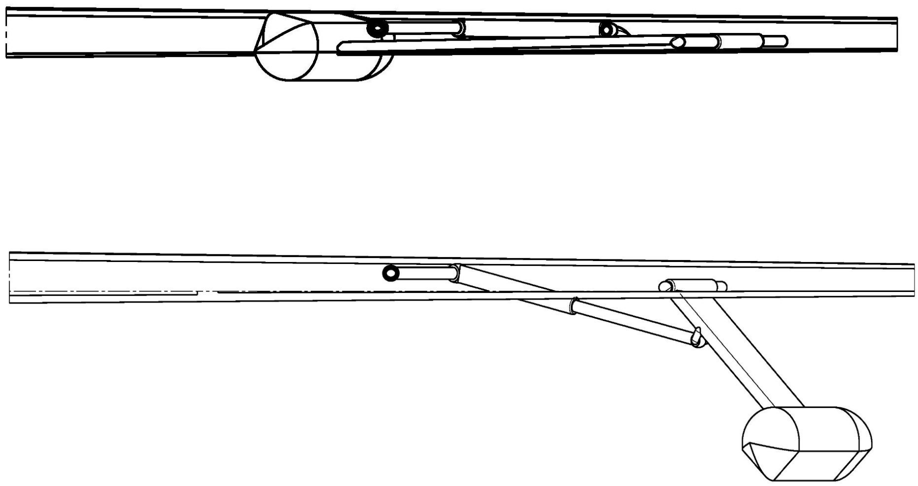

Figure 12.1: Side floats retracted in wing and extended.

12.1. Selection of connection mechanism

Although a good solution for lateral stabilisation, the side float also has adverse effects. Aerodynamic drag, additional loads on the wing and increased complexity are identified as the major adverse effects that should be analysed. A retractable mechanism with struts angled towards the wingtip minimises these adverse effects and is thus deemed to be the optimal solution. This concept is visualised in Figure 12.1. The criteria that can be used to evaluate different options for this subsystem, and ultimately to choose the most optimal design option, are explained in Subsection 12.1.1. Then different design options for this connection mechanism are presented and analysed to conclude at the most optimal design in Subsection 12.1.2.

12.1.1. Most important criteria for a connection mechanism

In order to compare different options, the criteria that make a distinct these options in their performance should be defined. Aerodynamic drag, Structural performance and complexity are identified as the three major criteria, with the first being the most important criterion.

Aerodynamic drag is considered the most important criterion, as the ability to fly in the transonic regime will require in the best scenario a large engineering effort to avoid shock-wave effects, and in less optimal scenarios will add a significant drag penalty. Shockwave effects would be disastrous for the feasibility of this high-speed long-range jet. This was also found in the sensitivity analysis explained in Section 2.3, where it was concluded that lift-to-drag ratio was an important parameter for the design performance. These arguments all support the conclusion that aerodynamic drag is the most important criterion for the connection mechanism.

Second, the influence on the structural performance of the wing is an important consideration. This criterion is twofold as the side float connection on the one hand imposes an additional load on the wing box, and on the other hand, the connection mechanism and potentially the storing mechanism adds complexity to the wing box structure.

At last, complexity is considered as a criterion, as complexity both adds cost and uncertainty to the design of the system and therefore should be avoided whenever possible.

12.1.2. Design Options and their performance

In order to find the best possible option to fulfil the requirements of this connection subsystem, first a tree with all possible design options is created. This tree can be found in Section F.1. Second, all clearly infeasible options are discarded. At last, the remaining options are all evaluated on the three design criteria by means of a tradeoff matrix, as in Table 12.3.

Although the option *Retractable in wing* has correctable deficiencies both regarding structural performance and complexity, it scores best on aerodynamic drag. Having identified aerodynamic drag as the most

important criterion in Subsection 12.1.1, it is concluded that this option is the most optimal. Even though, the risk that adverse structural performance or added complexity will influence the feasibility, should be mitigated as soon as possible. This can be done by additional structural analysis of the wing box. An approach for this is already given in Section 11.3.
An important finding is that the closer towards the fuselage the side floats is connected, the smaller the internal moment that is induced in the wing box structure because of the loads of the side float. Therefore, it is desirable to angle the connection mechanism towards the wingtip, and thus enabling it to be connected closer to the fuselage. Furthermore, in this manner, the side float is stored in a part of the wing closer to the fuselage, where the wing has a larger crossection. It should however be noted that the total internal moment caused by all forces acting on the wing box, is larger close to the root, and that thus storing the side float closer to the fuselage does potentially add more problems with the adjustment of the wing box. It is however expected that this disadvantage is cancelled out by the advantage that more room is available in the wing at that point. Considering everything, a retractable connection mechanism that stores the side float inside the wing, angled towards the wingtip, is deemed the most optimal design option.

Table 12.3: Tradeoff side float retraction mechanism.

	Aerodynamic Drag	Structural Performance	Complexity
Retractable in wing, angled towards wingtip	No drag during cruise at all	wing box should be adapted to fit side float, but no extra loads due to drag.	More complex wing box structure to fit side float.
Retractable in wing, angeled downwards	No drag during cruise at all	wing box should be adapted to fit side float, but no extra loads due to drag.	More complex wing box structure to fit side float.
Retractable in wing, angled towards fuselge	No drag during cruise at all	wing box should be adapted to fit side float, but no extra loads due to drag.	More complex wing box structure to fit side float.
Retractable to fuselage	Large drag during cruise and possible shockwave	Small moment at root	Nominal performance
Retractable to wingtip	Large drag during cruise and possible shockwave	Large moment at root	Nominal performance
Retractable to wing	Large drag during cruise and possible shockwave	Nominal performance	Nominal performance
Non-retractable mid-wing	Large drag during cruise and possible shockwave	Nominal performance	No mechanisms needed.
Non-retractable as downwards wingtip	Large drag during cruise and possible shockwave	Structure should be designed aerodynamically and large moment at root	No mechanisms needed.

12.2. Float sizing for lateral disturbances

The disturbing moments that the aircraft will encounter laterally during operations, will be primarily caused by wind and waves. The moments that need to be designed for, will be evaluated Subsection 12.2.1. The size and location of the side float will be determined in Subsection 12.2.2.

12.2.1. Quantification of lateral disturbances

This section is split up in two parts; one part for wave based disturbances, and one part for wind based disturbances.

Waves

Waves will try to roll the aircraft by changing its roll angle relative to the water surface. When the wave passes a side float, the float will try to emerge back from the water. This results in a moment that rolls the aircraft to an angle unequal to zero. Note that no matter what configuration is chosen, the aircraft will always have some roll angle in waves of sufficient amplitude.

As commonly encountered on open water, waves are a collection of simple sine waves of different periods and amplitudes. This makes it difficult to assign a single value to the wave height at any time, as sometimes the waves amplify, but other times they cancel out. In order to work around this statistical uncertainty, the significant wave height has been developed.

The significant wave height is a characteristic of the wave distribution at a given moment in time. It signifies the mean wave height of the highest third of the measured waves [21]. Typical wave heights are about half of the significant wave height. A typical distribution of waves can be seen in Figure 12.2.

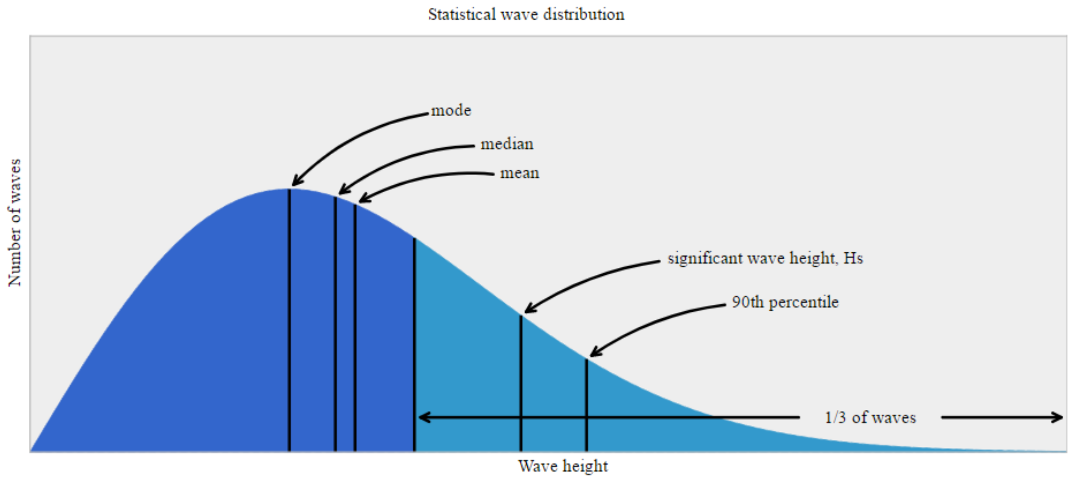

Figure 12.2: Qualitative view of the probability of different waves for a given significant wave height.

The costumer requirements dictate that the aircraft should be able to withstand waves of at least one meter. This wave height is assumed to corresponds to the significant wave height, as that is the wave height given in standard weather forecasts. EASA TCDS A.114 [11] dictates that the design wave height is the wave height at which 97% of the waves encountered during normal operations is lower than that. With a significant wave height of one meter, the required design wave height is approximately 1.5 meters.

Due to limited resources, only the expected extreme design case will be investigated. This extreme case is when the waves hit the aircraft perpendicularly. In a more detailed design phase, the effect of waves on the aircraft needs to be investigated with a wide spectrum of wave incidence angles and wave amplitudes/wavelengths. For now, the highest design amplitude (1.5m) is considered in three cases. These design cases are illustrated in Figure 12.3.

These cases have the following effects on the aircraft design:

- **Case A.** Only one float is submerged. This float will violently try to emerge from the water. In reality, this imposes the requirement that the float provides enough torque that it will rise and fall with the wave as it comes. The torque needs to be big enough to overcome the inertia of the aircraft.
- **Case B.** Only the fuselage is submerged. Due to the inherently unstable configuration of the fuselage less auxiliary floats, the aircraft will roll to a random side until one of the floats is on the water.
- **Case C.** Only the auxiliary floats are in the water. Due to their relatively small volume, the aircraft will sink until the hull has enough submerged volume to provide buoyancy again. As a result, the side floats will be fully submerged until the wave passes. Note that this case can only happen when the total distance between auxiliary floats is approximately equal to the wavelength.

Case A is the most driving for the side floats so this case will be further investigated. For simplicity, the wave is assumed to be a propagating sine wave with a constant velocity. Then, any point u on the wave has the height as described in Equation 12.1a. The relating acceleration is given in Equation 12.1b. Finally, the

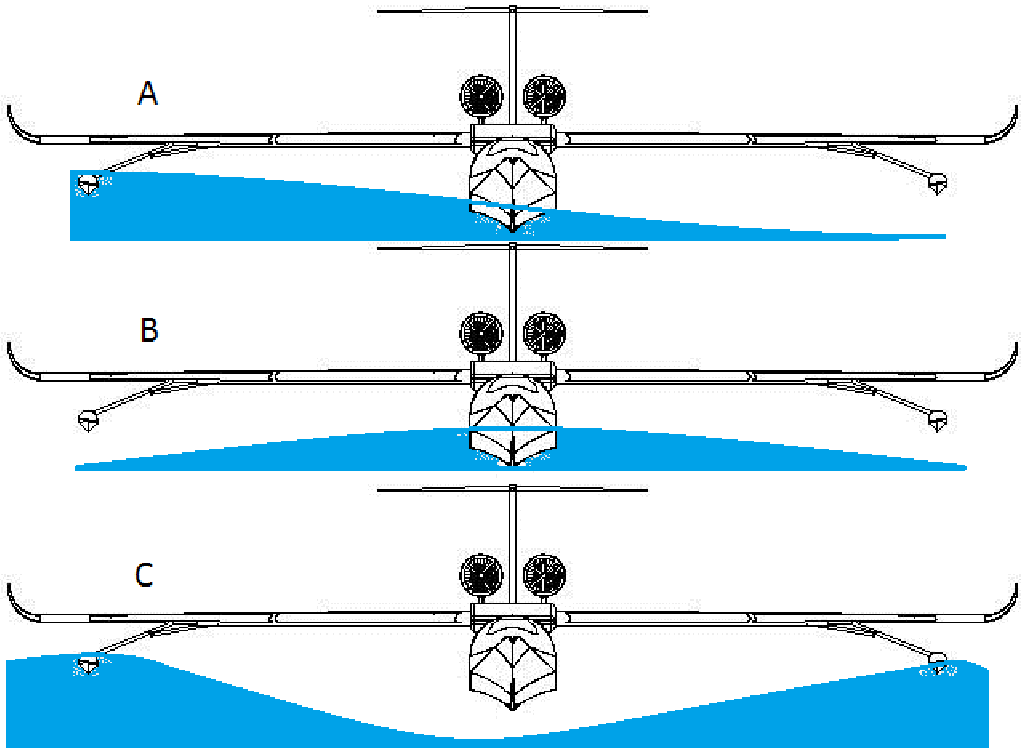

Figure 12.3: Preliminary view of the different cases of lateral wave interaction with the aircraft plus auxiliary floats.

maximum acceleration is given in Equation 12.1c.

$$u = A \cdot \sin\left(\frac{2\pi v}{\lambda} \cdot t\right) \tag{12.1a}$$

$$\frac{d^2u}{dt^2} = A \cdot \left(\frac{2\pi v}{\lambda}\right)^2 \cdot \sin\left(\frac{2\pi v}{\lambda} \cdot t\right) \tag{12.1b}$$

$$\left(\frac{d^2u}{dt^2}\right)_{max} = \pm A \cdot \left(\frac{2\pi v}{\lambda}\right)^2 \tag{12.1c}$$

This acceleration is related to the required torque using a modified version of Newtons second law seen in Equation 12.2a. Where the rotational acceleration is calculated in Equation 12.2b.

$$T = I \cdot \alpha \tag{12.2a}$$

$$\alpha = \frac{d^2u}{dt^2} \cdot \frac{1}{x_{sf}} \tag{12.2b}$$

The inertia term given in Equation 12.2a is estimated using the technique given Roskam V, page 17 [40]. A, λ and v represent the amplitude, wavelength and wave speed respectively. They are related to each other according to the methods presented by Holthuijsen [21].
For the most extreme design case, a wave amplitude of 1.5 meters is chosen. This wave height corresponds to a wavelength of 33 meters, and a speed of 5.6 meters per second. This wave height corresponds to a required torque of about 26 kNm.

Wind
Wind will try to roll the aircraft by depositing momentum into the aircraft when blowing against it. This phenomenon will work from any side, but only a wind direction fully perpendicular to the aircraft flight direction will be taken into account here. This is done because the biggest aircraft surface area will exposed to the wind in this case.
Oceanic waves are directly created from the wind. Therefore, the wave characteristics are derivative from wind characteristics [30]. The maximum significant wave height occurs when the energy put into the wave

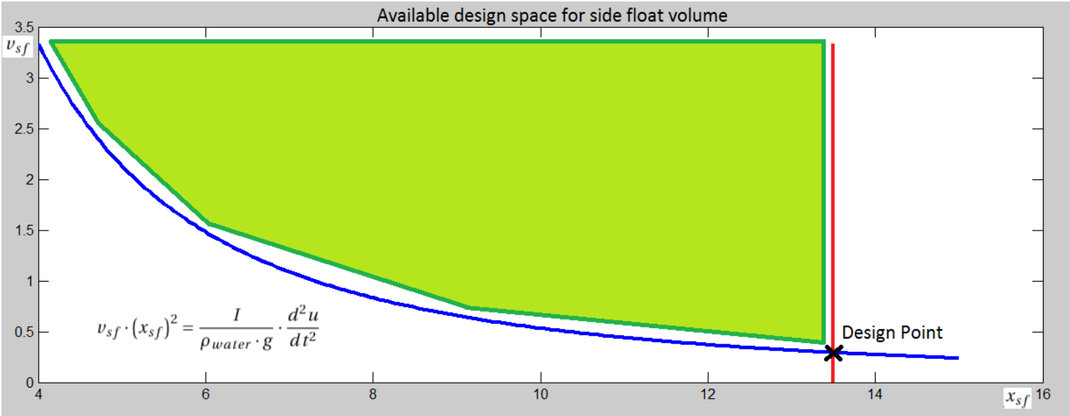

Figure 12.4: Permitted combinations of side float volume and location.

system by the wind is equal to the energy dissipating from the system by wave breaking. This knowledge relates the maximum design wave height to the maximum wind speed during water operations. A significant wave height of 1 meter corresponds with a wind speed of up to 8 meters per second [21]. This speed is taken as the design wind for the rest of the calculations.

The mass flow of the wind can be easily calculated with Equation 12.3a. Then, using Equation 12.3b the moment that the wind has on the aircraft is calculated. With a lateral area of 64 m^2 and moment arm of 2 meters, the moment experienced when lumping together all the mass of a single second is 7.6 kNm.

$$\dot{m} = \rho_{\text{wind}} \cdot A_{\text{lateral}} \cdot V_{\text{wind}} \tag{12.3a}$$

$$\dot{T}_{\text{wind}} = \dot{m} \cdot g \cdot l_{WL} \tag{12.3b}$$

12.2.2. Stabilising moment requirement

The total torque from the contributions as described in Subsection 12.2.1 needs to be counteracted by the auxiliary floats. The float torque is generated by submerging a part of the float at a distance from the aircraft centre line. The two design variables are the float volume and the float offset.

By rewriting Equation 12.2a into Equation 12.4, it can easily be seen that, due to the quadratic relationship between x_{sf} and v_{sf}, a maximised x_{sf} has more of a positive effect on the stability than a maximised v_{sf}. This principle is used as the basis for iterating for a optimum between the two.

$$V_{sf} \cdot \rho_{\text{water}} \cdot g \cdot x_{sf} = I \cdot \frac{d^2u}{dt^2} \cdot \frac{1}{x_{sf}} \rightarrow v_{sf} \cdot \left(x_{sf}\right)^2 = \frac{I}{\rho_{water} \cdot g} \cdot \frac{d^2u}{dt^2} \tag{12.4}$$

For structural reasons, the float can not be placed closer to the tip of the wing than 1.5 m This corresponds to a x$_{sf}$ of 13.5 m outboard of the aircraft centre line. With a total required moment of 33.6 kN m, a float volume of about 0.3 m^3 is sufficient to stay upright in the worst case scenario. The available design space is illustrated in Figure 12.4

In EASA ACDS A.114 [11] the rules with respect to compartmentalisation are given. These rules state that with any two compartments in the float flooded, there should still be enough buoyancy to stay upright in the worst case scenario. In order to get a 1.5 float scaling factor consistent with standard aircraft safety factors, it has been decided to get 6 compartments in the float. This results in a total float volume 0.45 m^3.

12.3. Structural sizing of the connecting element

The float needs to be connected properly to the wing. If the connection would fail, the aircraft will lose its lateral stability and lose the ability to operate safely. This section will first select a truss system that is compatible with the retraction mechanism chosen in Section 12.2. This will be done in Subsection 12.3.1. In Subsection 12.3.2 the relevant load cases will be discussed. Finally, the main structural members will be sized in Section 12.2.

12.3.1. Structural concept selection

In addition to the retraction concept selected in Section 12.2, the connection between the rotation point of the mechanism and the float needs to be designed as well. In Figure 12.5 the three considered concepts are displayed. Concept 1 has not been chosen because the resources involved in calculating the internal forces of statically in-determined structures. Concept 2 has not been chosen because wire bracing requires regular maintenance by experts that have become rare. Concept 3 is a relatively easy truss system with parallel cantilever beams at the top.

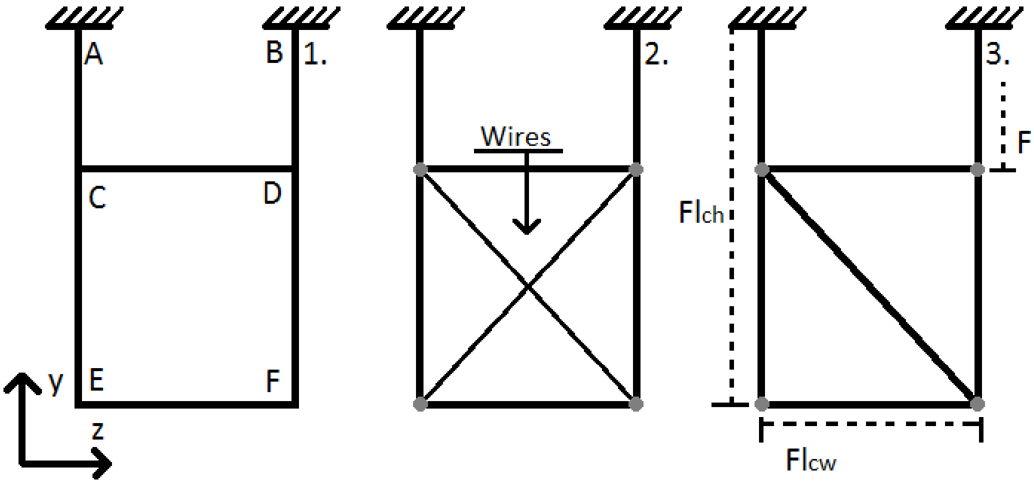

Figure 12.5: Three truss system concepts considered for the auxiliary floats.

Because this is still preliminary design, it is acceptable to trade some accuracy for speed of calculation. This makes Concept 3 ideal for this stage as it is primarily a simple truss structure. It is important to note however, that with more resources a lighter or more maintainable structure can be developed. Concept 1 for example can be designed using FEM software. This truss system can simply be joined together, reducing both production and maintenance cost.
The sizes of the truss system are given in Table 12.4. The relevant dimensions are indicated in Figure 12.5 and Figure 12.6. Note that the combination of these values is chosen such that the piston is able to fit in the area between the side float and the hinge point.

Table 12.4: Truss system sizes

Symbol	Description	Value [m]
Fl_{ch}	Float connection height	3
Fl_{cw}	Float connection width	1
Fl_{ph}	Piston connection height	0.75
Fl_{sh}	Float suspension	1.7
Fl_{p}	Lenght piston	3.7
X_{p}	Rotation point piston	8.5
X_{rot}	Rotation point trusses	11
X_{sf}	side float location	13.5

12.3.2. Load case analysis

In EASA ACDS A.114 [11] there are 2 load cases given for certification purposes of auxiliary floats. The first case is a landing impact force on the float as given via Equation 12.5. With a stall speed of 45 $\mathrm{m\,s^{-1}}$, a maximum landing weight of 31750 kg, a deadrise angle of 15 deg and an mass moment of inertia of 0.9 $\mathrm{kg^{-1}\,m^{-1}}$ (actually, ratio between float location and radius of gyration about z-axis).

$$F_{\text{impact}} = \frac{V_s^2 \cdot MTOW^{\frac{2}{3}}}{\tan(\beta_{sf})^{\frac{2}{3}} \cdot (1 + r_y^2)^{\frac{2}{3}}} \tag{12.5}$$

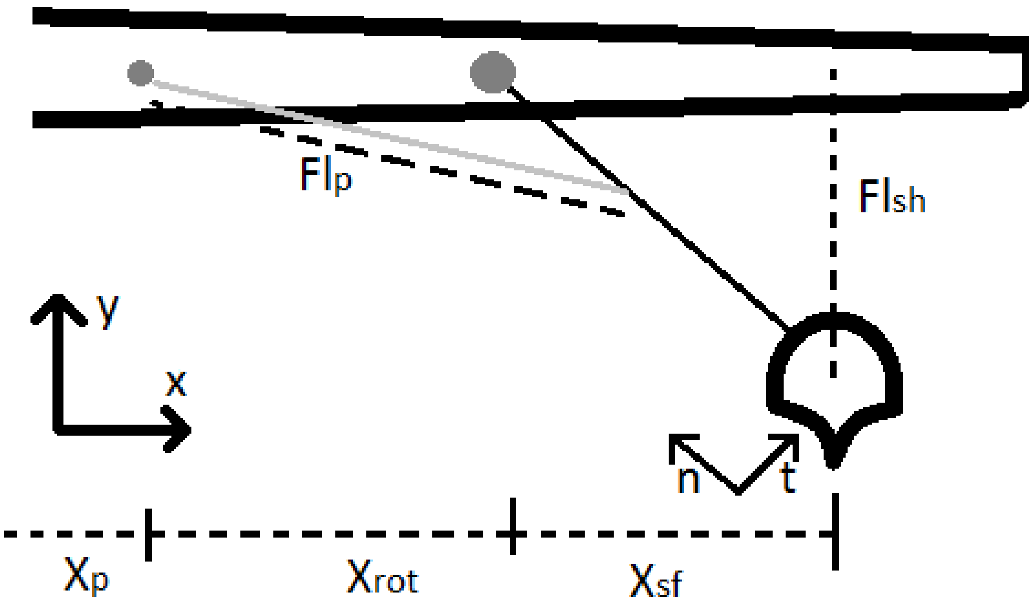

Figure 12.6: The truss retraction mechanism.

The second case is when the float is fully submerged while traveling at a significant portion of your stall speed trough the water ($0.6 \cdot v_{s0}$). The relevant equations are given in Equation 12.6a, Equation 12.6b and Equation 12.6c. The coefficient for side force (C_x) and drag (C_z) are 0.0036 and 0.0029 respectively [11]. Note that the side force can act both towards the aircraft and away from it.

$$F_y = V_{sf} \cdot \rho \cdot g \tag{12.6a}$$

$$F_x = C_x \cdot \frac{\rho}{2} \cdot V_{sf}^{\frac{2}{3}} \cdot (0.6 \cdot V_s)^2 \tag{12.6b}$$

$$F_z = C_z \cdot \frac{\rho}{2} \cdot V_{sf}^{\frac{2}{3}} \cdot (0.6 \cdot V_s)^2 \tag{12.6c}$$

The resulting forces from the three loadcases are then as displayed in Table 12.5. Because the structure is not pointed directly along the y axis, the F_y and F_x need to transformed to a normal and tangential force. The angle used for this coordinate transformation is $\tan^{-1}\left(\frac{x_{sf}-x_{rot}}{Fl_{sh}}\right)$. The resulting forces are also displayed in Table 12.5.

Table 12.5: Float forces for the considered load cases.

Loadcase	F_y [N]	F_x [N]	F_z [N]	F_n [N]	F_t [N]
Landing load	3800	0	0	2100	3100
Submerged loading ($+F_x$)	4400	8000	9900	-4100	8100
Submerged loading ($-F_x$)	4400	-8000	9900	9100	-900

Subsequently, the forces within the individual members can be easily calculated using simple statics equations at every individual node. The members AC and BD (refer to Figure 12.5 for node letters) are an exception to this, as they are two cantilever beams connected by a 2 force member. In Equation 12.7a through Equation 12.7c the derivation for the shear forces in Z direction for member AC and BD are displayed.

$$\Delta_{\text{bending}} = \frac{F \cdot h^3}{3EI}, \Delta_{\text{normal}} = \frac{F}{A \cdot E} \tag{12.7a}$$

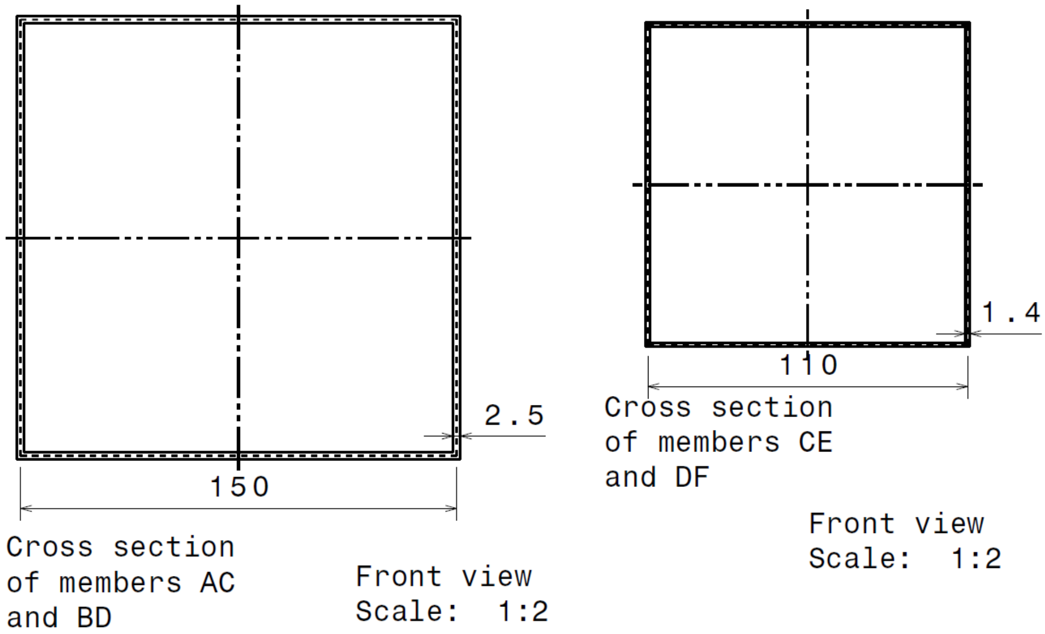

Figure 12.7: Cross sections of the selected beams.

$$\Delta_{BD,\text{tip,bending}} = \Delta_{AC,\text{tip,bending}} - \Delta_{CD_{\text{normal}}} \tag{12.7b}$$

$$\begin{bmatrix} \frac{h^3}{3EI_{AC}} & \left(\frac{h^3}{3EI_{BD}} - \frac{1}{A_{cd} \cdot E}\right) \\ 1 & 1 \end{bmatrix} \begin{bmatrix} V_{AC} \\ V_{BD} \end{bmatrix} = \begin{bmatrix} 0 \\ F_z \end{bmatrix} \tag{12.7c}$$

The forces that the individual members have to withstand are displayed in Appendix M for each separate load case. The F_n represents the normal force in the member, regardless of orientation. This means that the two force members only have a non-zero force here.

12.3.3. Preliminary structure sizing

In order to get a slightly more detailed look at the design of the side floats, the two main stiffening elements (AE and BF) have been sized. These members have been calculated as it gives a better indication on the impact of the floats on weight, cost, and manufacturing.
For these beams, simple bending, shear and compression theory was used to calculate the individual stress components [32]. To compute the design stress, the Von Mises yield criterion was used. In the calculations the following assumptions were used:

- Isometric materials are used for the beams. This means that just an universal E modulus can be used. In addition, no complicated design methods for the design of composite materials need to be used.
- The cross section has two axes of symmetry. This means that $I_{xy} = 0$. In addition, the shear flow calculation only has to be derived for one quarter of the cross section.
- The two beams AE and BF are symmetrically loaded, so the calculations only have to be done for one of the two beams.

Applying beam theory on a beam with the dimensions as given in Figure 12.7, the maximum Von Mises stress is given in Table 12.6. The load case for all maximum stresses is where the side float is submerged, and the F_x is directed outboard.
With the beams as displayed in Figure 12.7, the total weight of the beams is is 140kg. It is importatnt to realise that this weigt does not includthe weight of the piston and side float.

12.4. Future design considerations

For the preliminary design of the auxiliary floats a number of assumptions have been made. In this section the effect of these assumptions will be discussed. In addition, the effect of additional resources on the quality of the design will be discussed.

Table 12.6: Maximum Von Mises stresses and their locations.

Beam	Max stress [MPa]	location
AC	226	Top left corner, beam root
BD	226	Top left corner, beam root
CE	257	Right vertical, beam root
DF	257	Right vertical, beam root

The major assumptions and their effects are as follows:

- **Perpendicular waves** In reality, waves do not come in from a perfectly perpendicular angle. This means that the assumed pure lateral motion will in reality be a cross coupling of lateral and longitudinal motions. The effect of this on the lateral stability and the aircraft as a whole is unknown.
- **Rectangular rectangular frame** For the force calculations, the frame was assumed to be a rectangular one. This made the calculations less time consuming. Due to the sweep of the wing however, the frame needs to be a parallelogram to fit inside the wing when retracted. This means that a torsion component on the wing has been neglected for the frame.
- **Buckling is ignored** No buckling calculations have been performed on the frame. This means that the beams are not sized for it.
- **Hinged connections** For the preliminary design, the truss system has been assumed to have hinged connection points (no bending transferred). This made the preliminary evaluation less resource intensive. This results in a heavier preliminary structure.

In order to elevate the design from preliminary to detailed, more resources need to be allocated to this subsystem. The most effective ways to utilise these resources are by investing them in more detail assessments of wave dynamics and of the structural design.
By investing about one thesis worth of man hours in this design challenge, the effect of waves on the low speed dynamics of the aircraft can be looked at in more detail. Efforts should be focused around the cross coupling between lateral and longitudinal motions in waves. In addition, the dynamic response of the aircraft to a moving wave should be modelled in more detail.
The current structural design is fairly limited in its scope and connection to the real situation. By investing more man hours the design can be refined into a structure more representative of industry standard. Additional resources should first focus on generating more elegant concepts for the retraction mechanism. Preferably one that does not use a heavy piston for its retraction and extension. In addition, a more detailed force and stress analysis of the frame is required.
It is advised that extra resources are allocated to the wave analysis first. After that it is advised that the retraction mechanism is optimised. Finally, the structural design of connecting element should be performed.

13 Propulsion systems

The propulsion system has a big impact on the sustainability of the aircraft, since it produces most of the noise and emissions of the aircraft. The engines are also a significant part of the production cost of the aircraft. In the end, the Safran Silvercrest 2C turbofan engines were chosen to power the aircraft. Also, a low-noise propulsion system is required for delivering passengers to the shore, which comes in the form of a water jet.

Section 13.1 goes into depth on the selection of the turbofan engine and the fuel system. Section 13.2 explains the sizing and integration of the water jet propulsion system.

13.1. Regular propulsion system

This section shows the selection of the turbofan engine used on the aircraft as well as the fuel system layout of the aircraft. The chosen engine is the Safran Silvercrest 2C due to its low fuel consumption and high thrust to weight. The fuel system was designed to have redundancy and be able to pump the required amount of fuel to the engines on top of the wing.

13.1.1. Engine selection

From the thrust and wing loading diagram found in Appendix K the minimum thrust to weight ratio of 0.32 can be found to select the proper engine. This is limited by the landing stall speed and the TOP. Given that the maximum takeoff weight is 31 750 kg, the total required thrust is 22 400 lbf. This means 11 200 lbf per engine for a two engine configuration and 7470 lbf per engine for a three engine configuration. Since the design is very sensitive to a change in the specific fuel consumption, this parameter was given a high importance. In Table 13.1 the specific fuel consumption of the different engines is given. For some of the engines only the dry fuel consumption is known. This is the specific fuel consumption when in a standstill. The cruise specific fuel consumption is measured at Mach 0.8 at 35 000 ft. The dry specific fuel consumption of an engine is much lower than the cruise specific fuel consumption. When taking into account cost and sustainability, a two engine configuration outperforms a three engine configuration due to the lower maintenance cost and lower specific fuel consumption. Looking at the engines that deliver at least 11 200 lbf, the Safran Silvercrest 2C[1] shows the lowest specific fuel consumption. This engine is currently being developed and will power the Cessna Citation Hemisphere that will make its first flight in 2019. The engine developer Safran is also known for the LEAP engines[2] powering the new Boeing 737 MAX and Airbus 320neo.

13.1.2. Fuel system layout

The fuel system consists of all fuel tanks, lines, pumps and the engines. The layout of the fuel system is shown in Figure 13.1. The regulations in CS25 are not as strict on the fuel system as chapter 14 of the CFR[52], therefore this was taken as the start of the design. First the fuel tanks were placed, and their volume calculated. The wings were used for the placement of fuel tanks as seen in Figure 13.2. A centre fuel tank was created in the wings up to the float mechanism. Also, a tip fuel tank was created between the end of the side

[1] `https://www.safran-aircraft-engines.com/commercial-engines/business-jet/silvercrestr2c`
[2] `https://www.safran-aircraft-engines.com/commercial-engines/single-aisle-commercial-jets/leap/leap`

Table 13.1: Tradeoff table engines. [10][41]

Engine name	Takeoff thrust [lbf]	SFC [lb/(lbf·h)]	Mass [lb]
RR Allison AE3007A1	7580	0.36 (dry)	1586
AVCo Lycoming ALF502L-2C	7500	0.414 (dry)	1311
AVCo Lycoming ALF502R-3A	6970	0.408 (dry)	1336
GE CF-34-3B1	9220	0.346 (dry)	1670
PW 308	7000		1375
GE CF34-8C1	12 670	0.655 (cruise)	2335
Allied Signal TF507-1F	7000	0.700 (cruise)	1385
BR725	16 100	0.650 (cruise)	4742
Honeywell HTF7700L	7550		1534
GE CF-8C5B1	13 790	0.67 (cruise)	
TAY 611	13 850		
Safran Silvercrest 2D	11 450		2290
Safran Silvercrest 2C	12 000	0.57 (cruise)	2290

float mechanism up to 85% of the wing. The fuel tank is placed between 15 and 60% of the chord. The total volume of the tanks is 16 m^3. This gives a maximum fuel mass of 13 000 kg, just enough to store all fuel as can be seen in Table 4.4.

Secondly the placement of the engines has to be chosen. Due to spray underneath the wing, the engines can not be placed at that location. Also mounting them on the back of the fuselage will create the same problem. Therefore the engines had to be placed on top of the wing. This eliminates the chance of water ingestion into the engine. The added benefit to this is that the wing blocks some of the noise propagating into the cabin and to the earth, lowering noise pollution. The disadvantage is that simple gravity assisted fuel transfer is not possible and fuel pumps have to be constantly running.

The next parameter that should be chosen is the distance between the engines. The engines have a diameter of approximately 1 m. The engines were both placed one meter from the centre of the fuselage to eliminate the engine exhaust interfering with the vertical tail. The diameter of 1 m in combination with a little spacing between the engine and wing and the height of the fuel tank require the fuel to be pumped to the height of approximately 1 m. The pressure required to pump the fuel to this height is determined from Equation 13.1.

$$p = \rho_f \cdot g \cdot h \cdot n_{ult} \tag{13.1}$$

The ultimate load factor is included since the fuel is required to still supply the engines when this load factor occurs. This results in a required pressure of 29 kPa. This pressure has to be delivered to the fuel when operating at the maximum fuel flow rate. This fuel flow rate was calculated with Equation 13.2 for takeoff thrust with cruise specific fuel consumption.

$$\dot{m}_{f,max} = SFC \cdot T_{max} \tag{13.2}$$

This resulted in a fuel flow rate of 54 kg min^{-1}. Therefore it is required for every fuel pump on the aircraft to be able to pump the fuel at the rate of 54 kg per minute and generate a differential pressure of 29 kPa at that fuel flow rate.

The fuel system does not have the capability of dumping fuel. This was not required since the maximum landing weight is equal to the maximum takeoff weight. To comply with the regulations vents have been placed on the fuel tanks to prevent the buildup of fuel vapour, as seen in Figure 13.1. The aircraft has a refuelling point on both sides of the aircraft, as seen in Figure 13.1, to allow for more flexibility. The aircraft uses the refuelling system for fuel transfer. Also a cross feed valve is installed to equalise the fuel pressure to both engines.

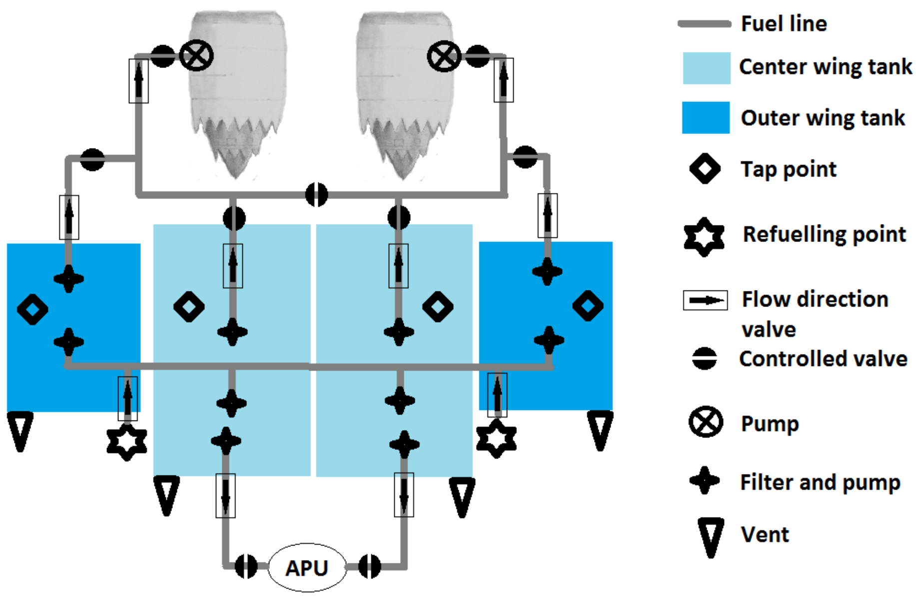

Figure 13.1: Layout of fuel system.

13.2. Waterjet propulsion system

For the design of the aircraft, watertaxi has become an important aspect of the design due to the amphibious capabilities of the aircraft. As explained in the midterm report [36], the waterjet is the most appropriate propulsion system to fulfil this function [36]. The waterjet especially excels in noise performance and easy structural integration which makes it a perfect propulsion system for water taxi. Furthermore, the waterjet can be used to manoeuvre on water and provide pushback. In this section, an elaboration of the water jet will be done on sizing and integration.

13.2.1. Waterjet system sizing

To choose the right waterjet system size, an estimation of the required power needs to be made. An estimation of the required power contains a tradeoff between taxi time, power and weight of the waterjet. As can be seen in Table 13.2, the required power of the waterjet that will be used is 37.0 kW and is based on the following:

- **APU**: Since the APU has an output power of 90 kW (Section 14.2), a waterjet input power of less than 90 kW saves a larger APU or an extra diesel/electric engine. With an average waterjet efficiency of about 60%, the minimum output power of the APU has to be 37.0 kW / 60% = 61.7 kW [16]. Therefore no additional engine has to be installed which saves weight and cost.
- **Drag hump**: As can be seen in Figure 13.4, between 6 and 11 $\mathrm{m\,s^{-1}}$ the drag and therefore the required power increases drastically. As a result, a taxi speed of 6 $\mathrm{m\,s^{-1}}$ is chosen to stay before the drag hump and to be able to use the APU as input power source.
- **Weight**: Based on statistical data, the relation between weight of the waterjet and power was found to be exponential as can be seen in Figure 13.3. Having a taxi speed of 6 $\mathrm{m\,s^{-1}}$ a satisfactory weight of 42.9 kg is obtained[3][4]. This weight is low compared to the whole aircraft and therefore the contribution to the c.g. range is of less concern (Subsection 11.1.1).
- **Taxi time**: With a taxi speed of 6 $\mathrm{m\,s^{-1}}$ (21.6 $\mathrm{km\,h^{-1}}$), a taxi distance of 6 km can be covered in 16.7 min. This is reasonable, since the average taxi time on land is 26 minutes (Subsection 8.1.2). Basically, a taxi a time of 16.7 min is the maximum, because when a 5 min faster taxi time was taken, the required power and weight would be out of bounds and the waterjet would be infeasible.
- **Cost:** Taking a waterjet of 37.0 kW the costs are reduced as well. First of all the waterjet is relatively small which reduces the cost price. Secondly the APU can be used to drive the waterjet system which saves an extra engine and complexity that directly saves costs.

[3] `http://www.mshs.com/ala_page.htm`
[4] `https://www.hamjet.co.nz/global/hj-series`

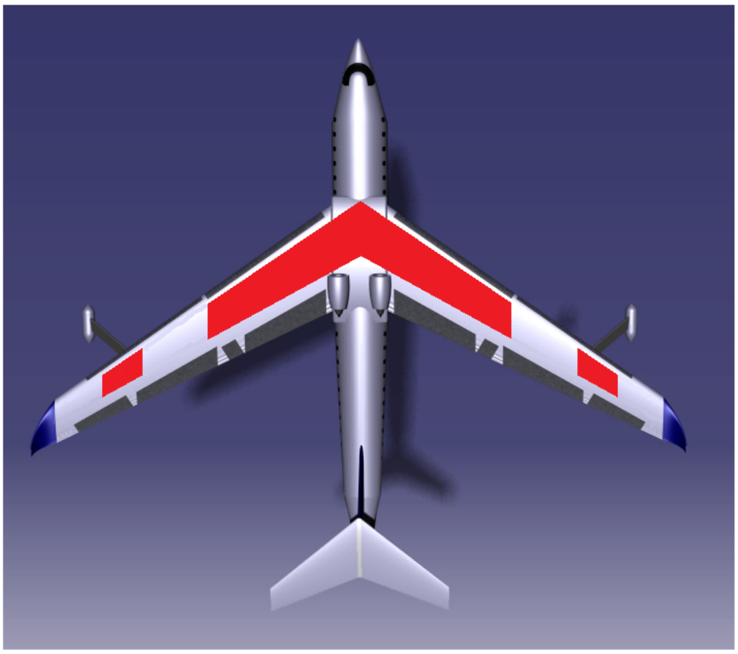

Figure 13.2: Position of wing tanks, as indicated in red.

Table 13.2: Water jet performance table.

Taxi speed [m/s]	Required Power [kW]	Weight [kg]	6 km taxi time [min]
5	20.5	40.4	20.0
6	37.0	42.9	16.7
7	104.7	54.7	14.3
8	211.7	80.5	12.5
9	331.5	123.9	11.1

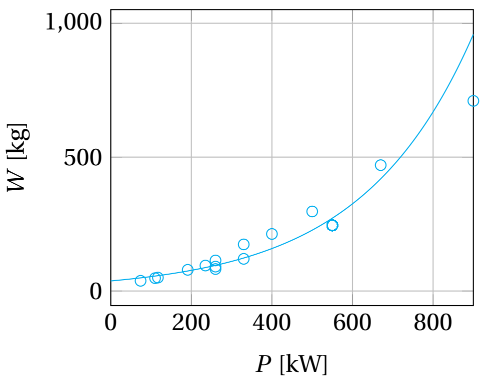

Figure 13.3: Weight to power relation waterjet

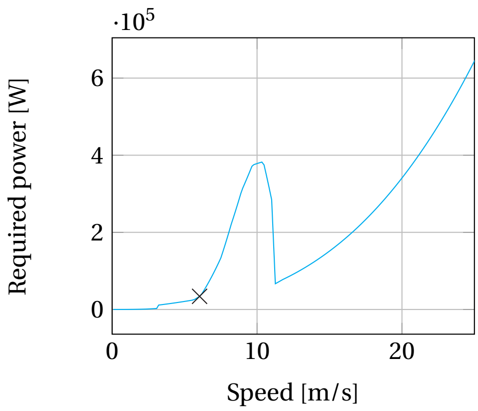

Figure 13.4: Power to speed relation waterjet

13.2.2. Waterjet system integration

In Figure 13.5 the integration of the waterjet into the back of the fuselage can be seen. The waterjet is made at scale in Figure 13.5 and it can be observed that the waterjet takes just a small space of the fuselage. Consequently, the waterjet does not have a big influence on the aircraft configuration and this also indicates that the waterjet can be integrated easily. As discussed in Subsection 13.2.1, the waterjet is coupled to the APU. In Figure 13.5 this is simplified by just one rod connecting the gear box of the APU (red) and waterjet (yellow). The blue tube represents the inlet of the waterjet and the water from the inlet is accelerated by the impeller inside the waterjet driven by the APU. Furthermore, the location of the waterjet at the end of the fuselage bottom is excellent, since this avoids interference with the pressure cabin and as a result complicated structures with sealings. Also, the placement of the waterjet at the end of the fuselage causes sublime manoeuvre capabilities. Because the moment arm is large, due to the fact that the waterjet located as far as possible from the c.g., therefore turns can be made easily.

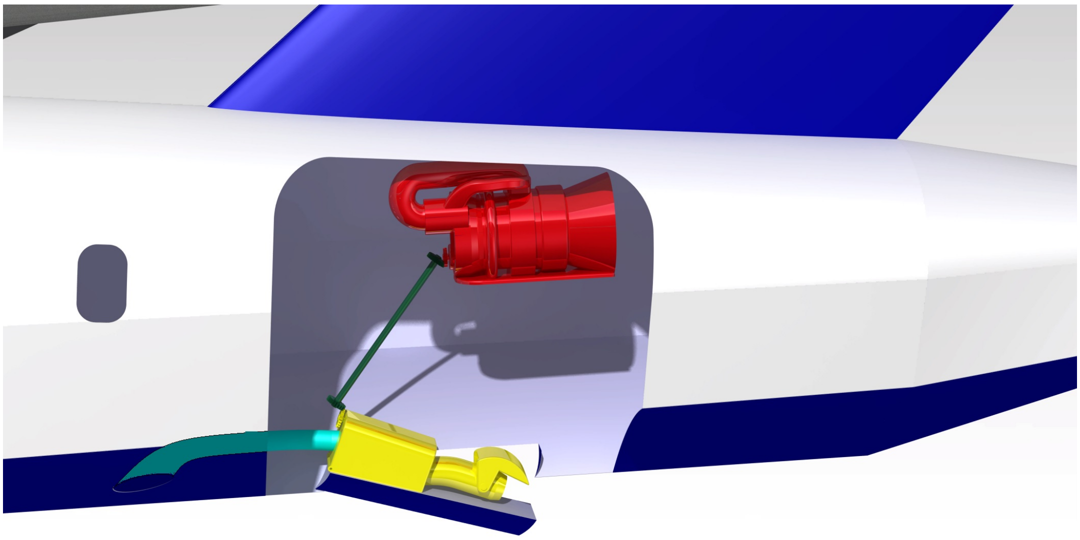

Figure 13.5: Overview of integration of the waterjet in the fuselage.

In addition, a N2-chart for the waterjet was made and can be found in Figure 13.6. This was done to get insight which elements are involved in the waterjet propulsion system along with their interrelations. As can be seen from the N2 chart, the cockpit controls all the systems directly and indirectly. The steer wheel and thrust lever are connected to the actuator and APU directly. These two are connected to the bucket and impeller respectively.

Cockpit	Steer wheel, thrust lever (reverse)		Thrust lever	
Direction of bucket	**Actuators**	Control force		
		Bucket		
Power delivery			**APU**	Power
Taxi speed				**Impeller**

Figure 13.6: N2-chart waterjet propulsion system.

14

Interior and supportive subsystems

In order to get a complete picture of the aircraft design, sizing of supportive subsystems is necessary. Furthermore, some of the supportive subsystems are essential to some of the aircraft's unique functions. Therefore, it is important for assessing its feasibility. First in Section 14.1, the landing gear system will be discussed. Due to the high centre of gravity position this system causes a concern on the feasibility of the aircraft. A tilted pivot landing gear was chosen for the design. Secondly in Section 14.2, the APU sizing is discussed. After that in Section 14.3, the interior concept of the aircraft is shown. Section 14.4 discusses some of the avionics and communication systems on board of the aircraft. This includes the flight deck, wifi, television and naval communication equipment. The suppliers of these subsystems will be Honneywell, Aerosat and Simrad®-yachting. Lastly Section 14.5 discusses the preliminary hydraulic architecture of the aircraft. It is deemed important to the aircraft, since it uses many hydraulic systems for for example deploying the side floats, landing gear and actuating the flight control surfaces. The hydraulic concept uses electric backup hydraulic actuation to save weight on the backup system.

14.1. Landing gear

The main landing gear that will be used on the aircraft is a gear with a tilted pivot. It consists of three struts of which one is foldable, one is an actuator and one has a shock absorber. This configuration can be compared with for example the F-16 which is shown in Figure 14.1. The main landing gear will have 8 wheels in total: two times four wheels at each side of the aircraft. The nose gear will be a regular nose gear having one strut with a shock absorber. This section describes the process of the landing gear positioning according to the loads acting on the front and main gear. Appropriate wheels will be selected and finally in water operation is assessed.

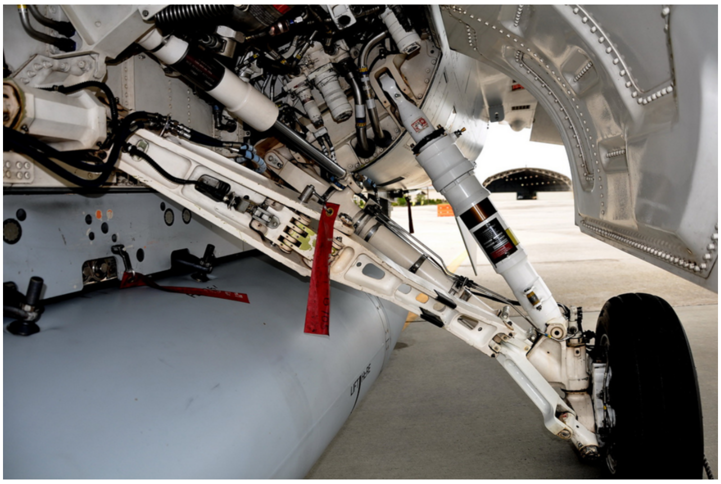

Figure 14.1: Landing gear of the F16 consisting of 3 struts (1 foldable, 1 actuator, 1 shock absorber)[1]

First of all it was decided to position the wheels such that a gap of 0.4 m was left between the underside of the wheels and the lowest point of the fuselage. This allows the aircraft to be pulled up ramps with a slope of 6.6° if, at the top, the slope changes directly from 6.6° to 0° degrees as analysed with CATIA. From this vertical wheel position the longitudinal position of the main gear followed, obtained using the aft centre of gravity location and using Figure 14.2 in which $\hat{A}$ is 15°, which is the minimal allowed angle. Using this location and moment equilibrium around the aft centre of gravity, the nose gear location could be obtained. The loads that are carried by the nose and main gear were assumed to be respectively 8 % of the takeoff weight and 92 % of the takeoff weight. The 8 % is a requirement in order to be able to steer the aircraft [33]. This leads to the following distances measured from the nose: $x_{ng} = 4.5$ m and $x_{mg} = 15.97$ m, being the nose gear and main gear location respectively. The landing gear characteristics are shown in Table 14.1

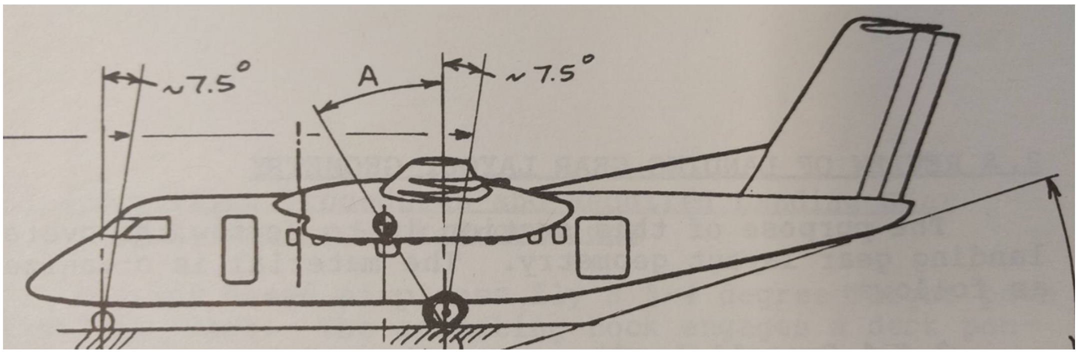

Figure 14.2: Main landing gear positioning where angle $\hat{A}$ needs to be larger than 15°. [40]

Having determined the location along the length of the fuselage, it had to be considered that the aircraft could potentially fall on its side when for example steering. Due to the relatively high centre of gravity of the aircraft, it was found out that the main landing gear would have to be positioned at a distance of 2.35 m of the centre of the fuselage cross-section. This means that the landing gear would have to stick out 1 m from the side of the fuselage.
As the current configuration did not allow for storing the landing gear in the wings due to the side floats already being stored there and due to fuel storing, it was decided to use a gear with tilted pivot as used in the F-16. This configuration consists of a foldable strut, an actuator an a shock absorber. The gear will be retractable and will be able to be stored at the hull step as there is still a lot of free space. The nose gear will also be retractable and stored under the cockpit.
The strut size of the nose gear could be analysed using [40] and will need a shock absorber with a stroke of (at least) 0.21 m. However, as [40] does not have a proper way to define the strut sizes for the tilted pivot,

[1] https://www.flickr.com/photos/mark233/8442201744

further structural analysis will have to be performed to analyse this configuration. When this analysis will be performed, attention will have to be paid especially to the moment generated by the main landing gear as this will be crucial for the size and weight of the struts.
The final step in the landing gear design was the selection of tyres. Goodyear aviation tyres were used: 2 Flight Eagle tyres (22x8.0-10) for the nose gear and 8 Rib tyres (26x10.0-11) for the main gear. These tyres were selected according to the load each wheel has to be able to carry, the inflating pressure and the speed it has to be able to operate on [2]. 8 main gear wheels are used as the main gear carries almost the whole weight of the aircraft and as it is easier to attach the struts (due to spacing between wheels that lie behind each other) if 4 wheels are used instead of 2 wheels. Table 14.1 shows the loads acting the gears and wheels and Figure 14.3 shows the used tyres.

Table 14.1: Gear characteristics.

		Value	Unit
Nose gear	Position from nose	4.5	m
	Total loading	24,909	N
	# wheels	2	\
	Static tyre loading	20,618	N
	Dynamic tyre loading	30,927	N
	Max operating speed	50.93	$m\,s^{-1}$
	Tyre	Flight eagle (22x8.0-10)	\
Main gear	Position from nose	15.97	m
	Total load	286,452	N
	# wheels	8	\
	Static tyre loading	38,313	N
	Max operating speed	50.93	$m\,s^{-1}$
	Tyre	Rib (26x10.0-11)	\

Figure 14.3: Used tyres: Flight eagle (left) and Rib (right). [3]

So, the landing gear configuration was chosen to be a regular nose gear with a main landing gear with tilted pivot consisting of three struts. These followed from the position of the landing gear which is rather remarkable due to the relatively more aft nose gear and the out sticking main gear. tyres have been selected and a structural analysis will have to be performed in a later design phase.
The only thing remaining is considering the fact that the landing gear has to be deployed while being in the water. This is to allow the aircraft being pulled out of the water as could be seen in the Subsection 6.2.1. As the location of the landing gear fairings comes directly in contact with the water, these will have to be sealed so that no water will come inside during takeoff and landing. In case of opening the landing gear inside the water, electric wires will have to be fully protected so no contact with water is possible. The whole inside of the fairings as well as the landing gear itself will have to be coated in order to be protected and will have to be treated after every flight it has been in contact with water. This in order to extend its life and thus reduce cost and increase sustainability.

14.2. Auxiliary power unit

This discussion will elaborate on the auxiliary power unit (APU) sizing and selection. The APU is a supportive subsystem that delivers power for all elements other than for thrust, which is delivered by the

[2] https://www.goodyearaviation.com/resources/pdf/databook_7_2016.pdf
[3] Made with https://www.goodyearaviation.com/tires/tires-by-segment.html?&market=G

main engines. Additionally, the APU may be used for starting the main engines. Primary considerations for sizing the APU for power required are nominal and peak power needed for on-board electronics, for starting the engines, and potential extra power supply uses of the APU. As a very detailed picture of the peak and nominal powers required is not available, because the design has not reached that level of maturity yet, reference business jets are used for estimating these values. When estimating the actual values for Jaeger Section N.1 will be used to ensure all components are included.
The reference business jets mentioned before almost exclusively use the Honeywell RE220 APU [4]. An exception is the Falcon 7X which uses the Honeywell 36-150 APU [5]. The former, weighing 108 kg, is capable of delivering 45 kW peak power. The latter, weighing less with 68 kg because it has the highest power-to-weight ratio currently available on the market[6], is capable of delivering a peak power of 90 kW. The cost specification of the APUs is unfortunately not disclosed by the manufacturer. However, it may be excpected that the 36-150 APU is more expensive than the RE220 APU, because of its high power-to-weight ratio. However, thinking on the scale of the total aircraft cost as opposed to a slightly higher APU cost, this is not such a big factor in trading off the APUs.
Trading off the APUs on power and weight performance, the choice for the 36-150 is evident. Additionally, in order to account for the situation that the Jaeger has similar power needs as the Falcon 7X, it is a logical choice to select the Honeywell 36-150 APU, of which an isometric render can be seen in Figure 14.4.

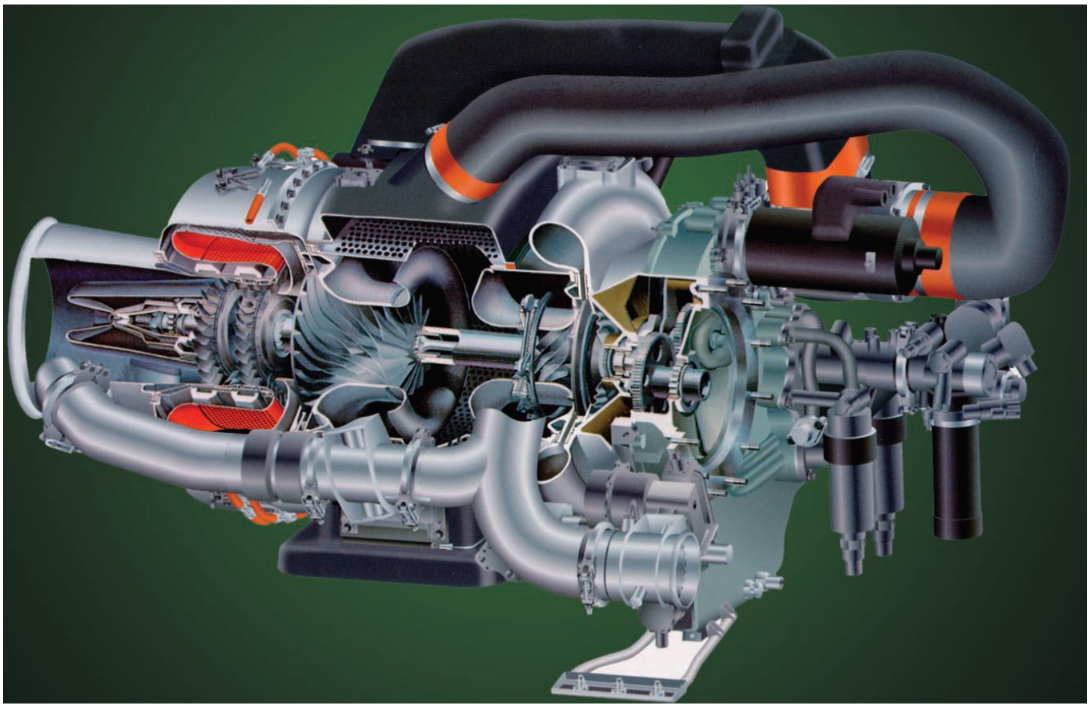

Figure 14.4: The selected Honeywell 36-150 APU, capable of delivering 90 kW peak power.

The placement of the APU in the fuselage is more forward than the placement of APUs in conventional aircraft. This way, the APU is guarded against water ingestion via its gas outlet during water operations. Additionally, the APU is placed closer to the water jet, such that the complexity of the shafts connecting the APU and the water jet is slightly lower. For a closer look on the integration of the APU with the water jet and the fuselage, the reader is referred to Section 13.2.

14.3. Interior

This section describes the interior of the cabin which is the section of the fuselage where the passengers stay during travelling. The design of the interior is usually done by an external party and therefore not studied in depth. With the current state of the design an impression of the interior is made with Sweet Home 3D which

[4]https://aerospace.honeywell.com/en/products/auxiliary-power-and-thermal/re220-apu
[5]https://aerospace.honeywell.com/en/products/auxiliary-power-and-thermal/36-series-apus
[6]https://aerospace.honeywell.com/BGA-Mechanical/

is shown in Figure 14.5. This interior configuration fits in the aircraft and holds eleven passengers. Other configuration could allow for more passengers. A shower, satellite TV, bed, and toilet is incorporated in this configuration. The curvature of the cabin is not taken into account and will shrink the cabin in width a little bit. For further design one can take into account the necessary interfaces for the interior such as the electricity and water lines. The first estimation, however, gives the impression that the requirements on the interior can be met.

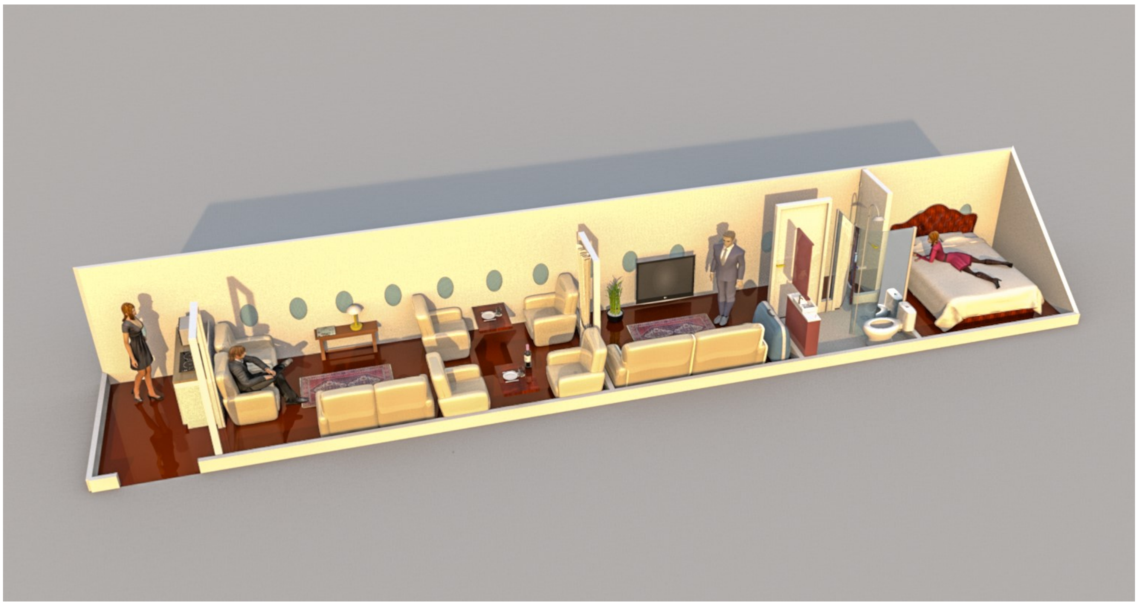

Figure 14.5: Impression of the interior.

14.4. Avionics

This section will discuss some of the main avionic subsystems of the aircraft, which are the cockpit systems and communication. Mostly the leading suppliers of the aerospace and maritime sector were visited to obtain the systems.

14.4.1. Cockpit

This part focuses on the interaction between the pilot and aircraft. Pilots have to be trained to interact with the avionics of the aircraft. To simplify the transition of pilots to the Jaeger aircraft, the avionics architecture used on the Jaeger shall have a similar layout to other business jets. Therefore the Primus Epic® 2.0+ [7] integrated avionics system designed by Honeywell was chosen to be used on the Jaeger aircraft. This is the latest generation of the Primus cockpit family, therefore integrating the newest technologies whilst still providing familiarity to the pilots. The Primus Epic® flight deck is used on different business jets like the Falcon 7X, Citation Sovereign and most Gulfstream models. The complete data handling block diagram is a confidential file held by Honeywell and therefore can not be provided, however a small part is discussed in Section N.2. The newest features of the Primus Epic® 2.0+ include amongst others:

- DynaCharts™, displaying the required information in charts directly to the pilot[8] instead of the charts themselves, therefore reducing workload.
- SmartView® synthetic vison system (SVS) [9], displaying the outside world on the primary flight display, thereby eliminating poor visibility as a safety factor and enhancing operational flexibility.
- Next generation Flight Management Systems [10], lowering cost and emissions by optimising the altitude, steps taken to this altitude, cruise speed and providing idle descent paths, all to allow for less emissions. It allows the customer to effectively trade between cost and time.

[7] https://aerospace.honeywell.com/en/products/cockpit-systems/primus-epic
[8] https://aerospace.honeywell.com/en/press-release-listing/2015/november/new-technologies-available-for-honeywell-primus-epic-c
[9] https://aerospace.honeywell.com/en/products/safety-and-connectivity/smartview-synthetic-vision-system
[10] https://aerospace.honeywell.com/en/products/cockpit-systems/next-generation-flight-management-systems

- TCAS Coupled Autopilot[11], ensuring quick and correct avoidance actions and allowing the pilot to monitor the flight path and assess the danger of the traffic alert. Due to the quick action no aggressive dives or climbs are required, ensuring passenger comfort and lowering risk of injury.
- IntuVue™weather radar [22], providing 3D weather information for improved hazard avoidance. It also features a 60 NM advanced turbulence detection radius, predictive hail, lightning and wind shear detection enhancing passenger safety and comfort.

14.4.2. Communication

This part shows the communication systems on board the aircraft. The general communication equipment required for communication on the aircraft band(108 to 137 MHz) to ATC, beacons and localizers, is part of the flight deck system and will not be discussed here. The Jaeger aircraft also requires a communication system for communicating with vessels. As discussed in Chapter 6, to be allowed on the water, an AIS-transponder, VHF-transmitter and radar are required. The marine VHF frequencies are between 156 and 174 MHz, therefore a separate transmitter for aircraft and vessels is required. These systems were chosen from the main suppliers for maritime traffic. Furthermore, television and internet shall be provided to the passengers. The equipment required for television and internet are discussed in the last part of this section.

The proposed VHF radio for vessels is the RS35 [12] produced by Simrad®-yachting. The system weights 1.63 kg, has a peak power of 81.6 W and costs around 502 euros [13].
The proposed AIS-transponder is the AIS650 transceiver [14] produced by Raymarine®. It weighs a mere 285 g, uses less than 3 W and costs 841 euros. This transceiver also allows the aircraft to receive the information of other vessels simplifying the landing operations.

The radar system of the aircraft will not be sufficient for operating on water, since no 360 degree field of view is achieved. The HALO™-3 pulse compression radar produced by Simrad®-yachting [15] was chosen to be on the aircraft. The cost of this appliance is around 4000 euros, it has a peak power usage of 150 W and weighs 26.8 kg [16]. This radar will be extended from the aircraft when landed on water. There will be a closed compartment in the main wing that, when the radar is not in use, the radar is stored in a way that does not disturb the aerodynamics of the aircraft.

Overall, the extra systems required for operations on water will not add significantly in overall cost, mass or power. Redesigning the systems for the aircraft would add significantly more cost to the subsystems. Therefore the equipment is directly implemented.

For the television and internet connection two different options are investigated in greater detail. The first is the FliteStream™T-220 system[17] by Aerosat. The second option is the EXEDE® system with the 2540 antenna configuration by ViaSat®. A tradeoff between the two systems is performed on the system characteristics mass, power, throughput and coverage. The results of the different systems can be found in Table 14.2. Coverage is deemed of high importance, since it increases passenger comfort. For this criterion FliteStream™T-220 scores the highest. The throughput of 40 Mbps of the FliteStream™T-220 system is deemed high enough especially, since the television can be used separately from this budget. Also the future FliteStream™T-320 will increase this speed if required by the customer. The FliteStream™T-220 has a significantly lower mass and a slightly higher power. The FliteStream™T-220 was therefore selected to be installed on the aircraft. There will be a new generation T-320 with higher throughput. This upgrade will be offered to customers.

[11] https://aerospace.honeywell.com/en/press-release-listing/2015/november/new-technologies-available-for-honeywell-primu
[12] http://www.simrad-yachting.com/en-US/Products/VHF-Radios/RS35-VHF-AIS-Radio-en-us.aspx
[13] http://www.marifooncenter.nl/Simrad-RS-35
[14] http://www.raymarine.eu/view/?id=558
[15] https://www.simrad-yachting.com/en-US/m/Products/Radar/Simrad-HALO-3-Pulse-Compression-Radar-en-us.aspx
[16] http://www.abe-inzenjering.hr/pdf/simrad_halo_radar.pdf
[17] http://www.aerosat.com/products/products_ife_antenna.asp

Table 14.2: Overview of specifications.

Criterion	FliteStream™T-220	EXEDE® 2540
mass	28 kg	44 kg
power	175 W	160 W
throughput	40 Mbps with separate live TV	100 Mbps
global coverage	All land, missing only parts of South Pacific, South Atlantic and Indian ocean	North America, Europe, middle east

14.5. Hydraulics

Where normal aircraft usually have three hydraulic systems, in which one is a backup, the Jaeger only requires two hydraulic systems. For the Jaeger aircraft the Electric Backup Hydraulic Actuation EBHA[18] will be used as the backup system. EBHA includes a small electric motor on every actuator to provide actuation in the case of hydraulic failure. The use of EBHA will lower the total weight of the hydraulic subsystem by eliminating the weight of the backup hydraulic system. This lowers overall fuel consumption and adds to a more sustainable aircraft. Also EBHA shows a lower maintenance cost [12]. EBHA is currently used on the Gulfstream G650 and Airbus A380, proving safe operations.

To make sure uneven deployment of flaps, slats and side floats is impossible, separate torque shafts will be used for these critical systems as a further redundancy against uneven deployment. The torque shaft for the slats is located inside the leading edge. The torque shafts of the side floats and flaps are located in the aft section of the wing just in front of the flap assembly.

The hardware block diagram shown in Figure 14.6 shows two main hydraulic systems and two electrical backup systems. It can be used as a tool to design the hydraulic system without forgetting any parts of it. It has four levels. The first level is the power supply level. This level shows where the power that is required for the system is generated. The second level shows the pumps. This is the level in which the hydraulic pressure is generated. Since the electrical backup does not require pressure, those lines go down to the third level directly. The third level shows the actuation mechanism and the fourth and final level shows the systems that are powered by the hydraulic system. This last level has some systems grouped. Main hydraulic lines carry the hydraulic fluid throughout the aircraft. At hydraulic separation points, the hydraulic fluid is separated from the main hydraulic line and runs through individual smaller hydraulic lines to each system. The number 1 hydraulic system provides the hydraulics to the left side systems of the aircraft. It also powers the rudder and the water jet bucket. The number 1 hydraulic system is pressurised by the left side engine. The number 2 hydraulic system provides the hydraulics to the right part of the aircraft. It also powers the landing gears. The number 2 hydraulic system is pressurised by the right side engine. The electric backup will consist of a left and right side system as well. The gears will be powered by the left side electric backup, whilst the rudder and water jet bucket will be powered by the right side electric backup. The gears, rudder and water jet bucket are powered by the opposite electrical backup system as the main hydraulics. This reduces the amount of systems that are backed up by each of the electric backup systems in case of a hydraulic failure in one of the main hydraulic systems. This lowers the electric power and also current required by each EBHA system in case of one of the main hydraulic systems failing, lowering the risk of electrical failure.

In addition, the main hydraulic system consists of hydraulic lines running from the turbo pumps to the actuators with a flow control valve installed before each actuator. These lines go back to a reservoir after which the hydraulic fluid flows through a filter back to the turbo pumps. The electric backup systems consists of computers and wires supplying electricity to the EBHA actuators that then use their electric backup actuation mechanism for controlling the systems.

[18] `http://ph.parker.com/us/en/electric-backup-hydraulic-actuation-ebha`

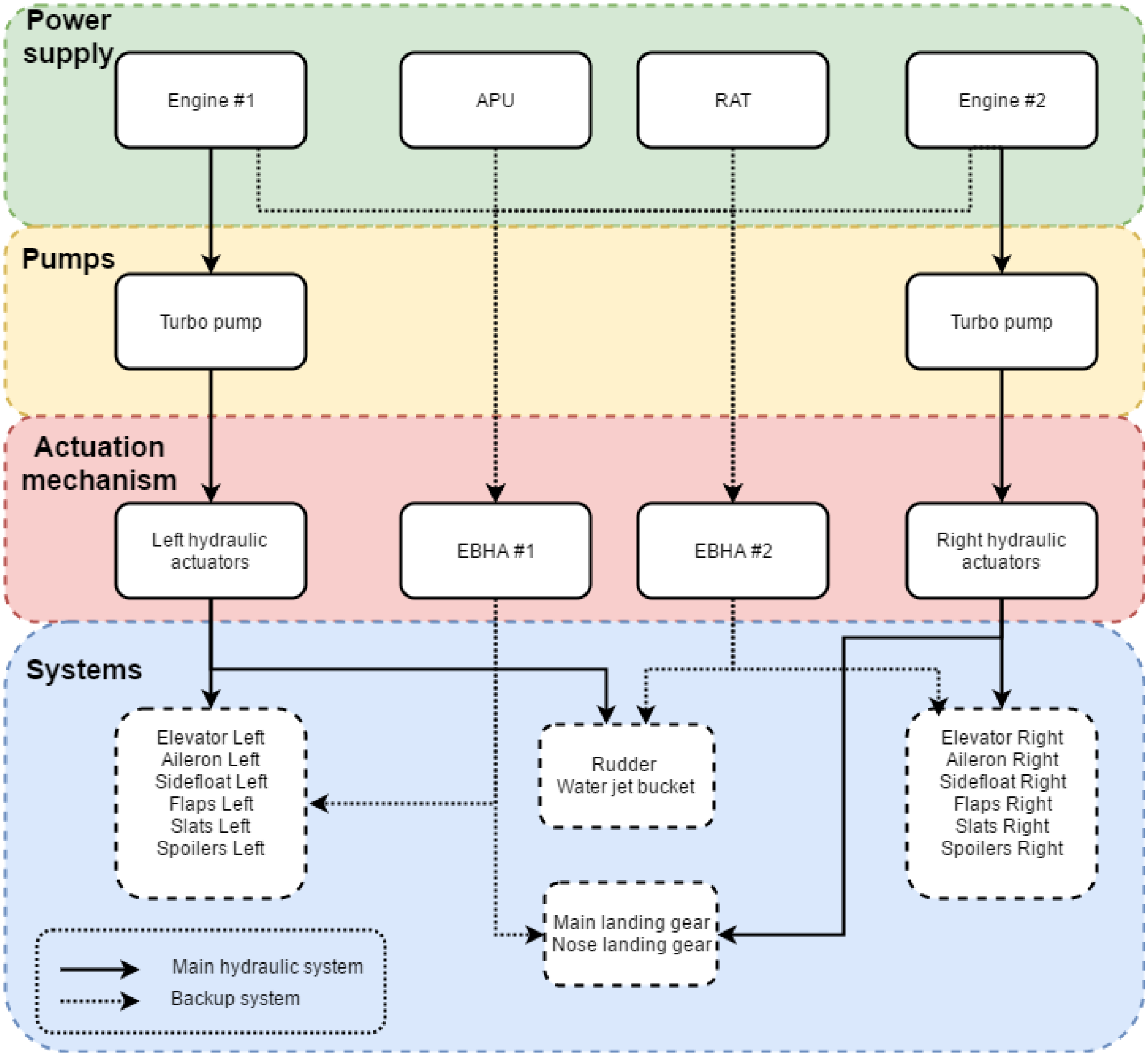

Figure 14.6: Hardware block diagram of the hydraulic system.

IV
The way forward

The current design is a combination of general preliminary design, and the design of critical subsystems and performance characteristics that were deemed critical on the feasibility of the design case. Furthermore, this report is only a snapshot of the current phase of the design, and should therefore not be limited to looking backwards, but should also give an indication of possible next steps. Chapter 15 gives an assessment on the state of the preliminary design, its current feasibility, and the largest risks still affecting this feasibility. Most importantly, Chapter 16 proposes actions that can be taken to mitigate the last risks still affecting feasibility.

15 Evaluation of the preliminary design

This project took off with the major goal of evaluating whether a water business jet would be feasible. By identifying the most critical risks for this feasibility, and mitigating these risks using a wide variety of analyses, it showed that it is likely that such a design is indeed feasible. Operations on water, complexity of side floats, too much hydrodynamic drag at takeoff and hydrodynamic instability were identified as critical risks on feasibility, and were all completely mitigated using analyses provided in this report. Furthermore, a list of requirements to satisfy a design case that would be an economic success in the market was developed and addressed. This chapter will first explain which of these requirements were met, and which were not in Section 15.1. Then, the risks that remain a threat to the feasibility are discussed in Section 15.2.

15.1. Evaluation of design requirements

This project started off by defining the requirements necessary to satisfy the design case. The method that led to these requirements was discussed in Section 2.2. In Appendix L, it is stated whether or not the preliminary design at the current state satisfies individual requirements, or whether further analysis is necessary for specific requirements. The most relevant requirements that were either not met, or for which it could not be concluded whether the Jaeger's preliminary design complied to the specific requirement, are discussed in the remainder of this section.

First of all, it can be seen that requirements 1.1-C and 1.1-D, with respect to the stall speed of the aircraft, are not met. In reality, the stall speed was set at $45\,\mathrm{m\,s^{-1}}$, in order to reduce the required flap and wing size. As analysed in Subsection 4.2.2, all landing and takeoff requirements are still met, and the structural load case was adjusted for a landing impact corresponding to a stall speed of $45\,\mathrm{m\,s^{-1}}$. Therefore, the higher stall speed does not pose any issues on the feasibility. Furthermore, it was required that the aircraft shall be able to transport 15 tonnes of cargo. This would drive the design to an unattainable extent, as described in Subsection 4.2.1. In Section 1.5, it is described that although the ability to transport 15 tonnes of cargo is a customer requirement, this requirement is actually of little relevance for the potential business case of the Jaeger. Therefore, reducing the maximum cargo that can be transported to 10 tonnes will render the design technically feasible, without having a significant impact on the business case.

Furthermore, there are some important requirements for which it cannot yet be concluded whether the final design complies with them. Most notable are REQ 3.0-F, which specifies a load factor while landing. Although the landing load factor is structurally manageable when modelled for a calm, flat sea, it is not yet known whether it is manageable when landing on a rough sea. The latter could lead to an unmanageable distribution of the load.

Moreover, although preliminary spray analysis showed no issues, further analysis should confirm whether this is indeed the case. It is however not likely that spray will have a large adverse effect on the design, due to the positioning of both the cockpit and the engines.

15.2. Feasibility assessment

This project set out to find a conclusion on the feasibility that the design of a Water Business Jet would be a commercial success. Throughout the project, the largest risks that were a threat on this feasibility were identified, as an indicator which subsystems and areas should be analysed with the highest priority. This process for example led to the fact that operational risks were almost fully mitigated, but however, it revealed even more complexity for the integration of the sidefloat and the wing. Currently, Figure 15.1 shows the areas that are the largest threat for feasibility. Many risks can be thought of that have both a low likelihood of occurring, and a low consequence when they occur. Because these risks are less relevant as they will only slightly influence the feasibility of the final design, all risks that would have fallen in the green area in this risk map, are not included in this section. This enables focus on the risks that actually do influence the final feasibility and can be found in Table 15.1. The remainder of this section will explain why these specific risks are worth mentioning here. A recommendation on how to mitigate these risks can be found in Chapter 16.

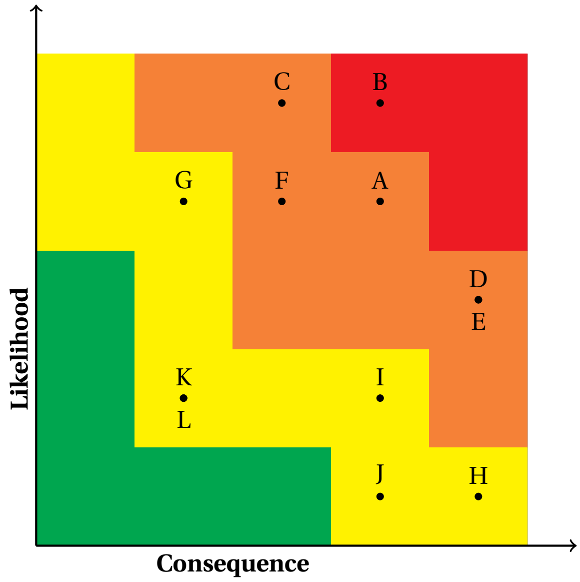

Figure 15.1: Risk map of final system.

Table 15.1: Legend for risk maps and section discussing corresponding risk.

Risk	Reference section
A: Aerodynamic CD0 Analysis	Subsection 11.1.2
B: Shockwave occurrence	Subsection 11.1.2
C: Landing on rough sea	Subsection 10.3.1
D: Hydrodynamic drag	Subsection 10.1.2
E: Change in seaplane regulations	Subsection 6.1.5
F: Change in subsystem masses	Section 4.1
G: Landing gear corrosion	Section 14.1
H: Water operations not possible	Section 6.1
I: Wing and side float don't integrate	Section 11.3
J: Sea traffic prohibits water operations	Subsection 6.1.3
K: Cost model inaccurate	Chapter 5
L: Aircraft shows porpoising motion	Subsection 10.1.3

Aerodynamic performance, considering both drag and shockwaves, is found to be the most critical risk on the feasibility. After all, the Jaeger is designed for both high speed and long range. Due to a large degree of uncertainty and little prior research on the effect of shockwaves around hull shapes, the aerodynamic shockwave effect is deemed a significant risk. A sensitivity as described in Subsection 4.2.1, would imply a range decrease of a little over 20 percent in the extreme case C_{D_0} would increase by 50 percent.
Furthermore, hydrodynamic performance is identified as an area into which further research should be done focusing on two aspects. First, stability and loads during landing on a rough sea, with waves up to 1 meter, should be analysed. Even though both stability while in rough water, and impact loads during landing on calm water have been researched extensively, little is known yet about a landing on rough sea.

Such a landing may result in more concentrated stress distributions. This can lead to larger stresses at specific locations, and furthermore, lead to an undesired moment that may cause the Jaeger to rotate. However, it is found in Subsection 10.3.1 that the larger the landing weight, the smaller the impact loads. Therefore, a more concentrated landing weight, for example on top of a wave, is expected to also reduce the loads. Moreover, it is expected that the differential moment due to rotation only acts on the aircraft for a short period of time. Taking all into consideration, it is thought that the risk that this effect will lead to a large impact on the feasibility, is not enormously large.

There are other risks that are not as critical as the ones mentioned above, but that are still important to consider in a further feasibility studies. Firstly, new regulations might pose the need for changes to the design, because at this point many regulations are often developed locally for small-scale applications of amphibious aircraft. It is possible that the Jaeger incites regulators to assimilate all local regulations into country-wide, or even global regulations. Such a scenario may lead to the need to change some parts of the design because of changing regulations.

Secondly, as many subsystems were only designed preliminary, their masses are estimated based on reference data. In case these masses change, this may influence the maximum payload and fuel weights, but may also change the centre of gravity. As a result, there may be need for a redesign of the wing, empennage, and control surfaces to maintain stability.

Lastly, it may happen that the side float retraction mechanism drives the wing box structure to an unattainable extent. Such a scenario would require a side float that would not retract inside the wing. This will unavoidably lead to an increase of drag during cruise. Relying on the sensitivity analysis for the current preliminary aerodynamic drag estimation, in the hypothetical case that drag would increase by 10 percent, range would reduce by 5 percent. Furthermore, the effect of possible shockwaves around the extended side float at Mach 0.9 are still unknown. As both long range and high speed were found to be a vital aspects of the business case in Chapter 1, it can be concluded that the consequence of this risk is severe.

At last, four risks are identified that should not be forgotten in a feasibility studies, but are less likely to cause significant changes to the total design. Firstly, these include corrosion of the landing gear due to extension while in water, which has a low consequence because wide knowledge is available on how materials react when in contact with seawater. Furthermore, this risk most likely only implies that it may be necessary that inspection of the landing gear would be required more often. This is not something that would have a large risk on the feasibility.

Second, if water operations in populated areas were impossible, this would have a significant impact on the feasibility of the Jaeger. However, this is not a likely event, as extensive research has been done on this in Chapter 6.

Thirdly, the final cost of the aircraft may deviate from the current planning in later stages of the design. Although the current model seems to comply with the robust three-dimensional least squares fit from reference data, the uncertainty of the results of later design stages inevitably implies uncertainty about the development of the cost in later stages of the design. Nevertheless, the model seems to be an accurate estimation for this preliminary state, and considering that it is rather conservative, it is thought that there is not a high probability of an overshoot in the orders of 10 %. Furthermore, smaller overshoots would not pose a large risk on the economic feasibility.

The fourth and last small risk, is that there is a risk that the aircraft is unstable during motion in the water. However, preliminary calculations indicate that the aircraft will be dynamically stable in the water.

It can thus be concluded that this Risk Analysis provides clear indicators of areas that need further design work, in order to arrive at an indisputable conclusion regarding the feasibility of this Water Business Jet Design. Concrete recommendations on how to assess the identified risks, are given in Chapter 16.

16
Conclusion and recommendations

Throughout Part II and Part III the current state of the design including results, conclusions and recommendations for further design efforts have been presented on a (sub)system level. Subsequently, Chapter 15 evaluated the current state of the design on a top-level by comparing it to the initially set requirements and performing a risk analysis. This chapter aims to put together these findings and give an action plan for the future. Section 16.1 presents the conclusions of the project, after which Section 16.2 elaborates on the recommendations for further efforts in studying the feasibility and development of the water business jet concept. A rough planning for the future which takes these recommendations into account is presented in Appendix O.

16.1. Conclusion

The objective of the design project was to develop a preliminary design of a high-speed, executive, amphibious aircraft and research its technical, operational, and economic feasibility. At the current state, an aircraft concept has been established and preliminarily sized. This design consists of a two-engine jet aircraft with a high wing, T-tail configuration. It has a hull shaped bottom of the fuselage, a waterjet propulsion system and retractable side floats for stability on water. The side floats and waterjet provide functions critical to the feasibility of the concept and were therefore designed in more detail than other subsystems.

Based on both a market and cost analysis the concept is expected to be highly competitive and profitable. At a sales price of 60 million USD break and with 100 units sold, a profit of approximately 2.4 million USD is made per aircraft. An average annual increase of 2.7% in long range business jet deliveries is anticipated for the coming ten years. Differentiation between the current products on this market is limited, whereas the unique selling point of the concept is the flexibility it provides with its amphibious capabilities. Being the first to bring a business water jet to the market imposes a large first mover advantage, based both on both reputation and knowledge.

Through research, design and evaluation efforts, the majority of initially set requirements and identified risks have been met and mitigated respectively. Firstly, an operational plan for landing and takeoff near major business-centric cities and at remote areas was created. It shows that no new large infrastructural development is required, and that community noise, maritime traffic, weather and current regulations at desired landing sites form no substantial limitations on operations. Furthermore a developed model indicates that it is likely the concept can overcome hydrodynamic drag during takeoff and taxiing. In addition, preliminary calculations have shown that spray will not form a threat during takeoff. Lastly, the design of the side floats has been proven to provide sufficient hydrostatic stability when subject to a wave height of 1 meter and to be integrable within the wing structure as well.

By means of a final risk assessment, it was concluded that at the current state aerodynamic performance is the most critical risk on the feasibility of the concept. CFD analysis identified shock wave formation at the hull of the fuselage when operating at Mach 0.8. It is uncertain what the resulting effects are on the performance of the aircraft. In addition, the method used for estimating the zero-lift drag and contribution of the hull has not been validated yet. The accuracy of these models is significant for the feasibility of the concept as the market analysis identified that the ability to achieve a long range at high speed is a critical

requirement.
Finally there are some other items which currently are a considerable threat to the feasibility. For hydrodynamics, the drag model has not been validated yet and little is known on the stability and impact loads during landing in rough water conditions. This has a direct influence on the side floats design and therefore could change the current assessment on the integration feasibility. Lastly, a change in regulations could endanger the operational aspects which make the concept unique.

16.2. Recommendations

In Section 16.1 it has been concluded that at the current state, the concept indicates technical, operational and economic feasibility, but still a couple of noticeable risks exist. Due to the overall promising results it is recommended to proceed with further efforts in studying the feasibility of and developing the water business jet concept. This section mainly focuses on the most urgent recommendations which are supported by means of work flow diagrams in Subsection 16.2.1, Subsection 16.2.2 and Subsection 16.2.3. Furthermore some additional recommendations considering operational and economic feasibility are made. In effect the recommendations can be viewed as mitigation strategy for the risks presented in Chapter 15.

16.2.1. Aerodynamic performance

Aerodynamic performance was found to be the most critical risk to the feasibility of the preliminary design in Chapter 15. This risk is twofold. Firstly, it was shown that shock waves are present at the hull of the fuselage when operating at high Mach numbers in Subsection 10.2.2. However, it is currently uncertain what the resulting effects of such shock waves are on the feasibility of the design. Therefore, it is highly recommended to dig deeper into this subject by doing an extensive literature study, and performing more research with use of computational models and experimental methods. This process is represented by phase 1 in Figure 16.1. If it turns out that this risk renders the current design infeasible, efforts should be directed to investigation of possibilities to solve this issue. This would mean evaluating new design options, for example a morphing step in the hull of the fuselage.
When the hull shape is feasible in terms of shock wave formation, the next aspect of the aerodynamic performance risk should be addressed. The method used for estimating the zero-lift drag has not been validated yet and the contribution of the hull of the fuselage has been based on merely statistical data. On top of that the method shows a high degree of sensitivity to exactly the hull contribution as presented in Subsection 10.2.1. Since the zero-lift drag largely influences the use of the aircraft at high speed and long range, it is important to obtain more certainty on the found results. Therefore, it is advised to validate the used method and if necessary establish a new model. This is visualised as phases 2 and 3 in Figure 16.1.
In the process a distinction between the aircraft with and without hull has been made. This is to ensure that first a solid preliminary phase drag model for parametric geometries is established in general, before efforts are directed on how to properly account for the hull. After this process has been performed, conclusions can be drawn with respect to the feasibility of the design in terms of aerodynamic drag.

16.2.2. Hydrodynamic performance

Hydrodynamic performance was identified as an area into which further research should be done. Two aspects in this topic form a risk for the feasibility of the design. First, little is known yet on operating the aircraft in rough water conditions such as the degree of stability during landing. It is recommended to establish a model which takes this situation into account and check whether it imposes constraints on the design or restrictions on the operations of the aircraft. This task is included within the work flow presented in Figure 16.2.
Furthermore, the model which was used for estimating the hydrodynamic drag during taxiing and takeoff has not been validated yet. If this drag turns out to be considerably higher it could have detrimental effects on the feasibility of the design, both technically and operationally. Therefore, it is advised to validate this model by means of a towing tank test, which has been described in detail in Subsection 10.1.2.

16.2.3. Structural performance

The last major recommendation concerns the development of structural model of the aircraft, which is visualised in Figure 16.3. This is required to address multiple risks identified in Chapter 15. These include the impact loads during landing on water in rough weather conditions, integration between the side floats and wing and the masses of different subsystems. The laid out process consists of two parts.

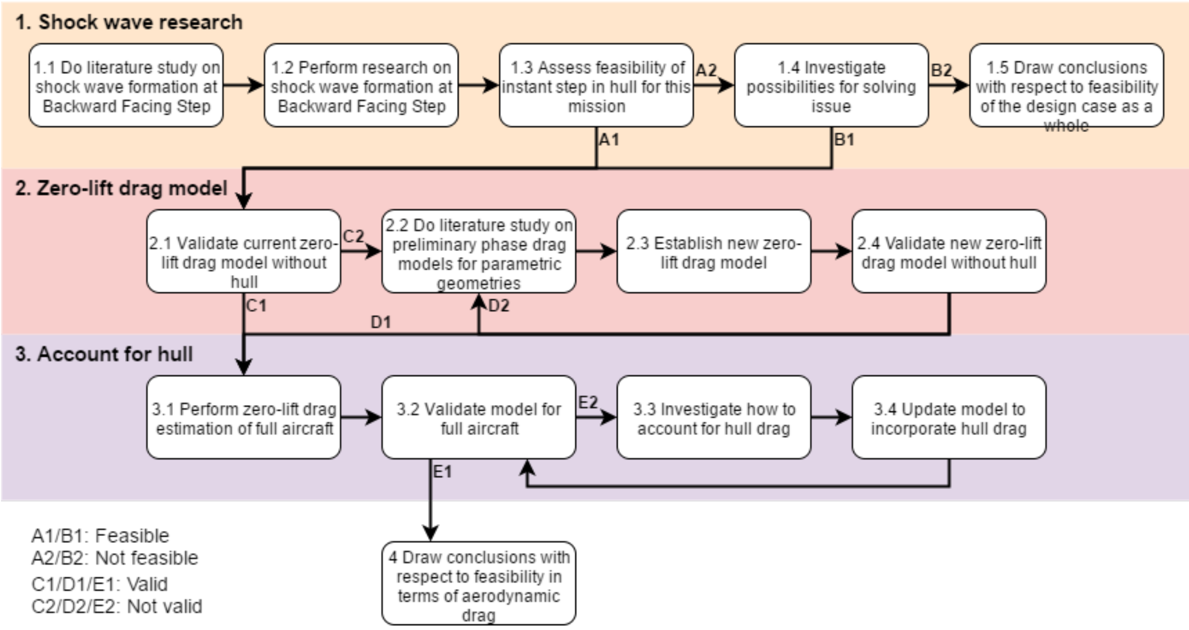

Figure 16.1: Recommended work flow for addressing risks concerned with aerodynamic performance.

First, an investigation into the load case should be performed. This has been done already into a large extent in Section 10.3, Section 11.3 and Chapter 12. However, it has to be extended to include the load case of landing rough water and loads originating from other subsystems.
The second part consists of the structural research. After a check on the structural feasibility of critical integration points, such as the side float and wing, the aircraft can be designed structurally for the established load case. Subsequently a more detailed mass estimation of different subsystems such as the empennage can be established. It should be kept in mind that the whole process is iterative due to the feasibility and validation checks at certain points. The purpose is to end up with a design which optimally balances structural integrity and mass of the aircraft.

16.2.4. Operations and cost model

Some additional recommendations which are less extensive are also provided. To start off, operations of the aircraft are susceptible to several small risks. Firstly few, non-uniform regulations are currently in existence regarding amphibious aircraft operations. There is a risk that new, less favourable regulations will be established. Secondly, it could turn out that the maritime traffic at major business-centric cities in the long run does impose restrictions on landing operations. Thirdly, the possibility exists that current infrastructure does not suffice for landing operations.
To mitigate the risk of an infeasible design or operations due to these three items, it is advised to proactively work together with the respective authorities and secure the desired operational plans. In addition, a more extensive research on maritime traffic should be performed as mentioned in Subsection 6.1.3.
Lastly, there is a chance that the cost model is inaccurate and that as a result the design would be economically infeasible. Therefore, it is recommended to use more sophisticated models as the design progresses and more detailed parameters can be taken into account.

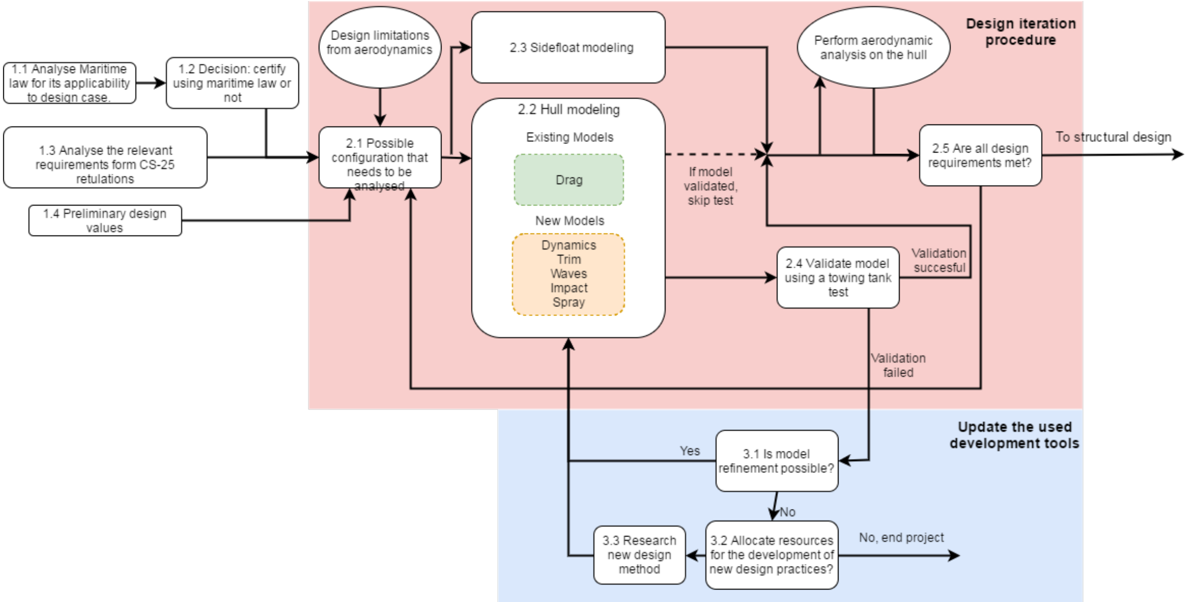

Figure 16.2: Recommended work flow for addressing risks concerned with hydrodynamic performance.

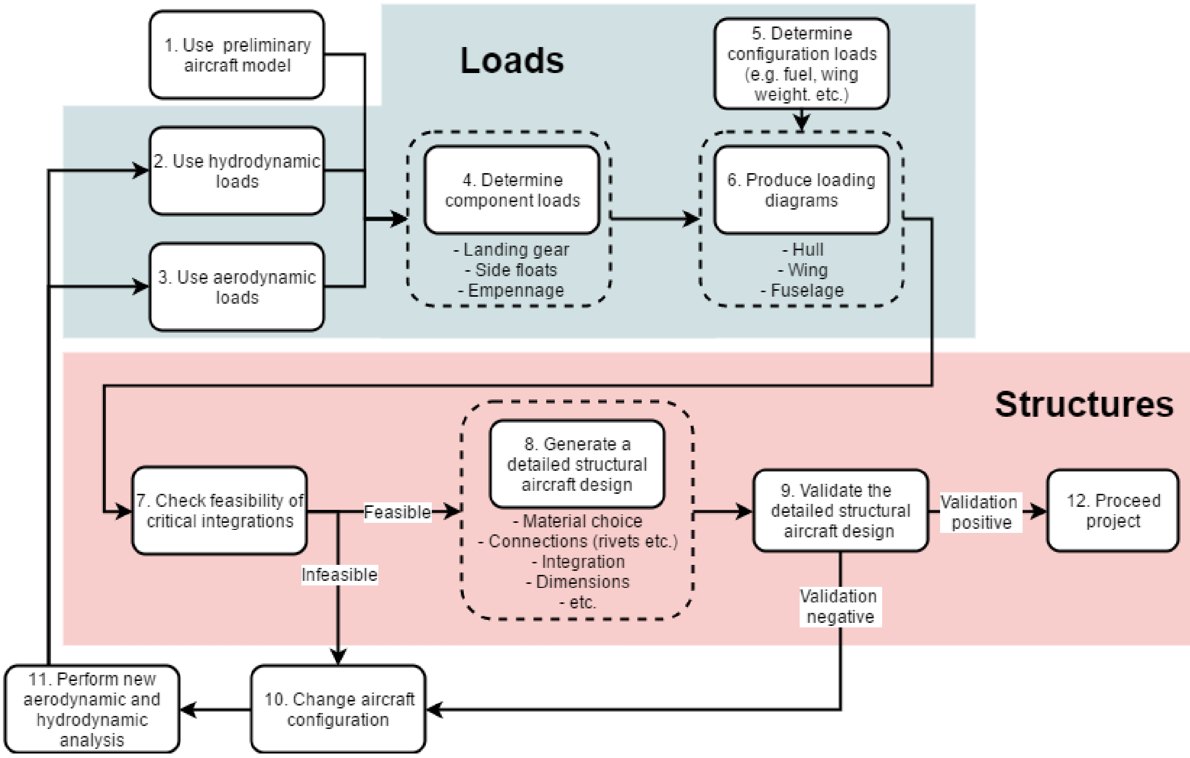

Figure 16.3: Recommended work flow for addressing risks concerned with structural performance.

A
CFD

A.1. CFD setup

CFD setup used to support the conclusions given in Subsection 10.2.2. See Figure A.2 for a visual representation and Table A.1 for the precise dimensions of the step and domain. The meshing was performed with three different setups, one for the top surface with a coarse mesh, one for the fuselage wall with very fine mesh and one for the remaining middle edges with a regular mesh. This was done to gain accurate results for the flow nearby the step and lower the computing time by making a coarse mesh far away from the surface of interest.

Table A.1: Coordinates of edge points of mesh.

Point	x [m]	y [m]	z [m]
1	0	0	0
2	0	0	0.2
3	0	3	0
4	0	3	0.2
5	1	0	0
6	1	0	0.2
7	1.7	-0.23	0
8	1.7	-0.23	0.2
9	6	-0.65	0
10	6	-0.65	0.2
11	6	3	0
12	6	3	0.2

The fuselage was modelled as a no slip wall. The inlet was modelled to be subsonic and have a inlet velocity equal to the required mach number in the u direction. The upper side and right side were modelled as openings with a relative pressure of 0 Pa and a normal velocity component. The sides of the domain were modelled as symmetry. The model was initiated with a velocity of $0\,\mathrm{m\,s^{-1}}$ across the domain and a temperature equal to the temperature at ISA 41 000 ft. For the remaining setups see Figure A.1.

Table A.2: Setup parameters for mesh.

Boundary	Top	Mddle	Wall
Maximum size	1.2	0.1	0.01
Height	1.2	0.1	0.01
Minimum size t	0.4	0.01	0.005

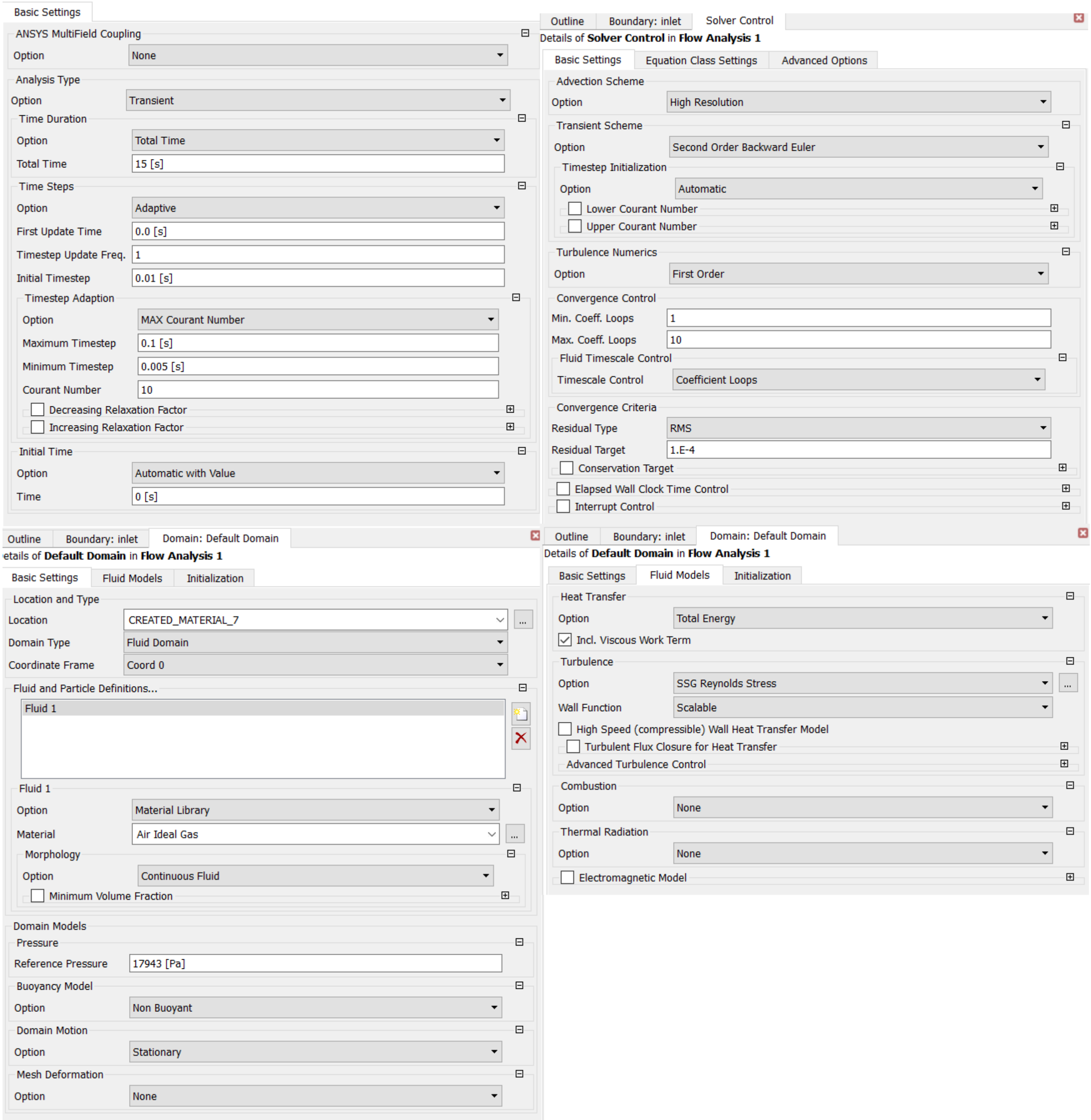

Figure A.1: Settings of CFD.

A.2. CFD results

The flow around the step is visualised here. These figures are used to support the conclusions given in Subsection 10.2.2 Each figure shows the fluid domain around the step. The air flows from the left to the right. On the bottom the domain changes direction twice. This was done to replicate the step on the aircraft. In the figures the aircraft would be upside down flying from the right to the left of the page.

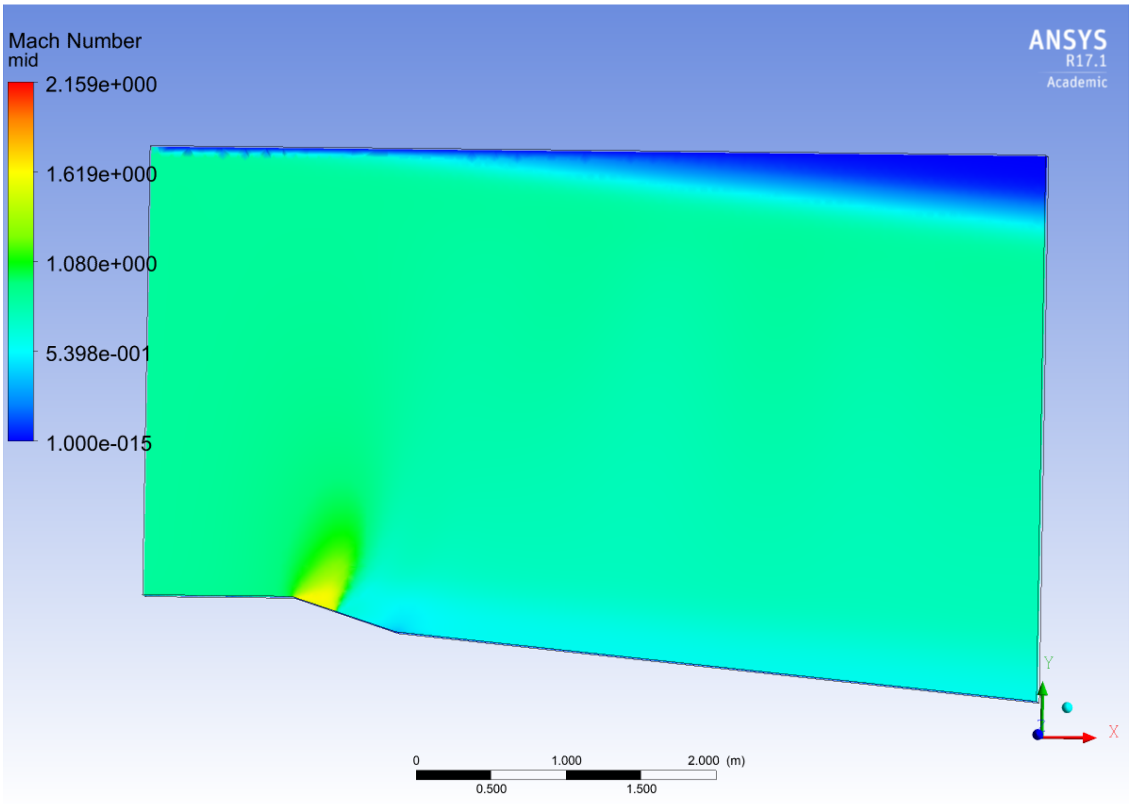

Figure A.2: Air flow of Mach 0.85 around the step

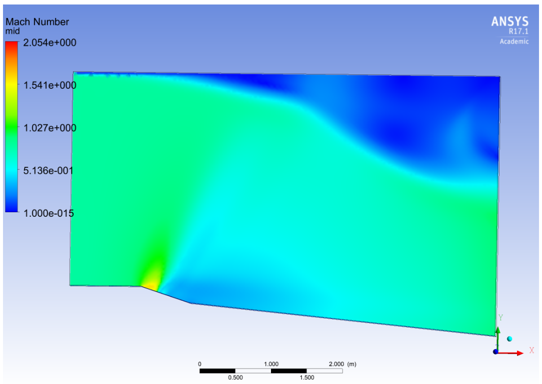

Figure A.3: Air flow of Mach 0.80 around the step.

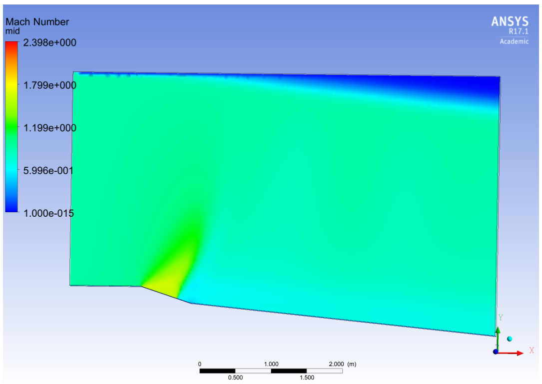

Figure A.4: Air flow of Mach 0.90 around the step

B

Air traffic control

Schematic detailing the architecture of the air traffic control in the United States of America. Detailed explanations can be found in Subsection 6.1.2

Figure B.1: Visualisation of Air Traffic Control system in the United States of America.

C

Maritime traffic

Table C.1 shows a number of coastal cities and their appeal as destination. Further explanations are given in Subsection 6.1.2.

Location	Reason for selection	Comments on maritime traffic
Amsterdam	Large city, possibility of easy access to information on location	Vessels on IJmeer travel in straight lines
Boston	#18 on GCEPI	Some scattering of vessels
Buenos Aires	#2 South-American city on Global City GDP list by Brookings Institution [38]	Anchoring spot far from city centre
Chicago	#8 route, #12 on GCEPI	Large shielded part in lake for harbour
Côte d'Azur	#1 & #7 route, #1 fastest growing route	Mostly pleasurecraft, traffic concentrates very close to shoreline
Dubai	#3 fastest growing route	On large scale busy but organised, near city centre (next to "The World") relatively low traffic density
Dublin	#16 on GCEPI	Little maritime traffic
Florida, Southeast coast	#2, #4, #10 route, #2 & #5 fastest growing route	Mostly pleasurecraft, traffic concentrates very close to shoreline
Geneva	#22 on GCEPI	Close to no maritime traffic
Helsinki	#14 on GCEPI	Little maritime traffic
Lagos	#8 fastest growing route	Some scattering of vessels, no maritime traffic on Lagos Lagoon
Los Angeles	#3 route, #7 on GCEPI	Maritime traffic concentrated near harbour
Mumbai	Asia	Maritime traffic concentrated at eastcoast
New York City, Lower bay	#2, #3, #4, #5, #8, #9, #10 route, #1, #4 fastest growing route, #1 on GCEPI	Some scattering of vessels
Oslo	#18 on GCEPI	Maritime traffic concentrated at several smaller harbours
San Fransisco	#23 on GCEPI	Close to no maritime traffic on upper part San Fransisco Bay
Sydney	#14 on GCEPI	Close to no maritime traffic outside Sydney harbour & Watson's Bay
Tel Aviv	#6 fastest growing route	Close to no maritime traffic
Toronto	#10 on GCEPI	Close to no maritime traffic
Vancouver	Large city, used as case throughout the entire project	Scattering of anchored vessels on Burrard Inlet, close to no maritime traffic on Straight of Georgie
Washington DC	#10 fastest growing route, #23 on GCEPI	Close to no maritime traffic
Zurich	#13 on GCEPI	Close to no maritime traffic
Hong Kong	Asia, #4 on GCEPI	Busy, mostly concentrated anchored vessels, mostly systematic travel routes
Singapore	Asia, #6 on GCEPI	Busy, highly concentrated anchored vessels, highly systematic travel routes, less traffic toward East
Shanghai	Asia, #18 on GCEPI	Busy, highly concentrated anchored vessels, extremely systematic travel routes with large area in between incoming & outgoing vessels
New York City, Upper bay	#2, #3, #4, #5, #8, #9, #10 route, #1, #4 fastest growing route, #1 on GCEPI	Highly scattered maritime traffic on a small area
Osaka	Asia, #16 on GCEPI	No systematic travel routes
Tokyo	Asia, #3 on GCEPI	Highly scattered anchored vessels, no systematic travel routes

Table C.1: Results of maritime traffic research. GCEPI = Global City Economic Power Index. [1]

[1] https://www.citylab.com/life/2015/03/sorry-london-new-york-is-the-worlds-most-economically-powerful-city/386315/. Retrieved 31-05-'17

D

Climates of New York, Vancouver and Hong Kong

The data from Table D.1 and D.2 is based on NASA's MERRA-2 Modern-Era Retrospective Analysis. The influence of these climates on the operations of Jaeger are discussed in Subsection 6.1.6.

Table D.1: Average maximum and minimum temperature for several business-centric cities in °C .

		Jan	Feb	Mar	Apr	May	Jun	Jul	Aug	Sep	Oct	Nov	Dec
New York[1]	max	3	5	10	16	22	26	29	28	24	18	12	6
	min	-3	-2	3	7	12	17	21	20	16	10	5	0
Vancouver[2]	max	7	8	11	14	17	20	22	22	19	14	9	7
	min	3	3	5	7	10	12	14	14	12	8	5	3
Hong Kong[3]	max	19	19	21	25	28	30	31	31	30	28	24	20
	min	15	15	17	21	24	26	27	26	24	24	20	16

Table D.2: Average wind speeds and 90^{th} percentile wind speeds for several business-centric cities in $\mathrm{km\,h^{-1}}$.

		Jan	Feb	Mar	Apr	May	Jun	Jul	Aug	Sep	Oct	Nov	Dec
New York[1]	average	9	9	9	8	7	6	6	6	7	7	8	9
	90^{th} percentile	14	14	14	12	10	9	8	8	10	11	13	13
Vancouver[2]	average	6	5	5	4	3	3	3	3	3	4	5	6
	90^{th} percentile	8	8	8	7	6	5	5	4	5	7	8	8
Hong Kong[3]	average	11	10	10	9	9	9	9	8	9	10	11	11
	90^{th} percentile	16	16	15	14	12	13	14	13	15	16	16	17

[1] `https://weatherspark.com/y/23912/Average-Weather-in-New-York-City-New-York-United-States`. Retrieved 20-06-'17

[2] `https://weatherspark.com/y/476/Average-Weather-in-Vancouver-Canada`. Retrieved 20-06-'17

[3] `https://weatherspark.com/y/127942/Average-Weather-in-Hong-Kong-Hong-Kong-SAR-China`. Retrieved 20-06-'17

E Data on reference aircraft

Table E.1: Data of reference aircraft for analysis of competitors and preliminary estimations. [24]

Aircraft	Passengers	Range [NM]	Cruise speed [M]	MTOW [kg]	Max PL [kg]	Sale price [million USD]	Noise level [EPNdB]	Max certified altitude [ft]	T-O Lenghth [m]	Cabin altitude [ft]
Embraer Legacy 600	13-14	3430	0.71	22500	2400	26.0	-	41000	1711	-
Embraer Legacy 650	13-14	3919	0.72	24300	2210	31.6	91.7	41000	1750	8000
Falcon 2000 S	10-19	3540	0.75	18600	2245	28.4	90.5	47000	1318	-
Falcon 2000 LXS	8-18	4075	0.75	19400	2245	33.7	91.0	47000	1794	-
Falcon 900 LX	12-19	4695	0.73	22226	2796	43.3	92.3	51000	1540	8000
Falcon 7 X	12-19	5760	0.79	31750	1996	53.8	-	51000	1740	3950
Falcon 8 X	12-19	6450	0.79	33100	2223	57.5	-	51000	1829	3900
Challenger 650	10-19	4020	0.73	21850	2200	32.4	90.3	41000	1720	7000
Global 5000	13-19	5520	0.81	41950	2341	50.4	89.7	51000	1689	4500
Global 6000	13-19	6147	0.81	45130	1710	62.3	89.7	51000	1976	4500
Gulfstream G450	14-19	4328	0.79	33840	2722	41.0	92.3	45000	1707	-
Gulfstream G550	16-19	6708	0.79	41275	2812	61.5	90.8	51000	1802	6000
Gulfstream G650	16-19	6912	0.84	45175	2948	66.6	88.3	51000	1786	2800
Gulfstream G650 ER	16-19	7437	0.84	47000	2948	68.7	88.3	51000	1921	2800

Table E.1 shows some basic data on reference business aircraft, as used in the market analysis of Chapter 1.

F
Side floats connection and interrelations

F.1. Side float connection design option tree

The design option tree from which the tradeoff in Subsection 12.1.2 are taken, is shown in Figure F.1.

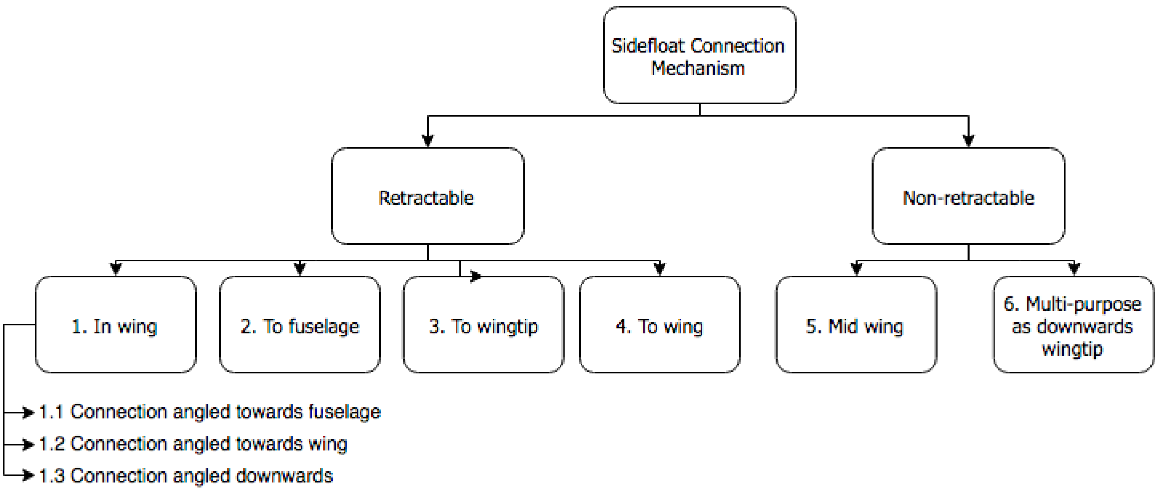

Figure F.1: Design option tree of side float connection.

F.2. Side float interrelations

The interrelations that the side float subsystem has internally. These interrelations are used to were used to determine the inputs and outputs of the subsystem with respect to the connecting subsystems in Chapter 12.

Cockpit	Extend/retract input			
Extended/retracted	**Actuators**	Side float 1 or 2 actuator failure	Provide rotation	Provide rotation
Extended/retracted		**Linkage between side floats (redundancy)**	Provide rotation through side float 2	Provide rotation through side float 1
	Provide support		**Side float 1**	
	Provide support			**Side float 2**

Figure F.2: N2-chart side floats.

G
Towing tank test speeds

Table G.1 shows the proposed towing tank speeds for the towing tank as described in Subsection 10.1.2. The first column shows the Froude numbers at which the aircraft will operate during takeoff and landing. The second column shows the corresponding speeds and Reynolds numbers for the full scale aircraft. Column three shows the towing speeds and corresponding Reynolds numbers for the larger model 1 used to test the lower speed regimes of the aircraft. Column four shows the towing speeds and corresponding Reynolds number for the smaller model 2 used to test the higher speed regimes. Note how the towing speeds of model 1 and model 2 do not exceed the maximum towing speeds of the towing tank facility. Furthermore both models will be tested three times at the same Froude number to map the deficiencies between the two models after correcting for the Reynolds number.

Table G.1: Relevant Froude numbers with the corresponding speeds and Reynolds numbers, for the full scale hull and the two proposed towing tank test models.

	Full scale (22.3 by 2.7 m)		**Model 1** (1.59 by 0.192 m)		**Model 2** (0.571 by 0.069 m)	
Froude number	Speed [$\mathrm{m\,s^{-1}}$]	Reynolds number	Speed [$\mathrm{m\,s^{-1}}$]	Reynolds number	Speed [$\mathrm{m\,s^{-1}}$]	Reynolds number
0.13	1.9	4.17×10^{7}	0.5	7.90×10^{5}		
0.25	3.7	8.33×10^{7}	1	1.58×10^{6}		
0.38	5.6	1.25×10^{8}	1.5	2.37×10^{6}		
0.51	7.5	1.67×10^{8}	2	3.16×10^{6}		
0.63	9.4	2.08×10^{8}	2.5	3.95×10^{6}	1.5	8.54×10^{5}
0.76	11.2	2.50×10^{8}	3	4.74×10^{6}		
0.89	13.1	2.92×10^{8}	3.5	5.53×10^{6}		
1.01	15.0	3.33×10^{8}	4	6.32×10^{6}		
1.14	16.9	3.75×10^{8}	4.5	7.11×10^{6}		
1.27	18.7	4.17×10^{8}	5	7.90×10^{6}	3	1.71×10^{6}
1.39	20.6	4.58×10^{8}	5.5	8.69×10^{6}		
1.52	22.5	5.00×10^{8}	6	9.48×10^{6}		
1.65	24.4	5.42×10^{8}	6.5	1.03×10^{7}		
1.77	26.2	5.83×10^{8}	7	1.11×10^{7}		
1.90	28.1	6.25×10^{8}	7.5	1.19×10^{7}	4.5	2.56×10^{6}
2.03	30.0	6.67×10^{8}	8	1.26×10^{7}		
2.11	31.2	6.94×10^{8}			5	2.85×10^{6}
2.22	32.8	7.29×10^{8}			5.25	2.99×10^{6}
2.32	34.4	7.64×10^{8}			5.5	3.13×10^{6}
2.43	35.9	7.99×10^{8}			5.75	3.27×10^{6}
2.54	37.5	8.33×10^{8}			6	3.41×10^{6}
2.64	39.1	8.68×10^{8}			6.25	3.56×10^{6}
2.75	40.6	9.03×10^{8}			6.5	3.70×10^{6}
2.85	42.2	9.37×10^{8}			6.75	3.84×10^{6}
2.96	43.7	9.72×10^{8}			7	3.98×10^{6}
3.06	45.3	1.01×10^{9}			7.25	4.13×10^{6}
3.17	46.9	1.04×10^{9}			7.5	4.27×10^{6}
3.27	48.4	1.08×10^{9}			7.75	4.41×10^{6}
3.38	50.0	1.11×10^{9}			8	4.55×10^{6}

H N2 chart

Analyses & requirements			Reference data, capacity requirements	Aero analysis	Hydro analysis	Hydro &market analysis	Aero analysis & performance requirements	Hydro analysis	Weight analysis, load case analysis	Aerodynamic & hydrodynamic analysis	MFW	Regulations, capacity requirements	Statistical data on aircraft power consumption	regulations on EBHA
customer requirements	**Operations**										Mission profile	Landing site analysis		
Aircraft mass & c.g.	limitations	**Mass & c.g.**				Mass & c.g.	Mass & c.g.	Mass & c.g.	Mass & c.g.	Mass & c.g.	Mass & c.g.			
		passenger placement and interior weight & c.g.	**Cabin**	Cabin geometry	Cabin geometry								Cabin power consumption	
Wing & empennage geometry		Wing & empennage mass & c.g.		**Wing & empennage**	Wing & empennage geometry		Wing & empennage geometry	Wing geometry	Wing geometry	Wing geometry	Wing geometry	Wing & empennage geometry		
Fuselage & hull geometry		Fuselage & hull mass & c.g.		Aerodynamic characteristics of fuselage	**Fuselage & hull**	Fuselage geometry	Aerodynamic characteristics of fuselage	Hull hydro capabilities	Fuselage geometry	Spray of fuselage	Fuselage & hull geometry	Fuselage geometry		
		WJP mass & c.g.			WJP geometric requirements	**Water Jet Propulsion (WJP)**							WJP power consumption	
		HLD & CS mass & c.g.		Aerodynamic characteristics flaps			**High-lift devices & Control surfaces (HLD & CS)**							
		SIdefloat mass & c.g.		Sidefloats storing requirements	Hydrodynamic capabilities, sidefloats storing requirements			**Sidefloats**			Sidefloats storing requirements	Side floats location		
		LG mass & c.g.			Landing gear storing requirements				**Landing Gear (LG)**		Landing gear storing requirements			
		Propulsion system mass & c.g.		Stability characteristics of engine placement			Stability characteristics of engine placement			**Propulsion System**	Fuel consumption			provide hydraulic pressure
		Fuel mass & c.g.		Fuel tank geometry	Fuel tank geometry					Fuel pumping	**Fuel Tanks**			
	Loading operations				(Un)loading system geometry							**(Un)loading system**		
		EPS mass & c.g.								Electrical power required			**Electrical Power System (EPS)**	provide power for backup system
							provide actuation	provide actuation	provide actuation			provide actuation		**hydraulics**

Figure H.1: N2-chart of the complete aircraft, as used for the system interactions in Subsection 4.1.2

I

Method for estimating the zero lift drag coefficient

This appendix presents the method used to estimate the zero lift aerodynamic drag for the fuselage, wing, empennage and side floats. Assumptions and limitations on a general level will be discussed, whereas assumptions and limitations for specific parts of the aircraft are discussed in their respective chapters.
The method is based on different models. For the friction drag, a full configuration drag estimation model developed by Gur, Mason and Schetz [19] was used. This model is aimed at early stages of the design phases for sub- and transonic aircraft configurations when computational fluid dynamics (CFD) is not yet possible. It includes induced, friction, wave and interference drag. It was found however that the Korn-Lock method, which is used in this model, is not an accurate predictor of wave drag in the conceptual design phase [53]. Based on this comparison study of Vargas and Vos, it was decided to use the Delta Method for estimation of the wave drag [13]. At last it was found that the method for estimating interference drag was not clarified upon enough for proper application. Therefore it was assumed to neglect the interference drag in the zero lift drag estimation. This assumption is backed by the fact that the contribution of the interference drag is small [19].
Main inputs for the methods are chosen in such a way that the method is convenient to apply in this phase of the design. This means that these parameters are usually known at this stage, and can still be changed to optimise the design for aerodynamic drag performance. Inputs include geometric parameters such as fuselage length, wing span and chord, and flight conditions such as Mach number and altitude.
The models for estimating the friction drag [19] and wave drag [53] [13] have been verified and validated individually in the respective studies. However, the developed method, which combines these two methods, for estimating the total zero lift drag, has not been validated yet. To be able to obtain a high degree of certainty on the results found with this method, validation in the form of for example wind-tunnel tests should take place. In addition, the assumption of neglecting the interference drag should be assessed as well.

J

Tradeoff table

Table J.1 shows the result of the original tradeoff as executed during the concept generation and selection phase in the midterm report [36]. The canard configuration with side floats was considered the best concept, as is clear from the table. However, during the detailed design phase the technical risk assessment based on the conceptual design showed that this concept was not feasible. It was therefore decided to continue the design with the T-tail configuration with side floats, as is described in Section 3.3.

Table J.1: Tradeoff table for the top level tradeoff. The numbers behind the criteria indicate the weight. The colours depict the score: correctable deficiencies (yellow); good, meets requirements (blue) and excellent, exceeds requirements (green).

Concept		Canard Sidefloats	Canard Wide body	T-tail Sidefloats	T-tail Wide body
Hydrodynamic performance (5)	Drag (0.5)	Small beam	Large beam	Small beam	Large beam
	Static stability (1)	Unrestricted stabiliser location	Limited stability	Unrestricted stabiliser location	Limited stability
	Dynamic stability (1.5)	Aft c.g. Slender body	Aft c.g. Wide body	Nominal c.g. Slender body	Nominal c.g. Wide body
	Buoyancy (1)	Trim angle at rest	Trim angle at rest	Comparable to ships	Comparable to ships
	Spray (1)	Small beam	Large beam	Small beam	Large beam
Aerodynamic performance (5)	Lift & drag (3)	Positive stabiliser	Positive stabiliser Wide body	Nominal	Wide body
	Stability (1)	Limited c.g. range	Destabilising hull	Nominal	Destablilising hull
	Controllability (1)	High manoeuvrability Good stall characteristics	High manoeuvrability Good stall characteristics	Deep stall possible	Deep stall possible
Structural performance (3)	Configuration (1)	Nominal	Nominal	Stall protection required	Stall protection required
	Water (2)	Nominal	Heavy fuselage	Nominal	Heavy fuselage
Development risk (3)		Both canard and sidefloats proven concepts	Transonic wide body unknown	Both T-tail and sidefloats proven concepts	Transonic wide body unknown
Passenger comfort (3)	Noise (1)	Aft engines No tail resonance	Aft engines No tail resonance	Nominal	Nominal
	Stability (1)	High length-to-beam ratio	Low length-to-beam ratio	High length-to-beam ratio	Low length-to-beam ratio
	Space (1)	Nominal	Increased area and volume	Nominal	Increased area and volume
Spinoff possiblities (1)		Low speed range	Low speed range Spacious cabin	Proven passenger cargo	Proven passenger cargo Spacious cabin

K
Wing and thrust loading

T/W and W/S diagram used to determine minimum thrust ratio in Section 13.1.

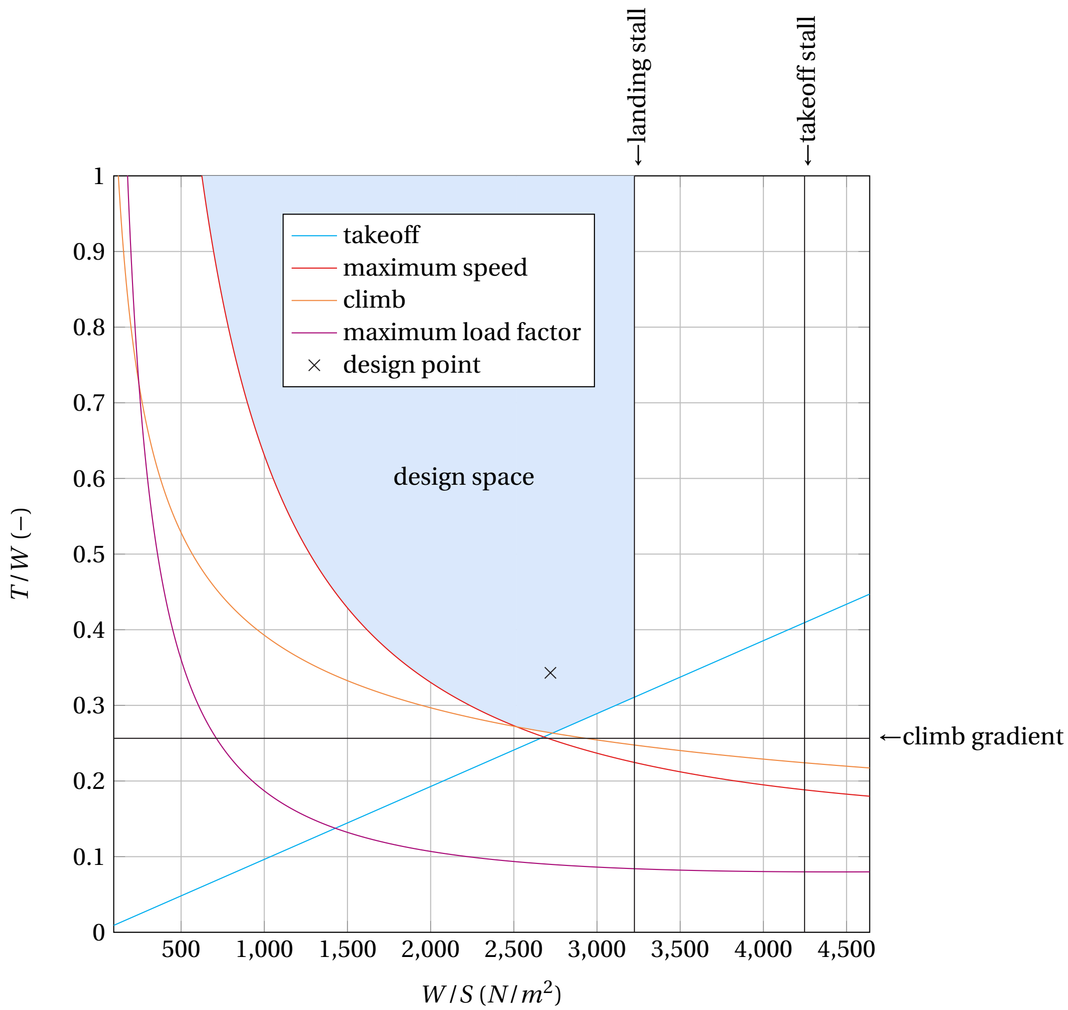

Figure K.1: Wing and thrust loading diagram.

L

Requirement compliancy matrix

In the following two tables, the most important requirements are shown. If a requirement is met, this is indicated with a green box. When there is still uncertainty, a yellow box is used and an unmet requirement is indicated with a red box. The last column shows the section in which this requirement is discussed.

Table L.1: Requirement compliancy matrix including the most important requirements and an indication of whether they are met and in which section the corresponding analysis can be found.

(Sub)parent	Identifier	Requirement	Section
Amphibious capability			
Autonomous operations	8.0-A	Refuelling shall be performable on water.	Subsection 6.2.2
	8.0-C	The passengers and crew shall be able to access the aircraft on water.	Subsection 6.2.1
	8.0-F	The cargo shall be able to access the aircraft on water.	Subsection 6.2.1
	9.0-A	De-icing shall be performable on water	
	10.0-B	A transportation system for the aircraft from landing site to the docking area shall be provided.	Section 13.2
	10.0-C	A transportation system for the aircraft from the docking area to the landing site shall be provided.	Section 13.2
	5.0-A	The aircraft shall provide the required movements during taxi on water.	Section 13.2
	10.0-A	Push-back capability shall be available on water for the aircraft.	Section 13.2
	4.1-I	The aircraft shall be capable of pitching up in takeoff configuration at rotation speed (Vr) on water	
	5.0-F	The aircraft shall provide enough thrust to overcome the resultant drag during takeoff on water	Subsection 10.1.2
	5.0-G	The aircraft shall provide enough thrust to overcome the resultant drag during takeoff on land	Subsection 4.2.2
	5.0-H	The aircraft shall be capable of taking off at maximum takeoff weight in land takeoff configuration in case one engine fails at V1 on a runway with a length of 2000 m CS-25.121	Subsection 4.2.2
	11.0-B	An emergency procedure for aborted takeoff on water shall be available	Section 6.3
	12.0-A	The aircraft shall be able to operate out of an airfield with a runway length of 2000 m on land	Subsection 4.2.2
	12.0-B	The aircraft shall have a balanced field length on water of 3000 m	Section 4.2 Section 10.1
	1.1-C	The aircraft shall provide enough lift to not stall at 41 $m\,s^{-1}$ in water landing configuration at MLW	Subsection 11.1.1
	1.1-D	The aircraft shall provide enough lift not to stall at 41 $m\,s^{-1}$ in land landing configuration at MLW	Subsection 11.1.1
	3.0-B	The aircraft shall be able to land on water with waves of at least 1 m high	Subsection 6.1.4 Subsection 12.2.1
	3.0-D	The aircraft shall be able to slow down from landing speed to a standstill within 1360 m on water without using reverse thrust	Subsection 10.1.2
	11.0-D	Procedures for landing on unsecured landing sites shall be provided	Subsection 6.1.2
	10.0-E	A long term parking solution shall be provided to the customer in case that the aircraft landed on water	Subsection 6.2.1
	12.0-F	The aircraft shall have a maximum wingspan of 30 m (access to airport and waterways)	Section 4.1
Interference with other operations	7.0-H	The aircraft shall be able to detect non-seaplanes	Subsection 6.1.3 Subsection 14.4.2

(Sub)parent	Identifier	Requirement	Section
Damages by environment	3.0-F	The aircraft shall be capable of carrying the impact loads of a load factor of 3.5 landing on water	Subsection 11.3.2
	3.0-C	The aircraft shall be able to land on land	Section 14.1
	3.0-G	The aircraft shall be capable of carrying the impact loads of a load factor of 3.5 landing on land	Section 16.2
	3.0-I	The aircraft shall be able to carry the critical water loads	
	3.0-A	The aircraft shall be watertight	Chapter 7 Section 14.1
	3.0-K	The aircraft shall have a resistance from corrosion by (sea)water	Chapter 7
	4.2-A	Spray during takeoff and landing shall not damage any aircraft system	Subsection 10.1.4
	4.2-B	Spray during takeoff and landing shall not be directly ingested into the engines	Subsection 10.1.4
	4.2-C	Spray during takeoff and landing shall not impair the vision of the pilots	Subsection 10.1.4
	3.0-H	The aircraft shall be capable of carrying the impact loads which can be encountered during flight without critical failure	
Dynamic stability	1.2-E	The aircraft shall be stable and controllable for all center of gravity locations during flight	Section 11.2
	4.1-B	The aircraft shall be hydrodynamically stable in all water operations	Subsection 10.1.3
	4.1-D	The aircraft shall be controllable in all water operations	Section 13.2
	4.1-F	The aircraft shall be able to perform all required manoeuvres on water	Section 13.2
	4.1-G	The aircraft shall not possess tip down tendency in all water operations	Subsection 10.1.1
Standstill stability	4.2-D	The aircraft shall be capable of floating on water without sinking	Subsection 10.1.1
Marketability			
	14.0-F	The nosie emission shall not exceed 70 dBA during takeoff and landing	Subsection 6.1.4
Luxurious passenger transport			
	12.0-C	The aircraft shall have a minimum of 10 VIP seats	Section 14.3
	12.0-E	The aircraft shall be able to transport 15 tonnes of cargo	Subsection 4.2.1
Long range			
	6.1-E	he aircraft shall have a minimum range of 4500 NM taking into account the NBAA IFR reserve fuel conditions	Subsection 4.2.1
Legal compliance			
Maritime law	13.0-E	The aircraft shall comply to maritime regulations	Subsection 6.1.5 Subsection 14.4.2
CS25	3.0-J	The aircraft shall be capable of carrying the gust and manoeuvre loads |as specified in CS-25	Subsection 11.3.1
	6.1-B	The aircraft shall be capable of reaching,ft within,min	
	13.0-C	The aircraft shall possess the required (emergency) exits as specified in CS-25 to evacuate the aircraft within 90 seconds	Subsection 6.2.1
Fast transport			
	6.1-C	The aircraft shall be capable of cruising at a cruise speed of mach 0.9	Subsection 10.2.1
	12.0-J	The aircraft shall be sold for a price of 60 million USD	Section 5.2

M

Forces on side float mechanism

Table M.1: The forces from the individual trusses described in Subsection 12.3.2 are given here.

	Impact load case					Submerges, F_x outboard					Submerges, F_x inboard				
Member	F_n	F_z	F_t	m_z	m_t	F_n	F_z	F_t	m_z	m_t	F_n	F_z	F_t	m_z	m_t
AC	300	0	6200	0	18800	15000	4700	16300	3500	49100	-5400	4700	-1800	3500	-5500
BD	2500	0	6200	0	18800	2000	5200	16300	3900	49100	-5100	5200	-1800	3900	-5500
CD	0	0	0	0	0	5200	0	0	0	0	5200	0	0	0	0
CF	0	0	0	0	0	10900	0	0	0	0	10900	0	0	0	0
DF	0	0	1500	0	7000	-4400	0	4000	0	18400	-4400	0	-500	0	-2000
CE	-2100	0	1500	0	7000	4100	0	4000	0	18400	-9100	0	-500	0	-2000
EF	0	0	0	0	0	-9900	0	0	0	0	-9900	0	0	0	0

N

Electrical systems

N.1. Electrical block diagram

Figure N.1 shows where the electricity of the aircraft is generated and how the power is stored or distributed towards systems within the aircraft. Since the power required for most subsystems is not known, reference aircraft are used for the total power estimation as described in Section 14.2.

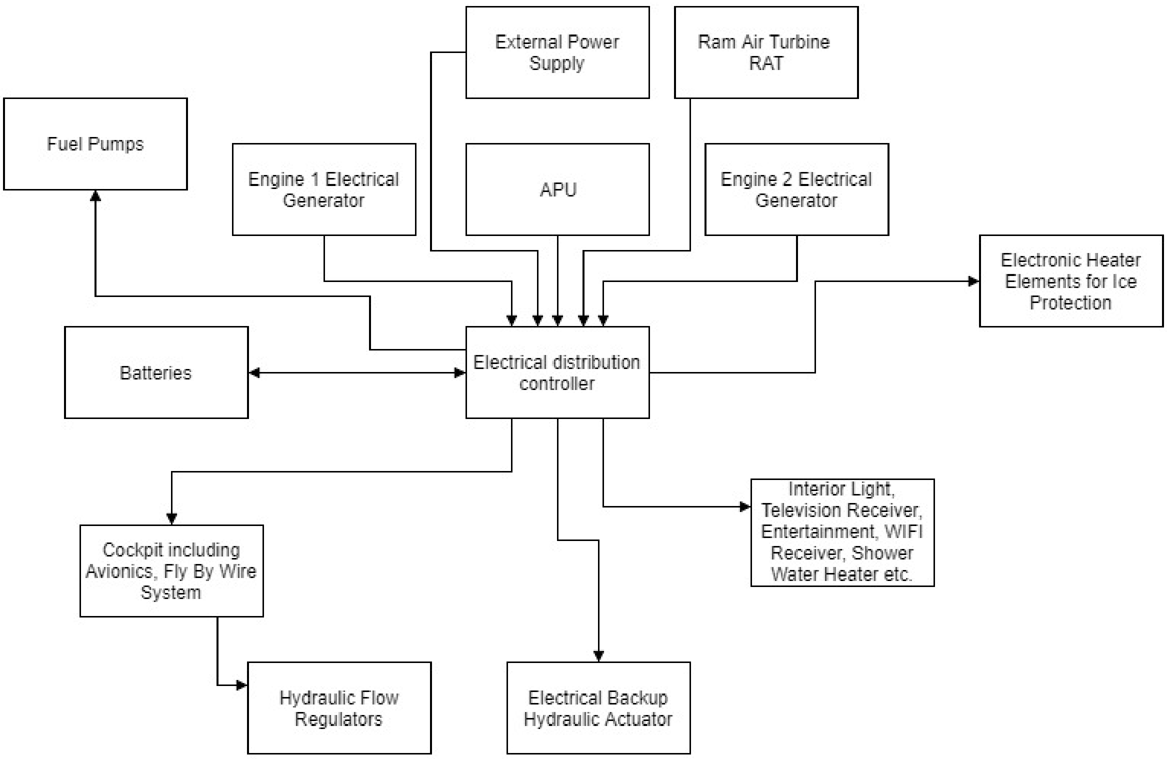

Figure N.1: Electrical block diagram of the complete aircraft

N.2. Side stick data handling

Figure N.2 shows one very small subsystem within the cockpit, namely the horizontal side stick displacement input for the fly by wire system. A variable resistor is used that varies the resistance with the deflection, where moving the flight control left decreases the resistance and moving it right increases the the resistance. A constant resistor is placed in series with this variable resistor. A constant DC source is linked to the variable resistance and constant resistor. This configuration is placed in parallel with itself for redundancy. The voltage over the variable resistor is measured by three fly by wire computers. This is required for redundancy since if one computer gives the wrong answer the aircraft can not determine what is the correct and what is the wrong answer. The same system is used for the vertical side stick displacement. Figure N.3 shows how the data is handled within the flight control subsystem.

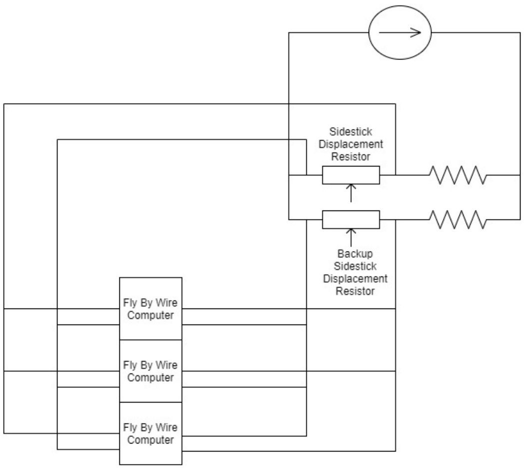

Figure N.2: Electrical diagram of side stick

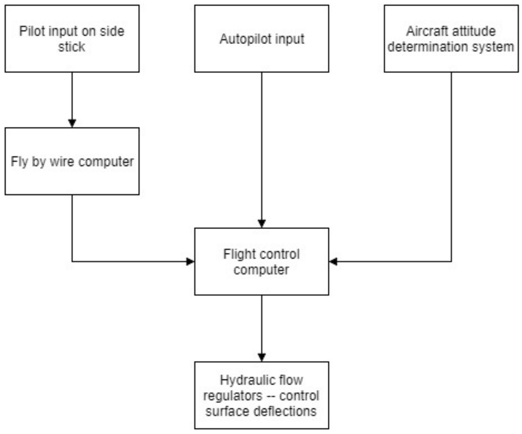

Figure N.3: Data handling block diagram of pilot control inputs

O Planning for further design efforts

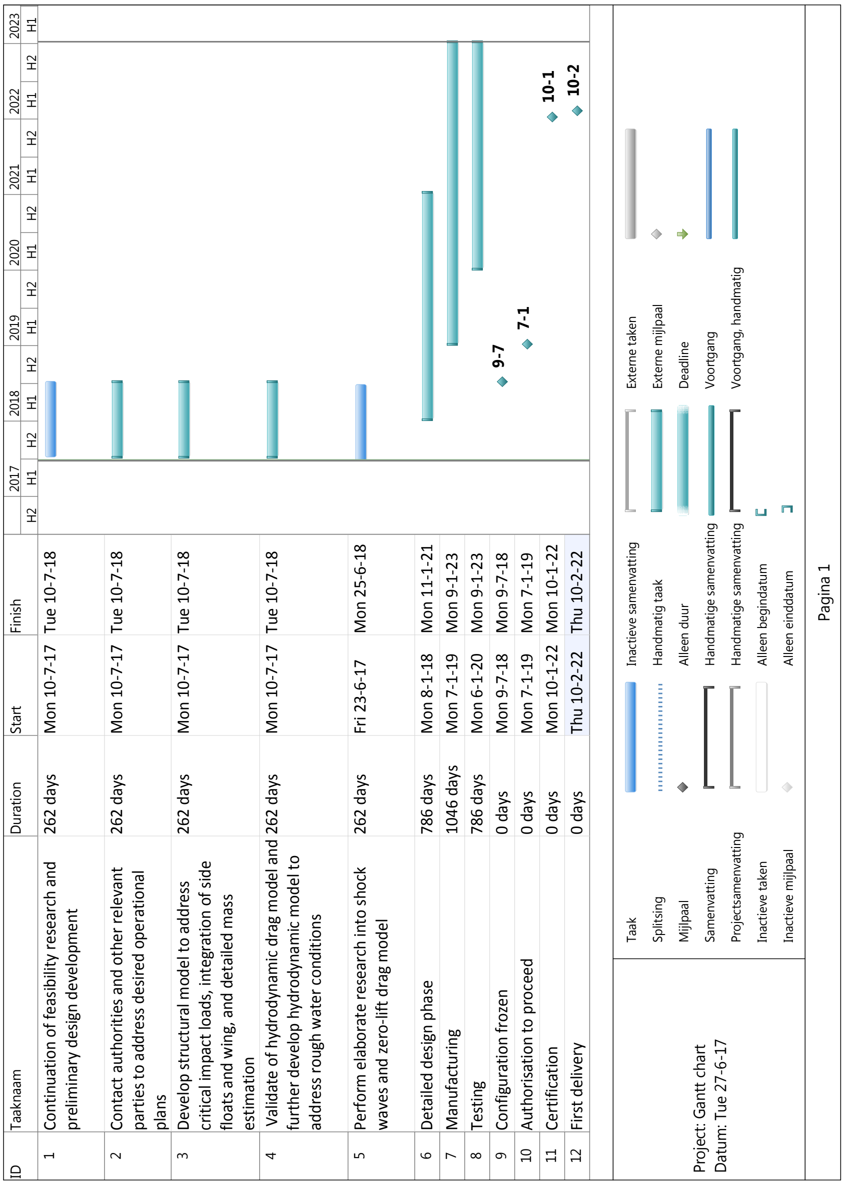

Figure O.1: Gantt chart for the way forward up to first delivery.

Figure O.1 shows the Gantt chart used in planning of the next design steps. Tasks 1 through 5 are based on the recommendations and elaborated upon in Section 16.2, including detailed work-flow diagrams. The general planning was based on the cost model as presented in Chapter 5.

P

Additional data on climb performance

Additional information on the climb performance of the aircraft in support of Subsection 4.2.3.

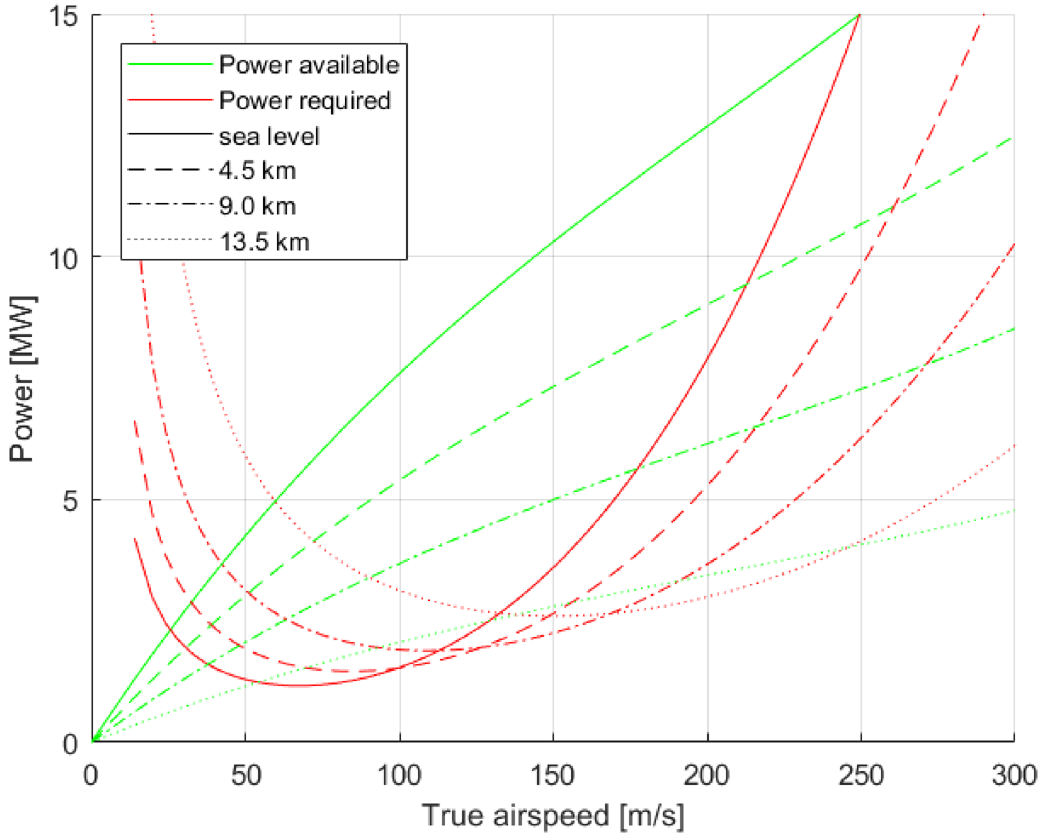

Figure P.1: Power performance at different altitudes.

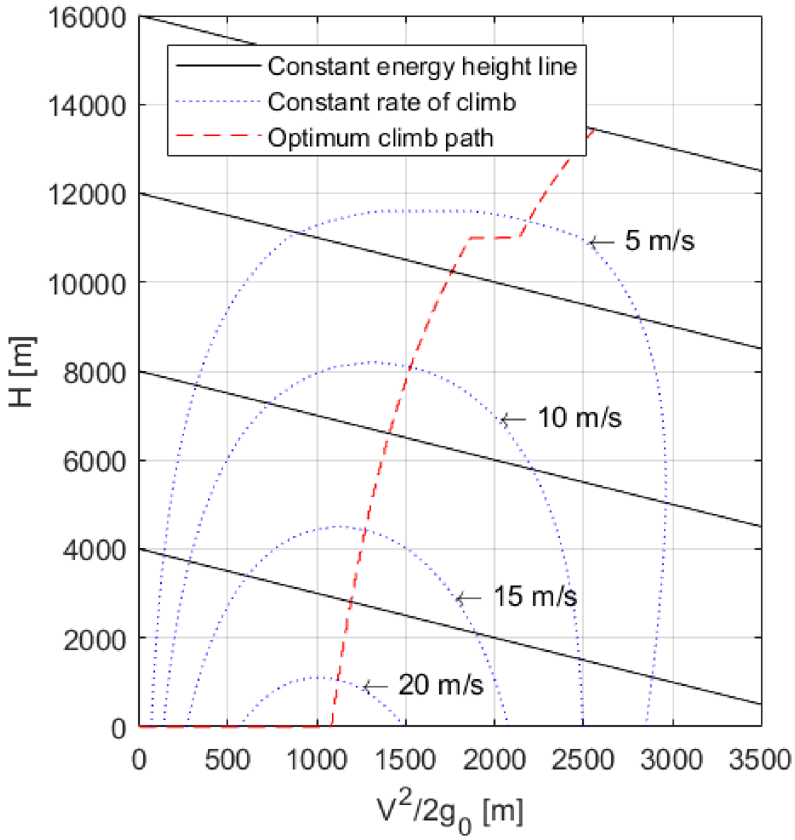

Figure P.2: A visual representation of the energy height method. Optimum climb path goes through constant energy height lines at the maximum rate of climb.

Q

Flying boat nomenclature

Figure Q.1 displays the common design variables used in the design of flying boats. Section 10.1 will go deeper into the design of the hull.

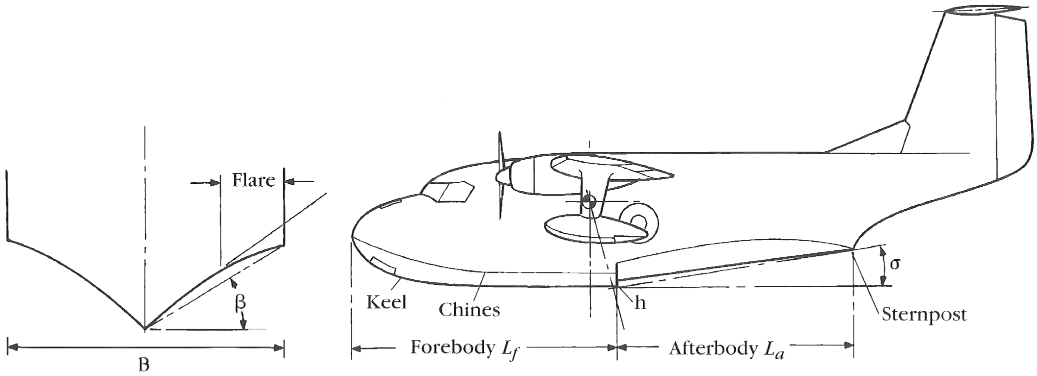

Figure Q.1: Parameters associated with specific symbols in a flying boat.

Bibliography

[1] E.R. Boeker, E. Dinges, B. He, G. Fleming, C.J. Roof, P.J. Gerbi, A.S. Rapoza, and J. Hemann. *Integrated Noise Model (INM).* Federal Aviation Administration Office of Environment and Energy, January 2008.

[2] J. M. Bryson. *Strategic Planning for Public and Nonprofit Organizations.* Jossey-Bass Publishers, 1995.

[3] A. Cervone and A. Elham. *Aerospace Design and Systems Engineering Elements II.* Delft University of Technology, 2016.

[4] *CAD 361 International Non-Public Transport Operations.* Civil Aviation Department Hong Kong, December 2016.

[5] N.E. Daidzic. Estimation of performance airspeeds for high-bypass turbofans equipped transport-category airplanes. *Journal of Aviation Technology and Engineering*, 5(2):4, 2016.

[6] J.P. Day and R.J. Haag. *Planing Boat Porpoising.* Webb Institute of Naval Architecture, 1952.

[7] N. Dickson. *Local Air Quality and ICAO Engine Emissions Standards.* International Civil Aviation Organization (ICAO), 2014.

[8] European Aviation Safety Agency (EASA). *Certification Specifications for Large Aeroplanes (CS-25)*, September 2007.

[9] C.N. Eastlake and H.W. Blackwell. Cost estimating software for general aviation aircraft design. *American Society for Engineering Education*, 2000.

[10] World Heritage Encyclopedia. Snecma silvercrest. *High-Bypass Turbofan Engines, Snecma Aircraft Engines, Turbofan Engines 2010-2019*, 2017.

[11] *Restricted Type-Certificate Data Sheet for Beriev Be-200ES-E.* European Aviation Safety Agency (EASA), November 2010.

[12] M. Fanliang. *Actuation System Design with Electrically Powered Actuators.* , Cranfield University, January 2011.

[13] R.C. Feagin and W.D. Morrison. *Delta method, an empirical drag buildup technique*, December 1978.

[14] F. George. Operators survey: Dassault Falcon 7X. *Aviation Week*, March 2016.

[15] *Aircraft noise report 2015.* German Aviation Association (BDL), 2015.

[16] P. Ghadimi, R. Shademani, and M.Y Fard. Performance assessment of the waterjet propulsion system through a combined analytical and numerical approach. *International Journal of Physics*, 1(2):22–27, 2013.

[17] E.K.A. Gill and G. La Rocca. *Systems Engineering and Aerospace Design.* Delft University of Technology, 2017.

[18] S. Gudmundsson. *General Aviation Aircraft Design: Applied Methods and Procedures.* Butterworth-Heinemann, September 2013.

[19] O. Gur, W.H. Mason, and J.A. Schetz. Full-configuration drag estimation. *Journal of Aircraft*, 47(4): 1356–1367, 2010.

[20] J.M. Hoekstra. *Introduction to Aerospace Engineering I.* Delft University of Technology, 2014.

[21] L.H. Holthuijsen. *Waves in Oceanic and Coastal Waters.* Cambridge University Press, 2010.

[22] *IntuVue™ 3-D Weather Hazard and Avoidance System.* Honeywell Aerospace, 2016.

[23] *Recommended Procedures: Resistance Uncertainty Analysis, Example for Resistance Test.* International Towing Tank Conference (ITTC), 2002.

[24] F.T. Jane, P. Jackson, K. Munson, and L. Peacock. *Jane's All the World's Aircraft.* McGraw-Hill, 2009.

[25] L.R. Jenkinson, D. Rhodes, and P. Simpkin. *Civil jet aircraft design.* AIAA education series. Arnold, 1999.

[26] Jetcraft. 10 year business aviation market outlook 2016-2025.

[27] C. Kassapoglou and R.C. Alderliesten. *Structural Analysis & Design.* Delft University of Technology, 2015.

[28] J.A. Keuning and M. Katgert. A bare hull resistance prediction method derived from the results of the delft systematic yacht hull series extended to higher speeds. *International Conference on Innovation in High Performance Sailing Yachts*, 2008.

[29] M. Kumar and V. A. Subramanian. A numerical and experimental study on tank wall influences in drag estimation. 2005.

[30] E.V. Lewis. *Principles of Naval Architecture.* The Society of Naval Architects and Marine Engineers, 3rd edition, 1989.

[31] M. McMillin. Bizav fleet to grow at 'tepid' rate over decade, report says. *Business Aviation*, 2017.

[32] T.H.G. Megson. *Aircraft structures for engineering students.* Elsevier, 2012.

[33] J.A. Melkert, R. Vos, and B.T.C. Zandbergen. *Aerospace Design and Systems Engineering Elements I.* Delft University of Technology, 2016.

[34] L.M. Nicolai and G.E. Carichner. *Fundamentals of Aircraft and Airship Design.* American Institute of Aeronautics and Astronautics, 2001.

[35] Water Business Jet, Delft University of Technology. *Baseline report.* Design Synthesis Exercise, Spring 2017.

[36] Water Business Jet, Delft University of Technology. *Midterm report.* Design Synthesis Exercise, Spring 2017.

[37] Water Business Jet, Delft University of Technology. *Project Plan.* Design Synthesis Exercise, Spring 2017.

[38] D.P. Raymer. *Aircraft Design: A Conceptual Approach.* American Institute of Aeronautics & Astronautics, 1989.

[39] *Study of the Global Business Jets Market 2015.* RnR Market Research, May 2015.

[40] J. Roskam. *Airplane Design.* DARcorporation, 1985.

[41] E. Roux. *Turbofan and Turbojet Engines: Database Handbook.* Ed. Élodie Roux, 2007.

[42] M. Saarlas. *Aircraft Performance.* John Wiley Sons, Inc., 2007.

[43] D. Savitsky. Hydrodynamic design of planing hulls. *Marine Technology*, 1(1), 1964.

[44] D. Savitsky and P.W. Brown. Procedures for hydrodynamic evaluation of planing hulls in smooth and rough water. *Marine Technology*, 13(4):381–400, 1976.

[45] D. Savitsky, M.F. DeLorme, and R. Datla. Inclusion of whisker spray drag in performance prediction method for high-speed planing hulls. *Marine Technology*, 2007.

[46] A.G. Smith. *The Full-Scale Air Drag of Some Flying-Boat Seaplanes.* Aeronautical Research Council, February 1956.

[47] J. Supamusdisukul. *Experimental investigation of wing-fuselage integration geomteries including CFD analyses.* , University of Maryland, 2008.

[48] *Cessna Longitude Citation Brochure.* Textron Aviation, 2016.

[49] D.B. Thurston. *Design for Flying.* TAB Books, 1995.

[50] E. Torenbeek. *Synthesis of Subsonic Airplane Design.* Springer Netherlands, 1982.

[51] A.A. Trani. *Fundamentals of Aircraft Performance.* Virginia Polytechnic Institute and State University, Fall 2006.

[52] *Aviation Maintenance Technician Handbook-Airframe.* United States Department of Transportation, Federal Aviation Administration (FAA), Oklahoma City, 2012.

[53] J.A. Vargas-Jimenez and R. Vos. *Development of a Wave Drag Prediction Method for the Conceptual Design Phase.* 54th AIAA Aerospace Sciences Meeting, 2016.

[54] M. Voskuil and R. Noomen. *Flight & Orbital Mechanics.* Delft University of Technology, 2016.

[55] H. Xia, P.G. Tucker, and S. Eastwood. Large-eddy simulations of chevron jet flows with noise predictions. *International Journal of Heat and Fluid Flow*, 30(6):1067 – 1079, 2009.